UNIVERSITY OF SUSSEX

Reactivity of a *syn*-Bimetallic Pentalene Titanium Complex: Synthesis of Alkyl Complexes and Related Adducts

Matthew K. Molloy

Submitted for the degree of Doctor of Philosophy

University of Sussex

September 2018

The work described in this thesis was performed under the supervision of Professor F. G. N. Cloke at the University of Sussex from September 2014 to September 2018. All work is my own, unless specifically stated otherwise. None of the work presented in this document has been previously submitted for any other degree at the University of Sussex or any other university.

Matthew Molloy

September 2018

ACKNOWLEDGEMENTS

I would like to thank Professor Geoff Cloke for introducing me to the fundamentals of inorganic chemistry during my undergraduate degree and his supervision and guidance over the course of my PhD project. Dr. Oscar Navarro also provided many useful discussions when planning my work, and I would like to express my gratitude for his input and advice.

Special thanks go to Dr. Nikos Tsoureas, from whose extensive laboratory experience and chemical knowledge I have learned a great deal. I also thank Dr. Alexander Kilpatrick for his early support and encouragement with the project and for his collaborative efforts for the collection of solid state NMR data. Dr. Jessica Frey and Dr. Alistair Frey also receive my thanks for their warm and welcoming introduction to Lab 14 in my first year.

Thanks are also given to colleagues Christopher Inman, Matthew Leech and Dr. Victoria Greenacre. Chris' sly sense of humour and easy-going personality were bright highlights of my time in Lab 14. I have had the privilege of completing both my undergraduate and postgraduate studies alongside Matt, and we have shared many good memories together. Finally, Dr. Greenacre's friendship and cooperation directly led to the crushing table tennis defeat of the University of Edinburgh at the 2015 RSC Dalton Meeting, an event documented here lest it ever be forgotten.

Additionally, I would like to thank:

Prof. J. C. Green

Dr. A. Abdul-Sada

Dr. I. J. Day

Dr. S. M. Roe

Dr. J. F. C. Turner

Prof. H. Cox

Dr. S. L. F. Hin

All members of Lab 14

The National Crystallography Service

My family, specifically Mum and Dad, who are immensely supportive of my work.

Summary of Chapter Contents

The introductory chapter of this thesis shall discuss the structure, binding modes and practical application of the pentalene ligand in organometallic chemistry. The synthesis and properties of the bimetallic titanium pentalene compound $[Ti(\mu:\eta^5,\eta^5\text{-}Pn^{\dagger})]_2$ **1.1** shall be focused upon in particular, as this compound is an important component of many of the experiments performed in this work. Examples of established transition metal cyclopentadienyl complex chemistry will also be discussed with a view to how the rationale behind these reactions may be applied to further the field of pentalene chemistry.

The second chapter of this thesis focuses entirely upon the dehydrogenation of amine-boranes, a process that **1.1** was found to catalyse. A discussion of the significance of this reaction and its real world applications will be presented, followed by a brief summary of existing catalytic species reported in the literature. The characterisation data obtained for a novel pentalene complex isolated from the reaction mixture will be analysed in detail.

Chapter Three describes the synthesis of a variety of titanium pentalene metal halide compounds with the objective of providing synthetic precursors for the isolation of further novel pentalene compounds. Efforts expended towards the optimisation of these synthetic routes shall also be discussed.

Chapter Four chronicles the further development of the chemistry discussed in Chapter Three, with the targeted synthesis of pentalene titanium metal alkyl complexes from pentalene titanium halides. The characterisation of these compounds, their stability and their reactivity is documented.

Chapter Five provides a summary of reactions performed between compound **1.1** and neutral L-type ligands. Highlights include the reaction of **1.1** with ethylene, butadiene and xylylisocyanide.

Abbreviations

$\{^1H\}$	Proton decoupled
[Ti]	Generic titanium catalyst
°C	Degrees Celsius
Å	Angstrom
Δ	Chemical shift, ppm
μ	Bridging species
η^n	Hapticity
acac	Acetylacetone
ADB	Aminodiborane
Atm	Atmospheres
BCDB	B-(cyclodiborazanyl)amine-borane
BCTB	B-(cyclotriborazanyl)amine-borane
BD	Butadiene
Bn	Benzyl
Bu	Butyl
CBC	Covalent Bond Classification
cm^{-1}	Wavenumber
COD	1,5-Cyclooctadiene
COT	Cyclooctatetraene
Cp, Cp*	Cyclopentadienyl, permethylcyclopentadienyl
CTB	Cyclotriborazane
Cy	Cyclohexyl
d	Doublet
1,2-DCE	1,2-Dichloroethane
DEPT	Distortionless Enhancement by Polarisation Transfer
DFT	Density Functional Theory
DME	Dimethoxyethane
DMSO	Dimethyl sulfoxide
EA	Elemental analysis
EDG	Electron donating group
EI-MS	Electron ionisation mass spectrometry
ESI-MS	Electrospray ionisation

Et ..... Ethyl

EWG..... Electron withdrawing group

ESD ..... Estimated standard deviation

FVP ..... Flash vacuum pyrolysis

g, mg..... Gram(s), milligram(s)

HOMO ..... Highest Occupied Molecular Orbital

HSQC ..... Heteronuclear Single-Quantum Correlation Spectroscopy

hv..... Photochemical process

Hz, KHz, MHz ..... Hertz, kilohertz, megahertz

^{i}Pr ..... Isopropyl

IR..... Infra-red

K..... Kelvin

kcal/mol..... Kilocalories per mole.

KHMDS ..... Potassium hexamethyl disilazide

K/Hg..... Potassium/mercury amalgam

LS-selectride ..... Lithium trisiamylborohydride, $[Li]^{+}[HB(CH_3CH^{i}Pr)_3]^{-}$,

LUMO..... Lowest Unoccupied Molecular Orbital

MAO, MMAO ..... Methylaluminoxane, modified methylaluminoxane

M ..... Multiplet

Me ..... Methyl

MS..... Mass spectrometry

m/z ..... Mass/charge ratio

n-Bu..... *n*-Butyl

NHC ..... N-Heterocyclic Carbene

NMR..... Nuclear Magnetic Resonance

OAc ..... Acetoxy group

Ph ..... Phenyl group

Pip ..... Piperidine

Pn, Pn*, Pn†..... Pentalene, permethylpentalene, 1,4-triisoproylsilylpentalene

PNP ..... N,N′-bis(diphenylphosphine)-2,6-diaminopyridine)

Pr ..... Propyl

p-TCD ..... 1,3-N,N'-di-*p*-tolylcarbodiimide

p-Tol ..... *para*-Tolyl group

R (group) ..... Generic hydrocarbon group

RPM ..... Rotations per minute

RT ..... Room temperature

SS ..... Solid state

^{t}Bu ..... *tert*-butyl

THF ..... Tetrahydrofuran

TIPS ..... Triisopropylsilyl

TMEDA ..... Tetramethylethylenediamine

TMS ..... Tetramethylsilane/trimethylsilyl (context-dependent)

TOF ..... Turnover frequency

TON ..... Turnover number

VT ..... Variable temperature

XRD ..... X-Ray diffraction

Table of Contents

"Why does this magnificent applied science which saves work and makes life easier bring us so little happiness? The simple answer runs: because we have not yet learned to make sensible use of it. […] Concern for the man himself and his fate must always form the chief interest of all technical endeavours; concern for the great unsolved problems of the organization of labor and the distribution of goods in order that the creations of our mind shall be a blessing and not a curse to mankind. Never forget this in the midst of your diagrams and equations."

Excerpt of a speech given by Albert Einstein, *The New York Times,* 16th February 1931.

"What upsets me about the job? Wasted talent. People could come to me, and they could go: "Excuse me David, but you've been in the business for twelve years. Can you just spare us a moment to tell us how to run a team? How to keep them task oriented as well as happy?" But they don't. That's the tragedy."

David Brent, *The Office*, 2001.

Chapter 1 - Introduction

The Pentalene Ligand

The discovery of ferrocene in 1951[1] and the elucidation of the η^5 binding mode of the cyclopentadienyl ligand[2] were seminal developments which marked the genesis of the field of organometallic chemistry as it exists today.[2] Many η^5-cyclopentadienyl sandwich compounds were soon synthesised, with a divergence in focus between focusing on altering the metal centre used (an approach adopted by Wilkinson)[3] and functionalising the Cp ligands.[4]

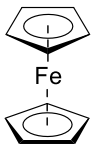

Figure 1.1 Ferrocene.

As the Cp ligand proliferated in subsequent decades, inorganic cyclopentadienyl sandwich compounds and related derivatives have found a diverse range of applications. These include catalysts used on an industrial scale for the synthesis of polymers,[5] enantioselective catalysts[6] and sandwich compounds capable of activating "inert" small molecules such as CO_2.[7]

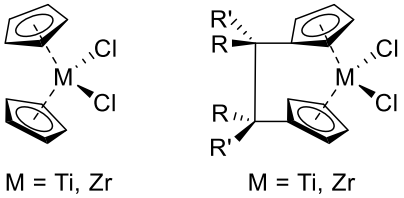

Figure 1.2 Examples of Ziegler-Natta cyclopentadienyl sandwich catalysts.[5]

Despite the extensive advancement of cyclopentadienyl chemistry, academic exploration of similar carbocycles has remained comparatively less developed.
The existence of pentalene was first postulated in 1922 by Robinson and Armit, who described the molecule pictorially as two fused cyclopentadienyl rings, speculating that it would likely possess aromatic character if ever isolated.[8] These predictions were later confirmed to be accurate if not completely correct. However, the difficulty of synthesising pentalenes without the use of modern synthetic techniques and equipment

proved formidable, resulting in a prolonged delay between the original theoretical predictions and practical confirmation by experiment. Le Goff finally succeeded in the synthesis of the first stable[9] pentalene species, hexaphenyldihydropentalene, exactly 40 years after the initial postulation of the existence of isolable pentalene molecules.

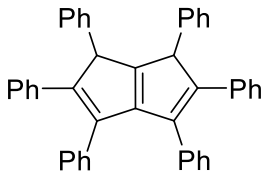

Figure 1.3 Hexaphenyldihydropentalene.

With the introduction of more reliable synthetic methods in the last decade, it has become evident that pentalene has many properties that make it ideal for stabilising low-valent, highly reactive metal centres. These include a flexible geometry, versatile electron donating properties and extensive scope for derivatisation allowing for highly customisable steric properties.

Multiple thorough reviews of contemporary pentalene chemistry have been published in recent years.[10,11,12,13] Rather than an exhaustive overview of the field, this introductory chapter shall instead seek to summarise the fundamental basics of pentalene chemistry. Naming conventions, binding modes adopted by the pentalene ligand and some seminal examples of organometallic pentalene chemistry will be presented, with a focus on transition metal pentalene complexes.

Anionic Pentalene Species and Related Nomenclature

Pentalene typically exists in a neutral or anionic state (effected by deprotonation around the ring). For clarity, pentalene, pentalene derivatives and related negatively charged species (such as those in **Figure 1.4**) shall be referred to by the generic descriptor "pentalene", unless otherwise specified.

Figure 1.4 Dihydropentalene and anionic derivatives.

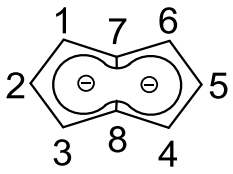

Figure 1.5 Formal pentalene numbering scheme.[10]

Figure 1.5 (*vide supra)* shows the numbering system used to formally denote specific carbons within a pentalene molecule. Carbon atoms 7 and 8 exist at the transannular bridge and are thus denoted "bridgehead" carbons, while atoms 2 and 5 are referred to as "wing tip" carbons.

Synthesis of Pentalene and Pentalenyl Species

The pentalene dianion, $[C_8H_6]^{2-}$, is essentially a doubly deprotonated derivative of dihydropentalene, C_8H_8. This would seem to insinuate that isolation of pentalene is a facile synthetic process; however, early organic preparations of pentalene derivatives required many synthetic steps and gave poor yields. This is due to the the propensity of pentalene to dimerise *via* [2+2] cycloaddition[14] a process driven by the electronic structure of the molecule. Unlike dihydropentalene, which is a 6π electron system, pentalene possesses 8π electrons, and is therefore defined by Hückel's Rule as anti-aromatic. Dimerisation results in the loss of anti-aromaticity and as a result is thermodynamically favourable, occurring even at very low temperatures.

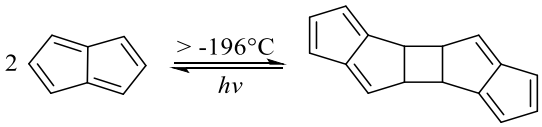

Scheme 1.1 Dimerisation of pentalene.

Organic methodologies often rely on the synthesis of complicated cyclic precursor molecules[15] followed by a rearrangement[16] to produce a final derivatised[17] pentalene; the significant complexity of this approach makes it impractical for facile access to pentalenes for use as ligands. While further refinements of organic routes to pentalene have reduced the number of synthetic steps required, performing these reactions at any temperature above -196°C still results in inevitable dimerisation from the moment the

species is formed in the mixture. This continues to result in a high degree of thermal sensitivity and sub-optimal yields, even with modern cross-coupling techniques.[18]

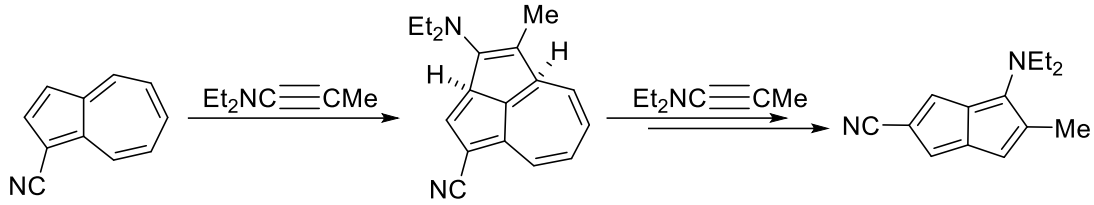

Scheme 1.2 Synthesis of a derivatised dihydropentalene.[15]

The first routes to inorganic complexes of pentalene were reliant on the conversion of a metal-bound cyclooctatetraene ligand into pentalene *in situ*, circumventing the difficulties encountered when making the ligand independently. The COT ligand, C_8H_8, is structurally analogous to a pentalene molecule lacking the bridgehead C-C bond.

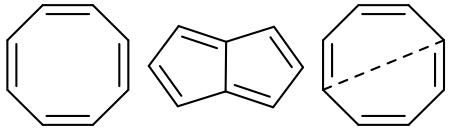

Figure 1.6 Cyclooctatetraene, pentalene and a depiction of the transannular C-C bond that relates the structures.

Reflux of a ruthenium cyclooctatetraene complex at 98°C was found to partially convert the COT ligand to pentalene through thermolytic rearrangement, resulting in the isolation of a bimetallic ruthenium pentalene compound. While this provides rational synthetic access to ruthenium pentalene complexes, the combination of low yield and the restriction of the resulting ligand to a set bimetallic ruthenium system with a (μ-η^5:η^5) bonding mode makes the utility of this type of synthetic procedure limited in scope.[19]

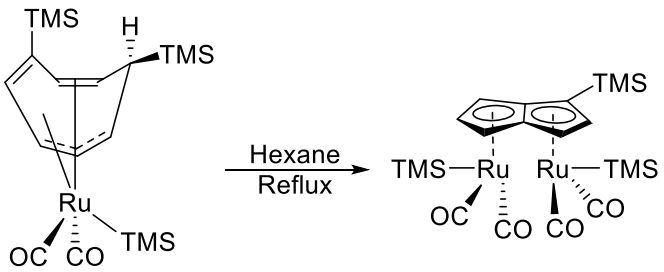

Scheme 1.3 Thermolytic rearrangement of COT to pentalene.[19]

Flash vacuum pyrolysis of cyclooctatetraene is one of the most reliable contemporary methods of dihydropentalene synthesis. Applied to the rearrangement of cyclooctatetraene to dihydropentalene by Jones and Schwab[20] in 1968, the technique was then further optimised by the Cloke group to achieve yields of up to 87%.[21] FVP apparatus allows exposure of small quantities of COT to extreme temperatures for very short periods of time under an inert atmosphere. The cyclooctatetraene is kept under a flow of nitrogen and drawn through a tube furnace *via* vacuum.[22]

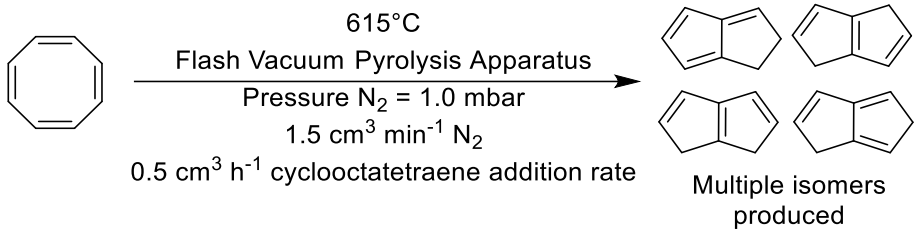

Scheme 1.4 Flash vacuum pyrolysis of cyclooctatetraene.[21]

The flow of COT is limited by a precision engineered needle valve, minimising the duration of time that the COT is heated. This produces optimal yield of dihydropentalenes while avoiding dimer formation. Collecting the dihydropentalenes in a -80°C trap then eliminates any further risk of thermally induced dimerisation. Pyrolysis of other precursors to form dihydropentalenes[10] has also been reported, including the thermally induced cyclisation of 5-cyclopentadienylidenemethyl-2-norbornene and isocyclopentadiene.

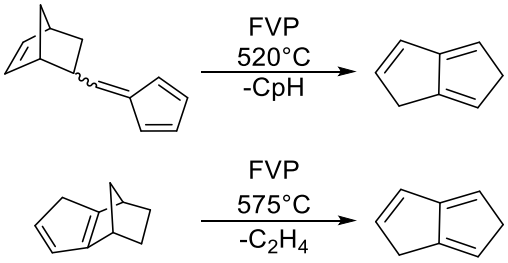

Scheme 1.5 Alternative precursors converted to dihydropentalenes[10] *via* flash vacuum pyrolysis.

Pentalene may be derivatised to encompass additional protective steric bulk (*i.e.* with the introduction of TMS or TIPS groups) and increase solubility in lipophilic solvents such as simple hydrocarbons.[23] Electronic properties may also be fine-tuned by the addition of electron donating substituents to further enrich the electron density of the

ligand π system. A protracted trial-and-error experimental approach is often required to establish which of these derivatised ligands is most effective for synthesis of a target complex. Pentalenes functionalised with excessive steric bulk may preclude desired reactivity at the metal centre or limit the possible binding modes of the ligand. Low-valent metal halides may fail to form a complex when reacted with these derivatives. While kinetic protection is desirable, a single ligand of η^8 binding is often insufficient to provide electronic stability to an electron deficient metal centre; a surplus of steric protection hinders formation of a sandwich configuration which may offset this and allow the synthesis of a stable species. Placing many electron donating groups around the pentalene ring may also cause issues with the synthesis of a complex; reduction of the metal centre can occur in preference to ligation of the pentalene group if the ligand is extremely electron rich and the metal is electron deficient.

One pathway to derivatives is to pre-include the desired groups in the precursors used before the synthesis of the pentalene ligand itself. This is the method for the 10-step synthesis of the permethylpentalene (Pn*) ligand, conceived by the O'Hare group.[23] Beginning from from the commercially available Weiss' salt ("WeissH_4"), methylation with MeI introduces the desired methyl groups at the 1, 3, 4 and 6 positions. This is followed by decarboxylation, oxidation and finally aprotic dehydration with LiCl[23] to produce the Pn*' precursor.[11]

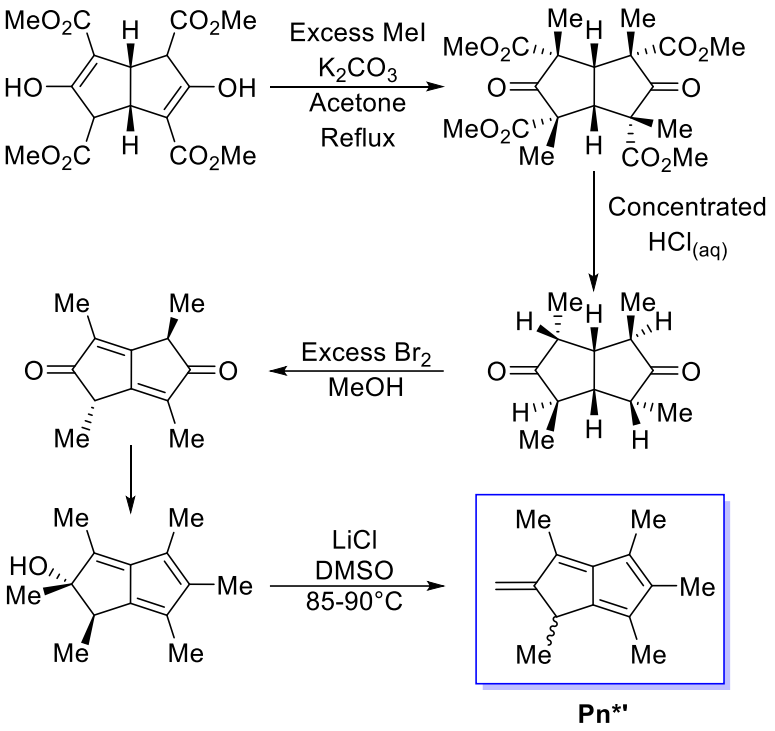

Scheme 1.6 Synthesis[11] of Pn*'.

While incompatible with many common reducing agents, Pn*' may be successfully treated with LS-Selectride ($[Li]^+[HB(CH_3CH^iPr)_3]^-$) to produce the hydropentalenyl monoanion *via* the direct addition of a hydride onto the conjugated alkenyl group jutting from the wing-tip carbon. Further deprotonation with *n*-BuLi yields the pentalenyl dianion lithium salt as an adduct with varying amounts of TMEDA. While this precursor would initially seem ideal for reaction with halogenated metal species, the salt suffers from poor solubility[23] and is extremely reducing both due to the dianionic nature of the pentalenyl ligand itself and the prevalence of electron-donating methyl groups. Thallium pentalene salts have seen general usage as "softer" pentalene transfer agents for many years; the O'Hare group has extended this technique to tin, using a reaction with Me_3SnCl to produce a mild neutral tin derivative. This species may also be converted to a more soluble *bis*-TMEDA dianionic salt by reaction with two equivalents of methyl lithium.

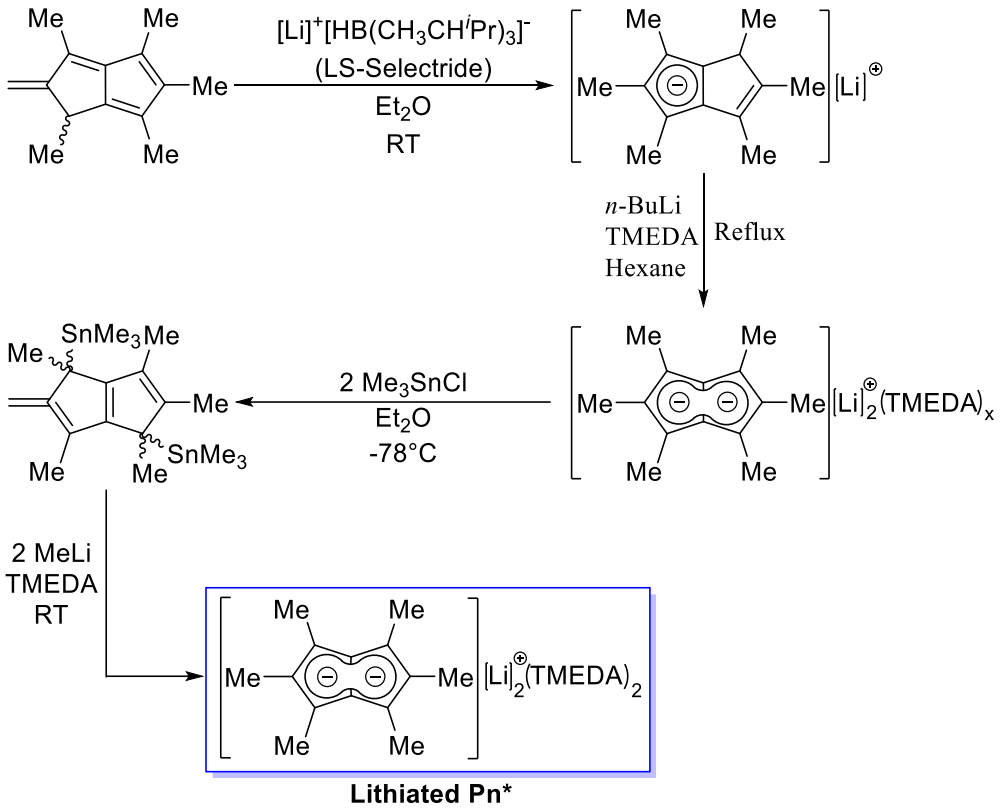

Scheme 1.7 Synthesis of the Pn* lithium salt.[24]

Other non-pyrolytic routes to substituted dihydropentalenes include cyclisation reactions performed upon cyclopentadiene tertiary amine complexes.[25]

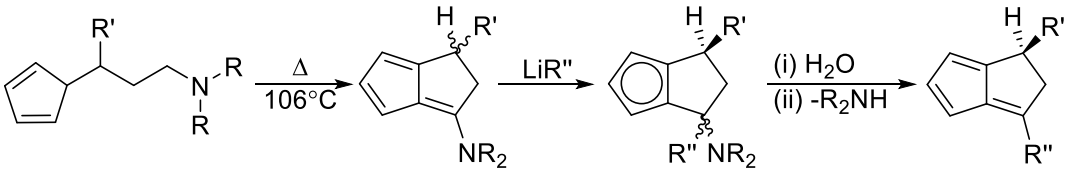

Scheme 1.8 Non-pyrolytic synthesis of a dihydropentalene.[25]

A method detailed by Baird and Reese[25] allows for the synthesis of both monosubstituted and unsubstituted dihydropentalenes in 30-40% yield. The reaction proceeds *via* a "foiled carbene" intermediate, in which the singlet-state Fischer-type carbene lone pair is stabilised by the diene p-orbitals.

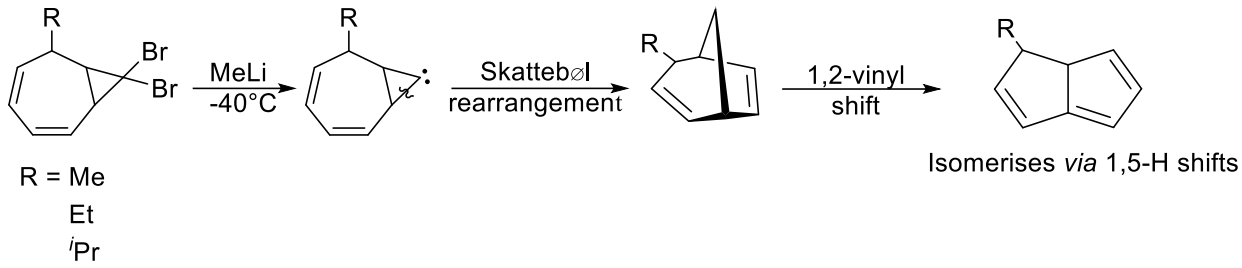

Scheme 1.9 Synthesis of pentalenes *via* the Skattebøl rearrangement.[25,26]

The most useful advantage of these methods is the avoidance of the technical and costly assembly of FVP equipment, though mediocre yields have thus far resulted in pyrolysis remaining the most efficient pathway for gram-scale synthesis.[10]

Modifications may also be made to generic unsubstituted dihydropentalenes *via* reaction of prepared pentalenyl dianion salts with electrophilic silyl transfer agents such as trimethylsilyl chloride and triisopropylsilyl triflate.[21] This is the method used in this project for the preparation of Pn† (the pentalenyl dianion with TIPS groups at the 1 and 4 positions). Addition of these silyl goups results in a neutral 6π species, necessitating a second double deprotonation with ^{n}BuLi or KNH_2 to produce the derivatised pentalenyl dianion salt. This deprotonation occurs exclusively at positions 1 and 4, owing to the increased acidity of the hydrogen atoms situated α to the silyl groups.[21]

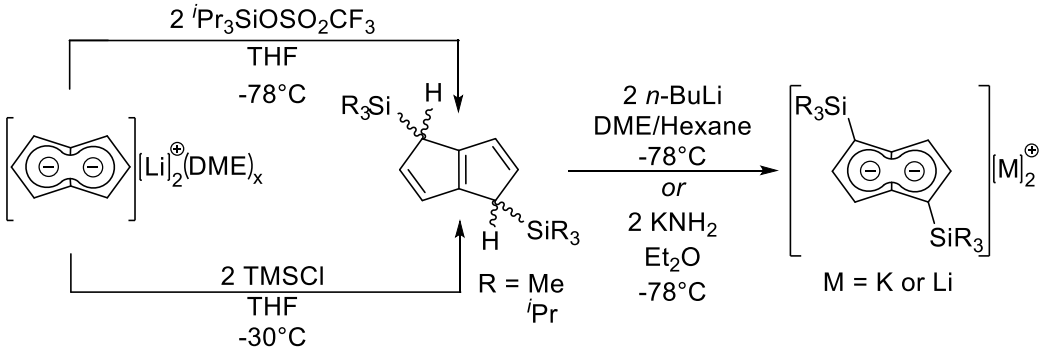

Scheme 1.10 Route to lithium and potassium pentalenyl dianion salts.[21,27]

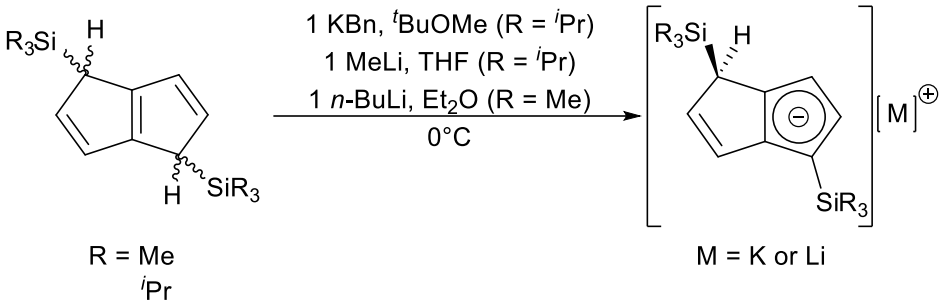

Scheme 1.11 Route to the substituted hydropentalenyl monoanion.[21]

Addition of silyl groups is also regioselective for the 1,4-positions at low temperature, a predisposition that pentalene shares with cyclooctatetraene. In the case of pentalene, this situates the TIPS groups *anti* to one another, providing maximum steric stability. Higher temperatures result in a mix of regioisomers.[21]

Heteronuclear analogues of pentalene have also been synthesised.[28] 4-azapentalenyl, in which bridgehead carbon 4 has been substituted for a nitrogen atom, exists as a singly anionic species isoelectronic with $[C_8H_6]^{2-}$.

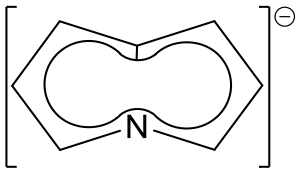

Figure 1.7 The 4-azapentalenyl monoanion.

In recent years, ring annulation reactions with metallabenzene have yielded the first pentalenes with a metal atom incorporated as part of the ring. Aza-metallapentalenes have also been synthesised, though aromaticity of these systems is contestable. Cyclisation reactions have been performed with osmapentalenes; however, no attempts have yet been made to use metallapentalenes as ligands in organometallic complexes. While predictions have been made that osmapentalene species retain a degree of aromaticity[29] it is probable that profound differences in the electronic structure of the molecule in addition to the increased bulk of the metal centre would make use of the molecule as a π donor ligand untenable.

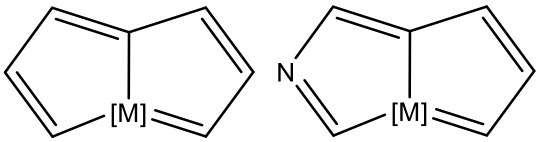

Figure 1.8 Metallapentalene and 2-aza-metallapentalene.

Hapticity and Geometry of Pentalene

The pentalenyl dianion is isoelectronic and isostructural with a dual, fused $[Cp]^-$ ligand, and isoelectronic with naphthalene[10] in the same way that the cyclopentadienyl monoanion is electronically analogous with benzene.

Computational studies on substituted pentalene species (such as 1,3,5-tri-*tert*-butylpentalene) have confirmed that the molecule is best considered an 8π *anti*-aromatic Huckel system.[30] Anti-aromatic systems follow a 4*n* electron count rule in opposition to aromatic systems, which generally obey Huckel's Rule and thus contain [4*n*+2] electrons. Aromaticity conveys stability upon a molecule due to the delocalisation of electrons around the structure providing a state of reduced energy. Anti-aromaticity produces the reverse effect, with delocalisation of 4*n* electrons producing a lower stability ground state comprised of valence bond orbitals in antiphase configuration.[31]

Dihydropentalene may be stabilised by the introduction of two additional electrons to create a 10π-aromatic system. This is the configuration associated with the pentalenyl dianion, which was first prepared by Katz and Rosenberg[32] *via* double deprotonation of dihydropentalene with *n*-BuLi, a procedure that has since become commonplace. Singular deprotonation of dihydropentalene is also possible, yielding a monoanionic dihydropentalenyl species possessing 6π electrons, partially aromatic with one delocalised ring system π bond.

It is notable that DFT studies have shown that the pentalenyl dianion does not necessarily donate all 10π electrons to a metal centre when a net loss of stability results. Counting the metal centre as fully oxidised (possessing zero electrons) and with the assumption that both pentalenyl ligands donate 10π electrons, $Ti(Pn)_2$ is a 20 electron system with two electrons occupying anti-bonding orbitals. Instead, partial donation of 9π electrons per ligand occurs with two π orbitals failing to overlap with the metal d-orbitals, resulting in a more stable 18 electron complex.[1] In theory, this also suggests that the dicationic species $[Ti(Pn)_2]^{2+}$ would be stable as an 18 electron complex with

full 10π donation from each ligand, though the oxidation state of the metal is ambiguous in such a complex, and no experimental evidence has been presented.[10]

Hapticity of the pentalene ligand is highly diverse.[10] Pentalene may contribute a maximum of 8 electrons to a metal complex through the adoption of six different binding conformations.[13] Electron donation in pentalene complexes is well described by the Covalent Bond Classification method (CBC), a neutral-metal counting scheme where ligands donating 2 electrons (*i.e.* π donation from a double bond) are described as "L" type. X type ligands describe one electron donation and Z type ligands donate zero electrons.

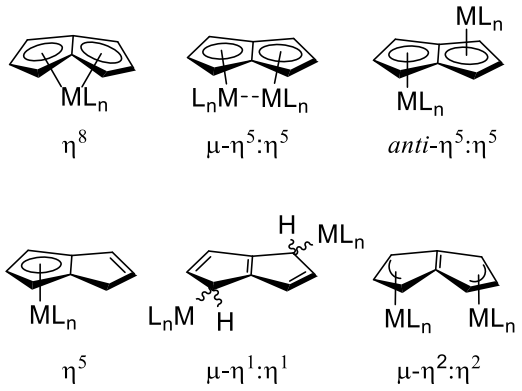

Figure 1.9 Pentalene binding modes.

Pentalene in η^8 complexes is an L_3X_2 type ligand, whereas pentalene displaying η^5 hapticity is defined as L_2X, mirroring the CBC classification of the cyclopentadienyl ligand.[33] Coordination mode is altered significantly by the electronics of a given metal centre: early transition metals require additional electron donation to remain stable, and thus η^8 pentalene complexes of the Group IV and Group V metals are particularly common. The η^5 binding mode most often results from the reaction of the hydropentalenyl monoanion with a metal halide; as only one ring system is aromatic, the η^8 binding mode is not possible. Pentalene also favours η^5 coordination when the metal centre is coordinatively saturated and electron rich, with late transition metals showing a greater affinity for this binding mode.[10]

The degree of "ring slip" is an important parameter in both multimetallic and monometallic μ:η^5-η^5 and η^8 complexes, and may be defined as the extent to which the metal centre(s) have moved away from the bridgehead carbons and towards the wing-tip carbons. This is denoted with the delta symbol (Δ).

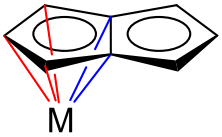

$$\Delta = \Sigma(M\text{-}C_{Bridge})/2 - \Sigma(M\text{-}C_{Wing})/3$$

Figure 1.10 Mathematical calculation of ring slippage.

In extreme cases, the drift caused by ring slippage can result in the conversion of an η^8 complex to η^5 ligation, though typically other ligands must be bound to the metal to stabilise the loss of electron donation caused by this transformation.
The geometry of pentalene is also versatile and the ligand may undergo distortion to further stabilise an "electron deficient" or kinetically unprotected metal centre. Molecules with $4n$ π electrons may deviate from planarity to avoid anti-aromaticity. This is observed in cyclooctatetraene, which is "tub" or "boat" shaped rather than a simple planar disc, existing as 4 separate π electron systems rather than one cohesive anti-aromatic group.

Pentalene does not distort to such a significant extent due to the transannular bond between the bridgehead carbons. However, the molecule still displays symmetry breaking as a result of the *pseudo*-Jahn-Teller effect.[10,31] To properly explain the role of this distortion in pentalene chemistry it is necessary to first explore the basic tenets of the Jahn-Teller effect. The conventional first-order Jahn-Teller effect describes geometrical alterations which occur in molecules with a degenerate electronic ground state. This degeneracy destabilises the molecule; in response, the geometry of the molecule is distorted to a similar symmetry group in which ground state is not degenerate (thus resulting in an increase in electronic stability). Prominent examples of this behaviour include the tetragonal compression or elongation of the axial bonds in octahedral complexes, converting from O_h to D_{4h} symmetry.

An example distortion is shown in **Figure 1.11**.

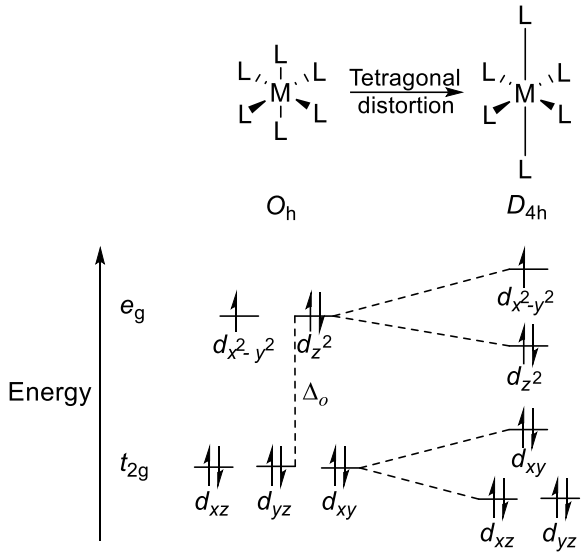

Figure 1.11 Jahn-Teller distortion of a d^9 octahedral compound with a doubly degenerate ground state, resulting in the lengthening of axial bonds.[34]

The key difference with the application of this same effect to pentalene is that the distortion of dihydropentalene is not due to a degenerate electronic ground state; DFT studies describe the ground state of pentalene as a filled, paired orbital of b_g symmetry, which is non-degenerate.[30] Instead, the geometrical distortion lessens the effective anti-aromaticity of the molecule by forcing the adoption of a less planar conformation; a deviation from planarity limits overlap of the π orbitals and thus limits conjugation. As a result, the transformation is more properly termed an example of a second order or *pseudo*-Jahn-Teller Effect. In practical terms, the aromatic dianion possesses D_{2h} symmetry and is consequently planar, while density functional theory has confirmed that this structural alteration causes dihydropentalene to possess C_{2h} geometry.[30]

In a sandwich complex, the pentalene ligands may twist out of perfect alignment along the vertical C_2 axis.[13] The hinge angle of a pentalene molecules provides a measure of the departure from planarity often exhibited by the ring system in η^5-η^5 complexes.[10] This is defined as the angle between bridgehead and non-wing-tip carbons and the wing-tip and non-wing-tip carbons.

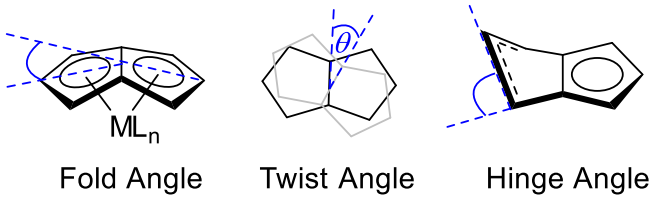

Figure 1.12 Pentalene fold, twist and hinge angles.

Pentalene may also fold across transannular bridgehead carbons when ligated to a metal centre.[10] Fold angle is influenced directly by the substituents bound to the metal; electron withdrawing ligands prompt greater folding at the bridgehead, bringing the rings closer to the metal centre and providing additional stabilisation. The degree of bending present is usually inversely proportional to the size of the metal.[13,35]

Bridgehead folding is particularly characteristic of η^8 early transition metal and f-block pentalene complexes, where the increase in stability afforded by stronger ligand-metal interaction and increased shielding of the coordination sphere offsets the lessening of ligand planar aromaticity.

Rotational orientation of the pentalene rings in a homoleptic sandwich complex can be described as “eclipsed” (when rings are overlapping when viewed top-down) or “staggered” (when one pentalene ligand is rotated 90° relative to the other). In actinide pentalene sandwich complexes, the additional steric bulk resulting from silylation of pentalene at the 1,4-positions results in limited rotation. This rigidity means that complexes of [Th(η^8-Pn†)$_2$] exist as separate *chiral* and *meso* diastereomers displaying D_2 and S_4 symmetry respectively,[13] while [U(η^8-Pn†]$_2$] has three diastereomers; an eclipsed conformation and two staggered arrangements differentiated by the torsion angles between the metal and wing-tip carbon atoms.

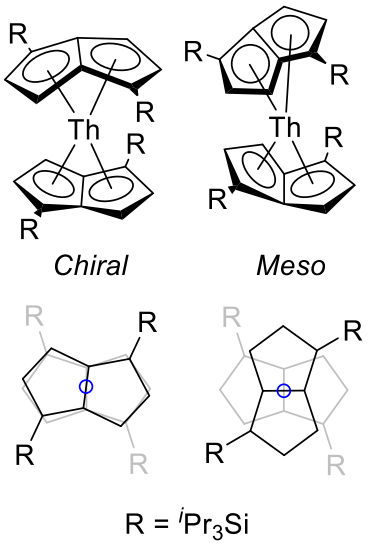

Figure 1.13 *Chiral* and *meso* diasteromers of [Th(η^8-Pn†)] demonstrating eclipsed and staggered conformations.[13]

DFT treatment of C_{2v} fragments of formula [M(η^8-Pn)] gives insight into the electronics behind the bonding of the pentalene ligand and provides a concise picture of the most common geometries adopted by ligated products. The π4 and π5 orbitals are the primary contributors to pentalene-metal bonding, while further ligation to the metal centre is determined by four metal-based frontier molecular orbitals.[13]

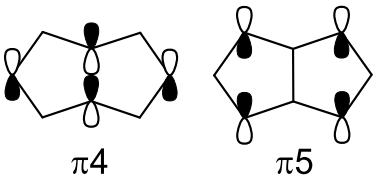

Figure 1.14 Dominant orbitals in M-Pn binding in monometallic pentalene complexes.

Facing outwards from the plane of the pentalene ligand and the metal centre itself, these molecular orbitals provide a strong affinity for trigonal geometry, while usage of all four MOs results in square pyramidal structures. The positions of the $6b_1$ and $7b_2$ metal-based MOs have particular impact on the geometry of Group IV [(η^8-Pn)MX_2] complexes. These orbitals lie perpendicular to the bridgehead carbons, and overlap with the positions of each X ligand, producing a characteristic pseudo-tetrahedral arrangement for η^8 pentalene non-sandwich compounds.

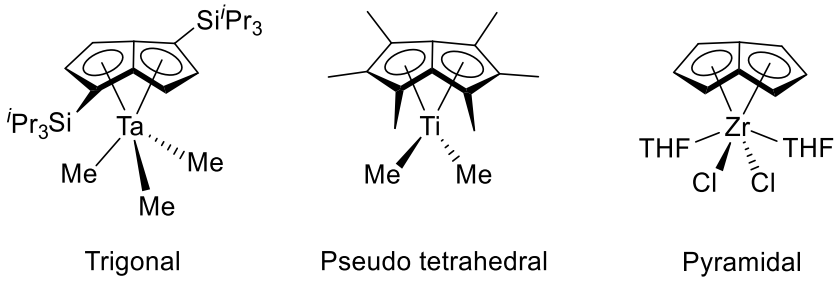

Figure 1.15 Literature examples[36,37,13] of monometallic η^8-Pn geometry.

The isoelectronic similarity between pentalene and two fused Cp rings allows for the symmetry groups of the $Ti_2(Pn)_2$ frontier orbitals to be described in likeness to a dual metallocene system.

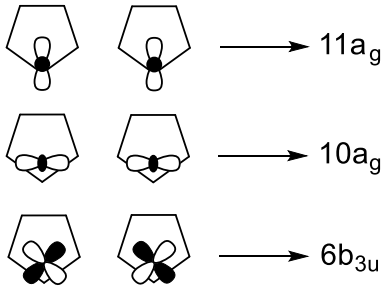

Figure 1.16 Symmetry group assignment of the frontier orbitals of $Ti_2(Pn)_2$ from isoelectronic analogy with two metallocene fragments.[38]

A fully detailed computational account of $Ti_2(Pn)_2$ is provided in a 2015 paper by Green *et al.*, including an in-depth explanation of the effects the frontier MOs have upon the binding of CO to [$Ti_2(\mu\text{-}\eta^5,\eta^5\text{-}Pn^\dagger)_2$)] (compound **1.1**).[38] The nature of the M=M double bond is further discussed; lowering of symmetry from D_{2h} to C_{2v} causes HOMO and HOMO-1 mixing responsible for the σ and π character of the Ti=Ti double bond.

Monometallic Pentalene Complexes

Synthetic Routes

The most common method for the synthesis of monometallic pentalene complexes is *via* salt metathesis of the pentalenyl salt species with a suitable metal halide. Heteroleptic cyclopentadienyl pentalene complexes may also be readily accessed by the reaction of a *bis*-cyclopentadienyl metal halide with a pentalene salt. The halide groups are substituted for the pentalene ligand by salt metathesis, while retaining the Cp ligand.

Jonas *et al.* reported one of the first documented examples of a folded η^8-ligated pentalene prepared by this method. Treatment of cyclopentadienyl vanadium halides with a lithium pentalene salt forms several mixed sandwich vanadium complexes featuring combinations of Cp and pentalene ligands.

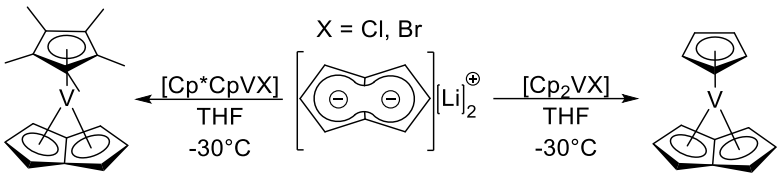

Scheme 1.12 Synthesis of the first η^8 pentalenes.[12]

Parallel to this development, Cloke *et al.* serendipitously synthesised an η^8 tantalum pentalene complex by a highly unconventional method. Taking $Ta(\eta^8\text{-}C_8H_4{}^{1,4\text{-TMS}})Cl_3$ and dehydrogenating with three equivalents of $[NH^iPr_2Et]Cl$ was found to result in transannular protonolysis of the COT ligand. This was followed by thermal rearrangement of the ligand to produce the 1,5-silylated pentalene ligand[39] *in situ*. The first Group IV η^8 pentalene complexes were soon after isolated by rational, planned synthetic methods (*vide infra*).

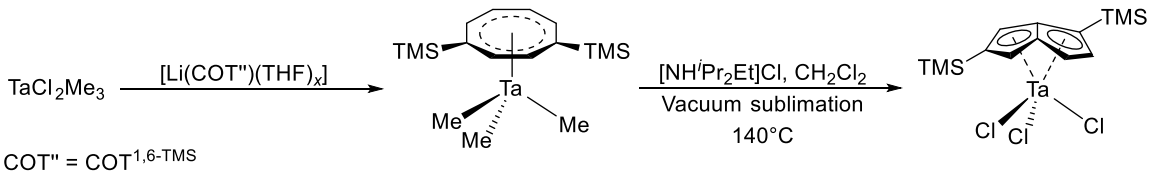

Scheme 1.13 Synthesis of an (η^8-Pn) tantalum complex.[39]

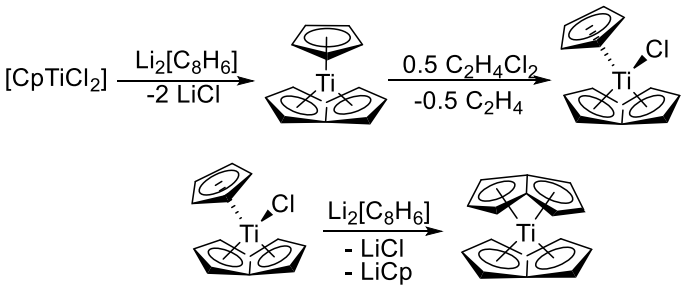

Scheme 1.14 Rational synthetic pathway to Group IV η^8 pentalene complexes.

The experimental procedure for the synthesis of η^5 monometallic hydropentalenyl complexes is simply a variation of the salt metathesis pathway used for the creation of

η^8 complexes. A reaction is typically performed between a halide salt of the desired metal and a monoanionic hydropentalenyl salt, though success of the reaction is metal dependent.[10] Only f-block and later transition metals possess enough electrons to be stable in such a configuration; early transition metals are typically electron deficient with only one η^5 site bound.[13] Such complexes may also be created serendipitously from reactions with pentalenyl dianionic salts; pentalene typically undergoes ring slipping to form η^5 complexes from an initial η^8 configuration when the electron count exceeds[40] 18, and thus heavier, more electron-rich metals show an affinity for this transformation.

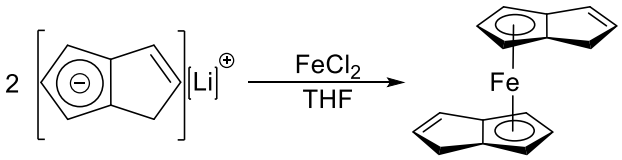

Scheme 1.15 Synthesis of an *anti* η^5, η^5 monometallic hydropentalenyl sandwich.[41]

Both heteroleptic and homoleptic monometallic f-block η^8 pentalene complexes have been reported. For some time, formation of f-block pentalene complexes was complicated by the poor suitability of lithium pentalene salts with f elements.

The high solubility of lithium halides creates practical issues with the separation of the desired product from halide waste; lithium salts also display a tendency to become incorporated into the final product (resulting in unwanted formation of "ate" compounds).[42] Potassium salts, by contrast, offer increased electron density at the alkali metal (and thus a stronger ability to displace the target halide group) and potassium halide waste is poorly soluble in hydrocarbon solvents, allowing for facile separation of contaminants from the reaction mixture. Reactions of f-block halides with potassium salts were more successful as a result, and a range of lanthanide and actinide $Pn^{\dagger}$ compounds have since been created.

Most f-block pentalene complexes exist in the +3 oxidation state; examples include [U(η^8-$Pn^{\dagger}$)Cp*], [Sm(η^8-$Pn^{\dagger}$)Cp*] and the mixed pentalene-hydropentalene sandwich complex [(η^8-$Pn^{\dagger}$)Sm[(η^5-$Pn^{\dagger}$H)]. The synthesis of these species is accomplished in identical fashion to transition metal pentalene complexes; *via* salt metathesis using appropriate metal halides. While d-block pentalene complexes can be synthesised from chloride or iodide salts, the electronegativity of the halide employed can be of greater consequence to the obtained result when synthesising f-block compounds. Use of a

ytterbium di-iodide as a starting material allowed for the synthesis of $[(\eta^8\text{-Pn}^\dagger)\text{Yb(THF)}_3]$, a rare example of an f-block pentalene complex in the +2 oxidation state.[42]

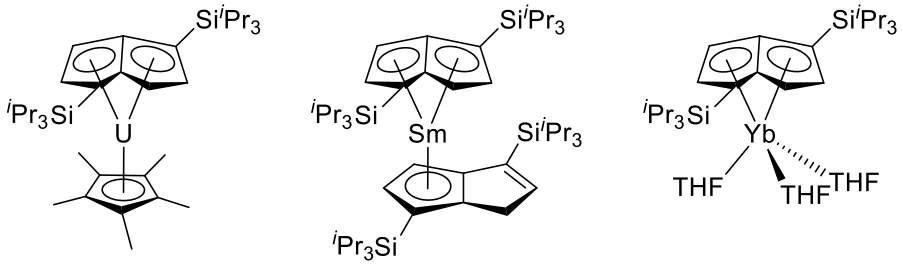

Figure 1.17 Examples of f-block pentalene compounds.

Properties and Applications

In 2002, the heteroleptic uranium (III) sandwich complex $[U(\eta^8\text{-Pn}^\dagger)_2\text{Cp*}]$ was successfully applied to reversible reductive activation of dinitrogen, producing an $[N_2]^{2-}$ group horizontally bridging two uranium centres.[43]

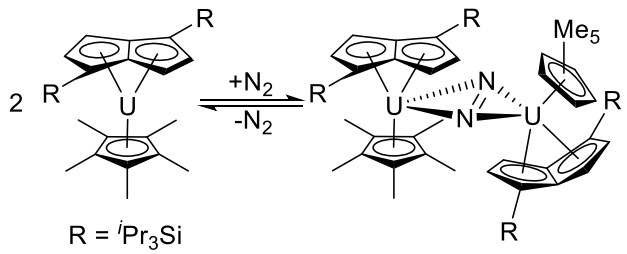

Scheme 1.16 Reduction of dinitrogen by a heteroleptic uranium pentalene complex.

The Cloke group later treated $[U(\eta^8\text{-Pn}^\dagger)_2\text{Cp*}]$ with one molar equivalent of the phosphaalkyne ^{t}BuCP. This produced a two electron reduction of the phosphaalkyne group, yielding a bimetallic uranium (IV) dimeric compound in which the uranium centres were bridged by the phosphaalkyne (**Scheme 1.17**).[44] Photoelectron spectroscopic studies have shown[45] that the C-P π system is 1.83 eV higher in energy than the phosphorus lone pair, making binding to a metal centre through side-on η^2 π bonding the dominant method of ligation of phosphaalkynes. The direct η^1 ligation mode of the phosphaalkyne in this bridged species through phosphorus provides an interesting contradiction likely due to the large amount of steric protection offered by the $\text{Pn}^\dagger$-Cp* sandwich.[44] This assertion is supported by the same mode of ligation

present in other compounds featuring spatially bulky ligands.[44]

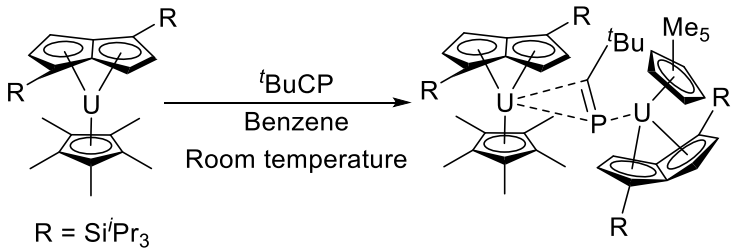

Scheme 1.17 Reduction of a phosphaalkyne.[44]

Pentalene complexes have also drawn attention as an alternative to the more familiar cyclopentadienyl Ziegler-Natta polymerisation catalysts. Several patents have been submitted featuring *ansa*-bridged Zr(IV) pentalene species that control polymer tacticity through the stereorigid nature of the catalytic site.

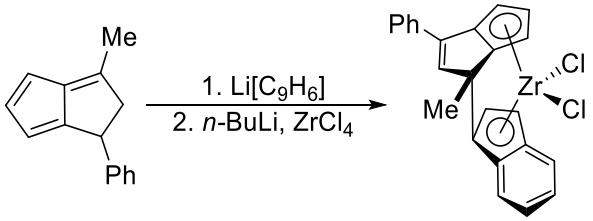

Scheme 1.18 An example of a patented Ziegler-Natta type *ansa*-sandwich catalyst utilising pentalene.[46]

Heteroleptic zirconium pentalene compounds have been shown to be efficacious catalysts for the formation of polyethylene.[47] The O'Hare group has made significant progress in using permethylpentalene mixed-sandwich Group IV complexes for the polymerisation of ethylene, with maximum efficiency obtained with [ZrCpCl(η^8-Pn*)] in the presence of MAO.[48]

Multinuclear Pentalene Complexes

Homonuclear Bimetallics and Multimetallics

As with monometallic hydropentalene sandwich complexes, multi-metallic pentalene complexes exist in *syn* and *anti* conformations. In a sandwich configuration, *anti* complexes display a staggered pentalene geometry rather than vertically eclipsing one another as in *syn* bimetallics. This can be exploited to create "chain sandwich" metallopolymeric structures by ligating the vacant coordination site to another η^5 pentalene species. A number of η^5:η^5 *anti*-complexes exist for both bimetallic and trimetallic pentalene species.

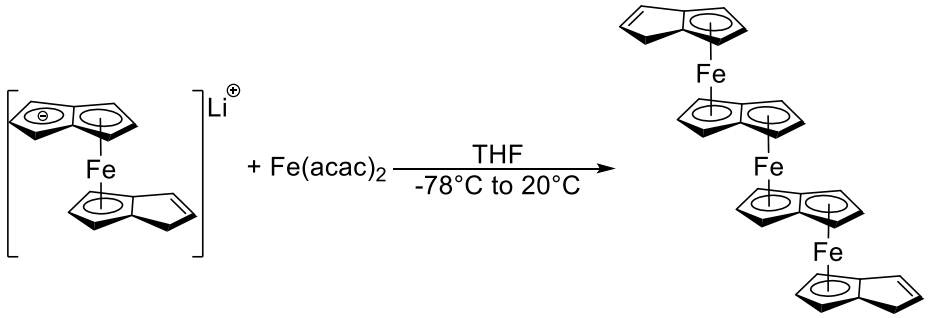

Scheme 1.19 Synthesis of an η^5 *anti*-trimetallic iron pentalene complex.[49]

Non-sandwich pentalene complexes of the later d-block elements with μ:η^5:η^5 bonding may also possess *syn* or *anti* arrangement and can be bound to Cp ligands to produce mixed sandwich compounds. L type ligands such as CO provide another alternative to the cyclopentadienyl group.

The first bimetallic pentalene complexes were synthesised prior to monometallic species and almost exclusively encompassed mid-to-late transition metals due to the high affinity of these elements for η^5 ligation. Extensive work was performed by Katz *et al.* on the creation of bimetallic nickel, iron and cobalt-centred pentalene compounds in 1972 *via* the reaction of dilithium pentalenyl dianion salts and an appropriate transition metal halide.[50] For these *syn*-bimetallics the μ:η^5-η^5 binding mode is common, with metals frequently forming metal-metal bonding interactions granting additional stability to the complex. Calculated bond order between metals is highest for early transition metals and decreases across the period with increasing atomic number. This correlates with increasing electron density in antibonding molecular orbitals, thus weakening metal-metal interactions. In these systems, the 18 electron rule may be used to give a

simplified prediction of metal-metal bond order. When each pentalene ring is treated as an L_2X donor to a single metal centre; the number of metal-metal bonds is then usually equal to the number of electrons necessary to bring the total electron count to 18. However, this generalisation is not valid for early transition metals. In the case of titanium, satisfaction of the 18-electron rule would result in formation of a quadruple metal-metal bond; instead DFT experiments describe the Ti-Ti interaction in $[Ti(Pn)_2]$ as a M=M double bond with both π and σ character.[38,51] This produces an electron count for each centre of 16. Each titanium atom is coordinatively saturated and possesses insufficient electrons to contribute to any higher metal-metal bonding order.

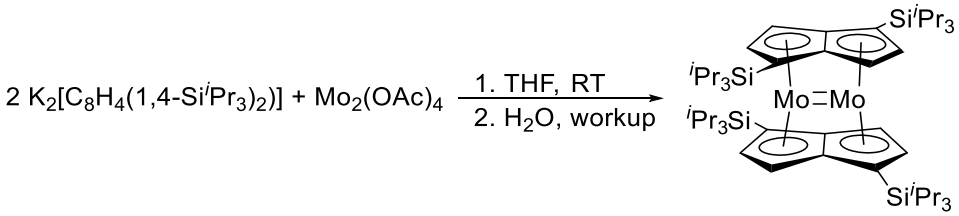

Scheme 1.20 A bimetallic *syn*-Pn† molybdenum compound exhibiting the metal-metal double bonding predicted by the CBC method.[52]

While proximity of metal centres to one another can prove a useful metric[51,53,54] for measuring the degree of metal-metal interactions present in a bimetallic complex, proximity itself does not guarantee the presence of these interactions.[55] *Syn*-permethylpentalene cobalt bimetallics reported by O'Hare *et al.* show no bonding interactions between the metal centres despite possessing shorter M-M distances than comparable COT complexes in which M-M single bonds exist.[55]

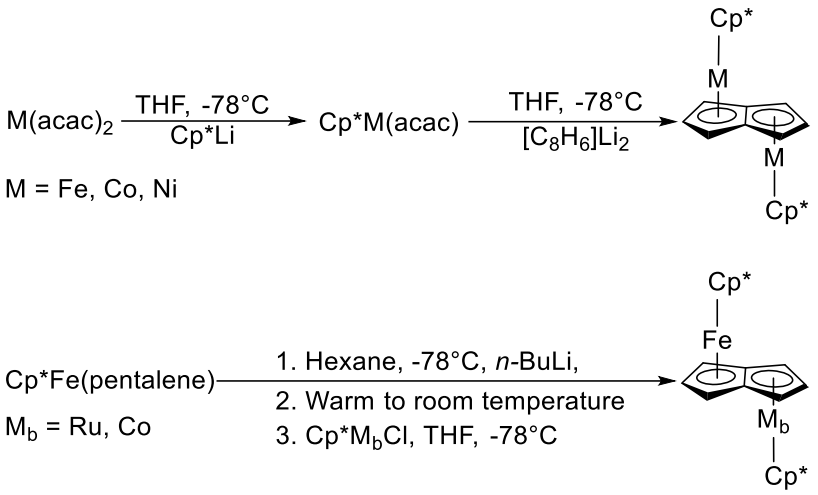

Scheme 1.21 Examples of synthetic pathways to d-block *anti*-bimetallic pentalene sandwiches.[42,49]

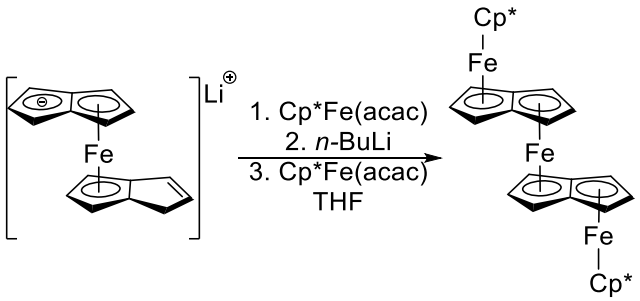

Scheme 1.22 Synthetic route to a trimetallic cyclopentadienyl-capped pentalene sandwich.[49]

The ability to connect multiple *anti*-bimetallic structures through pentalene ligands, cylopentadienyl groups and other similar π donating ligands such as indacenes[54] has potential applications for the synthesis of long chain metallopolymers.[56] The pentalene ligand allows for a large degree of electronic communication between metal centres through the π system, and having many metal centres allows for a variety of redox states throughout the polymer. Multimetallic systems with M-M bonds or connective π donor ligands may thus possess a range of conductive properties making them suitable for use as molecular wires or electronically "communitive" macrostructures.[35,54,57,58] The ability to derivatise pentalene is also attractive when designing these materials, as alkyl groups connected to the pentalene ring help to mitigate the solubility issues inherent when working with long chain polymeric systems.

Heteroleptic bimetallic systems with *syn* binding and multiple metal-metal interactions also exist, as in the case of $[V(\eta^5\text{-}C_5H_5)]_2(\mu{:}\eta^5,\eta^5\text{-}C_8H_6)$, isolated by O'Hare and Jones in 2003.[59]

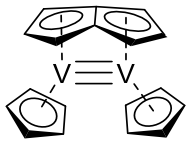

Figure 1.18 A mixed ligand bimetallic pentalene system featuring metal-metal bonding.[59]

As a Group V metal with an $[Ar]3d^34s^2$ configuration, an electron count of the complex (*vide supra*) should produce a value of 18 e^- per vanadium centre, rising to 36 electrons for the entire compound, making $[V(\eta^5\text{-}C_5H_5)]_2(\mu{:}\eta^5,\eta^5\text{-}C_8H_6)$ diamagnetic. However, in practice the ^1H solution state NMR behaviour is indicative of a paramagnetic system and the compound is not stable in solution.[59] Despite the M-M triple bond present, magnetic measurements have shown that V-V bonding is stronger in the more stable isoelectronic COT complex $[V(\eta^5\text{-}C_5H_5)]_2(COT)$.[10] This is possibly due to the 13° folding of the pentalene ligand, which keeps the centres in *syn* conformation but at the cost of stability due to the decreased orbital overlap.

Heteronuclear Bimetallics

Bimetallic pentalene complexes featuring two different metal centres are among the rarest synthesised examples of pentalene compounds. This is because the adaptable nature of pentalene coordination geometry may prove to be a hindrance rather than a benefit when attempting to sequentially bind different metals to the ligand.

If a η^5, η^5 *anti*-bimetallic pentalene complex featuring metals X and Y is desired, for example, metal X may instead preferentially form an η^8 monometallic compound or sandwich complex which precludes the subsequent addition of metal Y. Alternatively, metal X may simply form a homonuclear bimetallic through η^5, η^5 binding, with the stability granted by multiple M-M interactions providing a significant incentive for this to occur.

For this reason, many of the most effective precursors for synthesising heterometallic pentalene compounds feature pentalene coordinated η^5 to a metal centre while the other vacant ring site is coordinated to a substitutable stabilising cation, such as lithium. This allows the anionic ring system to be used directly upon a desired metal transfer agent, preserving the current ligated metal centre while allowing for the reliable addition of the second. In some cases, synthesis of these precursor complexes may occur serendipitously *via* unexpected coordination of a cationic species to the ring system (two novel complexes discovered by this route are discussed in Chapter 4). They may also be targeted rationally by performing a mono-deprotonation of a suitable derivative of dihydropentalene, reacting this hydropentalenyl anion with a metal transfer agent and then performing a second deprotonation and lithiation to yield the stabilised anion. Manriquez *et al*. were pioneers of this technique, using it to synthesise *anti*-pentalene compounds containing iron, cobalt, rhodium and ruthenium.[60,61]

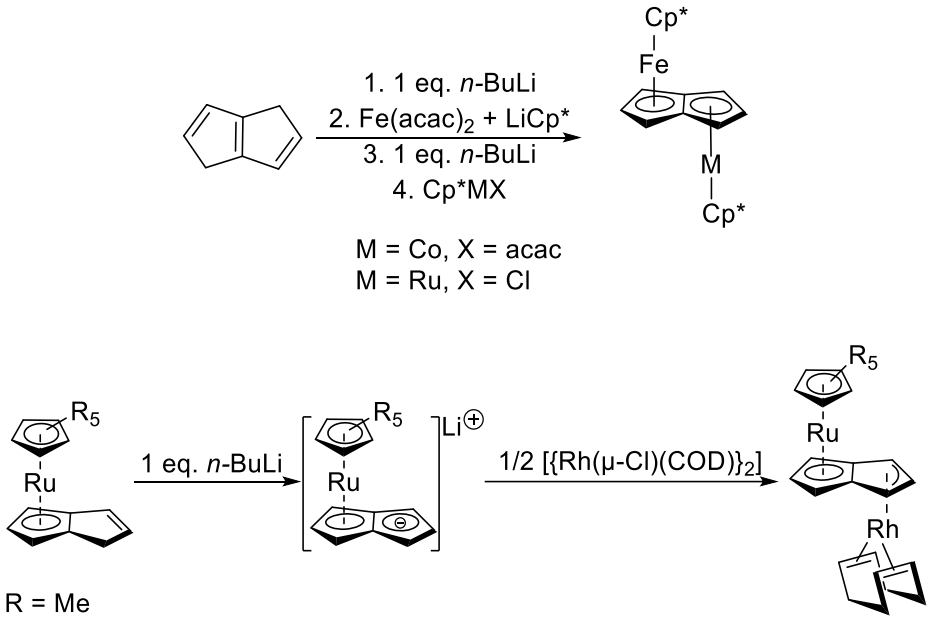

Scheme 1.23 Sequential lithiation to produce *anti*-heterobimetallic pentalene compounds.[60,62]

Creating mixed metal complexes has the obvious advantage of offering two separate sites of differing reactivity on one molecule. However, as with homobimetallic species, electronic communication through both direct M-M bonds and shared π donating ligands is also possible. In the case of a mixed metal system, electron density is no longer shared equally between two identical centres, instead the electronic influence of

the metal upon the system varies due to differences in electronegativity and redox potentials.[60,63] The Robin-Day classification system was developed in order to provide a formalism for the amount of influence each metal centre has upon a mixed valence system in which an unpaired electron is "shared" between the two centres. A Class III system shows a high degree of M-M electronic interaction and it is difficult to definitively pinpoint the exact oxidation state of either metal. Such a system may be a good candidate for inclusion in a metallopolymer with conductive properties due to a high degree of electronic communication. By contrast a Class I system describes two centres that have differing oxidation states that are clearly unique and confined to each centre (for example, one centre in the +2 oxidation state while the other is definitively +3). Such a molecule would have negligible electronic interactions between each centre. Effects on electronic properties across the molecule are not simply limited to the differing properties of each metal, but the symmetry of the ligands that make up the complex. Asymmetric ligands result in uneven electron distribution and this may also have significant effects on reactivity and electronic properties of the molecule or polymer.[60]

Heteronuclear metal-metal interactions can also be created by using a precursor material which already possesses a desirable M-M bond and labile ligands which may be displaced by a pentalene salt to furnish the complex. An interesting example of a *syn*-heterobimetallic Pn† sandwich was synthesised by a Cloke group student[64] *via* this method, using a carboxylate with a molybdenum-tungsten triple bond.

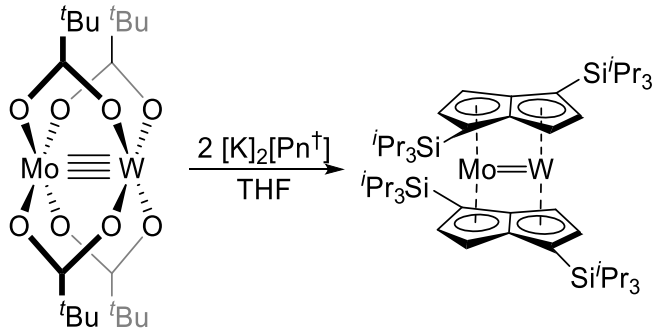

Scheme 1.24 A *syn* example of a mixed metal pentalene sandwich.[64]

[Ti(μ:η^5,η^5-Pn†)]$_2$

In 2013 the Cloke group reacted [K]$_2$[Pn†] with TiCl$_3$(THF)$_3$ to produce a mixture of two halogen-bridged titanium complexes in 4:1 ratio.[51] The most abundant of these complexes is mixed valency with a Ti(III) and Ti(IV) centre and three bridging chlorides. The other complex is homovalent, with two Ti(III) centres bridged by two chlorides. A subsequent reduction of these products with four equivalents (a slight excess) of potassium amalgam was found to yield the *syn*-homobimetallic sandwich complex [Ti (μ:η^5,η^5-Pn†)]$_2$, **1.1**.[51] The work described in this thesis primarily concerns the reactivity of compound **1.1** and subsequent experiments to functionalise the complex in order to produce novel, highly reactive titanium pentalene species. It is thus pertinent to discuss the reactivity profile previously established for **1.1** and its most salient chemical properties.

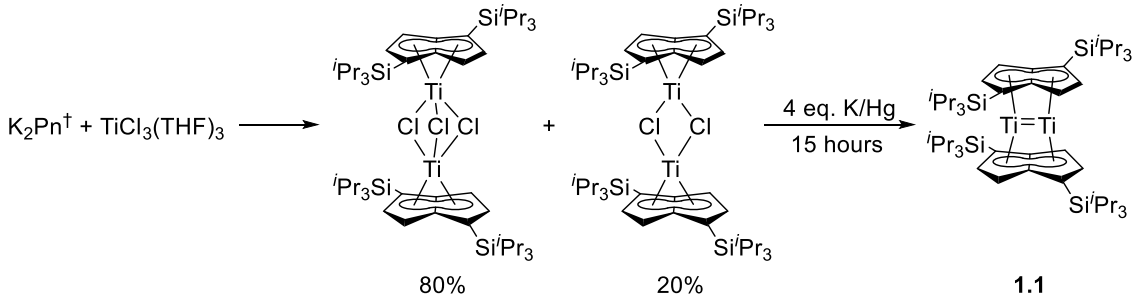

Scheme 1.25 Synthesis of **1.1**.

Parameter	Bond Length (Å)	Angle	(°)
Ti 1-Ti 2	2.399(2)	Hinge	3.80(8)
Ti-C$_a$	2.036(4)	Fold	20.12(8)
Bridgehead C-C	1.499(10)	Twist	8.72(4)
		C$_a$-Ti-C$_b$	155.2(2)

Table 1.1 Selected crystallographic metrics of **1.1**.

Possessing D_{2h} symmetry in the solid state with a significant bridgehead bend angle of 8.7 degrees, each Ti(II) centre in **1.1** has a total electron count of 16, with an L$_4$X$_4$ coordination classification. This compound is of substantial interest not only as the first synthesised bimetallic titanium pentalene sandwich complex, but also because the unusually short Ti-Ti distance of 2.399(2) Å provides experimental evidence of a rare

Ti-Ti double bond.[51] DFT calculations based on [$Ti_2(\mu:\eta^5,\eta^5\text{-}Pn)_2$] further describe the bond length for a double metal-metal bond with no symmetry constraints applied to the complex as 2.37 Å, in good agreement with the measured value for **1.1**.[38] Removal of symmetry constraints causes the C_{2v} configuration to correspond to a local energy minimum, with total energy of this configuration equal to the D_{2h} symmetry species within computational error. Four of the frontier orbitals of **1.1** are metal based, with three a_1 orbitals contributing to M-M bonding and one higher energy b orbital producing a M-M antibonding effect. The bent geometry of **1.1** maximises the overlap of the $5b_{1g}$ molecular orbital non-wing-tip carbon π system ($5b_{1g}$) with the metal centre due to the isolobality of dual Cp ring systems.[13,38]

DFT elucidates that the reduction of symmetry from D_{2h} to C_{2v} results in the mixing of the HOMO and HOMO-1 molecular orbitals, creating a bent hybrid orbital with both π and σ character. With the very low energy difference between the two symmetries, it is highly likely that the complex interconverts between D_{2h} and C_{2v} in solution. By extrapolation this also implies that the metal-metal double bond in the solution state thus possesses both σ and π character.[38]

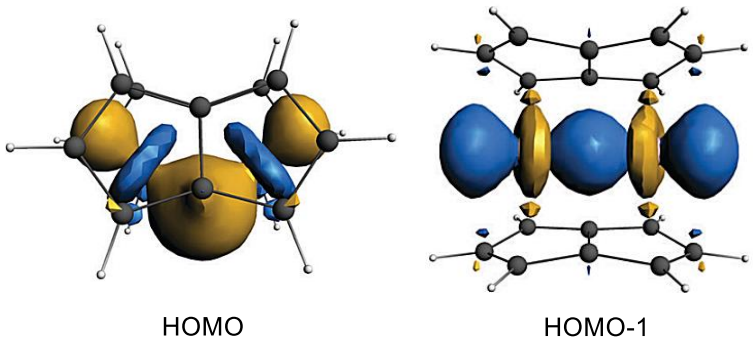

Figure 1.19 HOMO and HOMO-1 of Ti_2Pn_2 modelled as a C_{2v} structure.[51]

The presence of a titanium-titanium double bond presents opportunities for unique reactivity. Previous work with **1.1** has shown that it has the capability to reductively activate and interact with a variety of otherwise chemically inert small molecules such as CO and CO_2 in addition to the heteroallenes CS_2 and COS. Titanium is in the +3 oxidation state in these complexes, with cleavage of the metal-metal bond playing a key role in complex formation, resulting in reduction of Ti-Ti bond order to one or zero.

When **1.1** is reacted with one or two equivalents of CO, the M-M bond order decreases to one and formation of either *mono*- or *bis*-carbonyl adducts are observed, dependent of the stoichiometry of gas used. With an excess of gas, the structure alternates between

bis CO ligation with free CO present and a transient state in which a CO molecule is bound as an L-type ligand to each titanium atom and both centres are also bridged by a third CO molecule. Exclusive formation of the *bis*-carbonyl adduct is observed when **1.1** is exposed to two or more equivalents of CO_2 at room temperature. Reductive deoxygenation occurs, producing a mixture of the *bis*-carbonyl adduct observed in reactions with carbon monoxide and a bridging *bis*-oxo dimeric complex in which the M-M bonds are broken completely.[65] $[Ti(\eta^8\text{-}Pn^{\dagger})(\mu\text{-}O)]_2$ is also the exclusive product of reaction of **1.1** with oxygen; this is unsurprising given the highly oxophilic nature of titanium.

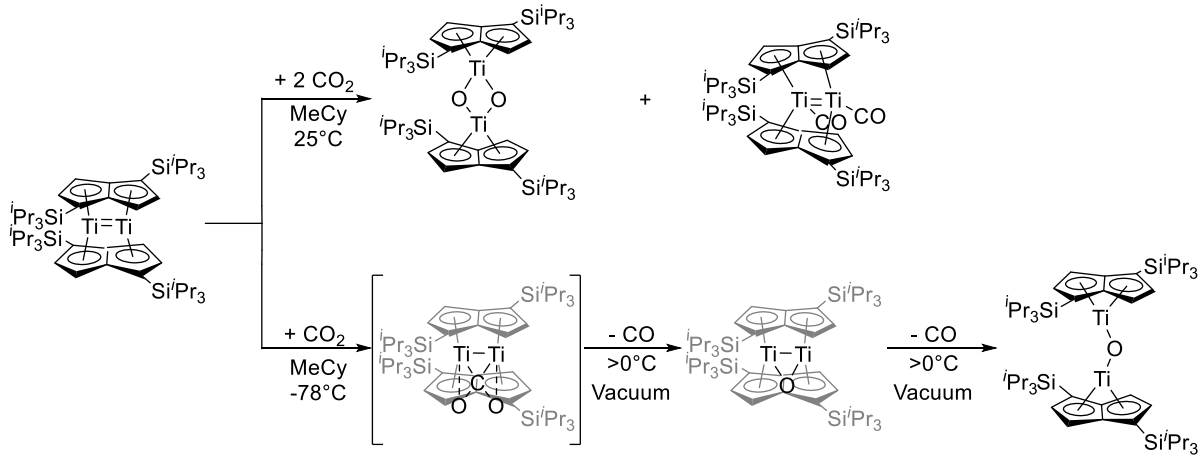

Scheme 1.26 Reductive deoxygenation of CO_2 .

At lower temperatures formation of a single carbon-bridged transition state is observed by *in situ* IR techniques, followed by loss of carbon monoxide to form a bridging *mono*-oxo complex with a Ti-Ti bond order of one.[65] This decays further at temperatures greater than 0°C, with loss of the metal-metal bond to give an oxo-bridged sandwich complex.

Compound **1.1** shows a strong predilection towards the formation of these dual heteroatom bridged bimetallic sandwiches. Reactivity of the Ti-Ti double bond is further exemplified when **1.1** is reacted with azobenzene or phenyl azide. Oxidative cleavage of the metal-metal bond results in a four e^- reduction[66] of azobenzene, producing an η^8-$Pn^{\dagger}$ pentalene sandwich bridged by two phenylimido ligands showing structural similarities to $[Ti(\eta^8\text{-}Pn^{\dagger})(\mu\text{-}O)]_2$.

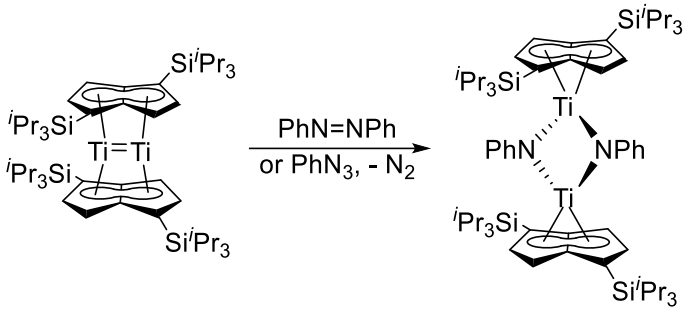

Scheme 1.27 Formation of phenylimido bridging ligands *via* reaction of **1.1** with phenyl azide and azobenzene.[66]

Methyl isocyanide was also reacted with **1.1**, due to its status as an isolobal analogue of CO. A colour change to purple[66] resulted, in addition to a ^{1}H NMR spectrum displaying eight separate aromatic pentalene environments; similar to the spectrum witnessed for the *bis*-CO adduct [Ti(η^8-Pn†)(CO)$_2$]. X-Ray diffraction analysis of the crystalline product confirmed formation of an adduct of **1.1** with the isocyanide moiety.

As would be expected from the previous results, **1.1** has also displayed reactivity towards heteroallenes including COS, CS_2 and 1,3-N,N′-di-p-tolylcarbodiimide (*p*-TCD). CS_2 and *p*-TCD form C_2 symmetric[66] adducts in which the entire molecule bridges the titanium metal centres while retaining the [μ:η^5,η^5-Pn†]$_2$ sandwich structure and a Ti-Ti single bond remains present. An extremely similar structural conformation was observed in a titanium pentalene borane adduct isolated from a catalytic reaction mixture further elaborated upon in Chapter 2.

COS also forms this bridged sandwich conformation,[67] though the complex swiftly decomposes upon warming above -40°C to yield a species in which CO separates from the bridging sulphide, giving a terminal CO adduct. This further progresses with the loss of CO to a dimeric *bis* bridged homovalent Ti(III) sulphide complex [Ti(η^8-Pn†)(μ-S)]$_2$, a sulphide variant of the familiar *bis*-oxo dimer.

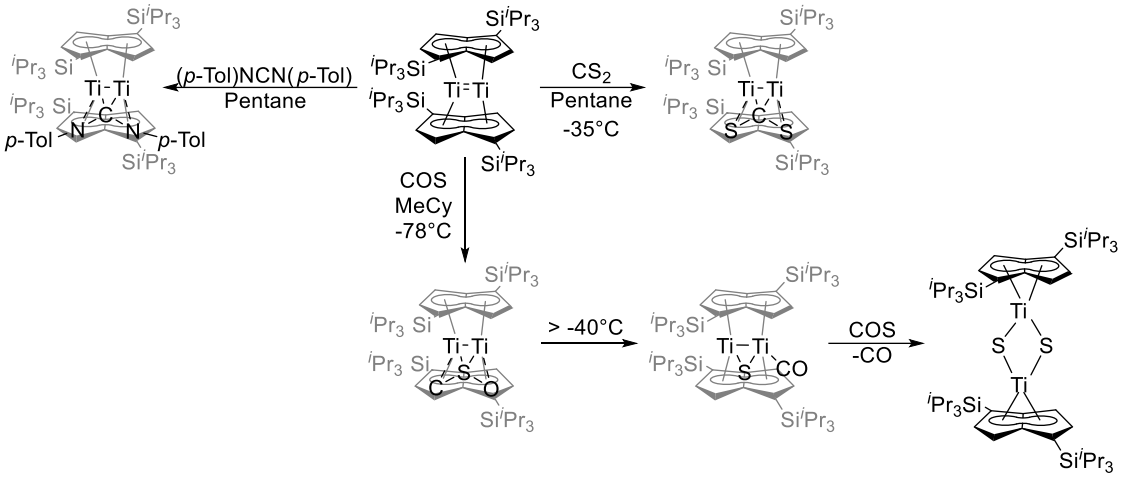

Scheme 1.28 Examples of heteroallene reactions with **1.1**.[66,67]

The first isolable monomeric titanium hydride, [(η^5-$C_5Me_4Ph)_2TiH$], was synthesised by hydrogenolysis of [(η^5-$C_5Me_4Ph)_2TiR$] by Teuben *et al.* in 1995.[68] Contemporary examples of titanocene hydrides and hydride cluster compounds have shown an affinity for C-H and N_2 activation,[69,70] making group IV pentalene hydrides a synthetic target of major interest.

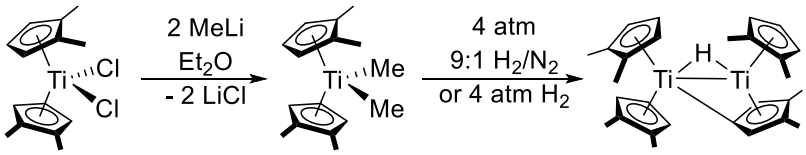

Scheme 1.29 Synthesis of a dimethyl titanocene compound followed by activation of a Cp C-H bond.[70]

As part of recent efforts to investigate the reactivity of **1.1** with strong σ-donating ligands, the Cloke lab reacted **1.1** with PMe_3 and the N-heterocyclic carbene 1,3,4,5-tetramethylimidazol-2-ylidene. While the former experiment produced no result, reaction with the NHC at 0°C in toluene resulted in the isolation of a titanium bridging hydride species, synthesised without the use of a reductant.[71]

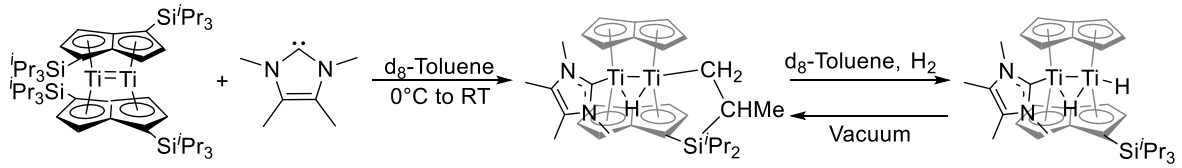

Scheme 1.30 Synthesis of bridging and terminal hydride derivatives of **1.1**. Non-interactive pentalene ring TIPS groups omitted after NHC binding for image clarity.[71]

NMR spectroscopic and X-Ray diffraction analysis of this compound confirmed that the bimetallic (μ:η^5,η^5) pentalene structure of **1.1** is unchanged, with coordination of the NHC to one metal centre and a resulting reduction of Ti-Ti bond order to one. The bridging hydride (which is placed equidistantly between the metal atoms) is generated *via* the abstraction of a hydrogen from one of the pentalene ring TIPS groups by the second titanium atom, in an example of C-H activation leading to "tuck-in" binding. Addition of hydrogen results in regeneration of the TIPS group through σ-bond methathesis, causing loss of the tuck-in interaction and simultaneous binding of a second hydride group in its place. To date, this is the only titanium pentalene hydride species reported.

Following the discovery of **1.1**, the O'Hare group has synthesised η^8-Pn* chloride compounds,[72] which served as the basis for the permethylpentalene alkyl complexes [Ti(Bn)$_2$(η^8-Pn*)] and [Ti(Me)$_2$(η^8-Pn*)].[73] Both of these species have recently been shown to conduct alkyl insertion chemistry with CO and CO_2 , the latter resulting in decarboxylation[27] to produce a titanium pentalene dicarboxylate compound.
This reactivity will be discussed in more significant depth in Chapter 4, which pertains to similar Pn† titanium alkyl species synthesised over the course of this project.

Chapter 2 – Catalytic Dehydrogenation of Amine-boranes with $[Ti(\mu:\eta^5,\eta^5\text{-}Pn^\dagger)]_2$

Introduction

With global concern mounting in recent years over reliance on finite energy sources and greenhouse gas pollution, development of environmentally friendly alternatives has become a prominent research focus. Hydrogen is readily combustible and produces only water as a waste product; for this reason it has long been regarded as a one of the most promising sources of abundant clean energy.[74] Flammable gases inherently pose safety risks and gas cylinders are heavy, difficult to refill without specialised facilities and pose further dangers when stored in bulk volume.

The two most prominent methods proposed for overcoming these problems involve the use of fuel cells or molecular hydrogen storage media. Fuel cells are similar in function (though not entirely analogous) to modern batteries and provide a physical construct inside which hydrogen and oxygen are electrolytically converted into H_2O. By avoiding the need to combust the gas, fuel cells remove mitigate safety concerns. Fuel cells still have significant drawbacks; unlike batteries or capacitors, fuel cells cannot "store" power, but only release it from the fuel on demand. The cells are therefore also dependent on having a continuous source of hydrogen fuel, usually stored in a canister as raw gas.

Chemical hydrogen storage media address this fuel sourcing problem directly. Inert or non-flammable substances containing large amounts of bound hydrogen act as the transport medium for the gas, which may be liberated *in situ* when needed *via* catalytic dehydrogenation.

Amine-boranes are a prime example of the latter group of hydrogen storage materials. The simplest amine-borane, ammonia borane (NH_3BH_3), is relatively inert, non-toxic and stable at ambient temperatures. Amine-boranes are also simple to synthesise *via* reaction of ammonia and a borane-dimethylsulphide adduct and contain a high volumetric and gravimetric percentage of hydrogen (19.6% by weight).[74] The strength of the B-N bond in NH_3BH_3 also favours loss of H_2 over dissociation into ammonia and borane, making the molecule stable even once dehydrogenation has occurred.[74]

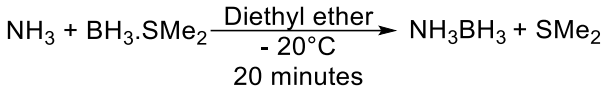

Scheme 2.1 Synthesis of ammonia borane.

Despite these useful properties, a catalyst able to efficiently liberate H_2 from the amine-borane under ambient conditions is still required if this class of compounds is to become viable as a hydrogen storage medium.[75] Transition metal complexes have been investigated thoroughly as candidates for this reaction in recent years, with iridium pincer complexes[75] and cyclopentadienyl sandwiches becoming particularly prominent in field literature as dehydrogenative catalysts.[76]

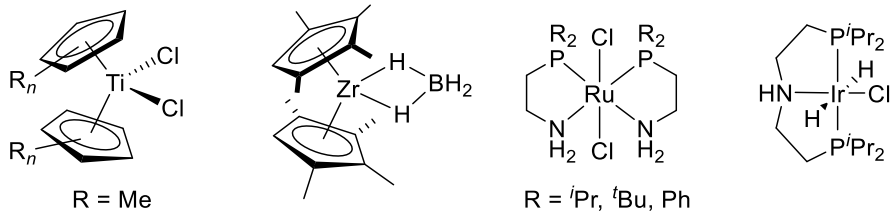

Scheme 2.2 Examples of d-block metal compounds implicated in amine-borane dehydrogenation reactions.[76–80]

To date, iron cyclopentadienyl sandwich compounds have produced the highest turnover frequencies at ambient temperature[79] and titanocene complexes featuring the Ti(II) oxidation state have also shown high activity.[81]

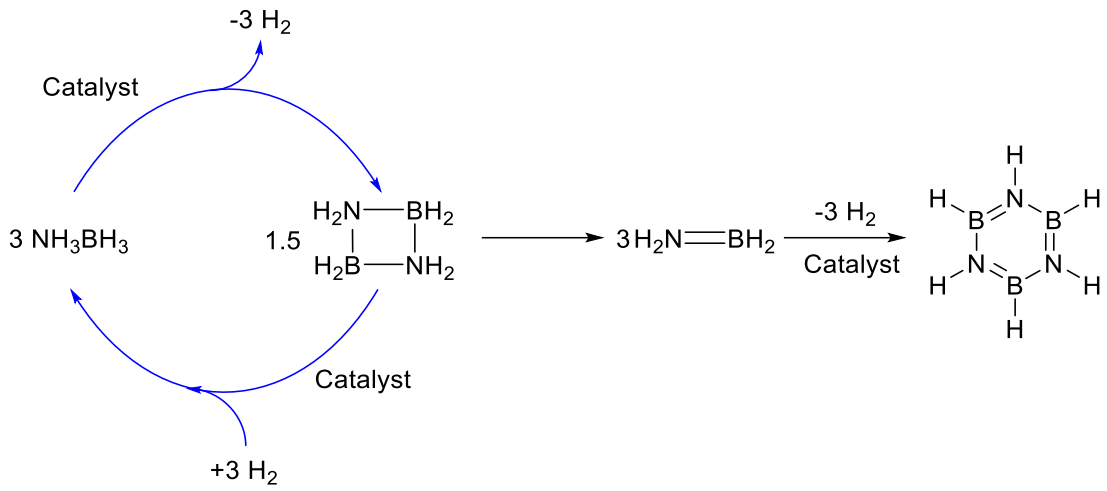

Scheme 2.3 Catalytic dehydrogenation of ammonia borane.

A simplified scheme (*vide supra*) displays the ideal behaviour of a dual-function ammonia borane dehydrogenation/hydrogenation catalyst. During the main cycle, highlighted blue, two equivalents of dihydrogen are lost from NH_3BH_3 to produce a cyclic four membered borane. The cycle can then be closed by catalytic hydrogenation, in theory allowing for the facile addition and removal of hydrogen on demand. In practice, reactivity of catalysts proves more complex; additional steps which break the reversibility of the dehydrogenation are shown with black arrows. The most active dehydrogenation catalysts often remove two equivalents of dihydrogen to form the four-membered dimer before further removal of hydrogen results in the formation of a nitrogen analogue of a C=B "borene" species. This double-bonded molecule is usually the final product of this reaction pathway when the feedstock consists of substituted amine-boranes such as dimethyl amine-borane, but in the case of ammonia borane a further combined dehydrogenation and cyclisation step may form borazine (the inorganic analogue of benzene) alongside polyborazylene and other cycloborane intermediates. Borazine possesses high thermodynamic stability and has been attributed to poisoning further catalysis within fuel cell systems.[82]

Most catalysts are mono-functional in practice. In cases where dehydrogenation halts at the dimeric borane stage rather than proceeding to subsequent irreversible loss of hydrogen, a second catalyst is still required to effect hydrogenation. Examples of dual-function catalysts capable of performing the entire cycle exist,[74] but these compounds often requiring more forcing conditions and give lower turnover frequencies.[79]

The Manners group has experimented with many d-block transition metal phophinoborane and amine borane dehydrogenation catalysts, including rhodium COD complexes, ruthenium carbonyl compounds, iron PNP pincer compounds and titanocenes. Initial experiments with Cp_2TiMe_2 for phosphinoborane dehydrogenation confirmed that this Ti(IV) species offers minimal catalytic activity.[83] However, experiments were also performed with [Cp_2Ti] Ti(II) compounds generated *in situ* by reaction of *n*-BuLi with appropriate titanocene dichloride compounds. These efforts yielded a range of high-activity group IV pre-catalysts suitable for amine-borane dehydrogenation. Further development of these compounds has produced Ti(II) systems capable of reliably catalysing the formation of variable chain length polyaminoboranes from amine-borane starting materials.[84]

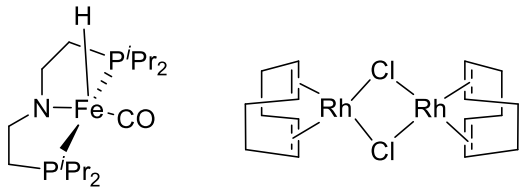

Figure 2.1 Examples of high activity iron and rhodium amine borane dehydrogenation catalysts.[79,83]

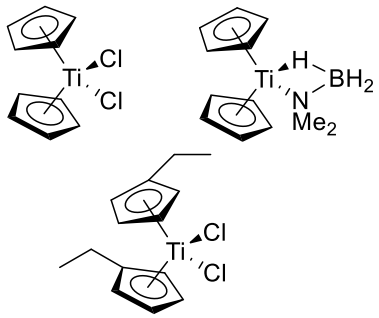

Figure 2.2 Titanocene precursors applied to the catalytic formation of polyaminoboranes.[81,84]

Despite progress in isolating d-block species responsible for the dehydrogenation of phosphinoboranes and amine-boranes, the mechanism of reaction remains poorly understood. A proposed mechanism for the formation of nitrogen-borene species from a titanocene catalyst was supplied by Chirik *et al.* in a 2007 paper, and relies on formation of a titanocene dihydride.[76] This catalytic cycle and its degree of relevance pertaining to pentalene bimetallic systems is discussed in depth in the results section.

The formation of a metal hydride species followed by reductive elimination appears near-universal as a mechanism amongst all d-block amine-borane dehydrogenation

catalysts.[76,77,81] While most of these hydrides are theoretical or transient species, some have proved isolable.[77]

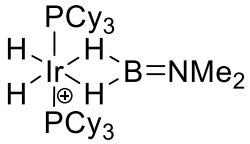

Figure 2.3 An isolated iridium dihydride species bound to dimethyl amine-borane.[77]

Given the literature precedent for the catalytic dehydrogenation of amine boranes with Ti(II) cyclopentadienyl complexes, amine-boranes were considered for reaction with **1.1**. Two amine-boranes were chosen for initial reactivity studies: NH_3BH_3 and $HNMe_2BH_3$. Additionally, test reactions were performed with NEt_3BH_3 to probe the necessity of α-hydrogen atoms in formation of catalytically active hydridic metal species.

Preliminary Reactions Between 1.1 and Ammonia Borane

Initial reactivity testing with NH_3BH_3 and **1.1** was conducted by 1:1 mixing of the solid amine-borane and crystals of the titanium complex. Upon addition of one mL of toluene at room temperature an immediate colour change from crimson to dark brown was observed; free hydrogen was absent from the ^{1}H NMR spectra recorded for multiple samples, though effervescence was clearly visible after addition of solvent. While the colour change provides a superficial indication of complex formation, proton NMR confirmed formation of a very complicated mixture at this stage of the reaction rather than a clear single product acting as a pre-catalyst or catalytic species. The 24 Pn-H signals observed in the ^{1}H NMR spectrum are consistent with a minimum of three asymmetric, diamagnetic pentalene complexes present in solution at this stage of the reaction. Unfortunately, none of these signals can be attributed to compounds that were later isolated, suggesting these unidentified species are likely intermediate borane adducts unique to this stage of reaction. The ^{11}B{^{1}H} NMR spectrum of the mixture shows only a broad borosilicate glass peak with no characteristic borane signals; this includes no signal attributable to NH_3BH_3. EI-MS analysis of aliquots of this reaction mixture also resulted in no rational fragments pertaining to these unknown compounds. The primary component of the EI-MS data was [Ti(Pn†)$_2$], which is commonly observed

upon fragmentation of **1.1** by electron ionisation techniques regardless of mixture composition.

Reaction of 1.1 with 3+ Equivalents of NH_3BH_3

Behaviour of the system changes drastically upon the addition of a minimum of three equivalents of NH_3BH_3 in toluene. Effervescence is observed immediately as before, with no apparent induction period, followed by a colour change to dark green.

Several simple control experiments were performed. To first guarantee the catalysis observed was homogeneous in nature, the reaction between **1.1** and NH_3BH_3 was intentionally spiked with mercury; heavy metals are known to poison heterogeneous catalysts by forming a surface-level amalgam with the reactive metal component.[85,86] Therefore if catalysis occurring is heterogeneous in nature, a complete loss of catalytic behaviour would be expected upon addition of mercury. However, no alteration in previously observed reaction behaviour was noted by ^{11}B and ^{1}H NMR. To ensure thermally induced coupling was not taking place at ambient temperature in absence of catalyst influence, NH_3BH_3 was heated to 40°C for two days and showed no evidence of dimerisation or hydrogen loss by ^{11}B and ^{1}H NMR.

Analysis of the reaction mixture composition to determine the products of the dehydrogenation was performed by ^{1}H, ^{11}B NMR spectroscopy and EI-MS. EI-MS proved the most useful characteristic technique, with the presence of the molecular ions of cyclotriborazane (CTB), B-(cyclotriborazanyl)-amine-borane (BCTB) and B-(cyclodiborazanyl)aminoborohydride (BCDB), all previously catalogued by R. T. Baker *et al*. in studies of amine-borane dehydrogenation with zirconium cyclopentadienyl catalysts.[87] Polyborazylene was identified as a number of fragmented integer value units of the polymer by EI-MS; dimers and trimers were the most common molecules observed. ^{11}B NMR spectroscopy is extremely useful for tracking the overall progress of the reaction; NH_3BH_3 is seen as a quartet at δ_B -12.33 ppm and the prominence of this peak decreases as a resonance attributable to polyborazylene rises at 28 ppm. Borazine was also observed at 31 ppm. ^{11}B NMR spectra generally varied in content with each sample analysed, likely due to the short lifespan of inorganic by-products formed over the course of the reaction prior to conversion to borazine or polyborazylene and the variable time scale of each reaction in toluene. A peak seen at

δ_B -5.50 ppm in one mixture is in perfect agreement with the reported literature value of BCTB.[87] A signal at -9.57 ppm was also present in another sample, indicative of CTB in solution.

It is therefore apparent that the mechanism for this reaction does not follow the repeatable cycle of dehydrogenation to form a cyclic four-membered dimer, instead progressing to trimerization of NH_3BH_3, producing the inorganic analogue of benzene. BCTB with borazine and polyborazylene as the final products of the reaction. BCDB and CTB are usually not seen in the spectra recorded since they are obscured by the probe borosilicate glass peak, which manifests as a broad resonance between δ_B -30 ppm to 40 ppm.

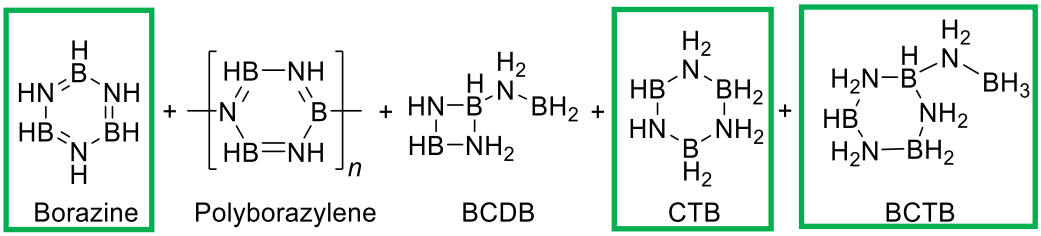

Figure 2.4 Inorganic products in solution identified by EI-MS. Outline boxes denote species also present by $^{11}B\{^1H\}$ NMR.

The ^1H NMR spectra obtained from the crude reaction mixture vary across repeat reactions; some spectra display no peaks representative of pentalene ring aromatic protons and broadened peaks are present δ_H ~ 7.87 ppm, 6.18 ppm, 5.91 ppm and 5.02 ppm. Other reactions showed 5-8 sharp pentalene protons at very weak integration values that did not correspond to any identified complex. However, one common component of the reaction was early formation of an asymmetric compound displaying 16 aromatic Pn-H environments. A single compound fitting this solution state NMR behaviour was isolated as green crystals from a filtered pentane solution of the reaction mixture stored at -35°C. Subsequent ^1H, $^{13}C\{^1H\}$ and $^{29}Si\{^1H\}$ NMR and X-Ray diffraction analysis identified this compounds as $[Ti(\mu{:}\eta^5,\eta^5\text{-}Pn^\dagger)]_2(\mu\text{-}BH_2NBH_3)$ **2.1**.

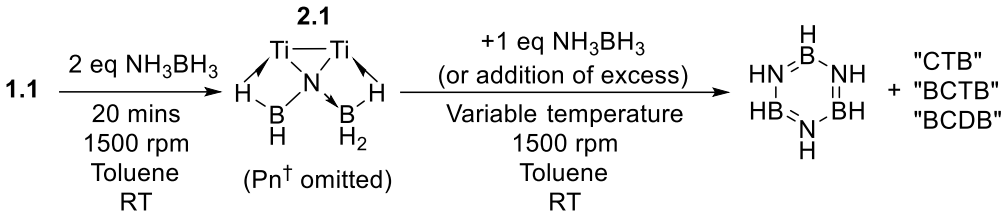

Scheme 2.4 Reaction of **1.1** with NH_3BH_3

Characterisation of [Ti(μ:η^5,η^5-Pn†)]$_2$(μ-BH$_2$NBH$_3$) (2.1)

The molecular structure of **2.1** obtained *via* X-Ray diffraction depicts a bimetallic titanium pentalene sandwich complex showing the same (μ:η^5,η^5) ligation mode as witnessed in **1.1**. However, the metal centres are now bridged by an amine-borane derivative fragment (BH_2NBH_3) comparable to a halved borazine ring.

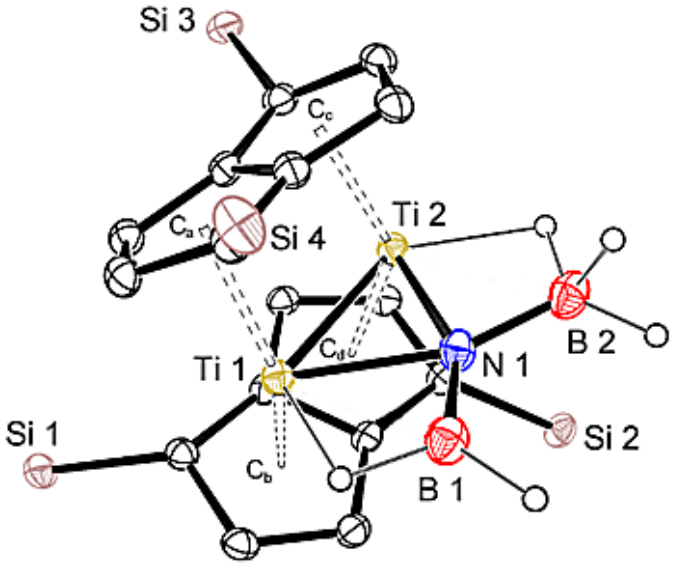

Figure 2.5 ORTEP diagram of **2.1**. Ellipsoids are shown at 50% probability. Ring hydrogen and ^{i}Pr groups omitted for clarity.

Parameter	Bond Length (Å)	Angle	(°)
Ti 1-Ti 2	2.450(2)	Hinge	4.29(4)
Ti 1-C_a	2.132(11)	Fold (ring possessing C_a)	2.79(3)
Ti 1-C_b	2.084(15)	Fold (ring possessing C_d)	2.73(3)
Ti 1-B 1	2.377(12)	Twist	6.46(3)
Ti 1-B 1 H	1.908(12)	C_a-Ti 1-C_b	145.97(4)
Ti 1-N 1	2.116(10)	C_c-Ti 2-C_d	135.06(3)
Ti 2-C_c	2.081(14)		
Ti 2-C_d	2.140(13)		
Ti 2-N 1	2.111(14)		
Ti 2-B 2	2.443(12)		
Ti 2-B 2 H	1.905(8)		
Bridgehead C-C	1.444(7)		
B 1-N 1	1.413(11)		
B 2-N 1	1.516(10)		

Table 2.1 Selected measurements for **2.1.**

The structure **2.1** bears a striking visual similarity to a bridged adduct compound formed when **1.1** is reacted with CS_2.[66]

When compared to **1.1**, the centroid-metal-centroid angle of **2.1** is reduced by 20 degrees; this is a rational alteration, given the addition of the amine-borane fragment between metal centres. The steric bulk adhered to one face of the structure causes the ring structure to hinge towards the unoccupied space. The centroid-metal-centroid angle of the metal centre labelled Ti 2 is also ten degrees more acute than the angle obtained for Ti 1. This is possibly due to the tetrahedral BH_3 group in close proximity to Ti 2, while Ti 1 is bound to BH_2 which is aligned flat to the Ti-Ti plane.

The Ti-Ti length of 2.451(2) Å differs by only 0.052 Å from the value of 2.399(2) Å measured for **1.1**. Ti-Ti single bonds in pentalene sandwich compounds have been reported in the region of 2.425(10) Å, though a mono-CO adduct of **1.1** which retains the double bond possesses a bond length of 2.405(5) Å.[88] Compounds in this work which display longer Ti-Ti interactions indicative of a single bond measure *ca.* ~2.6-2.7 Å.

The molecular structure of **2.1** suggests saturation of the coordination sphere of each metal centre due to the binding of the borane fragment, most likely resulting in loss of the double bond interaction. However, this cannot be confirmed through analysis of the bond metrics alone. DFT studies of the bond energetics may further elucidate the nature of the Ti-Ti interaction.

A minimum energy state theoretical structure for the formula [$Ti_2(Pn)_2B_2NH_5$] has been calculated by Professor Jennifer Green. The bond lengths measured for **2.1** are in very good agreement with this model.

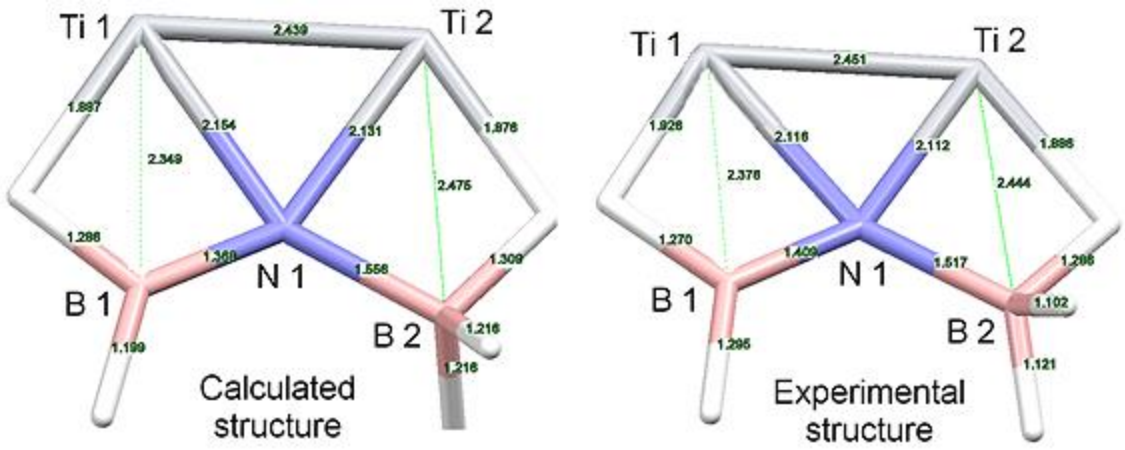

Figure 2.6 Comparison of bond lengths for calculated minimum energy structure of formula $Ti_2(Pn)_2(B_2NH_5)$ versus experimental structure of **2.1**.

Of particular note is the elongated length of the Ti-BH_3 bond at 2.443(12) Å; the existence of this bond is uncertain. The Ti-BH_3 distance of 2.443(12) Å is only marginally longer than the 2.377(12) Å bond of Ti-BH_2, however the BH_3 species is most likely coordinated to the central N atom *via* a dative bond from the nitrogen atom. This renders it a 4-coordinate species that interacts with the metal centre through a hydride interaction. X-Ray diffraction data processing software automatically draws a bond between the centre and the BH_3 group at this distance, though this bond is absent by default in the calculated structure, due to the slightly lengthened distance of 2.475(5) Å. The bond is drawn in **Figure 2.6** to provide a consistent comparative reference.

The solution state behaviour of **2.1** as analysed by ^{1}H NMR spectroscopy defies the expectations produced by the solid state structure. As the pentalene ring hydrogen environments are not symmetric, a ^{1}H NMR spectrum in agreement with the X-Ray data should display eight separate Pn-H environments only. In practice, the ^{1}H NMR spectrum of purified crystalline **2.1** contains 16 environments, consisting of 8 signals of equal integration and another set of 8 peaks of twice the area, giving an integration ratio of 2:1. This would appear to imply the existence of two pentalene compounds with ring hydrogen asymmetry in the sample, with a favoured conformation that exists at twice the relative concentration. Initial suspicions for this observation fell upon contamination

of **2.1** with a separate impurity, or degradation of the complex leading to formation of a separate compound lacking symmetrical ring hydrogens.

However, repeated recrystallisation and subsequent X-Ray analysis consistently resulted in the generation of the same solid state structure for **2.1**, with no anomalous morphologies or unit cell measurements to suggest the presence of any other compound. EI-MS of crystalline **2.1** supports the solid state structure as expected, exclusively providing a molecular ion of 965 *m/z* attributable to $[[Ti(\mu{:}\eta^5,\eta^5\text{-}Pn^{\dagger})]_2(\mu\text{-}BH_2NBH_3)]^+$. Using solvated samples of **2.1** displaying 16 Pn-H environments by ^1H NMR as a control returned an identical mass spectrum.

The validity of the diffraction analysis is once again lent credence by elemental analysis, which is in agreement with calculated elemental percentages for **2.1** with one unit of pentane contained in the crystal lattice (as observed in the refined structure itself). As with the EI-MS technique, microanalysis was performed on both solid crystalline **2.1**, and the powder obtained by re-dissolving these crystals in solution and removing the solvent *in vacuo*. The ^1H NMR spectrum again produced 16 distinct pentalene environments, yet all microanalytical results remained consistent with the solid structure of **2.1**.

In addition to the apparent existence of two separate inorganic compounds in the solution state, broad singlets in the ^1H NMR region of -0.39 and -2.77 ppm have relative integrations of two and three, suggesting these signals represent the BH_3 and BH_2 groups respectively. The large, broad residual borosilicate glass peak originating from the NMR probe and tube containing the sample proved a consistent barrier to useful analysis, preventing any BH signals attributable to **2.1** from being observed *via* ^{11}B NMR. $^{29}Si\{^1H\}$ NMR of **2.1** in solution shows four separate triisopropylsilyl regions at δ_{Si} -3.00 ppm, 2.42 ppm, 2.27 ppm and 2.05 ppm. This is characteristic of one asymmetric complex and in direct contrast to the ^1H NMR spectrum obtained from the same sample.

$^{13}C\{^1H\}$ NMR of **2.1** supports the ^1H NMR spectrum obtained, with 32 peaks visible in the aromatic pentalene carbon region, again denoting the existence of "two" compounds. Repetition of characterisation techniques confirms to a satisfactory standard that the "second" complex in solution cannot be the second half of a complex-bound borazine fragment ($[Ti(NH_2BNH_3)(\mu{:}\eta^5,\eta^5\text{-}Pn^{\dagger})]_2$ or the product of any kind of

decomposition in solution. A further control was established with the dissolution of 25 mg of crystalline **2.1** in toluene within a sealed vial.

The vial was left for two weeks at ambient temperature within a glovebox. The ^{1}H NMR of this sample remained identical to freshly prepared crystalline samples of **2.1**, with 16 Pn-H resonances, providing empirical proof that the compound is stable in solution.

To eliminate the possibility that **1.1** and **2.1** may react with one another to produce other species in solution, **1.1** was added to pure crystalline **2.1** in deuterated toluene and a ^{1}H NMR array experiment was conducted overnight. No reaction occurred.

Having discounted the possibility of complex instability or side reactions causing the observed spectroscopic discrepancies, it seemed most likely that the inconsistencies between the solution state ^{1}H NMR of **2.1** and X-Ray, EI-MS and EA data was caused by an inherent property of **2.1** itself. The differing number of pentalene TIPS environments between the ^{29}Si{^{1}H} and ^{1}H NMR spectra may implicate hydrogen-based interactions (specifically fluxional hydrogen exchange between the bound borane species) as the primary factor, though the difference between the two spectra within the same sample is still surprising.

Several groups have been able to isolate and analyse the solid state structure of transition metal inorganic intermediates in the dehydrogenation process.[76,77,81] The majority of these species exist as hydrides or are bound to a borane species *via* a hydride bridge. While the molecular structure of **2.1** suggests two metal-hydrogen interactions, there is no evidence for the generation of a separate hydride derivative of **1.1** forming at any point during catalysis.

These reported hydride species often demonstrate fluxional hydrogen exchange behaviour in solution,[76] and variable temperature NMR experiments were conducted in an attempt to establish if **2.1** also displays this tendency. ^{1}H NMR data details a minute drift of chemical shift over successive spectra recorded as the temperature is lowered; this shift change is reversible when warming the sample back to ambient temperature. This suggests that these minor alterations are simply a direct result of the temperature change itself rather than a property of the complex. Between the temperature range of -80°C to 60°C no resonance coalescence or integration change was perceptible between the two species.

Reviewing the characterisation data obtained, all evidence (including DFT studies) with exception of the ^{1}H and $^{13}C\{^{1}H\}$ NMR spectra fully support the conformation of **2.1** depicted by the X-Ray crystallographic structure. Despite lack of any conclusive VT NMR evidence, fluxional exchange of metal-ligated borane hydrogen groups remains the most plausible explanation for the discrepancies present in the solution state NMR data discussed above.

In a further effort to improve characterisation of **2.1** and obtain solid state NMR data, a sample was submitted to Oxford University. Solution state NMR was also repeated, including ^{11}B NMR performed with a boron-free probe insert and sample tube allowing for the exclusion of borosilicate glass peaks. This revealed two previously obscured peaks at δ_B 30.92 ppm and -5.50 ppm respectively. As the peaks are low integration, it is likely the δ_B 30.92 ppm peak corresponds to residual borazine present in the sample, generated shortly after the synthesis of **2.1**. -5.50 ppm is within the shift region typical of four coordinate boron species[82] and given the previous value of -4.34 ppm observed for BCTB, it is likely that this resonance corresponds to either the four coordinate BH or terminal BH_3 group present in this compound, also present in minute amounts due to incomplete conversion to borazine.

$^{29}Si\{^{1}H\}$ solid state data collected at 10 KHz spinning frequency depicts two broad environments at δ_{Si} 1.30 and -0.22 ppm while ^{11}B data produces four distinct broad environments. Unfortunately, these observations remain contrary to expectations based upon the X-Ray diffraction data for **2.1**, which would suggest that four silicon environments and two boron resonances should be visible by SS-NMR.

To concisely summarise this array of disparate data; the $^{29}Si\{^{1}H\}$ NMR spectrum, EI-MS, elemental analysis data and computational studies support the XRD structure consistently obtained for solid crystalline samples of **2.1**. However, ^{1}H and $^{13}C\{^{1}H\}$ NMR spectra depict resonances corresponding to two separate complexes present in solution, in contrast with expectations generated by the other data. Most surprising is the lack of support solid state NMR data lends to either the X-Ray diffraction pattern or the "2 complexes" implied by solution state ^{1}H and $^{13}C\{^{1}H\}$ NMR spectra.

Accepting that the ^{1}H and $^{13}C\{^{1}H\}$ NMR solution state characterisation of **2.1** is anomalous and considering the X-Ray structure the most accurate representation of the "true" conformation of the complex due to the bulk of EI-MS, ^{29}Si and microanalytical

evidence supporting this assertion appears the most valid conclusion at the present time, though no satisfactory explanation for the contradictory NMR data collected yet exists.

Further Study of the Reaction of 2.1 and 1.1 with NH_3BH_3 in Toluene

Despite outstanding issues with the characterisation of **2.1**, reactivity of the compound with ammonia borane was examined in further detail. The solubility of amine-boranes in toluene is very poor, with around one mL of toluene reaching saturation after dissolving only around one milligram of ammonia borane. However, all previous amine-borane reactions leading to the synthesis of **2.1** utilised toluene as a solvent; initially, this solvent was chosen due to a wide prevalence in field literature with other dehydrogenation catalysts.[76,81,89] Limited dissolution of NH_3BH_3 in toluene made establishing exact rates of reaction problematic, and stirring compounded this problem, with undissolved ammonia borane frequently adhering to the walls of a glass vessel rather than dissolving in solution as desired. Use of toluene was nonetheless kept consistent at this stage in order to eliminate any possible changes in reaction behaviour caused by solvent influence.

At five percent molar catalyst loading, time to 100% conversion of NH_3BH_3 assessed by $^{11}B\{^1H\}$ NMR varied from six hours to four days, establishing this solubility as the primary barrier to efficient catalysis. The absolute minimum catalyst loading still resulting in reactivity equated to 0.1 mol% of catalyst to ammonia borane, though these reactions do not proceed to completion and instead cease after around four hours.

Isolating crystalline **2.1** and mixing the solid with ammonia borane in toluene produces identical reactivity to direct reactions between **1.1** and NH_3BH_3, with no induction period prior to visible effervescence and full conversion of the amine-borane to borazine and polyborazylene over the course of around twelve hours by ^{11}B NMR.

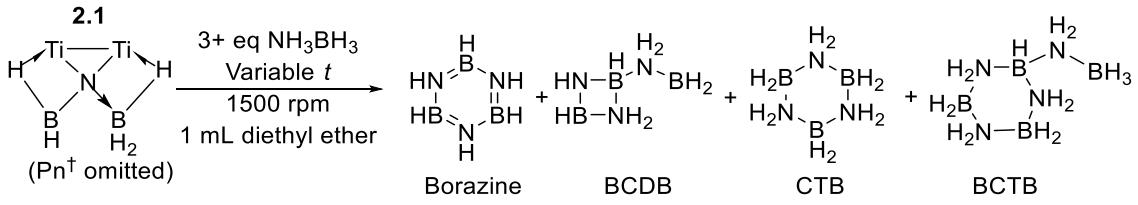

Scheme 2.5 Reaction of **2.1** with NH_3BH_3.

The formation of borazine is not visible by ^{11}B NMR until **2.1** is seen in solution *via* ^{1}H NMR spectroscopy and the resonances characteristic of **1.1** have been lost. It may be inferred from this observation that **1.1** is acting as a pre-catalyst in the formation of the active species directly responsible for the catalytic dehydrogenation.

If **2.1** is indeed an active component of the reaction, it logically follows that another titanium pentalene complex containing the second "half" of each borazine unit would exist in solution. As conclusive existence of this species has never been exposed by EI-MS, NMR spectroscopy or elemental analysis, it remains more probable that **2.1** is instead also acting as a pre-catalyst in formation of a further, directly active compound. This assertion is supported by the peak broadening regularly seen in ^{1}H NMR spectra of the crude reaction mixture, indicative of paramagnetism.

Reactions Between 1.1 and NH_3BH_3 in Diethyl Ether

Reactions between **1.1** and a standardised solution of NH_3BH_3 in ether display superficial visual similarities to reactions conducted in toluene. Visible effervescence and an immediate colour change to green are witnessed as before, though this green colour change also occurs with 1:1 stoichiometry, in contrast to the brown mixture formed with toluene. In spite of this colour change, at one equivalent of NH_3BH_3 in solution only compound **1.1** is observed by ^{1}H NMR spectroscopy, though the aliphatic region is considerably broadened between δ_H 2.48 and 1.46 ppm, preventing observation of the $^{i}PrCH_3$ triisopropylsilyl environments through obscuration.

Upon adding three equivalents of ammonia borane, ^{1}H NMR analysis provides formal confirmation that dehydrogenation occurs, with free H_2 observed at δ_H 4.5 ppm in C_6D_6. Borazine and polyborazylene signals are again observed by ^{11}B NMR at δ_B 30.59 ppm and 28.14 ppm respectively. The rate of reaction increases significantly with the solubility issues inherent to toluene removed, with reactions consistently running to completion (full conversion to borazine/polyborazylene) in 15 minutes at one mol% **1.1**, a TOF of 83.33 h^{-1}.

However, complex **2.1** is not observed by ^{1}H NMR spectroscopy in reactions performed in diethyl ether, validating suspicions that solvent choice may influence the reaction mechanism in addition to the rate of reaction. No clear characteristic aromatic resonances are observed, with the region instead extensively broadened into a series of

overlapping peaks. This is suggestive of a separate, paramagnetic species in solution. Initially it was considered that given the similarity between the reaction products and observations recorded, these resonances could correspond to an ethereal adduct of **2.1** or a subsequent catalytic species formed in solution from **2.1** that was previously unwitnessed.

To confirm or refute this, a crystalline sample of **2.1** isolated from a toluene reaction between **1.1** and NH_3BH_3 was dried thoroughly and dissolved in a stock ammonia borane diethyl ether solution. The ^1H NMR spectrum in C_6D_6 remains identical to that witnessed with reactions in toluene, with 16 sharp pentalene hydrogen environments. This provides compelling evidence that an entirely different species is responsible for the catalysis observed in reactions in Et_2O, though **2.1** is still capable of performing the same catalytic or pre-catalytic function in this solvent if pre-prepared in toluene. Unfortunately, this new compound has not yet been isolated successfully and thus remains uncharacterised.

Reactions between 1.1 and Aminodiborane (Toluene)

With the resemblance of the structure of **2.1** provided by X-Ray diffraction data to a "half-borazine" adduct, it was decided to explore reactions between **1.1** with a borane possessing a similar composition and structure to the this ligated "half-borazine". Aminodiborane (ADB, $NH_2B_2H_5$) was chosen for these reactions (*vide infra*). The objective of such reactions was to prompt the rational synthesis of **2.1** directly, allowing elucidation of the formation mechanism. Conversely, if **2.1** was not formed, it was intended that synthesis of a similar system would provide a point of reference for the data obtained for **2.1**.

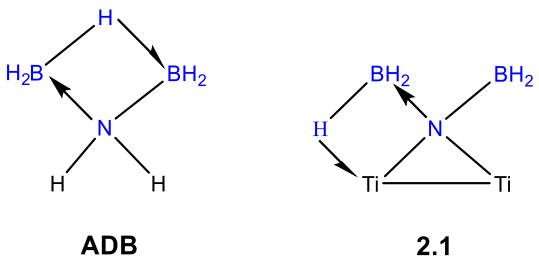

Figure 2.7 Aminodiborane and Complex **2.1**, with structural similarities highlighted.

Aminodiborane was synthesised in a procedure outlined by Chen *et al.* utilising a reaction of ammonia borane with BH_3.THF.[90] In comparison to the ten gram scale preparation described in the published procedure, the synthesis was conducted on a millimolar scale befitting the preliminary nature of the reactions. While practical, lowering the scale of the reaction did have some adverse effects, primarily complicating the removal of excess THF and impurities, as the volatile aminodiborane is easily lost *in vacuo* when synthesised in such small quantities. These impurities are detected post-filtration by ^{11}B NMR at δ_B 18.16 ppm, -11.13 ppm and -27 ppm, with the ADB resonance present at -26.88 ppm. EI-MS analysis did not imply the presence of any impurities referenced in comparable reactions in published literature, though the wide chemical shift range of the contaminants implicate a mix of boranes in states varying from two to four coordinate. Fortunately, the impurities also appeared to be inert, showing static integration ratios over the course of the reaction of ADB with **1.1**. The mixture of ADB and side products was also left in a THF solution for several hours, with no change in ADB or contaminant concentration, confirming presence of **1.1** is responsible for the reactivity and subsequent characterisation data obtained.

Despite visible effervescence and an instantaneous colour change to green when **1.1** is added to a given solution of ADB in toluene, complex **2.1** is not witnessed by ^{1}H NMR. Instead, one single asymmetric complex 2**.2** is observed in solution, with eight pentalene ring resonances between δ_H 7.28 ppm and 5.34 ppm. These are not comparable with any of the 16 recorded peaks for **2.1**.

^{11}B{^{1}H} NMR data confirms that the dehydrogenation of ADB progresses in an analogous fashion to the reactions between **1.1** and **2.1** with NH_3BH_3 with borazine and polyborazylene formation exhibited as signals at δ_B 31 ppm and 29 ppm respectively. As expected, polyborazylene is the primary product after three days of reaction time, though the reaction proceeds rapidly for the first 15 minutes after dissolution of the solids before rate falls dramatically. Interestingly, reactions conducted with **1.1** and ADB never proceed to full dehydrogenation of the starting material; the ADB resonance at δ_B -26.59 ppm is still present at 25% of the concentration of polyborazylene after several days. As with **2.1**, borane environments for **2.2** appear obscured by the borosilicate glass peak, though a series of resonances too broadened for clear interpretation appears apparent at δ_B 1.47 ppm to -8.43 ppm after formation of **2.2** is noted by ^{1}H NMR. Unfortunately, multiple repeat experiments did not yield a

crystalline sample of **2.2** of sufficient quality for XRD study. Analysis by EI-MS also failed to provide a characteristic fragmentation pattern, instead depicting only fragments of pentalene and [Ti($Pn^{\dagger}$)$_2$]. Nonetheless, the visual observations, dehydrogenation behaviour and ^{1}H and ^{11}B NMR spectra imply formation of a borane adduct of **1.1** with apparent increased catalytic rate when compared to **2.1**, but comparably poor longevity of catalysis prior to deactivation (*i.e.* an inferior TON). It is notable that **2.2** does not exhibit the same solution state behaviour that complicated the interpretation of the data collected for **2.1**. This would imply a lack of fluxional hydrogen exchange, possibly consistent with direct ligation of the ADB fragment to **1.1**, producing a complex similar to **2.1** in which the central nitrogen atom of ADB bridges both titanium centres and borane groups. The hydrogen interaction from one borane group to the second lends an asymmetry[90] to the bonding of the structure resulting in the observed eight ^{1}H NMR pentalene environments. The ^{1}H NMR spectrum of **2.2** also supports a lack of metal hydride interactions with the borane groups, showing no signals upfield of the aliphatic TIPS group peaks at around δ_H 0.85 ppm (discounting a weak resonance indicating presence of silicone grease at δ_H 0.26 ppm).

Unfortunately, while this description of **2.2** as a simple ADB pentalene compound adduct seemingly provides an internally consistent rationale for the characterisation data gathered, one critical contradiction in this model undermines its validity. The ADB adduct depicted shows no signs of dehydrogenation of the amine-borane fragment. Unless an ADB adduct is formed and remains at constant concentration in solution over the course of the reaction, it is therefore doubtful that the theoretical species depicted is **2.2**. Instead, it is probable that this complex would merely exist in solution as a transient species prior to dehydrogenation, and the actual asymmetric compound in the ^{1}H NMR spectrum remains unidentified. In absence of further characterisation data to provide an informed conclusion, any further interpretation of the spectroscopic information gathered would amount to speculation.

Attempts were also made to react ADB with **2.1**, though no evidence of a reaction was visible by ^{11}B and ^{1}H NMR spectroscopy. This suggests that the dehydrogenation occurring between **1.1** and ADB occurs only as a by-product of the formation of **2.2**; this also concurs with the cessation of borazine and polyborazylene production once **1.1** has been fully converted to **2.2**.

Reactions Between 1.1 and $HNMe_2BH_3$ (Toluene)

Even with the ongoing synthesis of increasingly efficient amine-borane dehydrogenation catalysts,[79] the exact mechanistic details of these systems remain elusive. In 2007, first row transition metals made a debut appearance in the literature when Keaton, Blacquiere and Baker reported catalytic nickel-NHC compounds.[82] This paper also provided the first tentative insight into mechanistic details. Baker *et al.* postulated that the first reactive step with substituted amine-boranes features B-H activation of the amine-borane to yield the species $R'RNBH_2$ σ bound to the metal centre in addition to the abstracted metal hydride. Subsequent β-hydride elimination from the N-H group then occurs.[82] In an interesting parallel to the findings of this work, Baker *et al.* were unable to find evidence of any nickel hydride species in solution by ^1H NMR spectroscopy, despite suspicion that such an interaction is instrumental in the operative mechanism.[82]

Chirik and colleagues developed this β-hydride elimination pathway[76] into a proposed catalytic cycle in order to explain the reactivity of a Ti(II) titanocene species with $HNMe_2BH_3$. In addition to the formation of a bound $R'RNBH_2$ group and metal hydride, the cycle also accounts for formation of a nitrogen-borene species which subsequently dimerises to form a four-membered inorganic analogue of cyclobutane. The role of titanium in this transformation is not formally elaborated upon, though the cycle still produces the most complete mechanistic description to date.

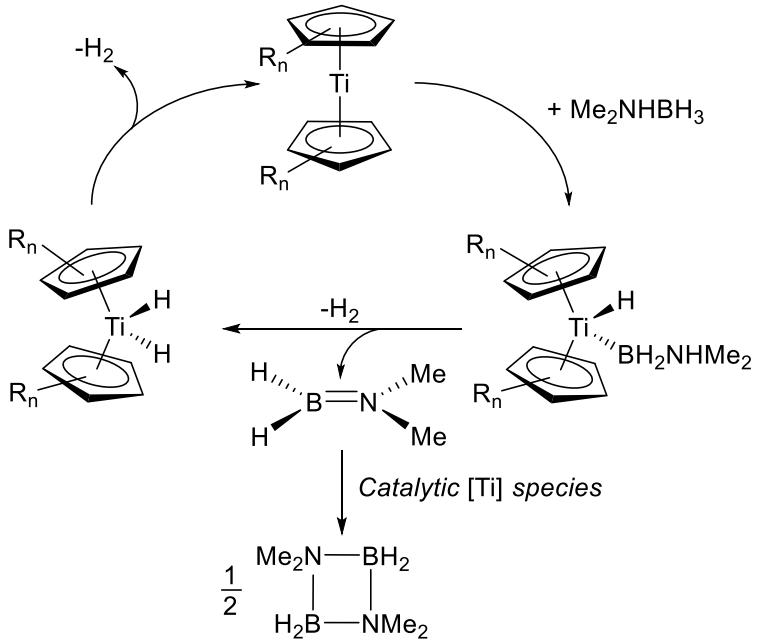

Scheme 2.6 Catalytic scheme proposed by Chirik *et al.*[76]

As with literature titanocene, iridium hydride and zirconium sandwich complexes,[76,80,81] compound **1.1** also proved capable of dehydrogenating substituted amine-boranes. Reactions performed with $HNMe_2BH_3$ and **1.1** in toluene resulted in visual observations consistent with previous catalytic reactions; immediate effervescence upon addition of solvent followed by a solution colour change from red to green. Reaction progress was again tracked most effectively *via* proton-coupled ^{11}B NMR.

The replacement of two amine hydrogen atoms with methyl groups places obvious limitations on the maximum extent of dehydrogenation that can occur over the course of the reaction. Formation of borazine requires trimerisation of three amine-borane units *via* the loss of H_2 from both the NH_3 and BH_3 groups. The ^{11}B NMR spectra of reaction mixtures support this deduction; the final dehydrogenation products (**Figure 2.8**) are in excellent agreement with the products characterised by Manners *et. al.*[81] and Chirik *et al.*[76] with observation of the borene species δ_B 38.09 ppm and the dimerised amine-borane structure at δ_B 5.41 ppm. A trimeric linear borane is also present in solution at δ_B 2.16 ppm.

High rates of reaction occurred using minimal loadings of **1.1**, with two mol% concentration of **1.1** producing full dehydrogenation to the cyclic dimer product within 15 minutes. Reaction rate continues to increase with greater catalyst concentration (with total reaction time measured at 10 minutes for 10 mol% loading). However, this trend is subverted upon approaching 1:1 stoichiometry; at this point a drastic reduction in catalytic ability is observed, with only around 70% yield (relative to starting material by ^{11}B NMR) of the dimerised species after 3 hours.

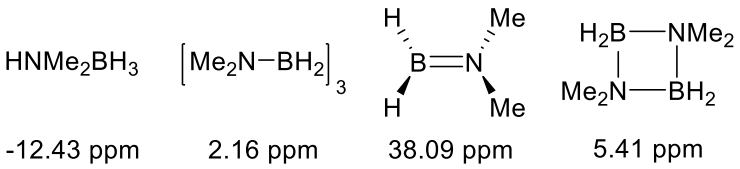

Figure 2.8 Species identified in solution and observed ^{11}B NMR chemical shifts.

^1H NMR of the reaction mixture is uninformative in comparison to reactions with ammonia borane, showing only a decrease in $HNMe_2BH_3$ over the course of the reaction at δ_H 3.46-2.63 ppm, with no visible signals corresponding to any novel pentalene complex. Heated (60°C) control reactions established that no dehydrogenation of $HNMe_2BH_3$ occurs thermally without the presence of a catalyst. As

catalytic dehydrogenation continues if more $HNMe_2BH_3$ is added to solution, the active inorganic complex responsible must still be present in the mixture despite the lack of ^1H NMR evidence for any pentalene compound in solution. This suggests the catalytic species is NMR silent due to paramagnetism, though no metal complex has yet been successfully isolated from the reaction mixture.

Reactions of 1.1 with Net_3BH_3 (Toluene)

With the observed consistency between the inorganic products isolated from reactions of **1.1** with amine-boranes and those reported in field literature, it was decided to further probe the N-H β-hydride elimination step discussed by the Baker and Chirik groups.[76,82] This was accomplished by performing reactions with Net_3BH_3, a substituted amine-borane lacking a proton situated on the α to the borane group. With the assumption that the Chirik *et al.* mechanism operates with bimetallic Ti(II) pentalene compounds, no catalytic dehydrogenation should be observed with this amine-borane; instead it was hoped that the reaction would halt upon formation of a titanium hydride and $Ti\text{-}BH_2Net_3$ species

However, effervescence was observed in combination with loss of ethylene[91] characterised by a ^1H NMR singlet at δ_H 5.25 ppm. Formation of $H_2B{=}Net_2$ was identified *via* proton coupled ^{11}B NMR as a triplet at δ_B 38.14 ppm. The ^1H NMR spectrum continues to display signals at chemical shift values characteristic of complex **1.1** after evolution of hydrogen, but these peaks immediately begin to broaden. After two hours, in C_6D_6 two broadened resonances at δ_H 6.91 and 6.22 ppm still remain (similar to δ_H 6.84 ppm and 6.24 ppm peaks seen in pure **1.1**, but in the course of a further hour these peaks widen until they merge with the baseline signal. A single broad peak is still observed at δ_H 6.07 ppm and the aliphatic region contains recognisable doublets assignable to pentalene TIPS environments despite additional broadening in this region. This would lend support to formation of a paramagnetic complex in solution, as appears to be the case with in $HNMe_2BH_3$ reactions with **1.1**. Unfortunately, no pure metal compound could be extracted from the mixture even with repeated attempts at crystallisation in a variety of solvents and the catalytic species thus remains unknown.

It is evident from the by-products identified, however, that this reaction demonstrates that α-hydride groups on the amine-borane reagent are unnecessary for dehydrogenation

catalysis with **1.1**. Further experiments would need to be performed to assess if this also the case for titanocene and iridium hydride species. The operative mechanism likely varies between catalysts used and compounds with two metal centres may bind wholly differently to monometallic systems.

While entirely speculative, an attempt has been made to construct a simple mechanism to provide some explanation of the observed chemical behaviour (**Error! Reference source not found.**). This scheme pairs literature predictions of the formation of a metal-hydride and σ-bound R_3NBH_2 group with the addition of bimetallic binding and γ-hydride interaction with an amine ethyl group CH_2.

While observed by-products are accounted for in this cycle, this mechanism does not take into account the presence of the unknown paramagnetic species, instead relying on hydrogen exchange between the two metal centres and subsequent elimination steps to furnish the products observed by ^{11}B and ^{1}H NMR spectroscopy. The scheme also neglects the possible existence of bridging hydride species. Presumably the paramagnetic compound in solution is a stable-state mixed valence system with a partially bound borane on one metal centre. However, it is imprudent to speculate further on the nature of this compound or the reaction mechanism itself, as this early proposed depiction remains unsubstantiated.

Conclusions

Complex **1.1** was reacted with ammonia borane, dimethyl amine-borane and triethyl amine-borane and found to catalytically dehydrogenate each to produce a range of products.

In the case of ammonia borane, the primary products at reaction completion were borazine and polyborazylene, confirmed by ^{11}B NMR and EI-MS techniques. Signal multiplicities of some minor inorganic products were not clearly defined even with the acquisition of ^{1}H coupled ^{11}B NMR spectra, though δ_B chemical shifts observed for borazine, polyborazylene, BCTB and CTB were consistent with reported literature values.[87]

Compound **2.1** was isolated from reactions between **1.1** and ammonia borane in toluene; exhaustive attempts were made to characterise the complex conclusively, though significant contradictions remain between ^{1}H NMR and EA, EI-MS, X-Ray, $^{13}C\{^{1}H\}$

and $^{29}Si\{^{1}H\}$ data. Variable temperature and solid state NMR did not resolve this conflict to any degree, instead introducing further ambiguity.

Complex **2.1** and **1.1** exhibit near identical reactivity with NH_3BH_3 in toluene, with neither displaying an induction period prior to catalysis and formation of **2.1** required before borazine is formed. It is thus clear that **1.1** acts as a pre-catalyst in the formation of **2.1**. However, it is not possible to conclude from current data whether **2.1** is an active catalytic component, or simply an intermediate or pre-catalyst to another active species.

Reactions performed between **1.1** and NH_3BH_3 in ether progress without formation of **2.1** by ^{1}H NMR analysis, suggestive of a different operative catalytic mechanism. When added to ether ammonia borane solutions, compound **2.1** displays the same NMR characteristics as in toluene, confirming **2.1** is not normally formed (or at least is not present other than as a transient intermediate) in this solvent.

Reactions conducted with aminodiborane resulted in synthesis of an asymmetric complex, **2.2**. The identity of this complex is thus far inconclusive, though it is most likely a dehydrogenated bimetallic adduct of ADB. Ultimately, these test reactions did not provide any further useful information regarding the structure or solution state behaviour of **2.1**.

Compound **1.1** showed catalytic behaviour consistent with literature reports of other transition metal catalysts when reacted with dimethyl amine-borane, though no metal complex could be isolated from the reaction mixture. ^{11}B NMR spectroscopy provides substantive evidence that complex **1.1** also catalytically dehydrogenates Net_3BH_3 despite the lack of hydrogen atoms on the amine group positioned α to BH_3. These α-hydrogen atoms are instrumental in the catalytic dehydrogenation mechanism recently proposed by Chirik *et al.*[76] and it would therefore appear that this reaction follows a novel mechanism with bimetallic pentalene compounds. It is possible that there is an involvement from the γ-hydride species of the nitrogen bound ethyl group, though more study of the system is needed. Isolation of a metal complex from solution would prove an invaluable asset for further understanding the mechanism of the catalysis observed.

General Experimental Considerations and Conditions

All reactions were conducted using standard Schlenk line techniques under argon, or alternatively performed under an inert argon or nitrogen atmosphere within an Mbraun glove box. Laboratory glassware was dried thoroughly in a 200°C oven.

All solvents were dried over sodium wire and transferred to a nitrogen atmosphere still before heating to reflux over potassium for a minimum of three days. Collected solvents were degassed and stored under argon in potassium mirrored ampoules, with the exception of THF and Et_2O, which were stored over 4 Å molecular sieves.

^{1}H, ^{29}Si and ^{13}C NMR experiments were performed using both a 400 MHz Varian NMR Spectrometer and a 500 MHz Varian NMR spectrometer. All spectra were collected in deuterated benzene at 303 K, unless stated otherwise. All NMR spectra were externally referenced to $SiMe_4$. All ^{13}C spectra were obtained at 100.5 Hz, while all ^{29}Si spectra were obtained at 79.5 Hz.

Elemental Analysis was performed by Desmond Davis at the University of Bristol and Stephen Boyer at the London Metropolitan University. EI and ESI mass spectrometry was performed upon samples by Dr. Alaa-Abdul Sada at the University of Sussex, using a 70 eV impact ionisation VG Autospec Fisons mass spectrometer.

X-Ray crystallography data was collected using an Enraf-Nonius FR590 diffractometer. Where noted, samples were sent to the National Crystallography Service at the University of Southampton. Solid state NMR data for compound **2.1** was collected by Dr. Alexander Kilpatrick at the University of Oxford. ORTEP-3 was used to present X-Ray structures pictorially[92] throughout this work and Olex2 was used to solve and refine XRD data sets.[93]

Procurement of Chemical Materials

Commercially Supplied Reagents

The following chemicals were purchased from Sigma-Aldrich: 2-butyne, $HNMe_2BH_3$, NEt_3BH_3, fumaronitrile and tetracyanoethylene.

Reagents were purified and stored in accordance with documented procedures dependent on the substance.[94] Technical grade (90%) NH_3BH_3 was additionally sublimed after purchase from Sigma-Aldrich to further increase purity.

Solutions of MeLi and *n*-Buli of 2.5 M concentration were procured from Acros Organics and concentration was regularly assessed before use by titration with diphenylacetic acid.

Cyclooctatetraene was purchased from Alfa Chemicals and stored in a refrigerator in absence of light. COT was vacuum transferred when selected for use.

Solids were dried thoroughly under vacuum conditions and stored in a glovebox under an argon atmosphere. Where appropriate, liquids transferred into ampoules, degassed and dried over 4 Å molecular sieves for a period of days before use.

Potassium solids used for the preparation of amalgams were acquired from Fischer Scientific and stored under oil. The oil was removed by a pentane wash and the solids were transferred into an argon atmosphere glovebox, in which the potassium oxide layer was removed manually with a scalpel prior to storage.

Synthesised Materials

Aminodiborane,[90] KNH_2, $H_2Pn^{\dagger,}$ $[K]_2[Pn^{\dagger}]$, $[Li(DME)_xPn^{\dagger}]$,[21,51] $MgMe_2$,[95] and $TiCl_3(THF)_3$ [51] were prepared by the referenced literature routes, purified and stored in an argon atmosphere glovebox.

Stored Materials

1,2-DCE,[96] adamantyl azide,[97] MeNC, $LiCH_2TMS$,[98] $TiCl_4.2THF$[99] and trityl azide were acquired and stored in the laboratory inventory before the beginning of this project. As with all purchased reagents, these chemicals were prepared and stored according to reported procedures[94,96–99] and used when needed.

Gasses used were stored in ampoules or pressurised metal containers previously purchased from Union Carbide. These reagents were of analytical-grade purity

(CO – 99.999%, CO_2 – 99.99%). Gas reactions performed using a T-piece were enacted only after thorough purging of the assembled apparatus with argon.

Isotopically labelled CO (^{13}CO 99.7%) was previously provided to the laboratory by Euriso-top, while labelled CO_2 ($^{13}CO_2$ 99%) was obtained from Cambridge Isotopes. Anhydrous ammonia was obtained from BOC Gases.

Starting Material Preparation and Synthesis of $[Ti(\mu:\eta^5, \eta^5\text{-}Pn^{\dagger})]_2$

R1.1) Synthesis of $[C_8H_6][Li(DME)_x]_2$

10.81 g (103 mmol) of cyclooctatetraene was measured out using a glass needle-valve regulated vessel with pressure-equalising side capillary and passed at a rate of 0.5 mL/hour through flash vacuum pyrolysis apparatus. The resulting mix of dihydropentalenes was collected in a trap cooled to -78°C. This orange solid was dissolved in 100 mL of pre-cooled hexane and transferred *via* cannula into a large round bottomed flask maintained at -78°C.

25 mL of pre-cooled DME (-78°C) was added to the reaction vessel. 90 mL of ^{n}BuLi was introduced to the orange mixture dropwise over *ca.* 3 hours. A grey suspension of $[C_8H_6][Li(DME)_x]_2$ was produced. After stirring for 1 hour, the reaction mixture was allowed to warm to ambient temperature. The mixture was then filtered within an argon glovebox using a porosity 4 sintered glass frit. The resulting solid was washed with four 100 mL aliquots of *n*-hexane and dried under vacuum conditions to give a mass of 15.15 g. ^{1}H NMR analysis in d^8-THF revealed the formula of the product to be $Li_2Pn(DME)_{0.6}$.

^{1}H NMR: $Li_2Pn(DME)_{0.6}$: δ_H 5.06 (4H, d, $^3J_{HH}$ = 2.89 Hz, Pn H), 3.43 (2H, s, DME CH_2, 3.27 (3H, s, DME CH_3).

Yield: 15.15 g (88.58 mmol), 86% with respect to cyclooctatetraene.

R1.2) Synthesis of $H_2Pn^\dagger$

4.16 g (8.73 mmol) of $[C_8H_6][Li(DME)_2]_2$ was placed within a Young's ampoule, suspended in 100 mL of THF cooled to -78°C and stirred vigorously. 5 mL (18.6 mmol) of TIPS triflate was added dropwise *via* cannula. The reaction mixture was warmed to 0°C in an ice bath. After removal of volatiles *in vacuo* the mixture was left to warm to room temperature. The solids were extracted with 150 mL of pre-cooled pentane and filtered *via* cannula to produce a yellow filtrate. The filtrate was concentrated under vacuum conditions until saturated, at which point it was cooled to -50°C. White crystals were isolated by filtration and washed with 2 x 10 mL aliquots of cooled pentane.
^{1}H NMR: δ_H 6.83 (2H, d, $^3J_{HH}$ = 4.68 Hz, Pn H), 6.68 (2H, d, $^3J_{HH}$ = 4.87 Hz, Pn H), 3.57 (2H, s, Pn H), 1.12 (6H, m, ^{i}Pr$_3$Si CH), 1.10 (18H, d, $^3J_{HH}$ = 6.43 Hz, ^{i}Pr$_3$Si CH$_3$), 1.03 (18H, d, $^3J_{HH}$ = 6.74 Hz, ^{i}Pr$_3$Si CH$_3$).

Yield: 2.42 g (5.85 mmol), 67% with respect to $[C_8H_6][Li(DME)_2]_2$

R1.3) Synthesis of $[K]_2[Pn^\dagger]$

A solid mixture of 3.10 g (7.20 mmol) of $[C_8H_6(Si^iPr_3\text{-}1,4)_2]$ and 0.816 g KNH_2 was placed in a Rotaflow ampoule and cooled to -78°C. 200 mL of -78°C. Diethyl ether was then added *via* cannula transfer under vigorous stirring. The mixture was left to equilibriate to room temperature overnight. The resulting orange solution was filtered through a Celite® packed Schlenk frit and volatiles were removed *in vacuo* to afford a tan coloured solid.
^{1}H NMR: δ_H 6.38 (2H, d, $^3J_{HH}$ = 3.46 Hz, Pn H), 5.74 (2H, d, $^3J_{HH}$ = 3.25 Hz, Pn H), 1.43 (6H, m, ^{i}Pr$_3$Si CH), 1.24 (36H, d, $^3J_{HH}$ = 7.30 Hz, ^{i}Pr$_3$Si CH$_3$).

Yield: 3.10 g (6.34 mmol), 88%.

R1.4) Synthesis of $TiCl_3(THF)_3$

12.56 g (81 mmol) of $TiCl_3$ was measured into a 500 mL Young's tap ampoule charged with 200 mL of anhydrous THF. The resulting purple mixture was left to stir overnight under reflux conditions (68°C), after which a blue solution and blue precipitate formed. The mixture was filtered and the blue precipitate was collected, with a second crop obtained from the mother liquor through repeated filtration. The solid was then dried *in vacuo* to give 25.55 g of a blue powder. 0.86 g of product was obtained as a second crop crystallised from the mother liquor. The identity of the blue powder was confirmed *via* comparison to ^1H NMR data previously obtained by Dr. Alexander Kilpatrick.
Yield: 26.41 g (71.28 mmol), 88%.

R1.5) Synthesis of $[Ti(\mu{:}\eta^5,\eta^5\text{-}Pn^\dagger)]_2$ (1.1)

3.03 g (8.21 mmol) of $TiCl_3(THF)_3$ was placed within a large (500 mL) ampoule equipped with a Rotaflow tap and magnetic stirrer bar and 50 mL of THF was added, creating a suspension. This solution was then cooled to 0°C in an ice bath. 4.02 g (8.14 mmol) of $[K]_2[Pn^\dagger]$ was placed within a small Schlenk flask and THF was added (30 mL).

The $[K]_2[Pn]$ solution was next added dropwise *via* cannula transfer. A colour change from bright blue to a a dark olive green was observed. Upon completion of the addition, the mixture was allowed to warm to ambient temperature and left to stir for 16 hours. The THF was then removed from the solution *in vacuo* and 100 mL of hexane was added, forming a green solution. The small stirrer bar previously used was removed from the ampoule and replaced with a large glass stirrer bar. Four stoichiometric equivalents of potassium was then introduced to the vessel in the form of 0.5% K-by-weight mercury/potassium amalgam (19.5 cm^3, 265 g, 34 mmol potassium). The mixture was left stir vigorously for 16 hours. After this time had elapsed, the mixture was a deep red colour. The solution was filtered through a Celite® packed frit and the solvent was removed under vacuum conditions. The product was extracted in pentane and crystallised from a saturated solution stored at -35°C.

Yield: 2.73 g (2.96 mmol), 67% (w.r.t $TiCl_3(THF)_3$).

^{1}H NMR: δ_H 6.82 (4H, d, $^{3}J_{HH}$ = 2.87 Hz, Pn H), 6.34 (4H, d, $^{3}J_{HH}$ = 2.85 Hz, Pn H), 1.17 (12H, m, ^{i}Pr$_3$Si methine CH), 0.92 (36H, d, $^{3}J_{HH}$ = 7.28 Hz, ^{i}Pr$_3$Si CH$_3$), 0.77 (36H, d, $^{3}J_{HH}$ = 6.81 Hz, ^{i}Pr$_3$Si CH$_3$).

EI-MS: *m/z* = 923 [Ti(μ:η^5,η^5-Pn†)]$_2^+$

Note: The heteronuclear spectra below were collected[51] by Dr. Alexander Kilpatrick and are documented for reference purposes. As **1.1** was identified by ^{1}H NMR spectroscopy and EI-MS after following an established synthetic preparation, repeat collection of these spectra was not necessary to establish that synthesis of **1.1** had been successful.

^{13}C{^{1}H} NMR: δ_C 133.4 (Pn C), 132.6 (Pn C), 111.3 (Pn C), 102.3 (Pn C), 19.2 (^{i}Pr$_3$Si CH$_3$ C), 19.0 (^{i}Pr$_3$Si CH$_3$ C), 13.4 (^{i}Pr$_3$Si CH C).
^{29}Si{^{1}H} NMR: δ_{Si} 4.32 (^{i}Pr$_3$Si Si).

Chapter 2 Experimental Data

R2.1) Reaction of [Ti(μ:η^5,η^5-Pn†)]$_2$ with NH$_3$BH$_3$ (1 equivalent)

50 mg (0.05 mmol) of **1.1** was placed within an ampoule. 4 mg (0.1 mmol) of NH_3BH_3 was added. The solids were dissolved in toluene (4 mL) and an immediate colour change to dark brown was observed. ^{1}H NMR analysis of the crude mixture was suggestive of 3 asymmetric compounds in solution, with the presence of 24 pentalene environments.

^{1}H NMR: δ_H 8.68 (1H, d, $^{3}J_{HH}$ = 2.49 Hz, Pn H), 8.12 (1H, d, $^{3}J_{HH}$ = 2.32 Hz, Pn H), 7.99 (1H, d, $^{3}J_{HH}$ = 3.58 Hz, Pn H), 7.87 (1H, d, $^{3}J_{HH}$ = 4.11 Hz, Pn H), 7.81 (1H, d, $^{3}J_{HH}$ = 3.40 Hz, Pn H), 7.69 (1H, d, $^{3}J_{HH}$ = 4.11 Hz, Pn H), 7.24 (1H, d, $^{3}J_{HH}$ = 4.11 Hz, Pn H), 6.86 (1H, d, $^{3}J_{HH}$ = 4.12 Hz, Pn H), 6.81 (1H, d, $^{3}J_{HH}$ = 3.40 Hz, Pn H), 6.69 (1H, d, $^{3}J_{HH}$ = 4.65 Hz, Pn H), 6.50 (1H, d, $^{3}J_{HH}$ = 3.40 Hz, Pn H), 6.45 (1H, d, $^{3}J_{HH}$ = 3.83 Hz, Pn H), 6.31 (1H, d, $^{3}J_{HH}$ = 2.83 Hz, Pn H), 6.13 (1H, d, $^{3}J_{HH}$ = 3.42 Hz, Pn H), 6.04 (1H, d, $^{3}J_{HH}$ = 3.06 Hz, Pn H), 5.97 (1H, d, $^{3}J_{HH}$ = 3.24 Hz, Pn H), 5.95 (1H, d, $^{3}J_{HH}$ = 3.47 Hz, Pn H), 5.85 (1H, d, $^{3}J_{HH}$ = 3.30 Hz, Pn H), 5.81 (1H, d, $^{3}J_{HH}$ = 2.89 Hz, Pn H), 5.70 (1H, d, $^{3}J_{HH}$ = 2.65 Hz, Pn H), 5.62 (1H, d, $^{3}J_{HH}$ = 2.89 Hz, Pn H), 5.49 (1H, d, $^{3}J_{HH}$ = 2.89 Hz, Pn H), 5.46 (1H, d, $^{3}J_{HH}$ = 2.78 Hz, Pn H), 5.34 (1H, d, $^{3}J_{HH}$ = 2.89 Hz, Pn H), 1.59 (18H, m, ^{i}Pr$_3$Si CH), 1.45-0.93 (^{i}Pr$_3$Si CH$_3$).

R2.2) Reaction of [Ti(μ:η^5,η^5-Pn†)]$_2$ with NH_3BH_3 (3+ equivalents)

100 mg (0.1 mmol) of **1.1** and 9 mg (0.3 mmol) of NH_3BH_3 were added to a small Young's valve sealed ampoule. The mixed solids were dissolved in toluene (10 mL). A colour change to green was observed over the course of 15 minutes. Complex **2.1** was identified in solution, and isolated from crystals of pentane at crystals were obtained from pentane at -35°C.

NMR of reaction mixture:

^{1}H NMR: δ_H 8.18 (1H, d, $^3J_{HH}$ = 2.98 Hz, Pn H), 8.04 (0.5H, d, $^3J_{HH}$ = 3.37 Hz, Pn H), 7.92 (1H, d, $^3J_{HH}$ = 2.98 Hz, Pn H), 7.86 (0.5H, d, $^3J_{HH}$ = 2.88 Hz, Pn H), 6.58 (1H, d, $^3J_{HH}$ = 3.18 Hz, Pn H), 6.56 (0.5H, d, $^3J_{HH}$ = 3.10 Hz, Pn H), 6.37 (1H, d, $^3J_{HH}$ = 3.44 Hz, Pn H), 6.05 (1H, d, $^3J_{HH}$ = 3.37 Hz, Pn H), 6.01 (0.5H, d, $^3J_{HH}$ = 2.92 Hz, Pn H), 6.00 (0.5H, d, $^3J_{HH}$ = 3.11 Hz, Pn H), 5.99 (1H, d, $^3J_{HH}$ = 2.98 Hz, Pn H), 5.93 (1H, d, $^3J_{HH}$ = 3.37 Hz, Pn H), 5.80 (0.5H, d, $^3J_{HH}$ = 3.37 Hz, Pn H), 5.72 (1H, d, $^3J_{HH}$ = 3.57 Hz, Pn H), 5.68 (0.5H, d, $^3J_{HH}$ = 3.37 Hz, Pn H), 5.57 (1H, d, $^3J_{HH}$ = 3.18 Hz, Pn H), 4.51 (s, free hydrogen), 3.09 (1H, s, unknown), 1.60 (6H, m, ^{i}Pr$_3$Si CH), 1.34 (6H, m, ^{i}Pr$_3$Si CH), 1.25-1.01 (56H, m, ^{i}Pr$_3$Si CH$_3$).

^{11}B NMR ($C_6D_5CD_3$), 399.5 MHz, -273.15 K): δ_B 28.52 (d, J_{BH} 136.24 Hz, borazine BH), -4.34 (s, br, "BCTB" BH), -9.57 ("CTB" BH), -20.91 (m, NH_3BH_3).
EI-MS: *m/z* = 965 $[Ti(\mu{:}\eta^5,\eta^5\text{-}Pn^\dagger)_2(BH_2NBH_3)]^+$; 878 $[Ti(\eta^8\text{-}Pn^\dagger)_2]^+$, 116 "BCTB" $[B_4H_{15}N_4]^+$, 87 "CTB" $[[H_2NBH_2]_3]^+$, 87 "BCDB" $[B_3H_{11}N_3]^+$, 81 "borazine" $[[HN{=}BN]_3]^+$, 79 "polyborazylene" $[[B_3H_4N_3]_n]^+$

Characterisation data for crystalline [Ti(μ:η^5,η^5-Pn†)]$_2$(μ-BH$_2$NBH$_3$) ***2.1***

^{1}H NMR (C_6D_6): δ_H 8.18 (1H, d, $^3J_{HH}$ = 2.98 Hz, Pn H), 8.04 (0.5H, d, $^3J_{HH}$ = 3.37 Hz, Pn H), 7.92 (1H, d, $^3J_{HH}$ = 2.98 Hz, Pn H), 7.86 (0.5H, d, $^3J_{HH}$ = 2.88 Hz, Pn H), 6.58 (1H, d, $^3J_{HH}$ = 3.18 Hz, Pn H), 6.56 (0.5H, d, $^3J_{HH}$ = 3.10 Hz, Pn H), 6.37 (1H, d, $^3J_{HH}$ = 3.44 Hz, Pn H), 6.05 (1H, d, $^3J_{HH}$ = 3.37 Hz, Pn H), 6.01 (0.5H, d, $^3J_{HH}$ = 2.92 Hz, Pn H), 6.00 (0.5H, d, $^3J_{HH}$ = 3.11 Hz, Pn H), 5.99 (1H, d, $^3J_{HH}$ = 2.98 Hz, Pn H), 5.93 (1H, d, $^3J_{HH}$ = 3.37 Hz, Pn H), 5.80 (0.5H, d, $^3J_{HH}$ = 3.37 Hz, Pn H), 5.72 (1H, d, $^3J_{HH}$ = 3.57 Hz, Pn H), 5.68 (0.5H, d, $^3J_{HH}$ = 3.37 Hz, Pn H), 5.57 (1H, d, $^3J_{HH}$ = 3.18 Hz, Pn H), 1.60 (6H, m, ^{i}Pr$_3$Si CH), 1.34 (6H, m, ^{i}Pr$_3$Si CH), 1.25-1.01 (56H, m, ^{i}Pr$_3$Si CH$_3$).

^{1}H NMR ($C_6D_5CD_3$), 399.5 MHz, -273.15 K): δ_H -0.39 (2H, br, s, weak, BH_2), -2.77 (3H, br, s, weak, BH_3).

$^{13}C\{^{1}H\}$ NMR: δ_C 139.6 (Pn C), 138.2 (Pn C), 137.5 (Pn C), 135.0 (Pn C), 131.1 (Pn C), 131.0 (Pn C), 130.9 (Pn C), 130.7 (Pn C), 130.6 (Pn C), 130.2 (Pn C), 130.0 (Pn C), 129.9 (Pn C), 126.4 (Pn C), 126.4 (Pn C), 126.3 (Pn C), 126.0 (Pn C), 125.3 (Pn C), 122.6 (Pn C), 121.0 (Pn C), 111.6 (Pn C), 111.4 (Pn C), 109.4 (Pn C), 109.0 (Pn C), 107.5 (Pn C), 107.4 (Pn C), 107.3 (Pn C), 105.41 (Pn C), 98.15 (Pn bridgehead C), 98.03 (Pn bridgehead C), 97.8 (Pn bridgehead C), 97.4 (Pn bridgehead C), 95.0 (Pn bridgehead C), 94.5 (Pn bridgehead C), 34.2 (^{i}Pr$_3$Si methyl), 23.9 (^{i}Pr$_3$Si methyl), 22.5 (^{i}Pr$_3$Si methyl), 22.0 (^{i}Pr$_3$Si methyl), 21.8 (^{i}Pr$_3$Si methyl), 21.7 (^{i}Pr$_3$Si methyl), 21.5 (^{i}Pr$_3$Si methyl), 21.2 (^{i}Pr$_3$Si methyl), 20.7 (^{i}Pr$_3$Si methyl), 20.6 (^{i}Pr$_3$Si methyl), 20.5 (^{i}Pr$_3$Si methyl), 20.2(^{i}Pr$_3$Si methyl), 20.0 (^{i}Pr$_3$Si methyl), 19.6 (^{i}Pr$_3$Si methyl), 19.2 (^{i}Pr$_3$Si methyl), 17.1 (^{i}Pr$_3$Si CH), 15.9 (^{i}Pr$_3$Si CH), 14.0 (^{i}Pr$_3$Si CH), 11.5 (^{i}Pr$_3$Si CH).
$^{29}Si\{^{1}H\}$ NMR: δ_{Si} -3.00 (*i*Pr$_3$ Si), 2.42 (*i*Pr$_3$ Si), 2.27 (*i*Pr$_3$ Si), 2.05 (*i*Pr$_3$ Si).
Solid state NMR:
$^{11}B\{^{1}H\}$ NMR (DEPTH, spinning frequency 15 KHz): δ_B 18.17, -10.30, -30.82, -38.03.
$^{29}Si\{^{1}H\}$ NMR (spinning frequency 10 KHz): δ_{Si} 1.30, -0.22
.EI-MS: *m/z* = 965 $[[Ti(\mu{:}\eta^5,\eta^5\text{-}Pn^{\dagger})]_2(\mu\text{-}BH_2NBH_3)]]^+$; 878 $[Ti(\eta^8\text{-}Pn^{\dagger})_2]^+$
Elemental analysis (calculated for $C_{54}H_{97}B_2Nsi_4Ti_2.C_5H_{12}$): C, 65.81 (65.94); H, 10.96(10.58); N, 1.70 (1.58)%.
Crystallographic data for $[Ti(\mu{:}\eta^5,\eta^5\text{-}Pn^{\dagger})]_2(\mu\text{-}BH_3NBH_2)$:

Formula weight 1037.22

Triclinic. Space group P-1, green block. A = 14.1717(9) Å, b = 14.2439(7) Å, c = 18.5527(9) Å, α = 88.783(4)° β = 69.177(5)°, γ = 64.739(5)°.

Volume = 3127.8(3) Å^3, T = 173 K, Z = 2, R_{int} = 0.0391, Cu(Kα) λ = 1.54178 Å

Maximum θ = 71.44 °, R_1 [I>2σ(I)] = 0.0511, wR_2 (all data) = 0.1478, GooF = 1.047.

Notes: Range and approximate integration values given for ^{i}Pr CH and ^{i}Pr CH_3 ^{1}H NMR due to high degree of peak overlap. Negative ppm peaks attributed to **2.1** BH_2 and BH_3 groups recorded in deuterated toluene ^{1}H spectrum with widened spectral window.

Solid state NMR spectroscopy was conducted by Dr. Nick Rees and Dr. Alexander Kilpatrick at the University of Oxford.

R2.3) Synthesis of Aminodiborane

50 mg (1.61 mmol) NH_3BH_3 was added to a small ampoule and dissolved in THF. 160 µL (1.60 mmol) of BH_3.THF was added *via* microsyringe. The solution was allowed to stir for 4 hours and filtered to remove a white precipitate. The resulting aminodiborane was concentrated by removal of excess THF *in vacuo* at 0°C.

^{1}H NMR: δ_H 3.35 (2H, t, $^3J_{HH}$ 6.52 Hz, aminodiborane NH), 1.52 (m, THF), 3.52 (m, THF).

^{11}B NMR: δ_B 18.09 (s, br, impurity), -11.17 (t, br, impurity BH_2), -21.34 (m, br, impurity), -26.88 (t, br, J_{BH} 153.14 Hz, aminodiborane BH_2).

R2.4) Reaction of [Ti(µ:η^5,η^5-Pn†)]$_2$ with Aminodiborane (excess)

50 mg (0.05 mmol) of **1.1** was added into a Rotaflow ampoule and dissolved in 1 mL of toluene. 0.1 mL of aminodiborane THF solution was added. An immediate colour change to brown was observed.

^{1}H NMR: δ_H 7.28 (1H, d, $^3J_{HH}$ 2.95 Hz, Pn H), 7.24 (1H, d, $^3J_{HH}$ 2.95 Hz, Pn H), 7.09 (1H, d, $^3J_{HH}$ 3.23 Hz, Pn H), 6.51 (1H, d, $^3J_{HH}$ 2.80 Hz, Pn H), 6.30 (1H, d, $^3J_{HH}$ 3.23 Hz, Pn H), 5.81 (1H, d, $^3J_{HH}$ 3.52 Hz, Pn H), 5.62 (1H, d, $^3J_{HH}$ 3.38 Hz, Pn H), 5.34 (1H, d, $^3J_{HH}$ 3.42 Hz, Pn H), 3.38 (2H, t, $^3J_{HH}$ 6.50 Hz, aminodiborane NH), 1.33-0.85 (70H, m, br, ^{i}Pr$_3$Si CH$_3$).

^{11}B{^{1}H} NMR: δ_B 31.85 (s, br, borazine BH), 30.52 (s, br, polyborazylene BH), 18.16 (s, br, impurity), -11.13 (s, br, impurity), -21.56 (s, br, impurity), -26.88 (s, br, aminodiborane BH_2).

R2.5) Reaction of [Ti(µ:η^5,η^5-Pn†)]$_2$ with 1 Equivalent of HNMe$_2$BH$_3$

40 mg (0.04 mmol) of **1.1** was added to a small Rotaflow ampoule. 2 mgs of solid $HNMe_2BH_3$ (0.04 mmol) was added and the mixture was then dissolved in toluene (1 mL). A colour change to brown was evident, with signs of effervescence.

^{1}H NMR: δ_H 3.47 (1H, s, $HNMe_2BH_3$), 3.19 (1H, s, $HNMe_2BH_3$), 2.91 (1H, s, $HNMe_2BH_3$).

^{11}B NMR: δ_B 38.17 (t, J_{BH} 122.80 Hz, $H_2B{=}Nme_2$ BH_2), 5.41 (t, J_{BH} 113.35 Hz, [H_2B-Nme_2]$_2$ BH_2), 2.16 (t, J_{BH} 108.02 Hz, [H_2B-Nme_2]$_3$ BH_2), -13.14 (m, $HNMe_2BH_3$ BH_3).

R2.6) Reaction of [Ti(μ:η^5,η^5-Pn†)]$_2$ with Net$_3$BH$_3$

20 mg (0.02 mmol) of complex **1.1** was mixed with 2 mg of $HNEt_3BH_3$ (0.02 mmol) and 1 mL of toluene was added. In addition to effervescence, an immediate colour change to purple was observed.

^{1}H NMR: δ_H 3.46 (1H, s, Net_3BH_3), 3.18 (1H, s, Net_3BH_3), 2.90 (1H, s, Net_3BH_3).
^{11}B NMR: δ_B 38.14 (t, J_{BH} 119.37 Hz, $H_2B{=}Net_2$ BH_2), 5.41 (t, J_{BH} 113.35 Hz, $[H_2B\text{-}Net_2]_2$ BH_2), -12.26 (m, $HNEt_3BH_3$ BH_3).

Chapter 3 – Pentalene Titanium Halide Complexes

Introduction

Salt metathesis and transmetalation reactions are some of the most powerful transformative tools in modern organometallic chemistry; instrumental whether seeking to synthesise a novel inorganic compound from simple precursors or modify an existing metal complex by exchanging bound ligands for new reactive functional groups.

Despite their prevalence and utility, these reactions are dependent on the displacement of a leaving group from the metal centre. For this reason, while the Ti-Ti double bond of compound **1.1** allows for interesting reactivity with heteroallenes and small molecules,[65,66] the lack of any bound leaving groups makes it a poor precursor for further derivative pentalene complexes, such as titanium metal alkyls or hydrides.

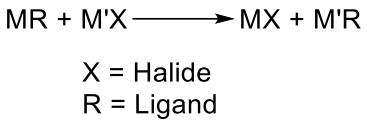

Scheme 3.1 Generic transmetalation reaction with a metal halide species.

To improve the compatibility of **1.1** with a wide range of nucleophiles and target novel pentalene titanium compounds, it was decided to react **1.1** with a range of halogen transfer agents, with the goal of creating titanium pentalene metal halide compounds while preferably retaining the Ti-Ti metal bond.

As previously mentioned in chapters one and two, in addition to their use as synthetic precursors, metal halides also have a history of practical use in the field of catalysis, most notably in the form of group IV metal dichloride Ziegler-Natta type catalysts.[5,100] Titanocene dichloride compounds have also seen increasing use as catalysts for organic transformations, such as the Pauson-Khand intramolecular synthesis of bicyclic cyclopentenones from enynes.[101] For this reason, performing reactivity studies of any isolated pentalene metal halides was also of interest.

In 2013 the O'Hare group succeeded[72] in synthesising $[TiCl(\eta^8\text{-}Pn^*)]_2(\mu\text{-}Cl)_2$. This was accomplished *via* two different synthetic routes. The first utilised addition of $PbCl_2$ to a reaction mixture of $TiCl_3.3THF$ and $Li_2Pn(TMEDA)_x$. The products formed prior to addition of $PbCl_2$ are not reported, though given the overwhelming similarity of the

reaction to that of $TiCl_3.3THF$ with $[K]_2[Pn^{\dagger}]$, it is likely a mixture of $[Ti(\eta^8\text{-}Pn^*)]_2(\mu\text{-}Cl)_3$ and $[TiCl(\eta^8\text{-}Pn^*)]_2(\mu\text{-}Cl)_2$ analogous to the $\eta^8\text{-}Pn^{\dagger}$ dimeric bridged chloride titanium compounds previously described in Chapter 1. $PbCl_2$ has previously been employed as a mild oxidant[102] to introduce chloride groups to Cp* titanocenes, making it a rational choice for further chlorinating this mixture.

However, yield for the reaction was limited to eight percent. This result was attributed by O'Hare *et al.* to the highly reducing nature of the permethylpentalene dianion component of the $[Li]_2[Pn^*]$ salt.[23,72] In a successful attempt to find a higher-yielding alternative, *cis*-$(SnMe_3)_2Pn^*$ was synthesised *in situ* and the use of $PbCl_2$ was avoided altogether by replacing the metal halide precursor $TiCl_3.3THF$ with $TiCl_4.2THF$, effectively pre-including the desired chloride groups before assembly of the pentalene sandwich structure.[72]

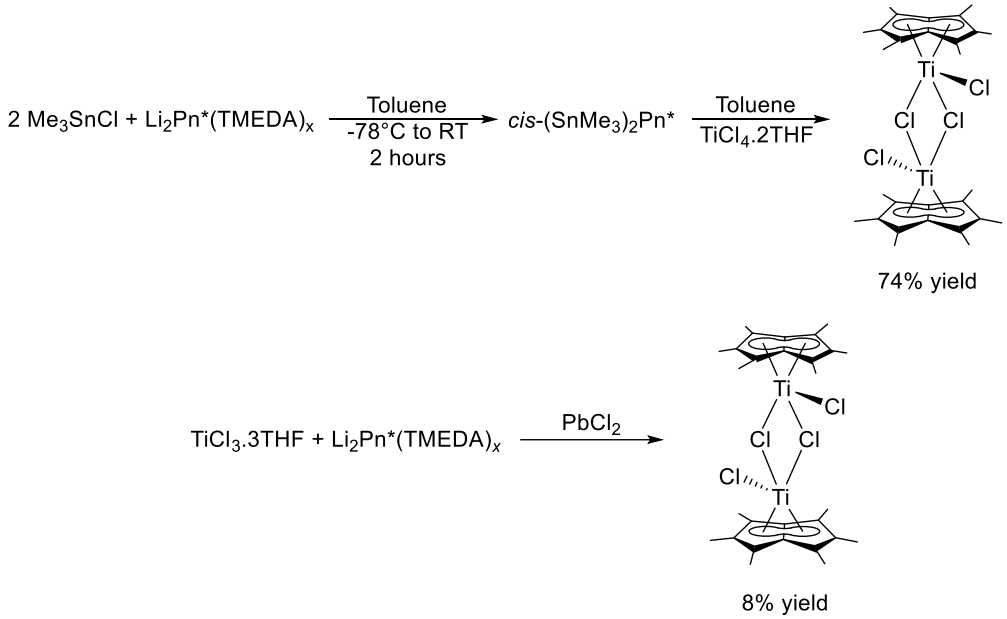

Scheme 3.2 Synthesis[72] of $[TiCl(\eta^8\text{-}Pn^*)(\mu\text{-}Cl)]_2$.

Once isolated, $[TiCl(\eta^8\text{-}Pn^*)]_2(\mu\text{-}Cl)_2$ was then reacted with both methyl and benzyl Grignard reagents to furnish the appropriate pentalene metal alkyl compounds.[73]

These methods served as a conceptual basis for the first attempts to synthesise an array of titanium metal halides with the $Pn^{\dagger}$ ligand, the details of which will be discussed in this chapter.

Synthesis of $[TiCl(\mu:\eta^5,\eta^5\text{-}Pn^\dagger)]_2$ (3.1), $[TiCl_3(\eta^5\text{-}C_8H_4^{\dagger,\ 3\text{-}tBu})]$ (3.2), $[TiCl_3(\eta^5\text{-}C_8H_4^\dagger)]$ (3.3) and $[TiCl(\eta^8\text{-}Pn^\dagger)]_2(\mu\text{-}Cl)_2$ (3.4)

The first method attempted for the synthesis of $[TiCl(\eta^8\text{-}Pn^\dagger)]_2(\mu\text{-}Cl_2)$ utilised reaction of **1.1** with two equivalents of $PbCl_2$ in pyridine.

Formation of $[TiCl(\eta^8\text{-}Pn^\dagger)]_2(\mu\text{-}Cl_2)$ was confirmed by EI-MS in the form of a molecular ion observed at 1067 *m/z*. Although this result initially appeared promising, work up of the reaction mixture failed to yield crystalline material and the ^{1}H NMR spectrum depicted many weak, sharp peaks unattributable to any pentalene compound. Reactions with $PbCl_2$ were therefore discontinued. The poor results of this experiment with the less electron rich[23] $Pn^\dagger$ ligand suggest that although it was asserted[72] that the reductive power of Pn* lithium salts was the primary cause of low yields obtained by the O'Hare group, $PbCl_2$ may simply be unsuitable for use with low valent titanium pentalene compounds.

The reaction of $[K]_2[Pn^\dagger]$ with $TiCl_3$.3THF cleanly yields[51] bridging chloride compounds **(A)** and **(B)** (**Scheme 3.3**). **(A)**, the primary product at 80% yield, is a mixed valence Ti(IV)/Ti(III) species with 3 bridging chloride groups. The less abundant compound **(B)** is a homovalent Ti(III)/Ti(III) bimetallic with two bridging chlorides.

By contrast, the mixture resulting from reacting the $Pn^\dagger$ dianion with $TiCl_4$.2THF produced a ^{1}H NMR spectrum depicting several extremely broad peaks unattributable to any rational pentalene complex, and the mixture proved intractable. The ^{1}H NMR data does contain two very weak signals at δ_H 5.96 ppm and 6.21 ppm; upon reviewing the data after successful isolation of $[TiCl(\eta^8\text{-}Pn^\dagger)]_2(\mu\text{-}Cl_2)$ **3.4** by a different synthetic route, these signals were later recognised as belonging to the pentalene environments of **3.4**. This provides retrospective confirmation that the reaction does produce the target compound, but in extremely poor yield.

In comparison to the tin pentalene transfer agent used specifically[72] by O'Hare *et al.* to "soften" the pentalenyl dianion, the electronegativity difference in $[K]_2[Pn^\dagger]$ results in comparatively "hard" donor properties. This may have had an influence on the disappointing outcome of the reaction, though given the successful isolation of pentalene compounds from the titanium tri-chloride precursor using the same potassium salt, this seems unlikely.

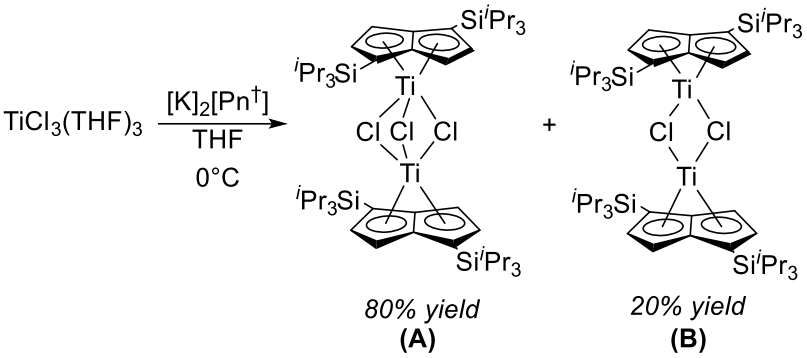

Scheme 3.3 Reaction of $[K]_2[Pn^{\dagger}]$ with $TiCl_3.3THF$.[51]

Given the lack of success with previous methodologies, it was next decided to experiment with direct reaction of halogenating agents with **1.1**. ^{t}BuCl was the first reagent chosen for these experiments; possessing a single chlorine atom, ^{t}BuCl allowed for convenient control of stoichiometry during sequential addition experiments. ^{1}H NMR spectra were recorded in intervals as each equivalent of ^{t}BuCl was added to the mixture. The reaction was conducted at -78°C, to preserve any thermally sensitive species in solution.

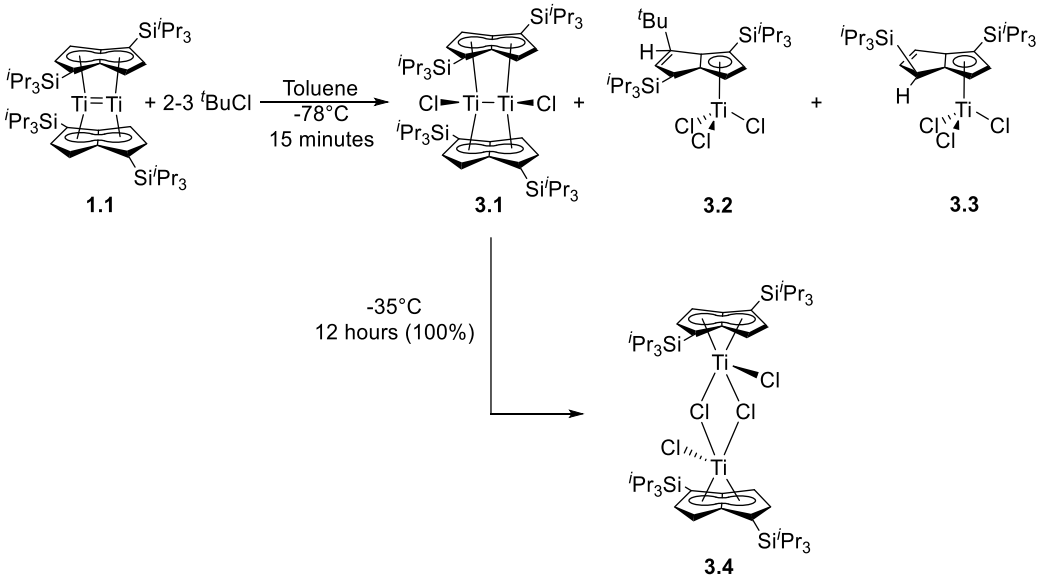

Scheme 3.4 Synthesis of $[TiCl(\mu{:}\eta^5,\eta^5\text{-}Pn^{\dagger})]_2$ **3.1**, $[TiCl_3(\eta^5\text{-}C_8H_4{}^{1,4\text{-TIPS, 3-}t\text{Bu}})]$ **3.2**, $[TiCl_3(\eta^5\text{-}C_8H_4{}^{1,4\text{-TIPS}})]$ **3.3** and $[TiCl(\eta^8\text{-}Pn^{\dagger})]_2(\mu\text{-Cl})_2$ **3.4**

With the addition of one equivalent of ^{t}BuCl, minor changes are visible in the ^{1}H NMR spectrum. Resonances characteristic of **1.1** at δ_H 6.82 ppm and 6.34 ppm remain the

most distinctive feature of the mixture, though around 20 additional peaks form in the aromatic region at around 25% of the integration of the **1.1** pentalene ring signals.

These peaks continue to grow as ^{t}BuCl is added. At three stoichiometric equivalents of ^{t}BuCl, the reaction proceeds to completion with the complete loss of peaks attributable to **1.1**. Analysis of the crude solution by ^{1}H NMR spectroscopy and EI-MS found evidence of two compounds: the metal halide sandwich compound $[TiCl(\mu{:}\eta^5,\eta^5\text{-}Pn^{\dagger})]_2$ **3.1** and a monometallic η^5-$Pn^{\dagger}$ titanium trichloride, $[TiCl_3(\eta^5\text{-}C_8H_4{}^{1,4\text{-TIPS, }3\text{-}t\text{Bu}})]$ **3.2** (*vide supra*). The most notable feature of this compound is the unexpected preference shown for η^5 ligation of the pentalene ligand and addition of a ^{t}Bu group to the pentalene carbocycle.

It was determined by a series of ^{1}H NMR array experiments that even at temperatures as low as -78°C, **3.1** begins to disproportionate into compound **3.4**, the targeted $Pn^{\dagger}$ analogue of $[TiCl(\eta^8\text{-}Pn^*)]_2(\mu\text{-}Cl)_2$. This is a rapid process at -35°C, with 80% conversion into **3.4** after only two hours. Full conversion, with no evidence of the presence of **3.1** by ^{1}H NMR spectroscopy, occurs after 12 hours at a storage temperature of -35°C. Raising the mixture to ambient temperature does not result in an increase in the yield of **3.4**; instead the complex degrades rapidly into a complicated mixture from which no pure compounds could be isolated. As a result of this behaviour **3.1** displays a very high degree of sensitivity to thermal conditions; reliable synthesis of **3.1** remains difficult at low temperatures and impossible above -78°C.

The final yield of **3.4** in solution by ^{1}H NMR is relatively poor, at 40% with respect to **1.1**. $[TiCl_3(\eta^5\text{-}C_8H_4{}^{1,4\text{-TIPS, }3\text{-}t\text{Bu}})]$ **3.2** is the main product of the reaction, accounting for the remaining 60% of the mixture. As **3.1** is the only product in solution that converts to **3.4**, it can be reasoned that halting the reaction as soon as possible results in a yield of 40% for **3.1** prior to formation of the dimeric bridged chloride compound, though this amount immediately begins to decrease over time.

Reactions with a large excess (ten equivalents) of ^{t}BuCl were performed to assess whether stoichiometry had any effect on the formation of this product; it was determined that reaction speed does not vary from addition of stoichiometric amounts of ^{t}BuCl, but yield of **3.2** increases until it is isolated as the sole product. **3.3** was serendipitously discovered in the same reaction mixture during X-Ray diffraction of crystalline material, but was not seen in the ^{1}H NMR spectrum of any ^{t}BuCl reaction

mixture, suggesting this species is formed in very low concentration. **3.3** shares the same η^5-Pn† ligation mode, but the pentalene-bound ^{t}Bu group is absent. The probable reasons for this were elucidated by further analysis of the TIPS group geometry seen in the X-Ray structure.

Characterisation of [TiCl(μ:η^5,η^5-Pn†)]$_2$ (3.1)

Complex **3.1** was observed by ^{1}H NMR spectroscopy five minutes after mixing **1.1** and ^{t}BuCl at -78°C in toluene. The ^{1}H NMR spectrum displays four pentalene ring hydrogen resonances at δ_H 8.10 ppm, 7.81 ppm, 6.19 ppm and 6.01 ppm. These observations are indicative of one compound of C_s symmetry retained in solution. EI-MS of the crude mixture yielded the characteristic molecular ion of 996 *m/z*.

Green/red crystals of **3.1** suitable for X-Ray diffraction were obtained on only one occasion from a THF solution stored at -35°C. Given the continuous conversion of **3.1** to the bridged chloride **3.4** in solution, attempts to further optimise the crystallisation of **3.1** instead consistently resulted in the isolation of **3.4** even with minimal solvent levels and storage at -78°C. This makes isolating crystalline material for the purposes of purification and further reactivity experiments impractical.

However, XRD analysis of a crystalline sample was successful in yielding a molecular structure (*vide infra*).

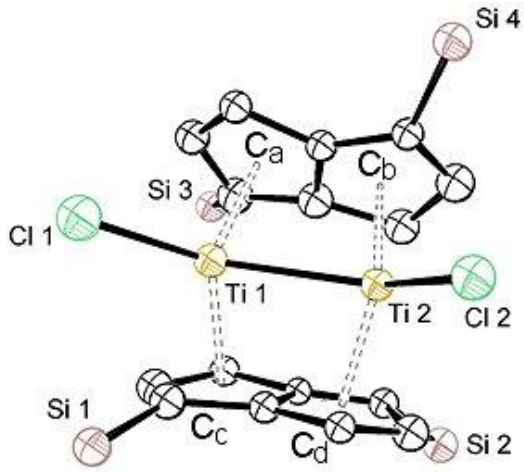

Figure 3.1 ORTEP diagram of **3.1**. ^{i}Pr and hydrogen groups omitted. Ellipsoids are shown at 50% probability

Parameter	Bond Length (Å)	Angle	(°)
Ti 1-Ti 2	2.681(9)	Hinge	4.04(14)
Ti 1-C_a	2.089(7)	Fold	8.07(4)
Ti 1-C_b	2.090(7)	Twist	4.70(3)
Ti 1-Cl 1	2.348(5)	C_a-Ti 1-C_b	137.40(2)
Ti 1-Ti 2	2.680(9)	C_c-Ti 2-C_d	136.40(2)
Ti 2-Cl 2	2.362(5)		
Ti 2-C_c	2.094(6)		
Ti 2-C_d	2.086(7)		
Bridgehead C-C	1.430(3)		

Table 3.1 Selected metrics for **3.1**.

A bimetallic Ti(III) halide species with an electron count of 16 per centre, the crystallographic data obtained for **3.1** supports retainment of the Ti-Ti bond. Measurements are represented in the table above and discussed further below, though the data obtained are of poor quality due to degradation of the crystal. This is reflected in an R_1 value of 0.2694, greater the values below 0.10 R_1 reported for other structures in this work. Metrics for this complex must therefore be taken as an approximation rather than definitive values.

The distance between the two metal centres is lengthened from 2.399(9) Å in **1.1** to 2.681(9) Å. This provides evidence for a bond order reduction to one.

Binding spatially bulky ligands to the metal(s) in a pentalene sandwich complex often results in a decrease in the C-M-C hinge angle from 180°, forcing the pentalene rings closer to one another. This is also observed in **3.1** with a metal-centroid-metal angle of 137.40°, significantly more acute than the value of 155.20° recorded for **1.1**. This degree of hinging alters the steric protection provided by the ligand, and is sufficient to preclude reactants from approaching from the obscured face. This results in a total preference for *cis* ligation of the halide groups, confirmed by lack of any evidence for formation of *trans*-isomers by ^{1}H NMR spectroscopy.

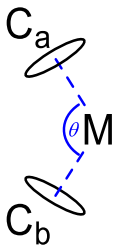

Figure 3.2 Centroid-Metal-Centroid Angle.

The metal-halide distances of 2.348(5) Å and 2.362(5) Å are in agreement with comparable literature values for titanocene chlorides and permethylpentalene metal halides.[72,76,103]

The twist angle measured between the two pentalene rings is 4.70°, a marked decrease from the 20.12° observed for **1.1**. This may be due to the diminished rigidity of the Ti-Ti single bond when compared to an M-M double bond interaction, allowing the structure the flexibility to settle into a conformation featuring minimal twist.

Fold angle, Ti-Centroid distances and bridgehead C-C length values remain consistent with those measured for **1.1**.[51]

Reactivity of [TiCl(μ:η^5,η^5-Pn†)]$_2$ (3.1)

Compound **3.1** remains perhaps the mot interesting halide synthesised by the ^{t}BuCl route due to the preservation of the Ti-Ti bond. Despite the propensity of the complex to convert to **3.4** in solution and difficulties encountered with crystallisation, further reactivity studies were attempted. Complex **3.1** was synthesised *in situ* and the methylating agent $MgMe_2$ was added. The results of this reaction are described in Chapter 4.

Characterisation of $[TiCl_3(\eta^5\text{-}C_8H_4{}^{1,4\text{-}TIPS,\ 3\text{-}tBu})]$ (3.2) and $[TiCl_3(\eta^5\text{-}C_8H_4{}^{1,4\text{-}TIPS})]$ (3.3)

Compound **3.2** is isolated as the primary product in reactions of 2-3 ^{t}BuCl with **1.1** and was analysed by ^{1}H, ^{13}C{^{1}H} and ^{29}Si{^{1}H} NMR spectroscopic techniques. **3.2** is stable in solution at ambient temperature.

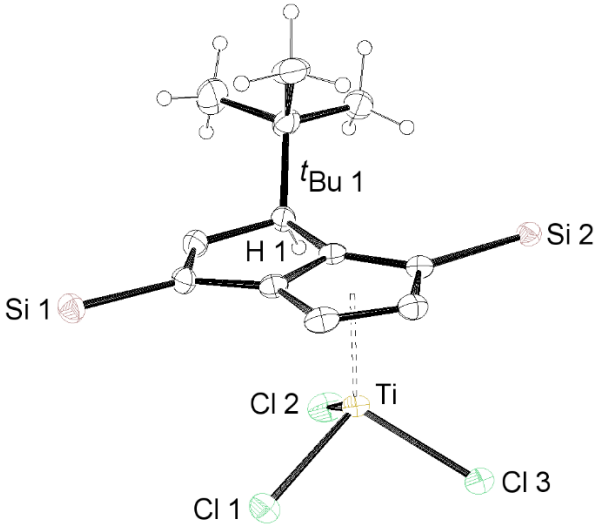

Figure 3.3 ORTEP diagram of **3.2**. Ellipsoids are at 50% probability. Hydrogens and ^{i}Pr groups omitted with exception of H 1 and the ^{t}Bu group.

Parameter	Bond Length (Å)	Angle	(°)
Ti -C_a	2.015(6)	Hinge	0.19(15)
Ti-Cl 1	2.239(10)	Fold	2.22(16)
Ti-Cl 2	2.233(10)	^{t}Bu-C-ring plane angle	24.65(13)
Ti-Cl 3	2.232(10)		
Bridgehead C-C	1.420(5)		

Table 3.2 Selected measurements for **3.2**.

The pentalene ligand exhibits the η^5 mode of bonding to a single titanium metal centre, which exists in a tetrahedral spatial conformation with three bound chloride atoms. This titanium centre possesses an electron count of 12, with a CBC coordination sphere definition of L_2X_4. Given this electron deficient state, it initially appears surprising that pentalene does not adopt an η^8 mode of ligation. While by no means definitive, applying cautious, reasoned speculation to the mechanism that results in the formation of **3.4** provides some insight into the geometry observed. In a reaction in which pentalene is

free to ligate η^8 to the metal centre, addition of a halide transfer agent would likely result in either direct formation of **3.4** as the metal-metal interaction is lost, or formation of a transient monometallic compound with two bound chlorides and elements of *pseudo*-tetrahedral geometry. This species would possess an electron count of 14 and would be free to immediately dimerise with another molecule to give **3.4**, a stable η^8 compound with "LX" bridging chlorides, counted at 16 electrons. **3.2** would not be observed. A similar process is postulated[72] by O'Hare *et al.* during the synthesis of $[TiCl(\eta^8\text{-}Pn^*)]_2(\mu\text{-}Cl)_2$.

In practice, although some formation of **3.4** is seen, **3.2** remains the dominant product even with strict adherence to two equivalents of ^{t}BuCl. This implies that the coordination of the pentalene ligand is being restricted during the reaction to give preference to η^5 binding. Addition of the ^{t}Bu group to the half of the pentalene carbocycle which shows no interaction with the metal centre causes partial loss of aromaticity of the pentalene ligand. This results in behaviour usually observed with the use of hydropentalenyl monoanionic salts of pentalene, which may only interact with the metal through one delocalised ring system with a maximum hapticity of η^5, akin to the L_2X binding mode of a cyclopentadienyl group. It is likely the titanium centre is offered steric stabilisation by the three chloride groups, which possess sufficient bulk to close the face of the coordination sphere unprotected by the pentalene ligand. It is perhaps surprising, given the tendency for titanium chloride species to dimerise when electron deficient, that ligation of three chlorine atoms occurs over coordination of two, which would allow for dimerisation to yield the theoretical *anti*-bimetallic Ti(III)/Ti(III) compound $[TiCl(\eta^5\text{-}C_8H_4{}^{1,4\text{-}TIPS,\ 3\text{-}tBu})]_2(\mu\text{-}Cl)_2$. This compound has 13 e^- per metal centre, doubling to 26 e^- for the entire system. Elevating the temperature of the reaction mixture is of future interest to determine if dimerisation can occur during formation of **3.2**.

The ^{1}H NMR spectrum of **3.2** displays 2 Pn-H signals at δ 7.22 ppm and 6.87 ppm, in integration 1:2 respectively. The greater integration of the δ_H 6.87 ppm peak corresponds to the equivalent wing-tip Pn-H environments adjacent to the TIPS groups. A third signal is present at δ_H 4.28 ppm corresponding to the allylic proton H 1, positioned on the carbon bound to the ^{t}Bu group. The ^{t}Bu group itself is seen as a singlet at δ_H 0.92 ppm.

Heteronuclear NMR supports the solid state structure, with eight pentalene carbon environments present by $^{13}C\{^{1}H\}$ NMR. The ring ^{t}Bu group is present at δ_C 36.3 ppm. The $^{29}Si\{^{1}H\}$ NMR spectrum shows two silicon environments at δ_{Si} 0.45 ppm and -0.88 ppm. Elemental analysis of crystalline material confirmed the validity of the predicted composition of the compound based on the solid structure of **3.2**.

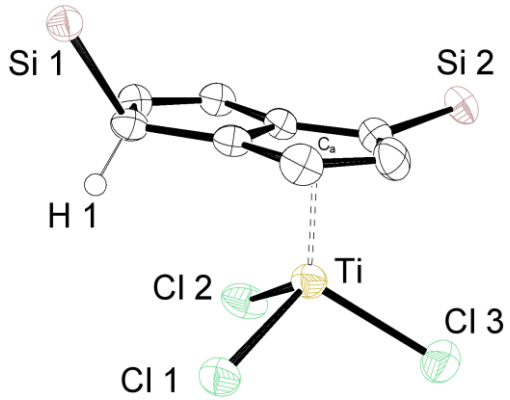

Figure 3.4 X-Ray structure of **3.3**. ^{i}Pr and hydrogen groups omitted for clarity, with the exception of H 1. Ellipsoids are shown at 50% probability.

Parameter	Bond Length (Å)	Angle	(°)
Ti-C_a	2.032(8)	Hinge	0.70(2)
Ti-Cl 1	2.229(14)	Fold	1.90(2)
Ti-Cl 2	2.248(14)	Si 1 to ring plane angle	38.20(2)
Ti-Cl 3	2.248(14)	Si 2 to ring plane angle	8.90(2)
Bridgehead C-C	1.430(6)		

Table 3.3 Selected bond length and angle measurements obtained from the crystal diffraction pattern of **3.3**.

Complex **3.3** (*vide supra*) was observed in a mixture with **3.2** by X-Ray diffraction, but by no other characterisation method, implying the presence of this compound in very low concentration. The compound displays the same η^5 pentalene binding mode as **3.2**, though no ^{t}Bu unit is bound to the pentalene ring.

Examination of the X-Ray diffraction data clearly shows a 38° deviation from planarity by one of the pentalene 1,4-triisopropylsilyl groups. By comparison, the TIPS group closest to the metal centre displays an angle of only eight degrees, comparable to other pentalene species synthesised in this work. This likely occurs due to protonation of the ring system, resulting in addition of a hydrogen atom at carbon position 1 – the same

carbon which binds TIPS group the pentalene ring. While no hydrogen atom is clearly defined by the X-Ray diffraction data, manual addition of a hydrogen group (H 1) to the carbon atom bound to the silicon group (marked as C 1) provides a rational explanation for the η^5 ligation mode. The precise source or mechanism of addition of the hydrogen group remains unknown, though hydride abstraction from the reaction solvent after activation of the ring system is the most likely possibility.

Optimised Synthesis of $[TiCl(\eta^8\text{-}Pn^{\dagger})]_2(\mu\text{-}Cl)_2$ (3.4)

The mixture of **3.4** and **3.2** produced by the ^{t}BuCl synthetic route was found to co-crystallise at -35°C to give green-red dichroic crystals distinguished visually only by minor visible changes in morphology. Given the similarity in solubility of the compounds, facile separation of each component was not possible.

As ^{t}BuCl also demonstrated an affinity for making undesired modifications to the pentalene ring, the ^{t}BuCl methodology was judged to be ill-suited to isolating these novel pentalene compounds for individual analysis. Other halide transfer agents were experimented with to determine if **3.4** or **3.1** could be isolated in exclusivity. Trityl chloride mimicked the reactivity of ^{t}BuCl, producing **3.1** (and thus **3.4** post-conversion). However, while **1.1** is completely consumed over the course of the reaction with trityl chloride when monitored by ^{1}H NMR spectroscopy, the characteristic resonances of **3.1** and **3.4** appeared very weak. Over 12 hours, the product signals did not show any increase in integration, with a large number of unidentified doublets instead appearing in the aromatic region of the spectrum. The reason for this is unknown, though such an observation is usually indicative of decomposition.

1,2-dichloroethane was then considered as an alternative, as it possessed several characteristics deemed useful for this reaction. Upon donating chloride groups to a metal, 1,2-DCE forms only ethylene as a waste product, which is easily removed *in vacuo*. 1,2-DCE is also a common laboratory solvent, and is cost-effective to procure and purify.[94] Finally, the reaction of **1.1** with ^{t}BuCl required two to three equivalents of the halide in solution to produce isolable pentalene compounds. Containing two halide groups per molecule, only one to two equivalents of 1,2-DCE would be necessary for the reaction to proceed to completion.

1,2-DCE proved effective in practice as well as theory. When reacted with **1.1**, **3.4** was reliably isolated as a dichroic crystalline material, although the final yield was poor (30%). No other chloride compounds were observed in solution by NMR spectroscopy.

Poor yield resulted from all attempts to synthesise metal halides from **1.1**, regardless of halide transfer agent used. It was thus decided to attempt addition of 1,2-DCE to the mixture of chloride bridged titanium compounds **(A)** and **(B)** resulting from the reaction of $[K]_2[Pn^{\dagger}]$ with $TiCl_3.3THF$. This was intended to synthesise **3.4** directly, without the prior requirement of isolating **1.1**, eliminating the need to reduce the mixture with K/Hg amalgam prior to conversion to the final metal halide compound.

Adding a slight excess (three equivalents) of 1,2-DCE at room temperature to a toluene solution of the chloride-bridging compounds slowly results in a subtle colour change from dark green to light emerald-green. ^{1}H NMR analysis of an aliquot sampled at this time shows the presence of small quantities of **3.4**, though **3.1** is absent. However, the reaction progresses very slowly at ambient temperature. Making the reasoned deduction that **3.4** is the primary thermodynamic product of the reaction given that **3.1** is isolated at very low temperatures and forms **3.4** with increasing speed when warmed, the temperature was increased to 90°C and the mixture was allowed to stir overnight. The resulting solution underwent a pronounced colour change to dark red. After analysis by ^{1}H NMR spectroscopy, this colour was found to be indicative of the large-scale formation of **3.4**. While **3.4** is dichoric red-green in the crystalline or powdered state, the compound is exclusively red in solution.

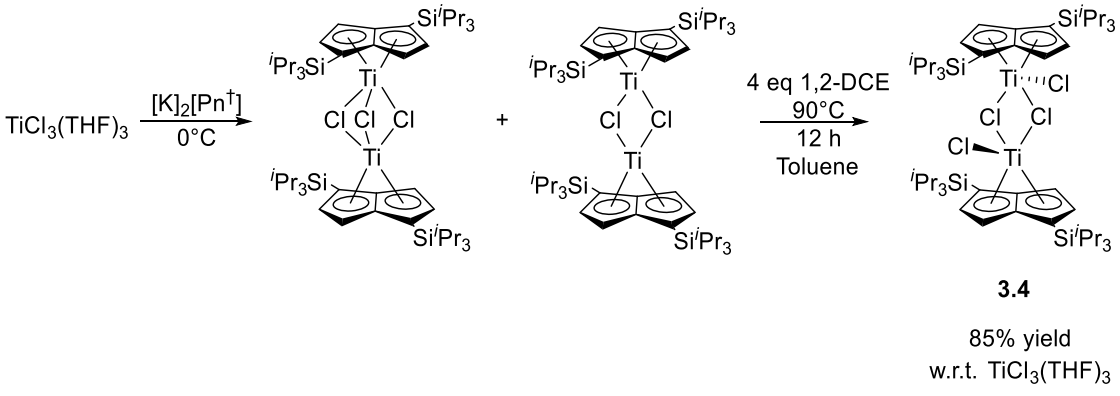

Scheme 3.5 Optimised synthetic route to **3.4**.

The yield of this new route was 80% of **3.4** obtained in absence of impurities. This significant improvement to the procedure allowed for efficient multi-gram scale isolation of pure **3.4**, instrumental in further synthetic experiments.

Characterisation of $[TiCl(\eta^8\text{-}Pn^{\dagger})]_2(\mu\text{-}Cl)_2$ (3.4)

Complex **3.4** is a dimeric, homovalent Ti(IV)/Ti(IV) ^{8}-Pn† complex with an electron count of 16 e^- per metal centre.

The ^{1}H NMR data obtained for **3.4** is consistent with a complex of C_{2h} symmetry on the NMR timescale, with two pentalene ring hydrogen environments at δ_H 6.21 ppm and 5.99 ppm. The 1,4-TIPS groups manifest as a single ^{i}Pr CH resonance at δ_H 1.24 ppm, while the ^{i}Pr CH_3 groups are seen at δ_H 1.11 ppm and 1.06 pm.

The stability of **3.4** allowed for full collection of heteronuclear NMR data. The ^{29}Si{^{1}H} NMR spectrum of **3.4** displays one silicon resonance at δ_{Si} 0.70 ppm, while the ^{13}C{^{1}H} NMR spectrum of the compound displays four pentalene carbon environments. Complex **3.4** was also characterised by EI-MS, which produced the characteristic molecular ion of 1067 *m/*z. Elemental analysis further corroborated this result, returning a composition consistent with all other methods of characterisation. X-Ray diffraction of crystalline material produced a solid state structure for the complex.

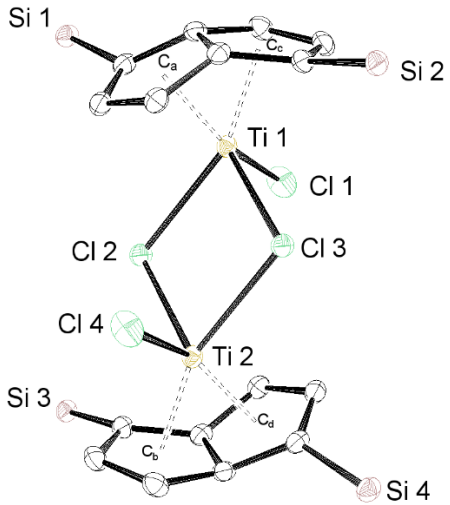

Figure 3.5: ORTEP view of **3.4**. Ellipsoids are at 50% probability, ^{i}Pr and hydrogen groups omitted.

Parameter	Bond Length (Å)	Angle	(°)
Ti 1-C_a / Ti 1-C_d	1.975(10)	Hinge	0.80(3)
Ti 1 - C_b / Ti 1-C_C	1.973(1)	Fold	31.80(3)
Ti 1-Cl 2 / Ti 2-Cl 1	2.313(2)	Twist	0.00(11)
Ti 1-Cl 4 / Ti 2-Cl 4	2.559(18)		
Ti 1-Cl 3 / Ti 2-Cl 3	2.423(16)		
Bridgehead C-C	1.460(8)		

Table 3.4: X-Ray structure length and angle measurements for **3.4**.

Bond lengths obtained from X-Ray diffraction analysis of **3.4** are in good agreement with bond parameters reported for the permethylpentalene analogue synthesised by O'Hare and co-workers. O'Hare *et al.* describe[72] a terminal Ti-Cl bond length of 2.359(10) Å, while **3.4** displays a shorter length of 2.313(2) Å.

3.4 possesses an average Ti-(μ-Cl) distance of 2.491(16) Å, comparable to the reported value of 2.485(1) Å for [TiCl(η^8-Pn*)](μ-Cl)$_2$. Fold angle differences between the structures amount to only two degrees.

Complex **3.4** was used extensively as a precursor for the synthesis of titanium pentalene alkyl compounds. The results of these reactions are discussed in detail in Chapter 4. Attempts were also made to assess whether **3.4**, **3.3** or **3.2** showed any catalytic activity towards the polyermisation of ethylene in combination with MMAO; unfortunately, no evidence of polymer formation was observed.

Attempted Synthesis and Characterisation of [Ti(μ:η^5,η^5-Pn†)]$_2$(μ-I) (3.5.1) and [TiI(μ:η^5,η^5-Pn†)]$_2$ (3.5.2)

In addition to targeting titanium chloride compounds, attempts were made to synthesise iodide analogues of these complexes.

Compound **1.1** was reacted with with 0.5 equivalents of iodine, accomplished *via* a stock solution of iodine in C_6D_6. The EI-MS spectrum of this mixture yielded a molecular ion value of 1052 *m/*z, consistent with the presence of a bimetallic pentalene sandwich compound with one bound iodide group. Very small purple crystals rapidly form from the reaction mixture once it is cooled to -35°C, and a sample was sent to the National Crystallography Service for XRD analysis. The structure obtained depicts a metal halide derivative of **1.1**, with the two titanium centres bridged by a single iodine

atom. Unfortunately, the data collected was very poor due to the restricted size of the crystals and repeated attempts to slow the rate of crystallisation to offset this were unsuccessful. In light of this, while bond metrics are discussed below, the structure obtained is not of publication standard and the data must be treated with caution.

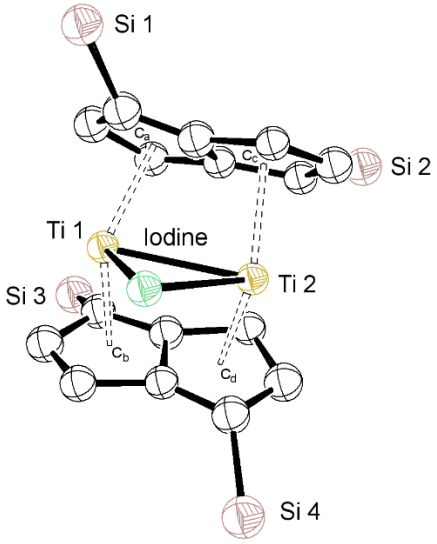

Figure 3.6 X-Ray crystal structure of compound **3.5.1**.

Parameter	Bond Length (Å)	Angle	(°)
Ti 1-C_a	2.185(2)	Hinge	1.80 (12)
Ti 1-C_b	2.095(4)	Fold	7.20(14)
Ti 2-C_c	2.102(4)	Twist	43.10(8)
Ti 2-C_d	2.130(5)	C_a-Ti 1-C_b	130.00(2)
Ti 1-Ti 2	2.648(8)	C_c-Ti 2-C_d	130.08(2)
Ti 1-Iodine	2.824(4)		
Ti 2-Iodine	2.825(4)		

Table 3.5 Selected metrics for crystal data obtained for **3.5.1**.

Compound **3.5.1** displays a near identical Ti-iodine bond length for each metal at 2.824(4) Å and 2.825(4) Å, placing the iodine group equidistant, bridging the metal centres. This value is elongated from average M-X bond distances of *ca.* 2.6 Å, suggestive of a weak bond.[72,103,104] The molecule exhibits folding along the bridgehead carbon-carbon bond at an angle of 7.20(14)°, consistent with a near-planar (μ:η^5,η^5-Pn†) sandwich conformation. This fold angle is slightly decreased compared to compound **3.1**, likely due to the greater size and centralised position of the iodine group. Centroid-metal-centroid angles for **3.5.1** follow the same pattern of one sided “hinging”

observed for **3.1**, but are more acute by 6-7°, showing that the centralised iodine has a greater effect than two terminal *cis*-chloride groups.

Unfortunately, supportive NMR evidence for this compound is limited. Crystals were isolated in low yield from the reaction mixture; a five milligram sample analysed by ^{1}H NMR produced no visible signals with the exception of deuterated solvent. It was unclear if this was due to the weak concentration of the sample, paramagnetism rendering the resonances too broad to observe, or a combination of both factors.

The ^{1}H NMR spectrum of the crude reaction mixture also provides little definitive support for the X-Ray structure obtained. With 30 mg of material in the sample, six sharp pentalene CH environments are observed at very low concentrations (approximately equal to C_6D_6 satellite peaks), ranging from δ_H 7.44 ppm to 6.50 ppm. Unreacted compound **1.1** is also observed at δ_H 6.82 ppm and 6.34 ppm.

A mono-iodide species should show asymmetry by ^{1}H NMR, displaying eight Pn-H environments. This geometry may be represented by the six peaks seen; given their low integration, it is possible two environments are obscured by the solvent. However, such a complex should also be paramagnetic, in contrast to the sharp and defined nature of these signals. Clear evidence of paramagnetism does exist in the ^{1}H NMR spectrum, with heavy signal broadening rendering the aliphatic region indistinct. If this broadening is representative of the mono-iodide in solution, it is possible that addition of 0.5 eq of I_2 to **1.1** results in an additional unknown diamagnetic, asymmetric di-iodide species that does not survive EI-MS analysis. This would also explain the presence of unreacted **1.1** confirmed present by EI-MS and ^{1}H NMR.

Reaction of **1.1** with one equivalent of I_2 produces a more straightforward ^{1}H NMR spectrum. Four signals characteristic of pentalene hydrogen groups are observed at δ_H 8.34 ppm, 8.20 ppm, 6.10 ppm and 6.03 ppm. This implies the synthesis of $[TiI(\mu{:}\eta^5,\eta^5\text{-}Pn^{\dagger})]_2$ **3.5.2**, which displays C_2 symmetry in solution consistent with a *cis*-di-iodide variant of compound **3.1**. EI-MS of this solution results in a second observation of the molecular ion associated with the mono-iodide at 1052 *m/z* despite no indication of the paramagnetic broadening or six previous ^{1}H NMR peaks observed in the spectrum of **3.5.1**. This is likely because the di-iodide compound breaks apart under the relatively harsh conditions used for EI-MS, producing the bridging mono-iodide *in situ*. In summary, while some compelling evidence exists for the formation of

compounds **3.5.1** and **3.5.2**, further characterisation of each species is required before a final conclusion can be made.

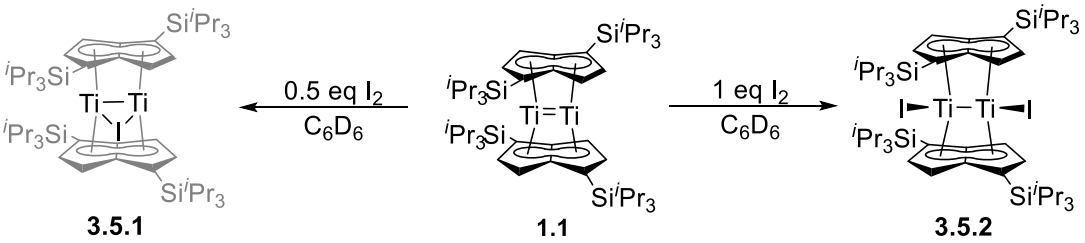

Scheme 3.6 Synthesis of **3.5.2** and **3.5.2**.

Synthesis and Characterisation of [(η^5-Cp*)Ti(η^8-Pn†)] (3.6)

Reaction of **3.4** with two equivalents of KCp* per titanium centre resulted in the synthesis of the paramagnetic Ti(III) mixed sandwich complex [(η^5-Cp*)Ti(η^8-Pn†)] **3.6**. Conventional ^{1}H and heteronuclear NMR analysis was of little use for characterising **3.6**, however EI-MS of a crystalline sample returned a spectrum of expected isotopic distribution, with one peak corresponding to the molecular ion, 597 *m/z*. The same EI-MS spectrum also yielded a prominent ion at 633 *m/z*, representative of [(η^5-Cp*)TiCl(η^8-Pn†)], however no further evidence of this mixed sandwich halide species was uncovered by other characterisation techniques. Isolated crystals were subjected to X-Ray analysis to yield a solid state structure.

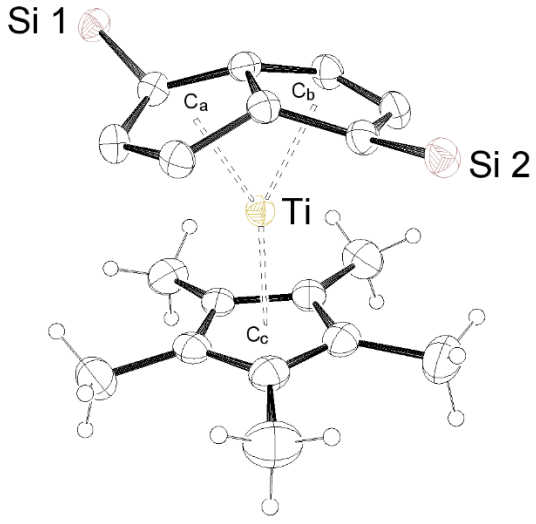

Figure 3.7 X-Ray diffraction diagram of complex **3.6**. 50% ellipsoid probabilities, pentalene hydrogen and ^{i}Pr groups omitted for clarity.

Parameter	Bond Length (Å)	Angle	(°)
Ti-C_a	1.954(10)	Hinge	0.79(6)
Ti-C_b	1.961(13)	Fold	35.22(3)
Ti-C_c	2.056(11)		
Bridgehead C-C	1.439(9)		

Table 3.6 Selected metrics and measurements for **3.6**.

The metrics obtained from the crystal structure of **3.6** are characteristic of η^8 pentalene ligation. Pentalene shows archetypal "umbrella" behaviour, folding at the bridgehead C-C bond to an angle of 35.22(3)°. This folding is also reflected in slightly reduced Ti-Centroid distances at 1.954(10) Å, in comparison to η^5 ligated pentalene compounds which typically show Ti-C_x distances of ~2 Å (this is observed in complex **3.1**, which possesses a Ti-C_a distance of 2.089(7) Å).

A literature precedent exists[105] for the oxidative addition of titanium Cp-Pn mixed sandwich complexes with 1,2-DCE or dibromoethane to give the corresponding mixed sandwich chloride or bromide. This was attempted for **3.6** with the goal of producing a metal halide derivative, but analysis by EI-MS and X-Ray diffraction confirmed no change in complex composition. The compound is the titanium analogue of the uranium species [(η^5-Cp^*)U(η^8-$Pn^\dagger$)], previously synthesised by the Cloke group and shown to bimolecularly bind and reduce dinitrogen to give a bridging diazenido $[N_2]^{2-}$ ligand.[43]

Conclusions

New pentalene titanium halide compounds were synthesised using several different methodologies, the most efficient of which was the targeted synthesis of [TiCl(η^8-$Pn^\dagger$)](μ-Cl)$_2$ **3.4** by reaction of 1,2-DCE with a mixture of [Ti(η^8-$Pn^\dagger$)](μ-Cl)$_3$ and [Ti(η^8-$Pn^\dagger$)](μ-Cl)$_2$.

Reactions between [Ti(μ:η^5,η^5-$Pn^\dagger$)]$_2$ **1.1** and ^{t}BuCl gave [TiCl(μ:η^5,η^5-$Pn^\dagger$)]$_2$ **3.1**, a bimetallic pentalene sandwich metal halide which retains the Ti-Ti bond of **1.1**, albeit with a reduced bond order of 1 confirmed by X-Ray diffraction analysis. The compound was highly sensitive to temperature and unstable in solution, with a propensity to dimerise to **3.4**. Many different reactions were performed between **3.4** and a variety of nucleophiles, however the majority of these experiments did not yield stable products.

Attempts were made to react the metal halide species isolated with ethylene in the presence of MMAO, but catalytic activity was not observed.

The ^{t}BuCl reaction also produced [$TiCl_3(\eta^5$-$Pn^{\dagger})$] compounds, which demonstrate restricted hapticity caused by unexpected ring substitution reactions by the halide transfer agent. However, these species remain stable at 12 e^- without degradation.

Reactions between **1.1** and 0.5 eq of I_2 in C_6D_6 resulted in the low-yield isolation of crystals of [$Ti(\mu$:η^5,η^5-$Pn^{\dagger})]_2(\mu$-I) **3.5.1**. As a paramagnetic compound, NMR spectroscopy proved ineffective for further characterisation. Early ^{1}H NMR experiments on the reaction between **1.1** and 1 eq of I_2 imply the possible formation of [$TiI(\mu$:η^5,η^5-$Pn^{\dagger})]_2$ **3.5.2**. However, both compounds lack full characterisation data and further experiments are required to confirm that these assignments are valid.

Finally, reaction of a KCp* salt with **3.4** yielded the mixed sandwich compound [$(\eta^5$-Cp*$)Ti(\eta^8$-$Pn^{\dagger})$] **3.6** in addition to the observation of [$TiCl(\eta^5$-Cp*$)(\eta^8$-$Pn^{\dagger})$] by EI-MS.

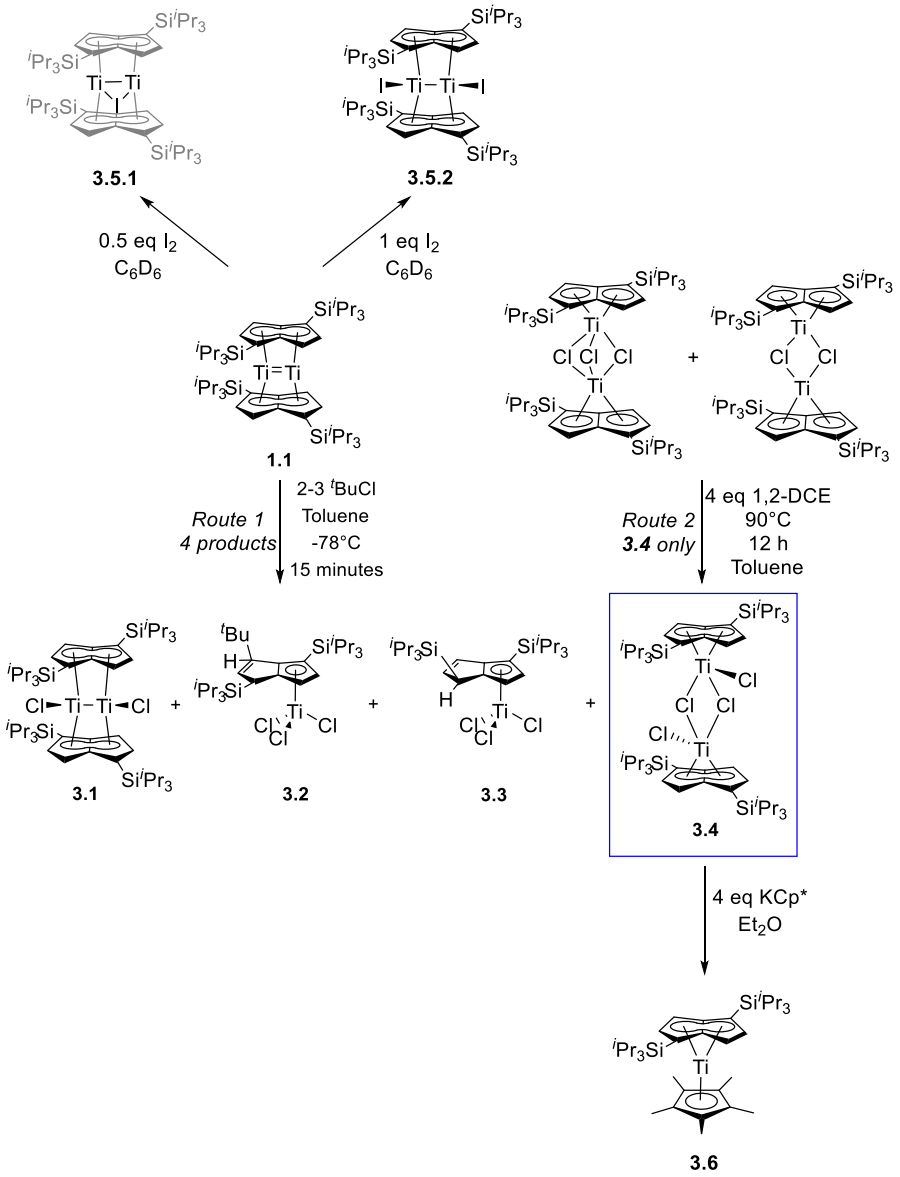

Scheme 3.7 Summary of isolated products (Chapter 3).

Chapter 3 Experimental Data

R3.0) Reaction of $[Ti_2(\mu{:}\eta^5,\eta^5\text{-}Pn^\dagger)]$ with $PbCl_2$ (3 Equivalents)

0.32 g (0.77 mmol) of $[K]_2[Pn^\dagger]$ was added to an ampoule equipped with a stirrer bar and dissolved in 10 mL of THF. 0.29 g (0.77 mmol) $TiCl_3(THF)_3$ was added to a Rotaflow ampoule charged with 100 mL THF. The $[K]_2[Pn^\dagger]$ solution was dropwise *via* cannula over two hours to the $TiCl_3(THF)_3$ solution under constant stirring. The reaction mixture was left to stir overnight.

The resulting green solution was taken into an argon filled glovebox and 0.65 g (2.34 mmol) of $PbCl_2$ partially dissolved in pyridine was decanted into the ampoule. The mixture was allowed to stir for 16 hours, after which an aliquot for EI-MS analysis was removed.

The ^1H NMR spectrum of this crude mixture features an extreme degree of broadening present in the aliphatic region. The aromatic region features many multiplets of unassignable origin.

EI-MS: *m/z* = 1067 $[[TiCl[(\eta^8\text{-}Pn^\dagger)]_2(\mu\text{-}Cl)_2]^+$

R3.1-R3.4) Synthesis of $[TiCl(\mu{:}\eta^5,\eta^5\text{-}Pn^\dagger)]_2$ (3.1), $[TiCl_3(\eta^5\text{-}Pn^{\dagger\text{-}3\text{-}tBu})]$ (3.2), $[TiCl_3(\eta^5\text{-}Pn^\dagger)]$ (3.3) and $[TiCl(\eta^8\text{-}Pn^\dagger)]_2(\mu\text{-}Cl)_2$ (3.4)

Addition of 3 equivalents of ^{t}BuCl to $[Ti_2(\mu{:}\eta^5,\eta^5\text{-}Pn^\dagger)_2]$

50 mg (0.06 mmol) of **1.1** was added to an ampoule fitted with a Rotaflow tap and 1 mL of toluene was added. 1.5 µL (0.18 mmol) of ^{t}BuCl was injected *via* a microsyringe. A colour change to bright red occurred over 12 hours. The sample produced red crystalline solids from a minimal volume THF solution stored at -35°C.

Yield $[TiCl_2(\mu{:}\eta^5,\eta^5\text{-}Pn^\dagger)]$ **3.1**: ~40% by ^1H NMR (pre-conversion).

Yield $[Ti(\eta^5\text{-}Pn^{\dagger\text{-}3\text{-}tBu})Cl_3]$ **3.2**: 22 mg (0.03 mmol), 58%.

Yield $[TiCl(\eta^8\text{-}Pn^\dagger)]_2(\mu\text{-}Cl)_2$ **3.4:** 40% by ^1H NMR (post-conversion).

Addition of 10 equivalents of ^{t}BuCl to [Ti$_2$(μ:η^5,η^5-Pn†)$_2$]

51 mg (0.06 mmol) of **1.1** was placed in a small Young's valve sealed ampoule and dissolved in 1 mL of toluene. 4.2 µL (0.60 mmol) of ^{t}BuCl was added *via* microsyringe. A colour change to bright red occurred over a period of 16 hours. Solvent was removed from the mixture *in vacuo*, the sample was filtered through a pipette packed with Celite® and the resulting solution furnished red crystals from pentane at -35°C.

Yield [Ti(η^5-Pn$^{\dagger\text{-3-tBu}}$)Cl$_3$] **3.2**: 33 mg (0.052 mmol), 89%.

*Characterisation data for [TiCl(μ:η^5,η^5-Pn†)]$_2$ **3.1**:*

^{1}H NMR (C$_7$D$_8$): δ_H 8.10 (2H, s, Pn H), 7.81 (2H, s, Pn H), 6.19 (2H, s, Pn H), 6.01 (2H, s, Pn H), 5.25 (ethylene), 2.92 (1,2-DCE), 1.78 (6H, m, ^{i}Pr$_3$Si CH), 1.53 (6H, m, ^{i}Pr$_3$Si CH), 1.18 (18H, d, $^3J_{HH}$ = 6.98 Hz, ^{i}Pr$_3$Si CH$_3$), 1.10 (18H, d, $^3J_{HH}$ = 7.04 Hz, ^{i}Pr$_3$Si CH$_3$), 1.04 (18H, d, $^3J_{HH}$ = 7.24 Hz, ^{i}Pr$_3$Si CH$_3$), 0.91 (18H, d, $^3J_{HH}$ = 7.04 Hz, ^{i}Pr$_3$Si CH$_3$).

EI-MS: *m/z* = 996 [(μ:η^5,η^5-Pn†)Ti$_2$Cl$_2$]$^+$

Crystallographic data for [TiCl(μ:η^5,η^5-Pn†)]$_2$ **3.1**:

Formula weight: 996.28

Monoclinic. Space group I2/a, red block. A = 20.0828(6) Å, b = 26.2576(7) Å, c = 42.5649(15) Å, α = 90° β = 91.830(3)°, γ = 90°.

Volume = 22434.1(12) Å^3, T = 173 K, Z = 24, R_{int} = 0.0911, Mo(Kα) λ = 0.71075 Å.

Maximum θ = 71.61°, R_1 [I>2σ(I)] = 0.2694, wR_2 (all data) = 0.7050, GooF = 3.199.

Note: Pn-H environments for **3.1** are listed as singlets without $^3J_{HH}$ values, as the multiplicity of the presumed doublet peaks in the aromatic region is poorly defined. Further ^{1}H NMR spectroscopy experiments were performed to rectify this, but data obtained from these repeats was poor, due to the decay of **3.1**. X-Ray data was solved and refined by the NCS at the University of Southampton. The data is unfit for publication due to degradation of the crystal, but provides corroborative evidence for the formation of **3.1** in combination with the ^{1}H NMR spectrum and EI-MS results.

Characterisation data for[$TiCl_3(\eta^5$-$Pn^{\dagger\text{-}3\text{-}tBu}$)] ***3.2****:*

^{1}H NMR: δ_H 7.22 (2H, d, $^3J_{HH}$ = 3.17 Hz, Pn H), 6.88 (1H, d, $^3J_{HH}$ = 3.00 Hz, Pn H), 4.28 (1H, d, , $^3J_{HH}$ = 1.68 Hz, allylic Pn ring hydrogen), 1.93 (3H, m, ^{i}Pr$_3$Si CH), 1.48 (3H, m, ^{i}Pr$_3$Si CH), 1.36 (9H, d, $^3J_{HH}$ = 7.51 Hz, ^{i}Pr$_3$Si CH$_3$), 1.19 (9H, d, $^3J_{HH}$ = 4.27 Hz, ^{i}Pr$_3$Si CH$_3$), 1.17 (9H, d, $^3J_{HH}$ = 3.68 Hz, ^{i}Pr$_3$Si CH$_3$), 1.10 (9H, d, $^3J_{HH}$ = 7.13 Hz, ^{i}Pr$_3$Si CH$_3$), 0.92 (9 H, s, ^{t}Bu CH$_3$).

^{13}C{^{1}H}NMR: δ_C 163.3 (Pn C), 160.9 (Pn C), 154.9 (Pn C), 147.3 (Pn C), 137.8 (Pn C), 137.4 (Pn C), 133.4 (Pn C), 117.6 (Pn C), 36.3 (Ring ^{t}Bu quaternary C), 30.0 (^{i}Pr$_3$Si CH$_3$), 20.5 (^{i}Pr$_3$Si CH$_3$), 19.5 (^{i}Pr$_3$Si CH$_3$), 14.5 (^{i}Pr$_3$Si CH$_3$), 12.6 (^{i}Pr$_3$Si CH), 12.4 (^{i}Pr$_3$Si CH$_3$), 12.2 (^{i}Pr$_3$Si CH), 12.1 (^{i}Pr$_3$Si CH).

^{29}Si{^{1}H}NMR: δ_{Si} 0.46 (^{i}Pr$_3$Si Si), -0.88 (^{i}Pr$_3$Si Si).

EI-MS: *m/z* = 626 [$TiCl_3(\eta^5$-$Pn^{\dagger\text{-}3\text{-}tBu}$)]$^+$

Elemental analysis (calculated for $C_{30}H_{55}Cl_3Si_2Ti$): C, 57.68 (57.55); H, 8.81 (8.85); N, 0.00 (0.00)%.

Crystallographic data for [$TiCl_3(\eta^5$-$Pn^{\dagger\text{-}3\text{-}tBu}$)] **3.2**:

Formula weight: 626.17

Triclinic. Space group P-1, red block. A =10.1440(13) Å, b = 13.5242(14) Å, c = 13.5962(14) Å, α = 97.419(8)° β = 104.342(10)°, γ = 102.106(10)°.

Volume = 1734.4(4) Å^3, T = 173 K, Z = 2, R_{int} = 0.0462, Cu(Kα) λ = 1.54184 Å.

Maximum θ = 70.77°, R_1 [I>2σ(I)] = 0.0628, wR_2 (all data) = 0.1832, GooF = 1.048.

Characterisation data for [$TiCl_3(\eta^5$-$Pn^{\dagger}$)] ***3.3****:*

Formula weight: 961.87.

Triclinic. Space group P-1, red block. A = 8.3350(3) Å, b = 13.6146(4) Å, c = 14.0238(6) Å, α = 107.435(3)° β = 94.924(3)°, γ = 92.561(3)°.

Volume = 1508.52(10) Å^3, T = 173 K, Z = 2, R_{int} = 0.0786, Mo(Kα) λ = 0.71075 Å.

Maximum θ = 29.75°, R_1 [I>2σ(I)] = 0.0628, wR_2 (all data) = 0.2569, GooF = 1.043.

Characterisation data for [TiCl(η^8-Pn†)]$_2$(μ-Cl)$_2$ ***3.4****:*

^{1}H NMR ($C_6D_5CD_3$), 399.5 MHz: δ_H 6.21 (4H, d, $^3J_{HH}$ = 3.42 Hz, Pn H), 5.99 (4H, d, $^3J_{HH}$ = 3.41 Hz, Pn H), 1.24 (12H, m, ^{i}Pr$_3$Si CH), 1.11 (36H, d, $^3J_{HH}$ = 7.31 Hz, ^{i}Pr$_3$Si CH$_3$), 1.06 (36H, d, $^3J_{HH}$ = 7.40 Hz, ^{i}Pr$_3$Si CH$_3$).

^{13}C{^{1}H}($C_6D_5CD_3$): δ_C 154.1 (Pn C), 131.1 (Pn C), 125.6 (Pn C), 123.8 (Pn C), 19.4 (^{i}Pr$_3$Si CH$_3$), 19.2 (^{i}Pr$_3$Si CH$_3$), 12.1 (^{i}Pr$_3$Si CH).

^{29}Si{^{1}H}($C_6D_5CD_3$): δ_{Si} 0.70 (^{i}Pr$_3$Si Si).

EI-MS: *m/z* = 1067 [TiCl[(η^8-Pn†)](μ-Cl)]$_2$]$^+$

Elemental analysis (calculated for $C_{52}H_{92}Cl_4Si_4Ti_2$): C, 58.64 (58.53); H, 8.6 (8.69); N, 0.00 (0.00)%.

Crystallographic data for [(Ti(η^8-Pn†)Cl)$_2$(μ-Cl)$_2$]:

Formula weight: 533.61 (1067.22 for dimeric unit).

Triclinic. Space group P-1, green block. A = 9.8565(6) Å, b = 12.0371(6) Å, c = 12.8455(5) Å, α = 106.943(4)° β = 92.153(4)°, γ = 93.671(5)°.

Volume = 1452.38(13) Å^3, T = 173 K, Z = 2, R_{int} = 0.0446, Cu(Kα) λ = 1.54184 Å.

Maximum θ = 71.39°, R_1 [I>2σ(I)] = 0.0482, wR_2 (all data) = 0.1378, GooF = 1.026.

R3.4.2) Alternate Synthetic Methods for [TiCl(η^8-Pn†)]$_2$(μ-Cl)$_2$ (3.4)

Sequential addition of ^{t}BuCl to [Ti$_2$(μ:η^5,η^5-Pn†)]

32 mg (0.03 mmol) of **1.1** was added to a Young's NMR tube and dissolved in d^8-toluene. 0.5 equivalency aliquots of ^{t}BuCl (1.15 µL, 0.015 mmol) were added once per day *via* microsyringe. Between additions, the NMR tube was allowed to stir on an automated sample holder. After 4 sequential additions over a period of four days (with ^{t}BuCl content totalling 4.8 µL, 0.06 mmol) a colour change to green was observed.

THF was used to fully re-dissolve the remaining sample, including a green residue largely insoluble in other solvents. Green crystals were obtained from a sample stored at -35°C.

Yield: 10 mg (0.01 mmol), 63%.

Addition of 2 equivalents of 1,2-dichloroethane to [$Ti_2(\mu{:}\eta^5,\eta^5\text{-}Pn^\dagger)$]

100 mg (0.11 mmol) of [$(\mu{:}\eta^5,\eta^5\text{-}Pn^\dagger)Ti_2$] was placed within a small Young's seal ampoule and dissolved in 2 mL of toluene. 18 µL (0.23 mmol) of 1,2-dichloroethane was added *via* microsyringe and the solution was stirred for 20 minutes. Red crystals of $[(\eta^8\text{-}Pn^\dagger)Ti]_2(\mu\text{-}Cl)_2$ were isolated after filtration through a Celite® pipette from pentane at -35°C. These crystals changed colour to green when dried further.

Yield: 40 mg (0.04 mmol), 72%.

Addition of 2 equivalents of 1,2-dichloroethane to a mixture of $[Ti(\eta^8\text{-}Pn^\dagger)]_2(\mu\text{-}Cl)_2$ and $[Ti(\eta^8\text{-}Pn^\dagger)]_2(\mu\text{-}Cl)_3$

3 g (8.09 mmol) of $TiCl_3(THF)_3$ was added to a large pressure-resistant Rotaflow ampoule and dissolved in 80 mL of THF. The ampoule was then cooled to -78°C and $[K]_2[Pn^\dagger]$ was added dropwise *via* cannula. The solution was allowed to warm to room temperature overnight, forming a green mixture of $[Ti(\eta^8\text{-}Pn^\dagger)]_2(\mu\text{-}Cl)_2$ and $[Ti(\eta^8\text{-}Pn^\dagger)]_2(\mu\text{-}Cl)_3$. 2.6 mL (3.25 g, 32 mmol) of 1,2-dichloroethane contained in a graduated ampoule was then added *via* cannula. The headspace was evacuated prior to moving the ampoule to an oil bath with a magnetic stir plate. The mixture was heated to 90°C for 16 hours and allowed to stir. Dichroic green/red crystals of $[TiCl(\eta^8\text{-}Pn^\dagger)]_2(\mu\text{-}Cl)_2$ were isolated from pentane after 12 hours in a glovebox freezer at -35°C.

Yield: 3.44 g (5.62 mmol) 80%.

R3.5.1) Reaction of [$Ti_2(\mu{:}\eta^5,\eta^5\text{-}Pn^\dagger)$] with Iodine (0.5 Equivalents)

50 mg (0.05 mmol) of **1.1** was added to a small ampoule equipped with a magnetic stir bar. 6 mg (0.025 mmol) of I_2 was added (benzene solution, 60.4 mg I_2/mL). An immediate colour change to brown was observed.

^{1}H NMR ($C_6D_5CD_3$), 399.5 MHz, 303 K): δ_H 8.68 (1H, d, $^3J_{HH}$ 3.15 Hz, Pn H), 7.44 (1H, d, $^3J_{HH}$ 2.04 Hz, Pn H), 7.03 (1H, d, $^3J_{HH}$ 2.31 Hz, Pn H), 6.89 (1H, d, $^3J_{HH}$ 2.58 Hz, Pn H), 6.82 (4H, d, $^3J_{HH}$ 2.25 Hz, **1.1** Pn H), 6.58 (1H, d, $^3J_{HH}$ 2.76 Hz, Pn H), 6.49 (1H, d, $^3J_{HH}$ 2.76 Hz, Pn H), 6.34 (4H, d, $^3J_{HH}$ 2.34 Hz, **1.1** Pn H), 5.76 (1H, d, $^3J_{HH}$ 3.97 Hz, Pn H), 5.71 (1H, d, $^3J_{HH}$ 3.28 Hz, Pn H), 0.92 (24H, d, $^3J_{HH}$ = 6.82 Hz, ^{i}Pr$_3$Si CH$_3$), 0.75 (18H, d, $^3J_{HH}$ = 7.20 Hz, ^{i}Pr$_3$Si CH$_3$).

Note: Extensive broadening witnessed in aliphatic region hinders accurate assignment, possibly indicative of presence of paramagnetic species.

EI-MS: *m/z* = 877 $[Ti(\eta^8\text{-}Pn^\dagger)_2]^+$; 1052 $[[Ti_2(\mu{:}\eta^5,\eta^5\text{-}Pn^\dagger)_2](\mu\text{-}I)]^+$;

Crystallographic data for $[Ti_2(\mu{:}\eta^5,\eta^5\text{-}Pn^\dagger)_2](\mu\text{-}I)$:

Formula weight: 959.58

Monoclinic. Space group $P2_1$, purple plate. A = 14.3755(11) Å, b = 14.1630(10) Å, c = 14.3835(12) Å, α = 90° β = 111.546(9)°, γ = 90°.

Volume = 2723.8(4) $Å^3$, T = 173 K, Z = 2, R_{int} = 0.0900, Mo(Kα) λ = 0.71075 Å.

Maximum θ = 28.15°, R_1 [I>2σ(I)] = 0.0116, wR_2 (all data) = 0.3284, GooF = 1.102.

R3.5.2) Reaction of $[Ti_2(\mu{:}\eta^5,\eta^5\text{-}Pn^\dagger)]$ with Iodine (1 Equivalent)

51 mg (0.05 mmol) of **1.1** was added to a Rotaflow ampoule equipped with a magnetic stir bar. 13 mg (0.05 mmol) of I_2 was added via benzene stock solution (60.4 mg I_2/mL) at ambient temperature. A colour change to purple was observed over 30 minutes. The solvent was removed *in vacuo* after 1 hour and purple crystals were isolated from pentane stored at -35°C.

^{1}H NMR ($C_6D_5CD_3$), 399.5 MHz, 303 K): δ_H 8.34 (2H, s, Pn H), 8.19 (2H, s, Pn H), 6.26 (1H, s, Pn H), 6.17 (1H, s, Pn H), 6.10 (2H, s, Pn H), 6.03 (2H, s, Pn H), 1.99 (6H, m, ^{i}Pr$_3$Si CH), 1.52 (6H, m, ^{i}Pr$_3$Si CH), 1.18 (24H, d, $^3J_{HH}$ = 7.33 Hz, ^{i}Pr$_3$Si CH$_3$), 1.10 (6H, d, $^3J_{HH}$ = 8.21 Hz, ^{i}Pr$_3$Si CH$_3$), 1.04 (3H, d, $^3J_{HH}$ = 7.51 Hz, ^{i}Pr$_3$Si CH$_3$), 1.00 (12H, d, $^3J_{HH}$ = 7.51 Hz, ^{i}Pr$_3$Si CH$_3$), 0.81 (12H, d, $^3J_{HH}$ = 7.21 Hz, ^{i}Pr$_3$Si CH$_3$).

EI-MS: *m/z* = 1052 $[[Ti_2(\mu{:}\eta^5,\eta^5\text{-}Pn^\dagger)_2](\mu\text{-}I)]^+$; 924 $[Ti(\mu{:}\eta^5,\eta^5\text{-}Pn^\dagger)_2]^+$; 877 $[Ti(\eta^8\text{-}Pn^\dagger)_2]^+$

Note: Multiplicity of doublets cannot be discerned in ^{1}H NMR of crude sample.

R3.6) Synthesis of [(η^5-Cp*)Ti(η^8-Pn†)] (3.6)

80 mg (0.08 mmol) of [TiCl(η^8-Pn†)]$_2$(μ-Cl)$_2$ was placed in a Young's tap ampoule with magnetic stirrer bar. 57 mg (0.33 mmol) of KCp* was added to the ampoule and the solids were mixed. 1 mL of ether was added, resulting in an immediate colour change to purple. The solvent was removed under vacuum conditions and the sample was crystallised from pentane after filtration through Celite®. Purple crystals were isolated at -35°C.

Yield: 78.33 (0.13 mmol), 82%.

EI-MS: *m/z* = 597 [Ti(η^5-Cp*)(η^8-Pn†)]$^+$, 633 [TiCl(η^5-Cp*)(η^8-Pn†)]$^+$.
Crystallographic data for [Ti(η^5-Cp*)(η^8-Pn†)Cp*]:

Formula weight: 597.92.

Triclinic. Space group P-1, lustrous purple block. A = 9.3269(5) Å, b = 12.8450(7) Å, c = 16.0210(11) Å, α = 77.597(5)° β = 77.869(5)°, γ = 78.305(5)°.

Volume = 1807.60(19) Å^3, T = 173 K, Z = 2, R_{int} = 0.0382, Mo(Kα) λ = 0.71073 Å.

Maximum θ = 26.49°, R_1 [I>2σ(I)] = 0.0587, wR_2 (all data) = 0.1578, GooF = 1.018.

Chapter 4 – Synthesis and Reactivity of Titanium Pentalene Metal Alkyls

Introduction

Academic interest in titanium metal alkyl species has existed since Herman and Nelson produced the first evidence for the existence of the titanium-carbon bond in 1953, through the reaction of phenyllithium and phenylmagnesium bromide with titanium isopropoxide in diethyl ether.[106] The resulting species, $C_6H_5Ti(OC_3H_7)_3$-$LiOC_3H_7$-LiBr-$(C_2H_5)_{20}$, was identified by elemental analysis of the reaction mixture. This development was followed two years later by the synthesis of the first titanocene alkyl and aryl compounds compounds by Summers *et al.*[107,108] Further transition metal cyclopentadienyl alkyl compounds developed by Wilkinson and Piper expanded the range of M-C bonded metallocenes to encompass iron, tungsten, molybdenum and chromium.[109]

The reactivity of metal alkyl compounds is defined by two functions of the metal centre; the ability to perform reaction mediation and the establishment of an electronegativity differential with respect to the ligand.

The primary role of the metal is universal in most every organometallic reaction and does not differ in the case of compounds with M-C bonds; the metal allows for the binding of multiple ligands (including the formation of transient reaction intermediates) and facilitates interactions between species that are ligated to the centre. The mechanism of ligation of a reagent to a metal, interaction between bound species and a final elimination step is ubiquitous in organometallic catalysis.[110] Metal-alkyl reactivity shows an entrenched reliance on these established and well-understood mechanisms and M-C bonded species often make effective catalysts simply because their mechanism of reactivity aligns conveniently with reaction mechanisms desirable for constructing a repeating catalytic cycle. Practical examples of metal-alkyl chemistry include catalytic hydroformylation and olefin polymerisation reactions.[47,110,111] Cyclopentadienyl sandwich complexes of the group IV metals, most notably zirconium, have seen widespread usage in the field of catalytic polymer synthesis, with many examples of homogeneous and heterogeneous systems.[110,112] Group IV catalysts have also been developed for use in “living” polymerisation.[113] Non-sandwich group IV cyclopentadienyl metal alkyl compounds displaying tetrahedral geometry also show

catalytic activity, though this is reduced in comparison to homoleptic sandwich structures.[114]

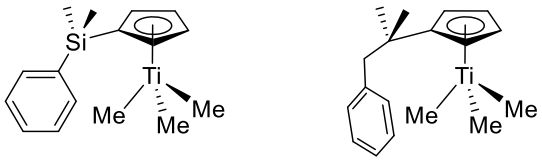

Figure 4.1 Titanium Cp "half-sandwich" trialkyl compounds suitable for olefin polymerisation.[114,115] Specialised variants have also been developed for trimerisation of ethene.[116]

The electropositivity of the metal relative to carbon is also important. The difference in electronegativity between titanium and carbon is such that a titanium alkyl complex can be aptly described as a stabilised yet highly reactive carbanion.[117] This allows the carbon bond to react with even strongly bonded electrophiles that would otherwise be considered chemically inert.[118]

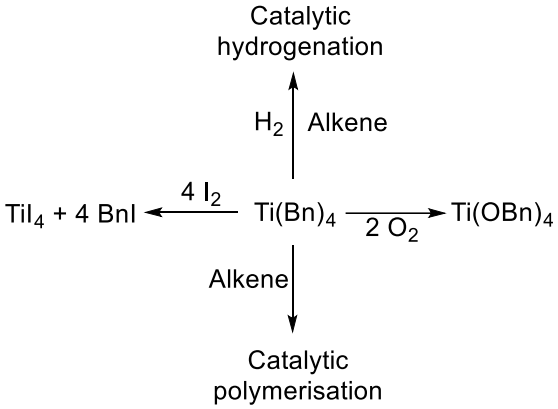

Scheme 4.1 Some examples of the diverse reactivity of tetrabenzyl titanium.[119]

In ideal circumstances, the addition of single carbon ("C1") units into molecules holds the potential to allow selective lengthening of a carbon chain by any desired amount of one unit increments. This would provide an effective synthetic pathway to simple organic feedstocks containing only one to two carbon units (such as ethanol or methanol), while simultaneously recycling waste materials.

CO_2 insertion reactions with metal-carbon bonds have been performed with f-block elements and transition metal compounds, including titanocenes.[120]

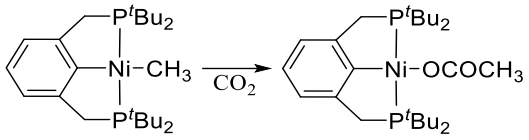

Scheme 4.2 Reaction of a PCP pincer ligand-supported Nickel alkyl compound with CO_2.[121,122]

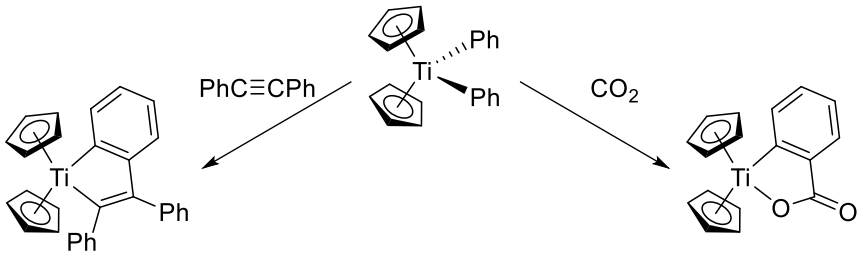

Scheme 4.3 Reactivity of $[(Cp)_2Ti(Ph)_2]$ with CO_2 and an alkyne.[119,123,124]

Metal-ligated hydrocarbons also serve as precursors for the synthesis of metal hydrides *via* σ-bond metathesis.[125] While hydrides may be synthesised by many methods, including direct reaction between metal halides and hydride sources, σ-bond metathesis is a non-reducing route, particularly effective for producing hydrides of early d-block metals. Many low valent early transition metal centres are readily reduced by direct reaction with reducing hydride sources, with the usual result of metal precipitation and degradation of the complex.

Alkyl ligands are also versatile with regards to net charge and coordination mode. The formation of cationic metal alkyl species (*via* methyl abstraction by the MAO co-catalyst)[114] has been determined a key step in the mechanism of homogeneous Group IV catalysts used for homogeneous alkene polyermisation.[112] Organolithium reagents consist of an anionic alkyl species stabilised by a counterion and have long held an important status in organic synthesis. Methyl groups are not limited to terminal binding and may bridge between centres. The C-H hydrogen groups may also engage in agostic binding to the metal core in circumstances in which the metal is electron deficient.

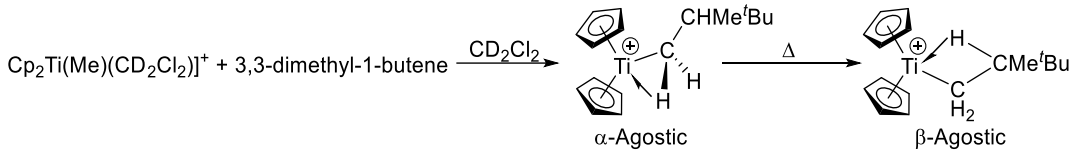

Scheme 4.4 The synthesis of cationic titanocene complexes displaying α-agostic and β-agostic hydrogen interactions.[126]

Unfortunately, the broad utility of transition metal alkyl compounds is tempered by their general instability, which often precludes isolation or stable storage.[127–129] In the 1950's, development of "binary" metal alkyls (species containing only M-aryl or M-alkyl bonds with no supporting ligands) was thought to be impossible without the influence of stabilising groups, examples including CO, the cyclopentadienyl ligand and substituted phosphines.[128] Stability of these species was initially assumed to be almost wholly dictated by coordinative saturation of the metal centre, or whether the complex was diamagnetic.[119] However, it was also recognised that β-hydride elimination is one crucial mechanistic pathway for the decomposition of such compounds and thus attempts were made to synthesise metal alkyl species lacking β-hydrogen groups. This resulted in the successful isolation of the first group IV binary tetrabenzyl and tetramethyl compounds.[119,130,131]

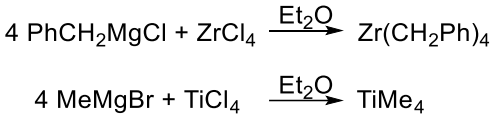

Scheme 4.5 Synthesis of $Zr(Bn)_4$ and $TiMe_4$ *via* reaction of Grignard reagent with metal tetrachloride.[119,127]

The reliance of metal alkyls and alkylidenes on stabilising ligand systems has lead to much investigation into defining the parameters that determine strength of the M-C σ-bond.[119,128,132,133] Metal-carbon σ-type interaction strengths vary between sp, sp^2 and sp^3 hybridised carbon species. In 1995, Per Siegbahn performed a detailed study of transition metal alkyl bond enthalpies using a combination of computational data and the comparison of documented experimental results. On average the M-CH_3 bond has an enthalpy of *ca.* 60 kcal/mol[134] while M-C σ-bonds to sp^2 carbon moieties are in the region of ~80 kcal/mol.[135] Continuing this trend, the strongest M-C σ-bond is exhibited by alkyne carbon groups, with a bond enthalpy in the order of 100-120 kcal/mol.[134] Siegbahn attributes this directly to the increased s-orbital character of the alkyne carbon sp hybridisation, resulting in a stronger σ-bond with the metal d-orbitals.[134] This same

logic explains why the inverse is also true; increase in p-character weakens the degree of s-d orbital overlap and the σ-bond decreases in strength.

The paper also notes that across the second row d-block elements, the earliest transition metals form M-C interactions with the greatest bond enthalpy values, with a noticeable decline in bond enthalpy between niobium and molybdenum. Metal carbon σ-bond enthalpy then steadily increases from molybdenum to ruthenium, before falling once again to a minimum of ~40 kcal/mol for the palladium-CH_3 bond. Siegbahn postulates that this is in large part due to the decrease in ionic character of the M-C bond as d-count of the metal centre increases. As the electron density around the metal increases, it is less positive with respect to the electronegative carbon atom, resulting in weaker ionicity in the bond between the alkyl and the metal. This translates directly to a net decrease in bond enthalpy and thus a weaker M-C σ-bond.[134]

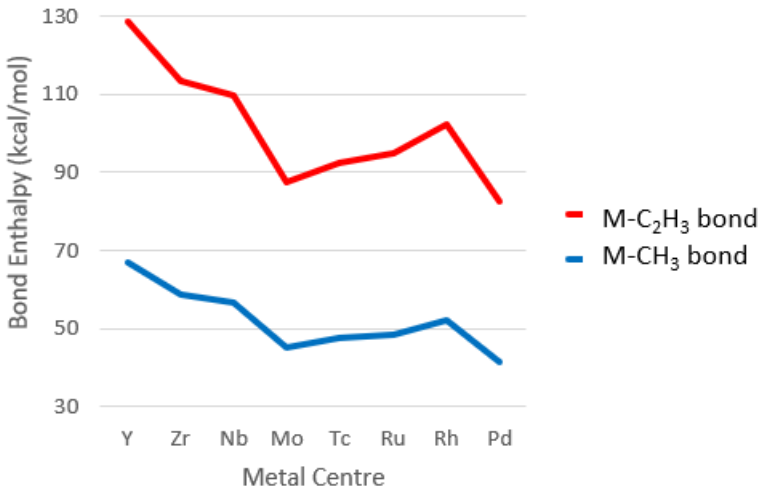

Figure 4.2 Chart depicting the differing enthalpy of the M-C bond for sp^2 and sp^3 metal-bound carbon species across the second row transition metals.[134]

Comprehensive bond enthalpy studies have disproved the earliest speculation that M-C bonds themselves are fundamentally too weak to be thermodynamically stable and this results in the decay of these compounds that is often observed. Instead, this research has indicated that the issue lies with the kinetic stability of metal alkyl species; they are inherently vulnerable to decomposing *via* any mechanism that that possesses a sufficiently low activation barrier, regardless of M-C bond strength.[134,136]

Common alternative routes for the decay of metal alkyls include α-hydride elimination and homolytic cleavage of the M-C bond; therefore even compounds synthesised with the intentional absence of β-hydrogen sites still display a tendency to degrade over time.[136]

Metal carbene complexes are a prominent category of transition metal alkyl derivatives. A metal carbene can be defined as any divalent carbon species which donates two electrons to a metal centre; these ligands may be broadly divided into Schrock and Fischer type carbenes (in addition to non-metallic carbenes, such as NHCs).

Fischer and Schrock carbenes are differentiated by the binding mode they adopt. Schrock-type alkylidenes are defined as X_2 ligands by CBC theory, while Fischer carbenes are L-type ligands.

Schrock-type alkylidenes have previously been isolated for d-block Cp and arene systems through reactions with neopentyl lithium and other alkyl transfer agents which lack β-hydrogen environments.[119] As with the synthesis of tetramethyl and tetrabenzyl titanium, this removes the β-elimination decay pathway and instead forces α-hydride abstraction from the alkyl ligand (commonly a neopentyl group or related ligand)[137] to generate the carbene species. As previously mentioned, this process is often a natural byproduct of the decomposition of an alkyl species; Schrock carbenes are therefore commonly formed during this decay, but only as transient species.[137]

The breakthrough that lead to the solation of Schrock alkylidenes as stable compounds was the purposeful inclusion of an electron donating group (commonly PMe_3) to retain the stability of the molecule.[25] The electronegativity gradient between carbon and the early-to-mid transition metals gives a degree of ionic character to the M=C bond present in Schrock alkylidenes, making the carbon strongly nucleophilic; addition of an adjacent σ-donor group therefore improves electronic balance of the system. Formation of Schrock alkylidenes is most commonly seen for high-oxidation state, early transition metal centres which are bound to stabilising π-donor ligands.[119]

Fischer carbenes bind in a format more similar to CO; the carbene σ-donates to the metal d-orbitals from the filled carbon lone pair orbital and π-back-bonding occurs from the metal d-orbitals to the carbon p-orbitals. This is stabilised by the presence of a π-acceptor ligand bound to the carbene.[138–140]

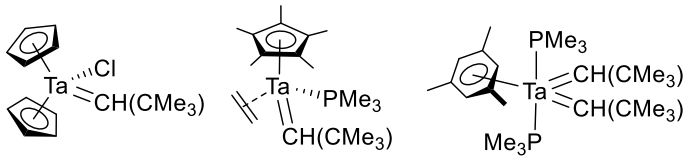

Figure 4.3 Examples of tantalum neopentylidene Schrock-type alkylidene compounds.[139]

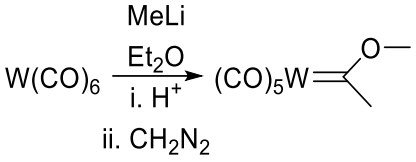

Scheme 4.6 Synthesis of the first Fischer-type carbene compound.[141]

As carbene chemistry has matured, DFT studies have elucidated the electronic properties and chemical reactivity of Schrock and Fischer systems[140] in far greater detail than described in this brief overview. Many comprehensive reviews of Fischer and Schrock d-block carbene synthesis and reactivity have been published.[142–144] When considering Group IV carbenes specifically, the 2008 publication *Metallocenes: Synthesis Reactivity Applications* dedicates an entire chapter to the diversity of titanocene chemistry and an extensive description of synthetic routes to titanocene carbene compounds.[145]

Routes to titanocene carbene compounds include controlled α-hydride elimination of metal alkyls (particularly prominent in the case of methyl titanocenes), synthetic access from Tebbe's reagent and reductive titanation of organohalides.[145] These methods are highlighted in **Scheme 4.7**, though many more have been omitted for purposes of brevity. Titanium alkylidene compounds have found use in organic synthesis for carbonyl olefination and alkene metathesis reactions.[146] Grainger and Munro have also provided a detailed overview of contemporary alkylidene chemistry, including use of carbene species for natural product synthesis.[140]

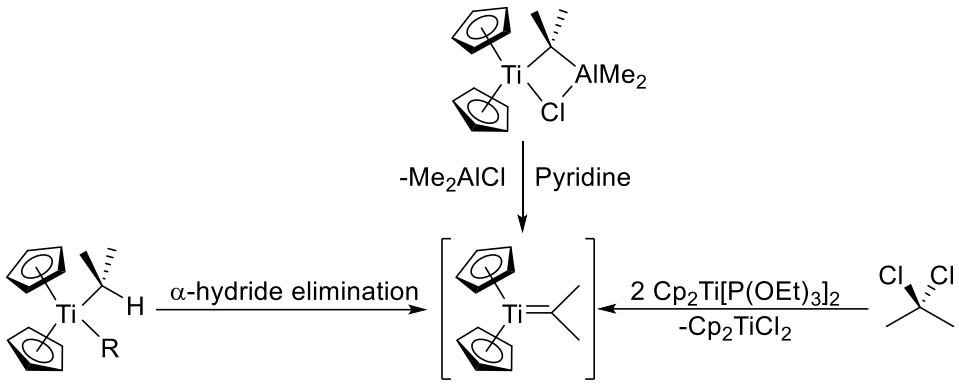

Scheme 4.7 Example methods for the synthesis of titanocene alkylidene compounds.[145,146]

Combined, the kinetic instability of transition metal alkyl compounds and the relative difficulty of synthesis of the pentalene ligand *versus* the cyclopentadienyl ligand has resulted in pentalene metal alkyl complexes remaining largely unexplored. Nonetheless, some examples of d-block pentalene metal alkyls have been reported recently. The O'Hare group synthesised *bis*-benzyl and *bis*-alkyl titanium-Pn* complexes in 2015, by reaction of $[Ti(\eta^8\text{-Pn*})Cl]_2(\mu\text{-Cl})_2$ with an appropriate Grignard reagent. These compounds were then successfully reacted with CO_2 to produce isolable double-insertion products.[67]

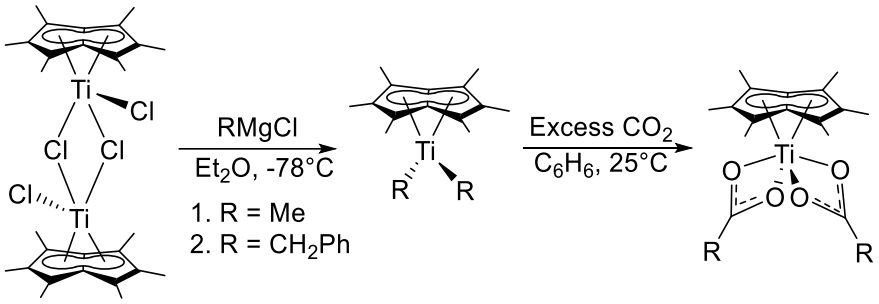

Scheme 4.8 Synthesis of titanium permethylpentalene metal alkyls and their reactivity with CO_2 .[73]

The reported isolation of $[Ti(Me)_2(\eta^8\text{-Pn*})]$ and $[Ti(Bn)_2(\eta^8\text{-Pn*})]$ was followed in 2016 by a further paper by O'Hare *et al.* describing the synthesis of zirconium and hafnium permethylpentalene alkyl compounds.

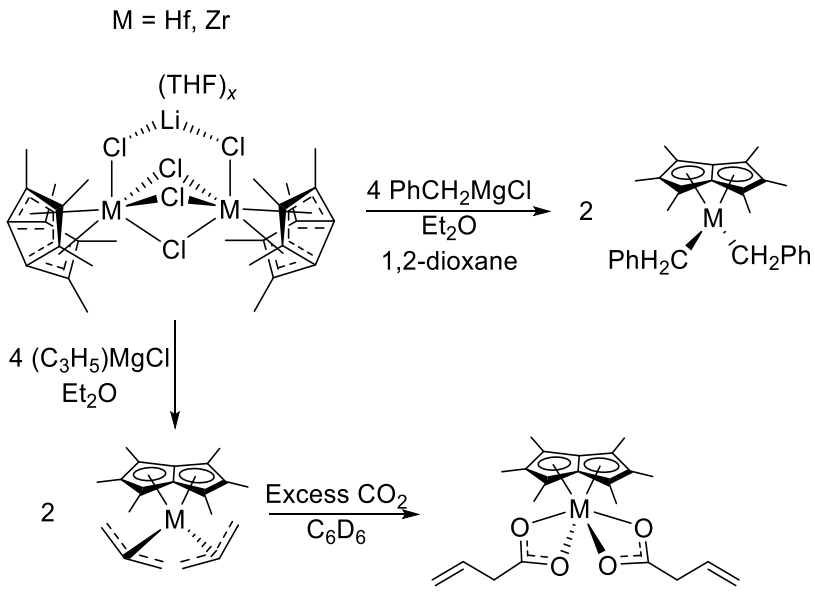

Scheme 4.9 Hafnium and zirconium permethylpentalene alkyl and allyl compounds, and formation of a derivative dicarboxylate.

This chapter will discuss the synthesis and reactivity of titanium pentalene metal alkyl species derived from the chloride compounds **3.1** and **3.4** described in Chapter 3.

Synthesis of [Ti(Me)$_2$(η^8-Pn†)] (4.1)

Initial attempts to synthesise [Ti(Me)$_2$(η^8-Pn†)] focused on the reaction of complex **3.4** with ZnMe$_2$. A stock of dimethylzinc was present in the laboratory inventory and it was therefore chosen as a convenient option for initial proof-of-concept reactions. Surprisingly, however, use of this methylating agent resulted rapid decomposition of **3.4** to an intractable mixture.

Given the poor results obtained, it was next decided to synthesise and purify a sample of MgMe$_2$ *via* an established literature method[95] and reattempt the reaction. Fortunately, use of this MgMe$_2$ yielded [Ti(Me)$_2$(η^8-Pn†)] **4.1** in 60% yield, as identified by the X-Ray diffraction analysis of red crystals isolated from a pentane solution at -35°C. The compound was further characterised by NMR spectroscopic techniques.

As 103imethylmagnesium is easily synthesised in significant quantities and produces **4.1** with a high degree of reliability, no further attempts were made to repeat the reaction with ZnMe$_2$ or alternate methylating agents. It therefore remains presently

unknown if $ZnMe_2$ is an unsuitable reagent for this reaction, or if the stock used was simply contaminated or degraded over a prolonged period of storage.

Compound **4.1** was found to be thermally unstable in solution, readily forming a yellow paramagnetic NMR silent product after *ca.* 15 minutes at ambient temperature. Mass spectrum analysis was performed on this crude solution and yielded only pentalene ligand fragments, confirming this decay. This behaviour is surprising, as [Ti(Me)$_2$(η^8-Pn*)] is reported stable indefinitely in solution even when heated to temperatures as high as 60°C.[73] Given the similarities in steric bulk between the Pn† and Pn* ligands, it would initially appear that the decay is driven by entirely by electronic factors, principally electron deficiency of the 14 electron complex. This is likely mitigated by the abundance of electron donating methyl groups on the Pn* ligand, resulting in a comparatively profound increase in stability. Electron count and degree of ligand donation certainly has a significant impact on stability of these species, as 12 electron compounds isolated degraded at *ca.* 50 seconds at ambient temperature. However, 18 electron Pn† alkyl derivatives were later isolated and remained highly sensitive to temperature in solution; this is suggestive that the EDG groups of Pn* provide a greater influence over stability than saturation of the coordination sphere with M-C bonds and other ligands.

Difficulties encountered with the removal of $MgCl_2$ from the final product proved a significant drawback to this synthetic method. Magnesium dichloride is typically eliminated by addition of 1,4-dioxane, followed by filtration of the resulting insoluble polymer without further issue. Upon addition of 1,4-dioxane, an immediate colour change from bright red to dark brown was observed. Analysis of this mixture by ^{1}H NMR spectroscopy once again confirms deterioration of compound **4.1**, forming a very complicated mixture containing dozens of peaks in the aromatic region. The reaction was repeated with dioxane taken from a separate ampoule to remove any possibility of solvent contamination or the presence of trace water, but this produced the same deterioration of the sample. As a result, the removal of $MgCl_2$ was accomplished by extraction in pentane followed by a minimum of two filtrations using Celite® and/or a Millipore syringe; this proved sufficient to isolate crystalline [Ti(Me)$_2$(η^8-Pn†)] in 70% yield after further optimisation detailed in the results section.

The optimum thermal conditions for the synthesis of **4.1** were established over multiple repeat experiments. Performing the reaction at -78°C for the duration of the experiment

results in a slow reaction rate; after one hour an aliquot analysed by ^{1}H NMR confirmed that **3.4** was still the primary component of the mixture.

Superior results are instead obtained by the addition of $MgMe_2$ to an ethereal solution of $[TiCl(\eta^8\text{-}Pn^{\dagger})]_2(\mu\text{-}Cl)]_2$ at -78°C, followed by warming to -30°C after the initial colour change to brown. This produces maximal yield of **4.1** after *ca.* 10 minutes, marked by a colour change to bright red, without any evidence of degradation in the ^{1}H NMR spectrum if the mixture is dried promptly.

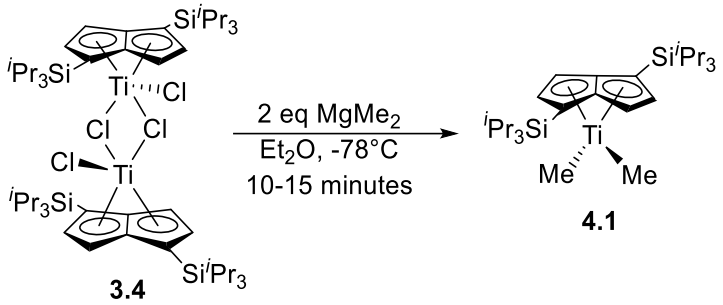

Scheme 4.10 Synthesis of **4.1**.

Experiments were also conducted successfully with THF, though apparent formation of an adduct to produce a bright purple colouration made visual distinction of the stages of reaction more complicated, resulting in lower yields. The THF adduct itself could not be isolated for crystallographic analysis, due to the reliance on dissolution in pentane prior to filtration in the work-up procedure. The presence of $MgCl_2$ predictably impedes any attempt at crystallisation.

Characterisation and Reactivity of $[Ti(Me)_2(\eta^8\text{-}Pn^{\dagger})]$ (4.1)

The ^{1}H NMR spectrum of $[Ti(Me)_2(\eta^8\text{-}Pn^{\dagger})]$ in C_6D_6 is typical of a complex showing C_2 symmetry in solution with two doublet resonances in the aromatic region δ_H 6.49 and 5.75 ppm. Both signals show characteristic proton ring proton coupling constants of $^{3}J_{HH}$ 3.30 Hz. One triisopropylsilyly methine C-H environment exists at δ_H 1.25 ppm and two doublets at δ_H 1.16 ppm and 1.14 ppm correspond to triisopropylsilyl CH_3 groups. A methyl resonance of integration six, denoting two symmetric metal bound methyl groups, is represented by a singlet at 0.66 ppm. This methyl group is also observed at δ_C 47.3 ppm in the $^{13}C\{^{1}H\}$ NMR, a shift value in good agreement with the C_6D_6 shift of δ_C 41.1 ppm recorded for the $[Ti(Me)_2(\eta^8\text{-}Pn^*)]$ Ti-CH_3 group.[73]

The $^{13}C\{^{1}H\}$ NMR spectrum also contains four pentalene carbon environments from δ_C 147.7-110.7 ppm. $^{29}Si\{^{1}H\}$ NMR spectroscopy displays a single silicon $Si^{i}Pr_3$ environment present at δ_{Si} 0.04 ppm. Attempts to perform elemental analysis of crystalline **4.1** were hindered by thermal instability. Multiple samples were prepared for analysis by EI-MS, but no characteristic molecular ion could be detected, suggesting the compound does not survive fragmentation.

X-Ray diffraction data was obtained from cubic red crystals of **4.1**, and further supports all spectroscopic data collected with the depiction of an η^8-coordinated pentalene *pseudo*-tetrahedral[42] titanium dimethyl complex.

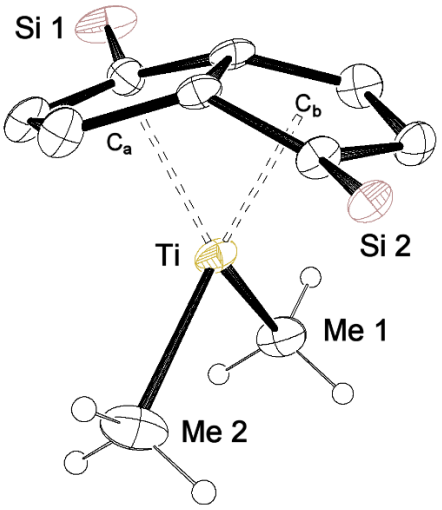

Figure 4.4 ORTEP diagram of $[Ti(Me)_2(\eta^8\text{-}Pn^{\dagger})]$ **4.1**, 50% probability ellipsoids shown with ^{i}Pr groups and selected hydrogen atoms omitted.

Parameter	Bond Length (Å)	Angle	(°)
Ti-C_a	1.946(11)	Hinge	0.49(5)
Ti-C_b	1.956(16)	Fold	34.54(3)
Ti-Me 1	2.121(17)		
Ti-Me 2	2.144(13)		
Bridgehead C-C	1.449(10)		

Table 4.1 Selected bond length and angle metrics for **4.1**.

Compound **4.1** is a Ti(IV) 14 electron system, with an ML_3X_4 classification defined by the CBC method. The metrics of complex **4.1** are expectedly similar to $[Ti(Me)_2(\eta^8\text{-}Pn^*)]$, with **4.1** displaying a significant fold angle of

34.54(3)° along the axis of the bridgehead carbons typical of η^8 pentalene coordination; by comparison, the fold angle of the Pn* analogue is 35.66(3)°. The Ti-Carbon distances for the bound methyl groups of each complex are also commensurate, with the Pn* dialkyl compound possessing Ti-Me C distances of 2.139(2) Å and 2.132(2) Å *versus* 2.121(17) Å and 2.144(13) Å for **4.1**.[73] The hinge angle of $[Ti(Me)_2(\eta^8\text{-}Pn^*)]$ is nearly double of **4.1** at 0.73(8)°, showing a greater distortion of the wing-tip carbons from planarity. However, as the hinge angle of **4.1** is 0.49(5)°, this amounts to a minimal deviation.

The reactivity of $[Ti(Me)_2(\eta^8\text{-}Pn^\dagger)]$ was of high interest due to the minimal steric protection offered by the compact methyl groups and potential to act as a C1 feedstock for insertion reactions. As the first metal alkyl synthesised over the course of this project, **4.1** was also an obvious candidate for σ-bond metathesis reactions with gaseous hydrogen to produce hydridic pentalene complexes. As with the metal halides isolated in Chapter 3, complex **4.1** also bears structural similarities to Ziegler-Natta type catalysts[5,112,117,147] and as a result, attempts were made to catalyse polyethylene and polypropylene polymerisation in the presence of MMAO. Addition of MMAO results in an immediate colour change to brown, though once again no evidence was found for the existence of any polymer species in solution after subsequent addition of ethylene or propylene. Control experiments were performed between $[Ti(Me)_2(\eta^8\text{-}Pn^\dagger)]$ and the gases in absence of MMAO, to confirm the co-catalyst was not rendering the pentalene complex inert. No reaction occurred and no further experiments of this nature were attempted.

Synthesis and Characterisation of $[Ti(OAc)_2(\eta^8\text{-}Pn^\dagger)]$ (4.2)

Reaction of **4.1** with one equivalent of carbon dioxide *via* Toepler pump at -78°C resulted in no evidence of reaction by ^1H and $^{13}C\{^1H\}$ NMR. This is consistent with reactions performed with $[Ti(Me)_2(\eta^8\text{-}Pn^*)]$[73] and in contrast to the titanocene species $Cp_2Ti(Me)_2$, which readily displays insertion of CO_2 into a single M-C bond (albeit with thermal[124] or photolytic[148] stimulus).

However, introduction of two stoichiometric equivalents of $^{13}CO_2$ was found to result in the insertion of CO_2 into each M-C bond to form a metal dicarboxylate compound, mirroring the literature precedent established by the O'Hare group.[73]

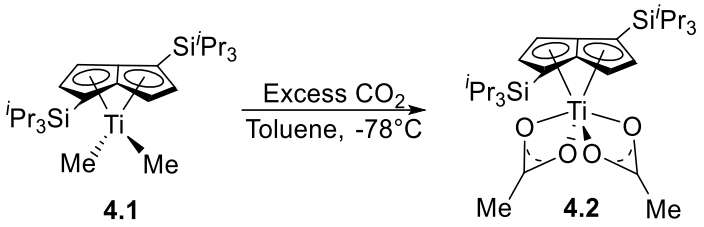

Scheme 4.11 Reaction of **4.1** with excess carbon dioxide.

Initial confirmation of CO_2 ligation was provided by $^{13}C\{^1H\}$ and ^{13}C NMR analysis in deuterated toluene, with the CO_2 carbon peak represented by a strong signal at δ_C 189.7 ppm. This presented as a quartet in the proton-coupled carbon spectrum, in keeping with the adjacent CH_3 group. The chemical shift value obtained is comparable to the analogous Pn* compound, which shows the O_2CMe CO_2 carbon at δ_C 188.5 ppm in C_7D_8. Free $^{13}CO_2$ was not witnessed in solution.

Unfortunately, despite possessing 18 electrons and a coordinatively saturated ML_5X_4 Ti(IV) titanium centre, **4.2** showed similar instability in solution to **4.1**, casting doubt on the previous assumption that degradation of these complexes is driven purely by electron deficiency. This made the use of ^{13}C labelled carbon dioxide particularly advantageous, as the increased isotopic abundance allows the bound CO_2 peak to be easily identified even in $^{13}C\{^1H\}$ NMR spectra collected over several minutes. The stability of the compound still proved a formidable hindrance to more thorough heteronuclear NMR analysis however, due to the necessary longevity of such experiments. This result would appear to support literature assertions that the strength of the M-C bond may be directly influenced by electron donating ligands bound to the metal centre.[128]

The ^1H NMR spectrum depicts two doublet signals at δ_H 6.60 ppm and 5.80 ppm, with coupling constants $^3J_{HH}$ of 3.47 Hz and 3.26 Hz respectively, typical of Pn-H ring environments. The methyl group experiences a downfield shift from δ_H 0.66 ppm in **4.1** to 1.66 ppm, indicative of proximity to the electron withdrawing CO_2 moiety. This CH_3 peak experiences geminal coupling with the ½ spin ^{13}C labelled CO_2 carbon to produce a doublet with coupling constant $^2J_{CH}$ = 6.58 Hz. The degradation of **4.2** may be tracked by the growth of many pentalene ring proton doublet peaks in the aromatic region of the ^1H NMR spectrum, most notably at δ_H 6.66 ppm and 6.46 ppm, sharing coupling constants of $^3J_{HH}$ 2.78 Hz.

A singular TIPS silicon environment would be expected from the $^{29}Si\{^{1}H\}$ NMR spectrum based upon the *pseudo*-tetrahedral geometry shared with **4.1**; instead, two peaks are seen at δ_{Si} 0.58 ppm and 0.26 ppm. The $^{29}Si\{^{1}H\}$ NMR experiment had to be performed for around 12 hours on a 15 mg sample to observe any resonances attributable to the pentalene TIPS groups; it was therefore impossible to avoid decomposition and as such, neither of these peaks likely corresponds to **4.2**. ^{1}H NMR analysis of the sample after 12 hours shows the presence of the aforementioned peaks at δ_{H} 6.66 and 6.46 ppm in exclusivity, with broadening of a number of other peaks the baseline in the aromatic region. The unknown diamagnetic compound could not be isolated or identified from samples of the mixture analysed by EI-MS, though $^{13}C\{^{1}H\}$ NMR data of **4.2** after around 10 minutes shows growth of a second bound CO_2Me CO_2 carbon peak at δ_{C} 190.7 ppm. This is suggestive that the compound formed by thermal decay retains the titanium M-CO_2 binding, and certainly warrants future investigation.

O'Hare *et al.* describe the O_2CCH_3 methyl group as a ^{13}C NMR resonance at δ_{C} 22.8 ppm in deuterated toluene. Surprisingly, although the methyl group possessed by **4.2** is clearly identified by ^{1}H NMR spectroscopy, it appears absent from $^{13}C\{^{1}H\}$ and ^{13}C NMR experiments, again possibly due to the degradation of **4.1** over the course of the data collection. However, a very weak multiplet is observed at 31.9 ppm in one proton coupled ^{13}C NMR spectrum of the compound, which is possibly suggestive of its presence. Similarly, decay of the compound resulted in around eight pentalene carbon environments in solution, indicative of the presence of at least two pentalene compounds, though the number of resonances continues to increase over time.

The structure was elucidated further by X-Ray diffraction analysis of single crystals of **4.2**.

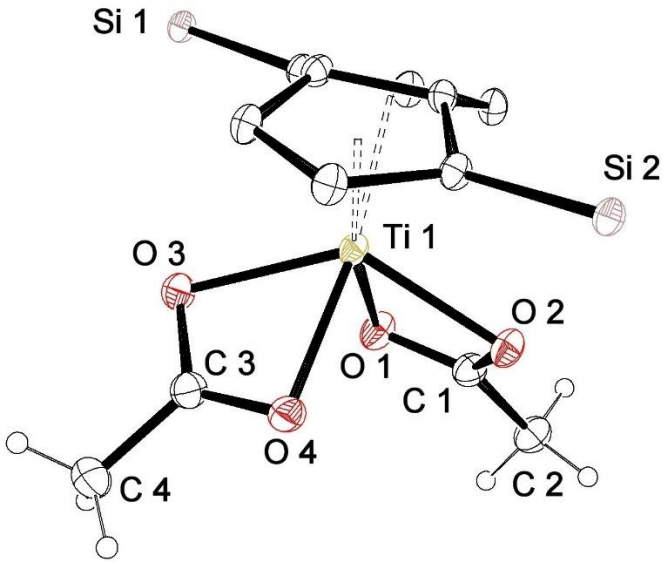

Figure 4.5 X-Ray diffraction structure of complex **4.2**. Pentalene ring hydrogen atoms omitted, ellipsoids at 50% probability.

Parameter	Bond Length (Å)	Angle	(°)
Ti-C_a	1.973(13)	Hinge	0.69(5)
Ti-C_b	1.970(8)	Fold	32.01(2)
Ti-O 1	2.146(9)		
Ti-O 2	2.121(8)		
Ti-O 3	2.137(7)		
Ti-O 4	2.123(13)		
Bridgehead C-C	1.463(5)		

Table 4.2 Selected measurements for complex **4.2**.

The heightened fold angle of 32.01(2)° observed for complex **4.2** is typical of η^8 pentalene coordination and is comparable to the folding of [Ti(OAc)$_2$(η^8-Pn*)], which is reported as 32.37(3)°.[10,73] Ti-O distances reported for the Pn* analogue by O'Hare *et al.* do not deviate significantly from measurements of **4.2**, as might be expected given the degree of structural similarity between the two compounds. The Pn* complex possesses Ti-O bond lengths from 2.139(14) Å to 2.149(14) Å,[73] compared to 2.123(13) Å to 2.146(9) for **4.2**. A notable but minor difference between the structures is the slight lengthening of the Ti-centroid distances in **4.2**, at 1.973(13) Å and 1.970(8) Å *versus* 1.958(2) Å and 1.955(2) Å, caused by the increased steric demand of the TIPS groups.

Reactivity of 4.1 with ^{13}CO

^{13}CO was reacted with **4.1** at -78°C, resulting in a visible colour change to pale yellow. The sample was warmed slowly to room temperature and analysed by ^{1}H and $^{13}C\{^{1}H\}$ NMR spectroscopy. As previously, the compound formed was unstable at ambient temperature, showing a colour change to brown after 10 minutes. Both $^{13}C\{^{1}H\}$ spectra obtained rapidly (20-30 scans) and over 12 hours showed no evidence of bound CO (which would be expected in the region of *ca.* δ_C 270 ppm, as seen with **1.1** carbonyl adducts).[38]

Several spectra obtained showed free CO is at δ_C 181 ppm, consistent with literature values (within minor shifts of plus or minus *ca.* 5 ppm dependent on solvent).[38,149,150]

^{1}H NMR spectroscopy proved unhelpful in determining the identity of the yellow compound in solution; signals observed are characteristic of a paramagnetic complex, with an incoherent aliphatic region in which only one very large singlet peak is apparent. The pentalene aromatic region is also broadened to the extent that signals merge with the baseline. The $^{29}Si\{^{1}H\}$ spectrum displays one highly broadened resonance at δ_{Si} 5.26 ppm; within the correct region for pentalene TIPS groups in a diamagnetic complex, but this is irrelevant in the case of a paramagnetic Ti(III) centre. Reactions between **4.1** and CO were discontinued in light of this disappointing result.

Reactivity of 4.1 with H_2 and NH_3

Several reactions between the dimeric chloride species $[TiCl(\eta^8\text{-}Pn^{\dagger})]_2(\mu\text{:}Cl)_2$ **3.4** and hydride sources were previously attempted in efforts to directly synthesise a titanium pentalene hydride complex. Reaction of with potassium hydride produced reduction of **3.4** to **1.1**, observed by ^{1}H NMR spectroscopy. Lithium triethylborohydride was experimented with as a less reducing alternative, attempting to circumvent undesirable reduction; however, an intractable mixture was formed from which no useful characterisation data could be extracted.

Following the previous failure of these reactions, isolation of **4.1**, a d^0 complex with Ti-R σ bonds, presented the possibility of facile metal hydride synthesis *via* M-C σ-bond metathesis.[125]

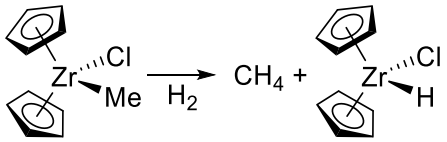

Scheme 4.12 Synthesis of Schwartz's Reagent *via* metathesis of the M-C σ bond with molecular hydrogen.[151]

A reaction of **4.1** with 2 atmospheres of hydrogen at -78°C was performed. Disappointingly, ^{1}H NMR analysis of the mixture at -60°C showed no evidence of bond metathesis, with only compound **4.1** present in solution addition to free H_2. Further warming of the reaction vessel to ambient temperature resulted only in decay of **4.1**. A sample left to crystallise at -80°C under an H_2 atmosphere produced small yellow block crystals visually uncharacteristic of **4.1**, but these decayed immediately upon any attempts at handling.

Compound **4.1** was also reacted with one equivalent of ammonia gas at -78°C. A colour change to yellow was noted, but the experiment ultimately produced an intractable yellow mixture in similar fashion to experiments with ^{13}CO.

Synthesis and Characterisation of [Ti(η^8-Pn†)(η^2-C$_8$H$_9$NCMe)$_2$] (4.3)

With the difficulties encountered with product stability in reactions between **4.1** and ^{13}CO, it was decided to next react **4.1** with an isocyanide moiety isoelectronic with carbon monoxide. The principle attraction of this class of molecules for this application lies with the wide variety of readily available derivatised isocyanides.[152,153] A stable adduct was successfully formed by the reaction of **1.1** with xylylisocyanide (complex **5.3**, see Chapter 5). This isocyanide was chosen again with the hope that its significant steric bulk would provide greater stability to the product.

The reaction produced a visual colour change to purple, also observed with the successful formation of other titanium pentalene isocyanide adducts.[66] Crystalline material from the solution was readily isolated and proved amenable to further study by X-Ray diffraction; the structure obtained is indicative of a monometallic, η^8 pentalene Ti(IV) complex with two bound iminoacyl ligands showing LX-type ligation.

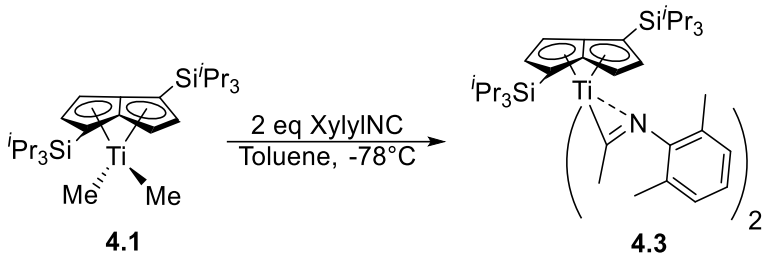

4.1 **4.3**

Scheme 4.13 Synthesis of compound **4.3**.

Each ligated iminoacyl group can now be seen to possess a terminal methyl substituent (the closest carbon atom of which is labelled C 2 in **Figure 4.6**, below), indicative of isocyanide insertion into both Ti-CH_3 bonds. The insertion of isocyanide groups into M-alkyl bonds is reported most often for the mid-to-late transition metals, particularly palladium.[154,155] To the best of the author's knowledge, **4.3** is the only present example of this type of isocyanide-alkyl insertion demonstrated with the pentalene ligand. An example of an osmapentalyne species experiencing isocyanide insertion into a M-C multiple bond also exists.[156]

Unfortunately, in contrast to the facile isolation of crystals and elucidation of the solid state structure, ^{1}H and heteronuclear NMR spectroscopy data gathered for compound **4.3** in solution unfortunately provided minimal characteristic information. The ^{1}H NMR spectrum of crystalline material shows evidence of both rapid decay in solution at ambient temperature and paramagnetism. ^{1}H NMR data obtained directly after formation of the compound displays seven broadened peaks in the aromatic region attributable to pentalene environments. The resonances at δ_H 6.71 ppm and 6.22 ppm display an integration of two, while the other five signals appear display half this integration.

All pentalene ring proton environments are broadened to the extent that they are observed as singlets, while the aliphatic region contains a mixture of singlets and doublets which change drastically in observed chemical shift and integration with each repeated collection of the spectrum over multiple ^{1}H NMR experiments. Each sample used was taken from the same crystalline material stored at -35°C, discounting the possibility of any change of sample composition prior to the ^{1}H NMR spectrum collection. The ^{1}H NMR spectrum was also gathered in deuterated cyclohexane, to better observe the aromatic region in absence of the benzene peak; however, no further resonances were seen. Instead signals in the aromatic region are show equal integration

with one another in this spectrum, with very low integration even with loading of 15 mg of material. The chemical shifts of these resonances bear no resemblance to those seen in the C_6D_6 sample, likely due once again to decay of the compound in solution; evidence of paramagnetism is also heightened, with an entirely indistinct aliphatic region showing very broad TIPS environments. This appears indicative that the decay product is paramagnetic, rather than the isocyanide insertion product itself.

This conclusion is supported by the formal electron count of **4.3**, which is defined as $18e^-$, and ML_5X_4 by the Green formalism, assuming η^2 side-on ligation of the isocyanide (as is depicted by the geometry of the solid state structure).[33] Such a compound should therefore be diamagnetic when observed by ^{1}H NMR spectroscopy, in contradiction to the ^{1}H NMR spectra obtained.

The Ti-Me resonance previously observed at δ_H 0.66 ppm in **4.1** is absent in **4.3**, as would be expected with insertion of the isocyanide group. Unfortunately, the isocyanide-bound methyl resonance is not clearly defined in the ^{1}H NMR spectrum. It is possible that the signal for this group is buried within the broadened and indistinct aliphatic region and is then lost as the compound decays over time. A singlet peak at δ_H 3.29 ppm possesses an integration value of three, possibly consistent with a single non-symmetric CH_3 group. This is consistent with the chemical shift of the nitrogen-bound CH_3 group in the MeNC adduct of **1.1**, which is reported at δ_H 3.25 ppm. However, this δ_H 3.29 ppm resonance was observed in only one ^{1}H NMR spectrum gathered within 5 minutes of dissolving **4.3** in C_6D_6 and was not present in subsequent NMR experiments. Repeat ^{1}H NMR experiments instead show a multitude of peaks between δ_H 2.38 ppm and 1.75 ppm, the existence of which varies with each data collection and with time. After two hours, a collection of highly broadened signals from δ_H 3.50 ppm to 0.20 ppm is seen in the ^{1}H NMR spectrum while, low integration sharp peaks rise at 2.00 ppm. As these changes occur, recognisable pentalene resonances in the aromatic region are lost entirely.

Further support for the deterioration of **4.3** in solution is provided by the $^{13}C\{^1H\}$ and $^{29}Si\{^1H\}$ spectra. The latter experiment shows no visible TIPS silicon resonances after data collection over a 12 hour period. $^{13}C\{^1H\}$NMR experiments depict eight separate pentalene environments, weakly apparent from the baseline, while a peak at δ_C 47.9 ppm is reminiscent of the Ti-CH_3 carbon peak at δ_C 47.3 ppm in **4.1**. This shift range is not characteristic of isocyanide-bound methyl groups.[66] Complex **4.1** is not observed in

the proton NMR spectrum, discounting the possibility that this $^{13}C\{^{1}H\}$ resonance is produced by remnant starting material. Widening the spectral window to δ_C 300 to -300 ppm did not result in any observation of isocyanide carbon resonances, reported at δ_C 289.2 ppm for MeNC reactions with **1.1**. Ultimately, despite attempts at deriving useful information from the ^{1}H and heteronuclear spectra obtained, the data gathered does not offer any significant useful insight given the propensity of the complex towards degradation in solution. The display of eight pentalene environments in the $^{13}C\{^{1}H\}$ spectrum, for example, cannot be used to reliably insinuate the presence of a single asymmetric species as it is entirely possible from the ^{1}H spectrum that multiple species are present in solution. Nonetheless, the spectrum obtained is reported in the experimental results section.

Repeated attempts at analysis by EI-MS failed to return a characteristic molecular ion; **4.3** does not survive fragmentation by this method. However, compound **4.3** remains thermally stable as a solid, and elemental analysis of a crystalline sample confirmed the validity of the atomic composition depicted by the X-Ray structure.

The IR spectrum of **4.3** most notably contains a ν(CN) stretch at 1642 cm^{-1}; this is exactly identical to the CN stretch reported for $[Ti(\mu{:}\eta^5,\eta^5\text{-}Pn^{\dagger})]_2(\mu\text{-MeNC})$ despite the status of **4.3** as an iminoacyl and $[Ti(\mu{:}\eta^5,\eta^5\text{-}Pn^{\dagger})]_2(\mu\text{-MeNC})$ as an isocyanide adduct.[66] However, other isocyanide compounds in the literature are not comparable; iron and ruthenium isocyanide compounds, for example, have reported ν(CN) stretches in the region of ~1800-1900 cm^{-1}.[157]

IR values related to the pentalene ligand TIPS environments, such as the asymmetric CH_3 stretch seen at 1463 cm^{-1}, remain identical with **1.1**.[51]

Group IV dimethyls possessing geometrically constrained ("cg") variants of Cp* rings have recently been successfully reacted with isocyanides to produce iminoacyl products similar in nature to **4.3**.[158]

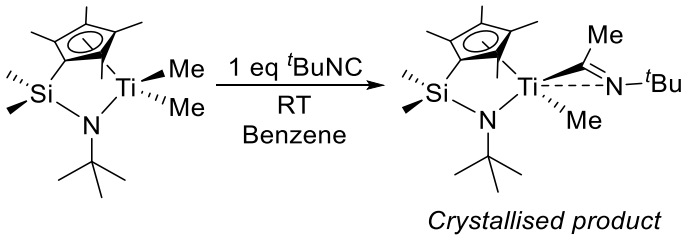

Scheme 4.14 Synthesis of titanium iminoacyl product by Norton *et al.*[158]

The Ti-N 1 distance of **4.3** is measured at 2.127(3) Å, in good agreement with the "cg" Cp* iminoacyl synthesised by the Norton group, for which a value of 2.073(2) Å is recorded. The titanium-carbon distance of 2.111(3) Å for **4.3** is also within 0.07Å of the literature value for this bond of 2.177(2) Å.[158]

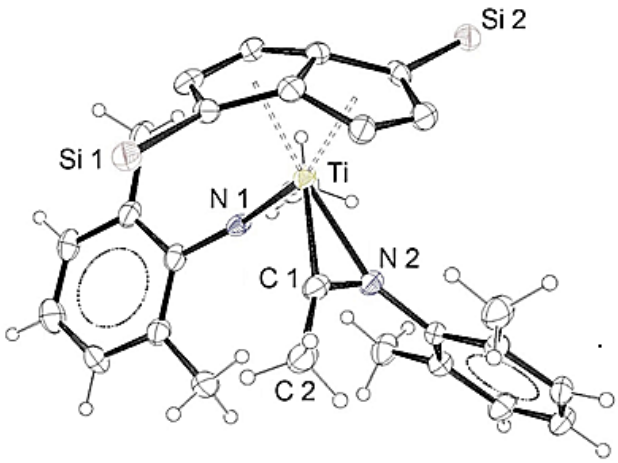

Figure 4.6 X-Ray crystal structure of complex **4.3**. Pentalene hydrogen atoms omitted for clarity, phenyl aromaticity highlighted.

Parameter	Bond Length (Å)	Angle	(°)
Ti-C_a	2.031(3)	Hinge	0.68(16)
Ti-C_b	2.010(3)	Fold	28.57(7)
Ti-C 1	2.127(3)		
Ti-N 1	2.128(3)		
Ti-C 2	2.111(3)		
Ti-N 2	2.146(3)		
Bridgehead C-C	1.452(3)		

Table 4.3 Tabulated metrics for **4.3**.

The crystallographic measurements attributed to **4.3** have several salient features. The pentalene fold angle is notably less extreme in **4.3**, reduced six degrees from 34.54(3)° in **4.1** to 28.57(7)°. This is likely due to the difference in formal electron count. While folding does provide increased steric protection, the degree of folding is typically driven by electronic requirements of the metal centre. As established previously, the loss of aromatic planarity of the pentalene ligand produced by the "umbrella" bridgehead C-C folding motif must be counterbalanced by the increased orbital overlap provided to the metal in order to preserve the stability of the molecule. With a $16e^-$ electron count, the

titanium core of **4.3** requires a lower degree of electronic stabilisation than titanium in the 14e$^-$ configuration of **4.1** and thus the fold angle is.

Hinge angle remains minimal in **4.3**, while bridgehead C-C length shows no deviation from the expected parameters of 1.43 Å-1.45 Å. The Ti-Centroid distances to C_a and C_b are lengthened slightly in comparison to the measurements taken from **4.1**, likely due to the proximity of the bulky 2,6-dimethylphenyl groups.

Synthesis and Characterisation of [Ti(Bn)$_2$(η^8-Pn†)] (4.4)

Although isolation of **4.1** and the dicarboxylate derivative **4.2** proves successful, it was apparent over the course of reactivity studies that the poor stability of the Pn† dimethyl compound was rendering attempts at isolation and characterisation of further novel species problematic. Given the reported existence of [Ti(Bn)$_2$(η^8-Pn*)], a similar Ti(IV) complex with a similar reactivity profile and greater steric protection for the titanium core,[73] synthesis of the Pn† analogue of this compound was a logical further step.

Two equivalents of potassium benzyl were reacted with complex **3.4** in toluene, resulting in a brown mixture. Red-brown crystals furnished from a TMS solution at -35°C were identified as the desired *bis*-benzyl compound [Ti(Bn)$_2$(η^8-Pn†)] **4.4** by X-Ray diffraction analysis.

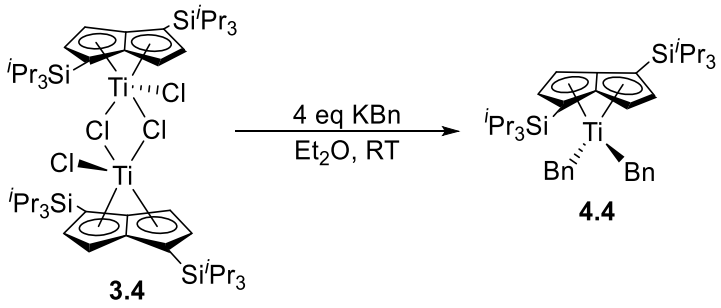

Scheme 4.15 Synthesis of **4.4**.

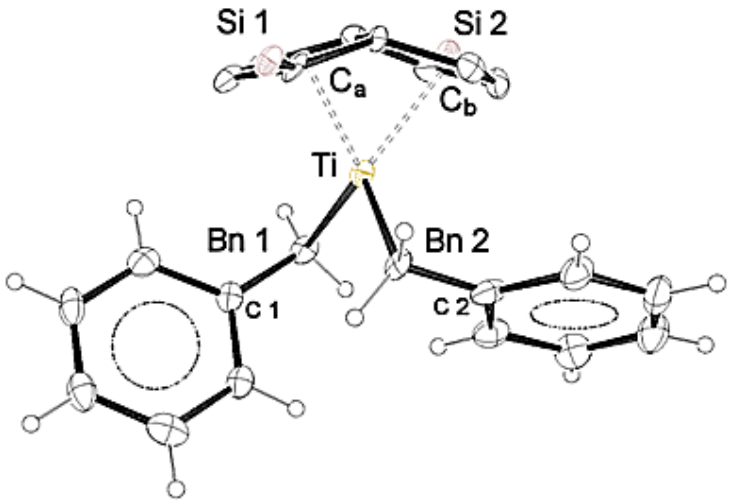

Figure 4.7 Molecular structure of **4.4**, pentalene ring hydrogen environments and TIPS carbon groups omitted. Ellipsoids at 50% probability.

Parameter	Bond Length (Å)	Angle	(°)
Ti-C_a	1.941(15)	Hinge	0.70(4)
Ti-C_b	1.947(16)	Fold	34.60(4)
Ti-Bn 1 CH_2	2.163(9)	Bn 1-Ti- Bn 2	110.70(4)
Ti-Bn 1 C 1	2.744(9)	Ti-Bn 1-C 1	102.40(4)
Ti-Bn 2 CH_2	2.225(8)	Ti-Bn 2-C 2	96.00(4)
Ti-Bn 2 C 2	2.927(9)		
Bridgehead C-C	1.455(11)		

Table 4.4 Selected measurements and bond lengths for complex **4.4**.

Initially, the synthesis of **4.4** was performed at -78°C. As suspected, however, the replacement of methyl groups with benzyl ligands grants the compound improved longevity in solution. Complex **4.4** shows increased resistance to thermal decay in comparison to **4.1**, degrading only when left in solution at ambient temperature for several hours. Future syntheses were thus performed without cooling, as the necessary duration of the reaction for 100% formation of **4.4** as indicated by ^{1}H NMR spectroscopy is only *ca*. 10 minutes and no evidence of unwanted by-products is observed in the proton NMR spectrum.

In spite of this positive development, isolating crystals of **4.4** proved particularly difficult. The lipophilic benzyl groups make the compound both extremely soluble in hydrocarbon solvents and liable to form an oily residue when saturated in solution. Crystals were only isolated successfully in one instance from cold tetramethylsilane. The difficulty of procuring [Ti(Bn)$_2$(η^8-Pn†)] as a crystalline solid combined with the

high average purity of the crude by ^{1}H NMR made *in situ* synthesis of samples the primary method for characterisation and subsequent reactivity experiments.

As with **4.1**, **4.4** possesses *pseudo*-tetrahedral geometry with C_2 symmetry in solution. ^{1}H NMR spectroscopy was performed in deuterated cyclohexane in order to avoid obscuring the aromatic environments of the benzyl group. Two pentalene CH signals are seen by ^{1}H NMR spectroscopy as doublets at δ_H 6.02 ppm and 5.61 ppm. Coupling constants recorded ($^{3}J_{HH}$ = 2.96 Hz and 3.01 Hz) are as expected for pentalene ring proton environments. The complex also showcases the ability of the Pn† ligand to generate facial enantiomerism when coordinated η^8 to a metal centre. The face presented to the metal dictates the orientation of the triisopropyl silyl groups when the metal bound ligands are constrained to a fixed conformation. As a result, two doublets are observed for the inequivalent benzyl CH_2 groups at δ_H 2.29 ppm and 2.18 ppm, each possessing an integration of two. Geminal coupling constants of $^{2}J_{HH}$ 10.26 Hz and 10.33 Hz were recorded, respectively. These values are in good agreement with reported methylene proton-proton coupling frequencies for cyclic systems.[159] In absence of facial enantiomerism, the symmetry of the molecule would instead produce a singlet of integration four. This is exactly what is seen[73] for [Ti(Bn)$_2$(η^8-Pn*)]; due to the universal placement of methyl groups around the ring system, the molecule remains identical regardless of the pentalene facial orientation and the benzyl CH_2 resonance is located at δ_H 1.82 ppm in C_6D_6. This upfield shift relative to **4.4** is likely due to the difference in NMR solvent combined with the greater electron donation of the Pn* ligand to the titanium centre resulting in the metal showing greater EDG character.

Lack of signal crowding in the aromatic region due to use of d_{12}-cyclohexane allowed for facile assignment of benzyl aromatic peaks, displayed here pictorially for convenience.

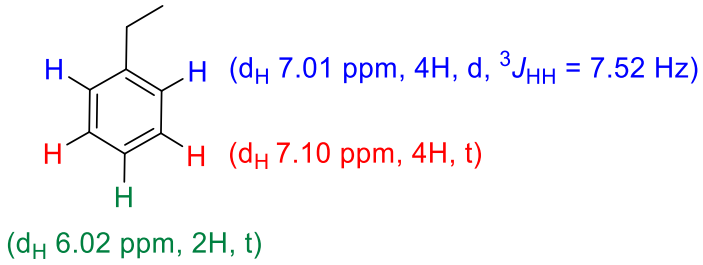

Figure 4.8 Aromatic proton environments present in the ^{1}H NMR spectrum of **4.4**.

One silicon environment is observed for **4.4** by $^{29}Si\{^{1}H\}$ NMR spectroscopy at δ_{Si} 0.21 ppm, further supporting the solid state structure. The increased bulk of the benzyl substituents in **4.4** proved sufficiently robust to withstand EI-MS analysis and a molecular ion of 663 *m/z* was obtained, indicative of a fluorine adduct of **4.4**. Fluorinated compounds are as calibrants for mass spectrometer apparatus[160] and this is the most likely source of the fluorine ion.

The $^{13}C\{^{1}H\}$ NMR spectrum of **4.4** in C_6D_{12} displays four pentalene carbon environments in addition to a single resonance at δ_C 66.4 characteristic of the benzyl CH_2 carbon atom.[73,161] The aromatic environments are depicted in **Figure 4.9**.

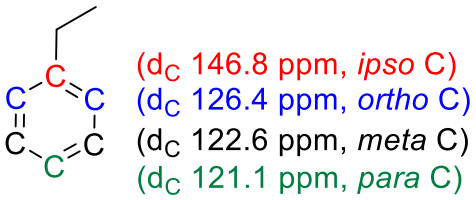

Figure 4.9 Aromatic benzyl ring carbon environments for **4.4**, as identified by $^{13}C\{^{1}H\}$ NMR.

The crystallographic measurements for **4.4** are, as expected, congruent with the Pn* analogue compound [Ti(Bn)$_2$(η^8-Pn†)]. The fold angles of each complex are within one degree of one another, with values of 33.14° for the Pn* complex and 34.60(4)° for **4.4**. Distances between carbons C 1 and C 2 and the titanium centre are elongated by 0.13(9) Å in comparison to the value of 2.61(3) Å reported for tetrabenzyl titanium by Bassi *et al.*[162]. Complex **4.4** shows a Ti-CH_2 distance of 2.163(9) Å characteristic of an η^1 M-C bond, once again in good agreement with the Ti-CH_2 bond length of 2.13(3) Å displayed by Ti(Bn)$_4$. The Ti-Bn 2-C 2 angle of 96.00(4)° is significantly wider than the most acute comparative angle measure for tetrabenzyltitanium[162] (88.00(2)°) and similar to the largest measurement, 98.00(2)°. The Ti-Bn 1-C 1 angle of 102.40(4)° for **4.4** *versus* 108.00(2)°-116.00(2)° for Ti(Bn)$_4$ remains similar between compounds. Together, these metrics discount the possibility of the benzyl moiety displaying an η^3-LX coordination mode; the bond lengths observed are too long and acute angles would be expected if the aromatic ring system was interacting with the metal centre, rather than the widened bond angles obtained. Ti-centroid distances between **4.4** and compound [Ti(Bn)$_2$(η^8-Pn*)] differ by only 0.02 Å.

Reactions with ^{13}CO and $^{13}CO_2$ were attempted with **4.4** as with **4.1**; unfortunately, in contrast to the success found with [Ti(Bn)$_2$(η^8-Pn*)], no spectroscopic evidence was found for the formation of any novel species.

Synthesis of [TiMeCl(η^8-Pn†)]$_2$(μ-Cl) (4.5)

The dimeric "half-sandwich" η^8-pentalene structural motif of **3.4** has been reported extensively in the literature; mixed ligand tantalum and yttrium systems were reported in 2001 by Cloke[42] and more recent examples of this arrangement include permethylpentalene zirconium compounds featuring bridging methyl groups.[163]

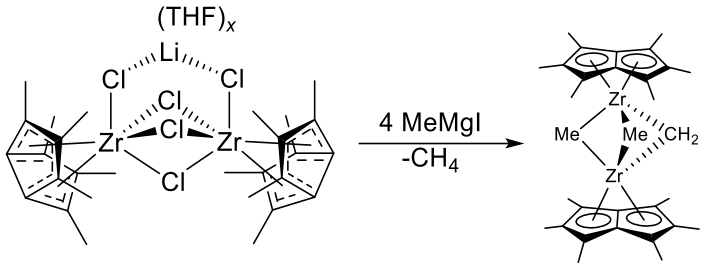

Scheme 4.16 Synthesis of a bimetallic zirconium η^8-Pn* dimer with alkyl substituents.[163]

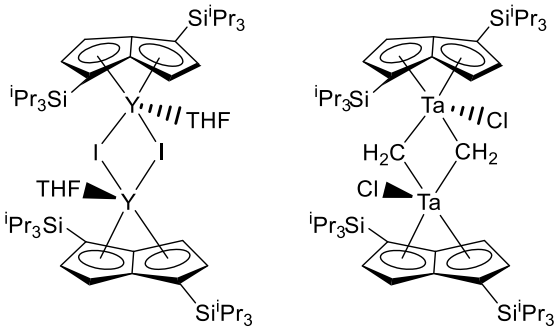

Figure 4.10 Examples of mixed ligand η^8-Pn† dimers.[42]

It therefore seemed plausible to target partial methylation of **3.4**, allowing retainment of the bridging chloride groups and half-sandwich motif, while substituting the terminal M-Cl ligands for reactive alkyl species. This was initially attempted by the reaction of one molar equivalent of $MgMe_2$ with **3.4**. Conditions were chosen to mimic the synthesis of the dimethyl compound; the sample was cooled to -78°C for 10 minutes during the addition of $MgMe_2$, followed by an identical work-up. Although this synthetic method appeared rational, [Ti(Me)$_2$(η^8-Pn†)] was produced in low yield with no evidence by ^1H NMR analysis for the *mono*-methyl complex in solution.

[TiMeCl(η^8-Pn†)]$_2$(μ-Cl)$_2$ was instead serendipitously discovered during optimisation of the synthesis of **4.1**, when the reaction of two equivalents of $MgMe_2$ with **3.4** was halted prematurely. Surprisingly, this method of adding a seeming excess of $MgMe_2$ at -78°C and quenching the reaction after 40 seconds by removal of solvent *in vacuo* proved both reliable and repeatable. The solution must be kept at -78°C as the solvent is removed; an increase in temperature prior to this point results in complete conversion to **4.1**. The sample is isolated as a brown film, extracted in pentane and doubly filtered through Celite® to produce a bright red saturated solution visually undiscernible from **4.1**. However, ^{1}H NMR analysis of the mixture performed at this point in the procedure confirms that **4.1** is absent from in solution, and [TiMeCl(η^8-Pn†)]$_2$(μ-Cl)$_2$ **4.5** is the sole product.

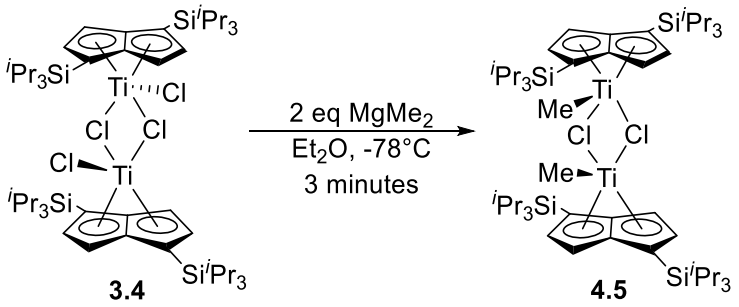

Scheme 4.17 Synthesis of complex **4.5**.

Several further attempts were made to simplify and rationalise the synthetic method by performing the reaction for the same brief duration while halving the amount of $MgMe_2$ used under the same reaction conditions. In contrast to expectation, this appears to actively hinder formation of the *mono*-methylated bridged dichloride in favour of the terminal dimethyl complex. The reason behind this observation is difficult to explain, though it is apparent that an excess of methylating reagent at very low temperatures is paradoxically advantageous for partial methylation. It is possible that a lower concentration of $MgMe_2$ simply slows the reaction rate for *mono*-methyl complex formation to an extent that it progresses to the dimethyl titanium compound (in reduced yield) faster than the *mono*-methyl is formed. At the time of writing, controlled mixing of **3.4** and **4.1** has not yet been performed; it is possible that the dimethyl complex also interacts directly with **3.4** in solution as it forms, to yield **4.5**.

Crystals of **4.5** were isolated from a pentane solution and analysed by X-Ray diffraction.

Characterisation of $[TiMe(\eta^8\text{-}Pn^{\dagger})]_2(\mu\text{-}Cl)_2$ (4.5)

The solid state structure of **4.5** depicts a complex of C_{2h} symmetry, similar to the parent complex $[TiMe(\eta^8\text{-}Pn^{\dagger})]_2(\mu\text{-}Cl)_2$. As with **3.1**, the Ti(IV) centre has a CBC classification of ML_4X_2, producing a 16 electron compound.

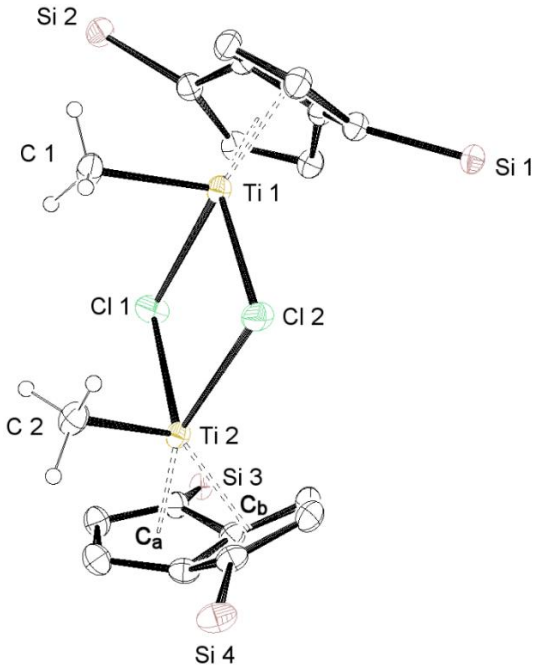

Figure 4.11 X-Ray structure of **4.5**, ellipsoids at 50% probability with pentalene hydrogen and ^{i}Pr groups omitted for clarity.

Parameter	Bond Length (Å)	Angle	(°)
Ti-C_a	1.973(5)	Hinge	0.93(17)
Ti-C_b	1.979(4)	Fold	31.18(15)
Ti-Me 1	2.163(3)	Twist	51.77(15)
Ti-Cl 1	2.419(7)		
Ti-Cl 2	2.566(9)		
Bridgehead C-C	1.454(4)		

Table 4.5 Selected metrics for complex **4.5**.

As **4.5** is effectively a hybrid of the dialkyl complex **4.1**, with the bridging chlorides of **3.4**, it is pertinent to compare the metric measurements of **4.5** to each of these molecules. The Ti-Me C distance in **4.5** equates to 2.163 Å, only a 0.02-0.04 Å deviation from the Ti-Me C σ-bond distances of **4.1**. Ti-centroid distances are also near-identical between compounds at 1.975(10) Å in **3.1** *versus* 1.973(5) Å in **4.5**.

The twist angle between the plane of each pentalene ligand in **4.5** is increased by 51.77(15)° in **4.5** over **3.1**, in which twisting is negligible. This is due to the *cis*-placement of methyl groups, which results in twisting of the rings in opposite directions to adopt the most stable steric conformation. Distances between the titanium centres and bridging chloride atoms in each complex are also similar, with a value of 2.559(18) Å recorded for **3.1** against 2.566(9) Å for **4.5**.

In contrast to **3.1**, the ^{1}H NMR spectrum of **4.5** displays one sharp doublet of integration four at δ_H 6.35 ppm ($^{3}J_{HH}$ = 3.57 Hz) and one broadened singlet of equal integration at 5.85 ppm. Extensive broadening in the aliphatic region also occurs, obscuring the triisopropyl silyl methane CH groups, though the TIPS CH_3 environments are still seen at δ_H 1.15 ppm and 1.11 ppm. Surprisingly, the methyl groups themselves are not visible in the ^{1}H NMR spectrum at ambient temperature. ^{1}H-^{13}C{1H} HSQC experiments denote a correlation a peak at δ_C 48.6 ppm and a signal at 1.08 ppm, buried beneath the broadened region of the ^{1}H NMR spectrum; it is likely this signal corresponds to the Ti-Me group.

^{29}Si{^{1}H} NMR corroborated the symmetry of the solid state structure with one TIPS silicon environment observed at δ_{Si} 0.45 ppm. EI-MS of the crystalline sample produced the molecular ion at 1026 *m/z*, though elemental microanalysis was rendered impossible by thermal degradation of **4.5** to an intractable oil.

Synthesis and Characterisation of [Ti(CH$_2$^{t}Bu)$_2$(η^5:η^1-Pn†(Si(^{i}Pr)$_2$CH$_3$CHCH$_2$)][Li(THF)](4.6)

However, in the case of pentalene, it may be possible for the Pn ligand itself to provide sufficient electron donation, particularly in the case of electron donating substituents placed around the ring as in the case of Pn*.

As discussed in Chapter 1, a reaction recently performed by the Cloke group between **1.1** and an NHC species produced a novel bimetallic sandwich bridged metal hydride.[71] Although the reactivity of pentalene compounds with other carbene species has been explored, isolation of a pentalene metal-carbene complex is yet to be reported in field literature.[10] This made the synthesis of such a complex an attractive goal.

The reaction of complex **3.4** with four molar equivalents of neopentyl lithium (one equivalent for each chloride group) was performed at -78°C in THF, producing a colour

change to bright blue signifying the formation of a new compound, **4.6**. The identity of this compound was confirmed as the *anti*-bimetallic $[Ti(CH_2{}^tBu)_2(\eta^5{:}\eta^1\text{-}Pn^\dagger(Si(iPr)_2CH_3CHCH_2)][Li(THF)]$ *via* X-Ray diffraction of isolated crystalline material.

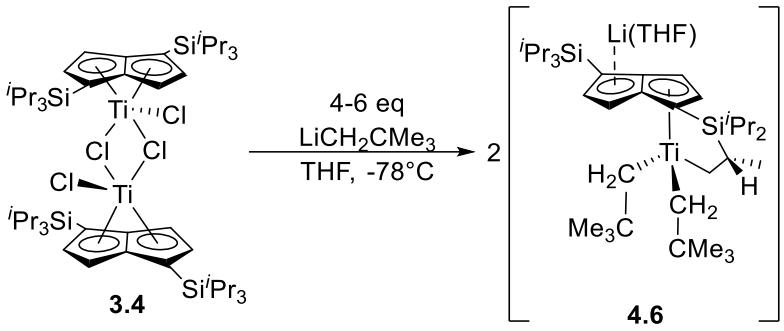

Scheme 4.18 Synthetic scheme for compound **4.6**.

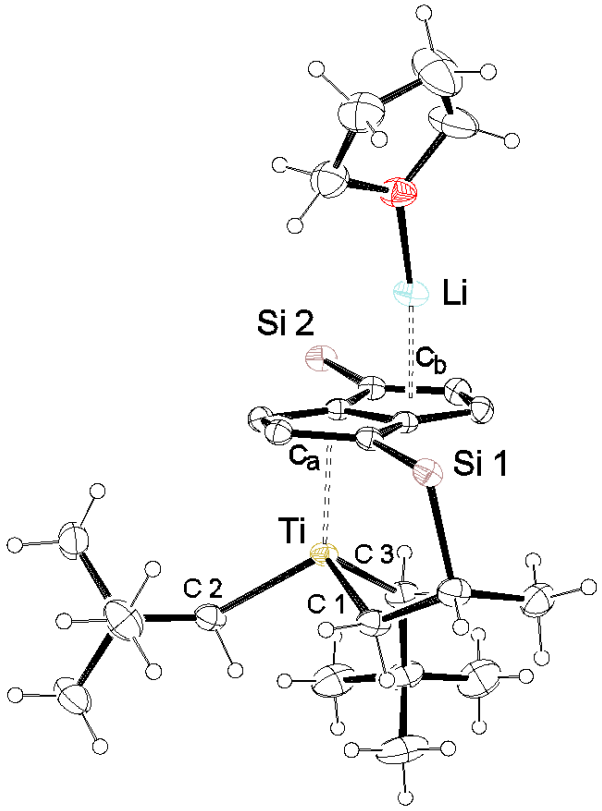

Figure 4.12 ORTEP model of complex **4.6**, ellipsoids at 50% probability.

Parameter	Bond Length (Å)	Angle	(°)
Ti-C_a	2.0871(19)	Hinge	2.14(2)
Li-C_b	1.840(16)	Fold	3.63(4)
Ti-C 1	2.124(14)		
Ti-C 2	2.097(2)		
Ti-C 3	2.135(12)		
Bridgehead C-C	1.451(9)		

Table 4.6 Selected bond lengths and angles for complex **4.6**.

As can be observed from the ORTEP diagram of **4.6**, the complex is an *anti*-heterobimetallic system comprised of a single pentalene ligand showing η^5-ligation to two different metal centres; titanium and lithium (which is also bound to a THF molecule). Lithium is ligated to one anionic half of the pentalene ring, acting as the counterion to preserve charge neutrality while the second half of the ring is bound η^5 to titanium. The solid state structure also confirms the existence of a tuck-in bond from one pentalene TIPS methyl environment to the titanium core. This is in part a result of the electron deficiency of the Ti(IV) centre, which has a total electron count of only $12e^-$ even after metathesis of the methyl group and subsequent binding of CH_2. Four stoichiometric equivalents of neopentyl lithium allows for full substitution of the chloride groups; after loss of the bridging chloride bond present in **3.4**, it is likely the β-silicon effect is responsible for preferential formation of the TIPS tuck-in over coordination of another neopentyl lithium unit. The presence of silicon creates a predilection for formation of a cationic CH_2 species prior to the titanium atom binding, resulting in the consistent isolation of **4.6** with no other products observed.

The compound proved extremely sensitive to temperature conditions. Cooling is critical to compound stability during synthesis and storage; at ambient temperature, complex **4.6** degrades in solution within 50 seconds, showing a pronounced colour change from bright red to yellow-brown. This prohibited use of NMR spectroscopic techniques for characterisation; decay was observed even when the sample was stored in a cardice-packed dewar immediately prior to transfer to the NMR spectrometer. Crystals obtained for diffraction analysis also begain to deteriorate upon the sample slide, necessitating the fastest possible transfer time of single crystals to the diffractometer cryostream.

As the characterisation of **4.6** is heavily reliant upon X-Ray data, analysis of the bond metrics is of particular importance for identifying the nature of the Ti-C bonding

interactions. The Ti-C 1 distance describes the bond length between the titanium centre and the tuck-in CH_2 carbon, and is measured at 2.124(14) Å. This is consistent with a Ti-C σ-bond, being comparable with the value of 2.121(17) Å for **4.1** and 2.142(2) for **4.9**, the only other titanium pentalene tuck-in complex isolated in this work, discussed in depth later in this chapter. A significant difference between **4.6** and **4.9** is that the tuck-in interaction in **4.9** does not originate from a pentalene TIPS methyl group but instead from a TMS group donated by a separate ligand. Nonetheless, the Ti-C distances are very similar, differing by only ~0.02 Å.

The Ti-C 2 distance of 2.097(2) Å is the shortest Ti-C distance recorded of any compound in this work, though it shows similarity to the Ti-C 1 distance of 2.098(3) Å seen in complex **4.7**, a similar *anti*-lithiated η^5-pentalene compound with titanium showing tetrahedral geometry. This shortening of the Ti-C bond is often observed in carbene compounds, with values of ~1.9-2.00 Å reported for a range of iron, platinum and palladium alkylidene compounds.[138] This short bond length apparently does not correspond to any increase in bond or compound stability. M-C σ-bond length was a common metric in early attempts to quantify metal alkyl stability, but this method was found to be flawed. In a 1972 review of M-C σ-bonds, Geoffrey Wilkinson states: "Attempts to correlate only M-C bond lengths with thermal stabilities are doomed to failure and […] arguments based on thermal stabilities of transition metal aryl compounds […] based on shortened metal-carbon bond distances are without adequate support".[128,164]

Schrock-type alkylidene complexes often show a near-180° M-C-C angle between the metal due to agostic interactions between proximal hydrogen atoms and the metal centre.[138,165,166] The Ti-C 2-CH_2 angle of **4.6** is instead 137.663(4)° with no evidence of any CH agostic interactions. Combined, these observations and deductions based on electronic configuration strongly suggest that no carbene complex is formed. Instead, the Ti-C shortening is simply indicative of a strengthened titanium alkyl bond. If any as-yet unobserved transient Schrock-type carbene species does form, it is clearly unstable, most likely due to the limited electon donation provided from the η^5-conformation of the pentalene ligand.

Fold angle is minimal with regard to the angle of *ca.* 30° seen in η^8-pentalene compounds, at only 3.64(3)° for **4.6**. However, this degree of folding is quite pronounced for an *anti*-bimetallic pentalene compound, as seen in comparison to the

anti-complexes **4.7** and **4.8**, which show fold angles of 1.20(3) Å and 0.00(9) Å respectively. A slight deviation of one TIPS group in **4.6** from relativity parity with the pentalene plane is caused by the tuck-in interaction. Due to the rigidity of the pentalene ring, this causes increased bending of one half of the ring relative to the other. Compound **4.7** possesses very similar geometry to **4.6**, but the fold angle is only one third of the value due to the lack of this tuck-in binding from the ring TIPS group.

The discrepancy index of the X-Ray data collected for **4.6** is 0.0447, an R_1 percentile of 4.47%. This is indicative of a good fit between the diffraction data collected and the structural model produced by data refinement and suggests that the ORTEP diagram displayed is a reliable depiction of the compound.

Given that elemental analysis and NMR spectroscopy were rendered impractical by stability issues, it was desirable to obtain a corroborative mass spectrum of the complex if possible. A sample was prepared for ESI-MS analysis and kept at -78°C after synthesis. When loaded into the mass spectrometer apparatus as rapidly as possible (within 30 seconds of synthesis), this approach proved effective and the molecular anion $[Ti(\eta^5\text{-}Pn^\dagger)(\eta^1\text{-}CH_2Si^iPr_2Pn^\dagger)]^-$ was successfully observed at 603 *m/z*.

A review by Lappert *et al.* provides an excellent reference for alkylidene $^{13}C\{^1H\}$ NMR resonances; the alkylidene carbon is observed at chemical shifts as high as δ_C 230-360 ppm, dependent on the EDG or EWG nature of adjacent groups.[138,167] For this reason it is especially unfortunate that **4.6** is unamenable to analysis by heteronuclear NMR, as such a signal would prove definitive of the presence of a titanium carbene species or lack thereof. In the absence of $^{13}C\{^1H\}$ NMR data, the existence of a carbene interaction in this compound based on the other characteristic data obtained seems very unlikely, however. Schrock type carbenes are X_2 ligands; ligation of an X_2 group in addition to the three present X donors in **4.6** would exceed the available valence electrons of the titanium centre and produce a cationic core. While many examples of cationic carbene complexes exist,[138] observation of the complex anion by ESI-MS proves that **4.6** does not contain this type of interaction.

As previously discussed, incorporation of a heteroatom bound to the carbene carbon atom is integral to the development of Fischer-type carbenes[138] and thus neopentyl lithium is a wholly inappropriate reagent for the targeted synthesis of such a compound. Formation of Schrock alkylidenes is also preferential for high oxidation state early

transition metals, while examples of Fischer carbenes are usually isolated for later d-block elements in low oxidation states.[138,139,145] Nonetheless, if this logic is ignored for the sake of further speculation, coordination of a Fischer-type L-donating carbene would result in a Ti(III) centre with an electron count of $13e^-$, making the complex paramagnetic. Despite initial decay of the compound, the crude ^{1}H NMR spectrum of **4.6** collected as soon as possible after synthesis does not show strong evidence of paramagnetism. The aliphatic region is comprised of a complicated array of sharp peaks and the aromatic signals attributable to pentalene (seen at δ_H 6.67 and 6.17 ppm) and shows no sign of broadening. These two pentalene ring protons rapidly decrease in integration to yield no visible pentalene environments as the aliphatic region becomes increasingly complicated. This is suggestive that any remaining pentalene species become paramagnetic and are NMR silent, though the compound of initial greatest concentration is clearly diamagnetic.

In summary, no evidence for a metal-alkylidene interaction exists and the X-Ray structure of **4.6** depicting a trialkyl compound with a single tuck-in interaction from the pentalene TIPS group appears to be accurate.

Synthesis and Characterisation of $[Ti(CH_2TMS)_3(\eta^5\text{-}Pn^\dagger)][Li(THF)_2]$ (4.7)

Compound **3.4** was next reacted with six equivalents of $LiCH_2TMS$. Visual characteristics of the reaction were identical to those seen during the formation of **4.6**, with the same colour change to bright blue indicative of THF adduct formation remaining consistent. X-Ray analysis of the red crystals isolated by work-up of the reaction mixture depict the *anti*-heterobimetallic complex, $[Ti(CH_2TMS)_3(\eta^5\text{-}Pn^\dagger)][Li(THF)_2]$ **4.7**. This formula was also supported by ESI-MS data, with the observation of the molecular ion at 653 *m/z* (minus one fragmented TMS group).

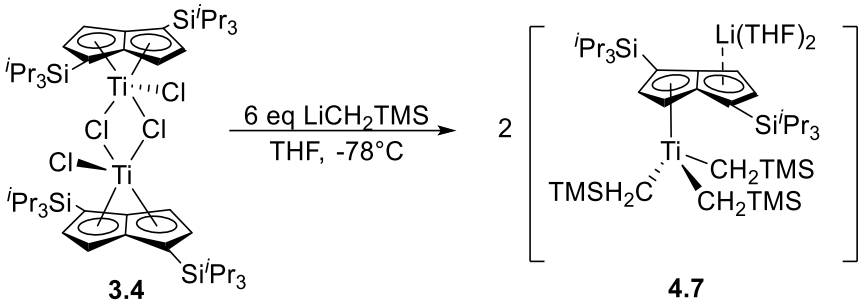

Scheme 4.19 Synthesis of **4.7**.

Attempting the synthesis of **4.6** or **4.7** in a non-coordinating solvent results in immediate decay of the complex to an intractable mixture. It is therefore clear that the presence of coordinated THF is required to stabilise the *anti*-lithiated product. Use of excess $LiCH_2TMS$ in stoichiometries greater than six equivalents consistently produced complex **4.7**.

Complex **4.7** shows greater stability in solution than **4.6** and displays a notable change in colour from red to orange over 10 minutes as opposed to a delay of seconds. After a period of several hours, the colour of the sample progresses to dark brown, with the intermediary orange colouration caused by the presence of both pure **4.7** and intractable decay products.

The ^{1}H NMR spectrum of crystalline **4.7** shows four peaks attributable to aromatic pentalene ring proton environments at δ_H 7.09 ppm, 6.65 ppm, 6.54 ppm and 6.12 ppm. The aliphatic region shows no evidence of paramagnetic broadening, instead depicting complete asymmetry of pentalene TIPS environments with a large number of partially overlapping, sharp doublet and multiplet peaks. The sum integration of these peaks is 42, consistent with two non-equivalent pentalene TIPS environments. Combined, these results suggest formation of an asymmetric monometallic pentalene species similar in structure to **4.6**. This is further supported by the presence of three separate TMS CH_3 proton resonances at δ_H 0.42 ppm, 0.35 ppm and 0.00 ppm, the integration of each producing a value of nine, for a sum total of 27 hydrogen atoms. Identification of the CH_2 groups is more difficult, as doublet peaks in the region δ_H 1.87-1.64 ppm overlap significantly, though the total integration value of these signals implies the presence of six hydrogen atoms.

Despite the notable colour change at ambient temperature, heteronuclear NMR data collected over *ca.* 12 hours appear mostly consistent with the solid state structure and

ESI-MS results. The $^{29}Si\{^{1}H\}$ NMR spectrum was collected over 16 hours and depicts five silicon environments, as would be expected for three asymmetric silicon TMS environments and two inequivalent pentalene TIPS signals. Seven pentalene carbon signals are present in the $^{13}C\{^{1}H\}$ NMR spectrum. Five peaks are distributed between δ_C 126.9 ppm and 93.9 ppm, characteristic of aromatic pentalene carbon environments. Two further signals at δ_C 81.9 ppm and 79.7 ppm are indicative of two non-symmetric pentalene bridgehead carbon atoms, again supportive of the X-Ray diffraction data gathered. It appears that the eighth pentalene environment is buried underneath the C_6D_6 peak, which the uppermost visible Pn ring carbon environment appears directly adjacent to. Three $LiCH_2TMS$ signals appear at δ_C 35.4 ppm, 31.4 ppm and 24.8 ppm. The latter signal appears extremely weak in the $^{13}C\{^{1}H\}$ NMR spectrum and was initially identified by a ^{1}H-^{13}C HSQC correlation experiment performed upon a concentrated (30 mg) sample. Also present are eight separate $^{i}Pr_3Si$ methyl carbon environments between δ_C 22.1 ppm and 19.6 ppm. Six TIPS CH carbon environments are present between δ_C 13.9 ppm and 11.9 ppm, showing complete inequivalence of all methine CH environments present in both TIPS groups. From this observation, it would follow that the TIPS CH_3 environments would also be inequivalent, producing a total of 12 signals; instead eight are observed. This is likely due to the close proximity of each TIPS CH_3 carbon peak, the overlap of which obscures the remaining four resonances. Finally, three separate TMS CH_3 carbon environments are seen from δ_C 2.8 ppm to 0.0 ppm. As with **(4.6)**, no evidence was observed for carbene environments in the $^{13}C\{^{1}H\}$ spectra collected.

^{1}H NMR spectra collected for **4.7** after prolonged data collections at ambient temperature show that pentalene signals attributable to **4.7** have weakened significantly and new, broad singlet peaks form over time at δ_H 6.91 ppm and 6.03 ppm. These signals show equal integration to those representative of compound **4.7**, and are therefore present at a sufficient concentration to influence $^{13}C\{^{1}H\}$ and $^{29}Si\{^{1}H\}$ data. A cautious interpretation of the data is therefore necessary at this stage despite the apparent correlation between the heteronuclear spectra obtained and other characterisation data.

The ^{7}Li NMR spectrum of **4.7** is symptomatic of this decomposition, and shows three environments instead of the single signal that would be expected from the geometry of the solid state structure or the other NMR spectra collected. The signal observed at δ_{Li} -6.95 ppm shows highest magnitude, with the next environment at -6.87 ppm displaying only one fifth of the relative integration value. Finally, the third environment is seen as a very weak, broad peak at -6.76 ppm and possesses an integration value relative to the largest peak of only 0.04. While open to interpretation, in combination with the observed colour change over time, this result would seem to imply that the peak at δ_{Li} -6.95 ppm at the greatest concentration can be attributed to the lithium environment of **4.6**, while the other two signals result from less concentrated decay products forming at variable rates.

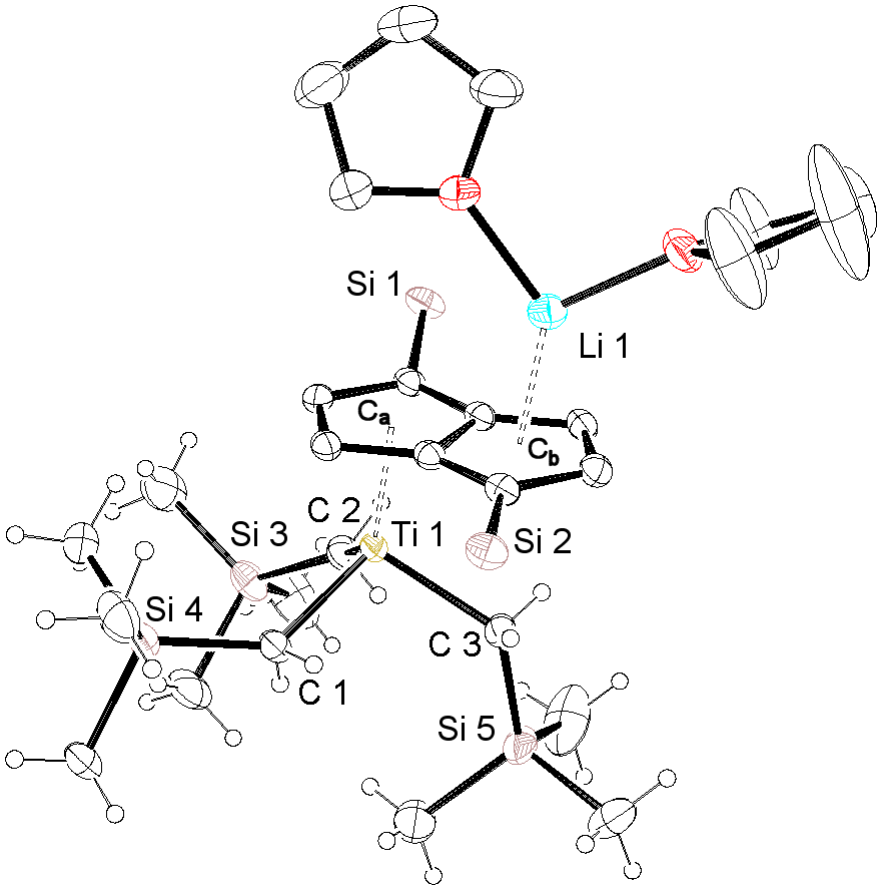

Figure 4.13 X-Ray crystallographic structure of compound **4.7**.

Parameter	Bond Length (Å)	Angle	(°)
Ti-C_a	2.092(4)	Hinge	1.06(3)
Li-C_b	2.082(5)	Fold	1.20(3)
Ti-C 1	2.098(3)		
Ti-C 2	2.113(3)		
Ti-C 3	2.114(3)		
Bridgehead C-C	1.448(2)		

Table 4.7 Selected bond lengths and metrics for complex **4.7**.

Complex **4.7** is isoelectronic with **4.6**, with a formal electron count of 12, and shows the same tetrahedral titanium geometry. However, the tuck-in interaction between the pentalene TIPS group and the titanium core is absent, replaced instead with binding of three CH_2TMS ligands. The presence of **4.7** as the sole product of the reaction persists even with increased concentration of $LiCH_2TMS$, an excess of which increases yield of **4.7** but otherwise has no effect on the final product. Similarly, further decreasing the amount of $LiCH_2TMS$ in solution does not result in any tuck-in behaviour to compensate, but simply decreases yield of **4.7**.

Compounds **4.6** and **4.7** are particularly intriguing from a synthetic standpoint as they combine the reactivity potential of a pentalene stabilised, low valent titanium-alkyl system with the synthetic flexibility of a stabilised anion present on the ligand itself. This allows for the direct reaction of the lithiated pentalene with electrophilic metal halide salts in classic salt metathesis reactions, making these species potentially excellent precursors for the synthesis of both *anti*-homobimetallic and *anti*-heterobimetallic pentalene metal alkyl complexes.[61,168]

Of the two complexes, **4.7** is better adapted to this use by simple virtue of its apparent increased longevity in solution. When conducted on a small scale with adequate preparation (including *in situ* synthesis of the lithiated complex), salt metathesis reactions with titanium pentalene complexes often proceed successfully to completion within minutes at temperatures as low as -78°C, making issues of compound decay less prohibitive. This is seen specifically with the reaction between $[TiCl(\mu{:}\eta^5,\eta^5\text{-}Pn^\dagger)]_2$ **3.1** and $MgMe_2$ later in this chapter.

Functional groups ligated to the second metal centre can also be modified with relative ease prior to reaction with **4.7**, giving access to a vast number of derivatisations. As this compound was synthesised towards the end of practical experiments conducted over the

course of this project, this reactivity has not yet been explored, though it may prove a tantalising prospect for future investigation.

When assessing the solid state structure of **4.7** *versus* **4.6**, the singular steric difference between the neopentyl group and the TMS group lies with the larger atomic radius of silicon at 111 pm *versus* 70 pm for carbon. In combination with the very similar electronics of both systems, this variation does not seem significant enough to explain the omission of one neopentyl group in favour of a tuck-in interaction with the TIPS group and the ultimate reason that **4.7** shows overwhelming preference for three CH_2TMS ligands remains unknown. A review of metal alkyl chemistry published by Schrock and Parshall does state[119] that first row transition metals may only bind a maximum of three units of the $LiCH(TMS)_2$ ligand due to steric demands; while this ligand is larger, this further hints that it is possibly sterically preferable for **4.6** to adopt a tuck-in conformation with the pentalene TIPS group over addition of a third neopentyl group. Again, this leaves the question of why CH_2TMS groups do not produce the same result unanswered. Schrock discusses ligand hydrogen abstraction as a driving force in the formation of tuck-in compounds resulting from alkyl complex degradation.[119] As one unit of the metal-bound alkyl unit is lost due to thermal degradation, a CH_3 group from a ligand in close special proximity may tuck-in to compensate for this.

The example ligand described in this literature exploration of tuck-in formation is the Cp* methyl group. The electron withdrawing nature of the ring π-system increases the acidity of the ligand CH_3 protons above that of any other metal-bound alkyl group, resulting in preferential deprotonation and binding of the Cp* ligand substituent. As **4.6** decays so rapidly, it is therefore plausible that the compound initially forms in similar fashion to **4.7**, with three neopentyl ligands and a titanium centre in tetrahedral arrangement, bound η^5 to pentalene. This species is essentially transient, as one neopentyl group is immediately lost and the TIPS CH_3 group in proximity to the EWG pentalene π-system then forms the tuck-in complex isolated and observed by X-Ray diffraction analysis. Since **4.7** is comparatively stable, the tuck-in compound is not formed as quickly and thus is not observed in the crystalline state if the solution is kept cold. Though this is somewhat speculative reasoning, further attempts at crystallising **4.7** after visual signs of degradation have been noted at ambient temperature would prove this line of logic correct if a similar tuck-in complex is isolated from this partially decayed mixture.

As with **4.6**, the small degree of hinging and folding is characteristic of μ:η^5,η^5 pentalene binding. Ti-C bond lengths are consistent with both literature values[67] for M-C σ-bonds and those measured over the course of this work, though as compared with **4.6**, the Ti-C 1 length displays a degree of shortening. Given the lack of evidence for any alkylidene-type interaction, this appears to simply be evidence of a strong Ti-C σ-bond, as with **4.6**. A repeat $^{13}C\{^1H\}$ NMR experiment conducted at reduced temperature with a concentrated sample would be worthwhile in order to definitively rule out the presence of a carbene resonance, as spectra collected with a widened spectral window unfortunately showed extensive decay.

Synthesis and Characterisation of [(Ti(Me)$_3$)$_2$(μ:η^5,η^5-Pn†)] (4.8)

Complex **4.8** was isolated serendipitously as a single crystal from a micro spatula previously used to manipulate a crystallised sample of **4.1**. The ^1H NMR spectrum of the bulk sample of **4.1** showed no resonances suggestive of secondary species in solution, providing the implication that **4.8** is present in only minute quantities. Nonetheless this singular sample of **4.8** produced a strong diffraction pattern depicting an *anti*-bimetallic titanium complex bridged by 1,4-triisopropylsilyl pentalene with η^5,η^5 hapticity.

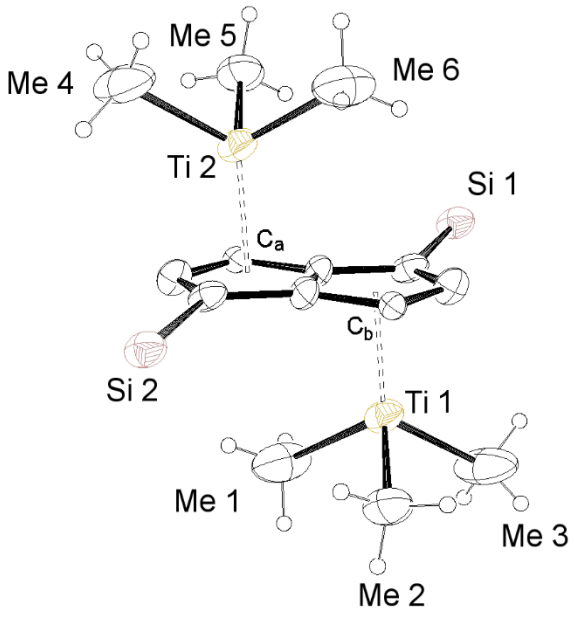

Figure 4.14 X-Ray crystallography structure of complex **4.8**.

Parameter	Bond Length (Å)	Angle	(°)
Ti-C_a	2.082(16)	Hinge	1.80(4)
Ti-Me 1	2.074(12)	Fold	0.00(9)
Ti-Me 2	2.080(18)		
Ti-Me 3	2.073(12)		
Bridgehead C-C	1.442(5)		

Figure 4.15 Measurements taken from the crystallographic model of complex **4.8**.

The most notable metrics of **4.8** are the fold and hinge angles. The compound shows near zero degree of folding (with room for deviation within the ESD value) and does not deviate from planarity; this is common amongst *anti*-bimetallic species.[62] The hinge angle, however, is comparatively high at 1.80(4) Å, resulting in a slight upturn of the wing-tip pentalene carbons. Ti-Me distances show a minor degree of shortening in comparison to **4.1** and are considerably shorter than the Ta-Me distance of 2.326(3) Å reported[169] for [$TaMe_2Cl(\eta^8$-$Pn^{\dagger})$], which shows a similar tetrahedral arrangement.

An attempt was made to devise a repeatable, rational synthesis of **4.8**. A method of synthesising $TiMe_3Cl$ from $TiCl_4$.2THF first reported by Schlegel *et al.*[170] was used to produce a suitable metal precursor for reacting with a pentalene salt. The mixture was kept at -78°C and further $TiCl_4$.2THF was added at this temperature, resulting in a comproportionation reaction to give $TiMe_3Cl$ as the principle product. Further reaction with ½ an equivalent of $K_2Pn^{\dagger}$ was then performed with the desired goal of producing exclusively producing **4.8**. A very similar method has been used previously by the Cloke group for the synthesis of *anti*-bimetallic lanthanide pentalene complexes.[10]

Unfortunately, despite these efforts, this procedure simply yielded complex **4.1** with no other complexes present in solution when the sample was analysed by ^{1}H NMR spectroscopy and EI-MS.

Reactivity of $[TiCl(\mu{:}\eta^5,\eta^5\text{-}Pn^{\dagger})]_2$ (3.1) with $MgMe_2$

When ^{t}BuCl is added to **1.1** at -78°C within one mL of toluene, the solvent can be removed after 30 seconds to give a powder brown in colour with a mild green hue. Due to the extreme sensitivity of **3.1** in solution, it is difficult to provide infallible evidence that this powder is a pure sample of compound **3.1** at this stage of reaction. Taking a sample of the solid to analyse by NMR spectroscopy or EI-MS was unviable. However,

since **3.1** was repeatedly observed as the major product by ^{1}H NMR in cold samples five minutes after addition of ^{t}BuCl (albeit with small quantities of **3.4** in evidence), it is a reasoned extrapolation from this data that **3.1** is most likely formed in isolation at the immediate beginning of the reaction.

It was decided to attempt a reaction of $MgMe_2$ with **3.1** *in situ* to test if displacement of the halide groups was possible, potentially yielded a unique Ti-Ti bonded dimethyl (μ:η^5,η^5-Pn†) sandwich.

Any minor delay in handling the brown powder, even at -78°C, resulted in its degradation to a much darker, intractable brown substance, in keeping with the properties of **3.1** in solution. To counter this, a separate solution of $MgMe_2$ in THF was prepared (with a slight excess of $MgMe_2$ due to the poor solubility of the complex) and cooled to -78°C prior to isolation of the brown powder. Upon obtaining the dried powder, the solvated methylating agent was transferred to the vessel immediately.

Interestingly, addition of this THF solution rapidly results in a bright purple mixture. This observation is in keeping with what is seen during the formation of [(Ti(Me)$_2$(η^8-Pn†)] when the reaction is performed in THF (with this colour change likely due to the formation of an as-yet unisolated THF adduct). When dissolved in THF *sans* addition of a methylating agent, neither the brown powder or any other identified chloride compounds (including **3.2**, **3.3** and **3.4**) display any such colour change. Instead these complexes merely become red in colour, as when dissolved in any non-binding hydrocarbon solvent.

With this observation providing some tentative evidence for the formation of a new species, the sample was kept cold and left to crystallise. Stability increased significantly after addition of the methylating agent and no degradation to the brown substance was witnessed. An aliquot taken from the crude sample was analysed by ^{1}H NMR spectroscopy. The resulting spectrum was remarkably clean without purification work-up and contained only one unknown species. This unknown complex displays eight separate, sharp pentalene hydrogen resonances, suggesting an asymmetric conformation.

Several useful deductions can be made from this result. It is apparent that the species in solution (hereby referred to as **4.1.U**) is novel, as none of the previously isolated chloride or alkyl species exhibits eight equal integration pentalene peaks by ^{1}H NMR.

This spectrum also disproves any formation of **3.4** prior to addition of $MgMe_2$, as [$(Ti(Me)_2(\eta^8\text{-}Pn^{\dagger})$] is formed in this case, and there is no evidence for this complex observed in solution. Finally, the spectrum also disproves any possible rearrangement of a transient dimethyl sandwich to the theoretically more stable [$(Ti(Me)_2(\eta^8\text{-}Pn^{\dagger})$] by this same absence.

If a simple replacement of the chlorides by methyl groups had occurred to create a bimetallic sandwich with Ti-ligated methyls, the symmetry of **4.1.U** would remain fundamentally similar to **3.1**. The complex would be diamagnetic with a total of 34 electrons, with the observation of four Pn-H environments by ^{1}H NMR. However, methyl groups may be terminal or bridging, raising the possibility of one non-bridging and one-bridging methyl group between the metal centres. This would concur with the inequivalence of the pentalene ring hydrogen environments observed for the unknown purple mixture. EI-MS analysis of the mixture also supported this preliminary evidence for existence of the methylayed sandwich species, returning a molecular ion peak at EI-996 *m/z* characteristic of $[[TiMe(\mu{:}\eta^5,\eta^5\text{-}Pn^{\dagger})]_2]^+$.

Complex **4.3** also displayed promise as a more stable precursor for the synthesis and identification of **4.1.U**. Reaction of **4.3** with a reducing agent to effect a two electron reduction (one e^- per metal centre) would theoretically allow for the abstraction of both chloride groups to yield $[TiMe(\mu{:}\eta^5,\eta^5\text{-}Pn^{\dagger})]_2$. This reaction was performed using potassium amalgam in THF, and as with the direct methylation route, a colour change to bright purple was observed over several hours. Unfortunately however, after two hours of vigorous stirring the complex had been reduced to the point of decay, yielding a slurry of Ti(0) and unligated pentalenes.

Analysis by ^{1}H NMR spectroscopy of an aliquot taken from the mixture shortly after K/Hg was added was in excellent agreement with the eight Pn-H resonances observed for **4.1.U**, though the integration of each peak was significantly weaker (presumably due to the early stage of reaction). Due to time constraints, this reaction has not yet been repeated over a shorter duration, however this would be of future interest in addition to experimenting with milder reducing agents.

Synthesis of [Ti(η^8-Pn†)(η^2-$CH_2SiMe_2NSiMe_3$)] (4.9)

Reactivity studies of **3.4** were not limited to the use of alkylating agents. A wide variety of experiments with nucleophilic sodium and potassium salts were performed, the majority of which proved unsuccessful and thus have not been elaborated upon in further detail. Reactions with sodium hydride and lithium superhydride resulted in immediate decomposition of the compound, while potassium methoxide was found to reduce **3.4** to complex **1.1**, seen by re-emergence of characteristic pentalene ring proton signals at δ_H 6.82 ppm and 6.34 ppm in the ^{1}H NMR spectrum. Other reagents such as $MgEt_2$ and KCH_2TMS showed initial colour changes suggestive of successful reaction but subsequently formed intractable mixtures.

Over the course of these experiments, compound **3.4** was reacted with a non-nucleophilic base, KHMDS. KHMDS has seen recent use in the reliable generation of both NHC species[171] and mesoionic variants of these species referred to as aNHCs (abnormal N-heterocyclic carbenes)[172] *via* deprotonation.

As reactions with $LiCH_2TMS$ and neopentyl lithium had showcased the lithiation of one half of the pentalene ring system, it was of interest to see if any similar 139etalation would occur with a mildly nucleophilic potassium species in absence of direct attack upon the metal halide. The formation of a TIPS tuck-in during the synthesis of **4.7** also demonstrated the ability of the electron deficient titanium centre to dehydrogenate proximal methyl groups, potentially allowing for an interaction with the TMS groups of KHMDS. However, even with this loose rationale in place, the reaction was initially performed merely as a curiosity, with no strong expectation of isolation of a specific product.

The reaction proved successful, producing a colour change when **3.4** is reacted with one equivalent of KHMDS to brown. The resulting ^{1}H NMR spectrum of the crude mixture displays eight sharp signals in the aromatic region, suggestive of formation of an asymmetric compound retaining two pentalene ligands. However, the compound degrades quickly in solution and the aliphatic region appears broadened. After *ca.* two hours the compound deteriorates almost completely, forming a complicated mixture of complexes when analysed by ^{1}H NMR spectroscopy. Even when analysed rapidly after the colour change is observed, the ^{1}H NMR spectrum shows seven different TMS environments of varying integration, which appears to imply that decay of the compound starts almost immediately at ambient temperature.

Unfortunately, repeated attempts to crystallise this species from a variety of solvents failed to yield material suitable for X-Ray analysis. Attempts were made to analyse the crude mixture by EI-MS, but further details of the identity of this compound were unforthcoming.

Reaction of **3.4** with two or more equivalents of KHMDS resulted in the formation of a second complex, **4.9**, which was successfully isolated and proved stable in solution.

Characterisation of [Ti(η^8-Pn†)(η^2-$CH_2SiMe_2NsiMe_3$)] (4.9)

Although KHMDS is typically employed as a non-nucleophilic reagent,[171] the solid state structure of **4.9** shows complete displacement of the halide groups of **3.4** by KHMDS to yield an η^8-pentalene, non-symmetric monometallic complex. Both compound **3.4** and KHMDS lose their dimeric structure, with one bis(trimethylsilyl)amide "half-unit" of the KHMDS molecule bound to the titanium core. Ligand binding to the metal centre encompasses formation of a tuck-in metal alkyl bond from one TMS group of the amide and X-type bonding (confirmed by bond length, below) from the nitrogen atom.

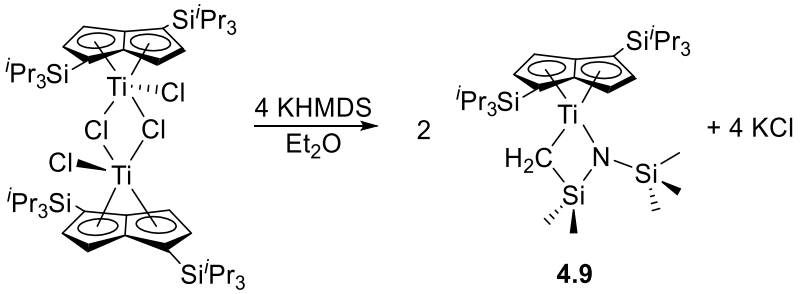

Scheme 4.20 Synthesis of complex **4.9**.

Formation of compound **4.9** is not observed unless two or more equivalents of KHMDS are present. This is the correct stoichiometry for the formation of four equivalents of KCl, allowing for the complete substitution of the chlorine environments of **3.4**.

The ^{1}H NMR spectrum of **4.9** shows four pentalene ring proton environments between δ_H 6.36 ppm to 5.91 ppm. This asymmetry also results in inequivalency in the tucked-in KHMDS TMS CH_2 proton environments, causing this group to manifest as two separate CH doublets at δ_H 1.64 ppm and 1.49 ppm. The $SiMe_2CH_2$ group methyl environments are observed as singlet resonances at δ_H 0.51 ppm and 0.29 ppm. This δ_H 0.29 ppm

resonance occurs at the exact same chemical shift as a TMS CH_3 resonance in the reaction mixture resulting from the reaction of one equivalent of KHMDS with **3.4**. However, the integration of each group differs significantly (3H *versus* 6H) and no other traces of **4.9** are observed in the ^{1}H NMR spectrum of that mixture; these groups are therefore unlikely to be related.

The second TMS environment in the ^{1}H NMR spectrum of **4.9** has completely equivalent methyl groups, producing one large singlet peak at δ_H 0.14 ppm with an integration value of nine.

Assignment of the ^{1}H NMR spectrum is further supported by $^{13}C\{^1H\}$ data, which contains eight independent pentalene carbon environments. $^{13}C\{^1H\}$-^{1}H HSQC experiments confirm that a signal observed at δ_C 48.3 ppm corresponds to the Ti-CH_2 carbon atom, displaying an expectedly similar chemical shift to the δ_C 47.3 ppm value seen for The Ti-methyl carbon in **4.1.** TMS carbon environments are seen as three separate resonances at δ_C 5.6 ppm, 5.1 ppm and 3.1 ppm.

The $^{29}Si\{^1H\}$ spectrum of **4.9** shows two resonances attributable to the pentalene TIPS environments at δ_{Si} -0.04 and -0.08 ppm, with one further signal at δ_{Si} -3.37 ppm indicative of one TMS silicon group. As the TMS silicon environments are not symmetrically equivalent, it follows that one silicon further environment should be present in this spectrum. The TIPS group signals are grouped tightly, overlapping at the base, providing the possibility that a further silicon peak is buried beneath these signals. However, given the similarity of the TMS silicon environments in **4.9**, it seems highly unlikely the "missing" resonance would be downfield shifted to the extent that the TIPS group resonances would obscure it; the shift difference between δ_{Si} -0.08 ppm and -3.37 ppm is significant. Alternatively, despite the chemical inequivalence of each TMS group, it is possible that the silicon atoms are close to magnetic equivalency in the ^{29}Si spectrum as they exist in near-identical environments with three alkyl substituents each. It is therefore possible that the signals for each silicon environment overlap and do not prove distinct in the observed spectrum. This explanation still does not satisfactorily account for the ^{1}H and $^{13}C\{^1H\}$ NMR signals recorded, however, which clearly imply that the TMS environments differ enough to be clearly identified as separate peaks. Another resonance was seen at -34.88 ppm, though this was later determined to be a recurrent impurity of unknown origin in the C_6D_6 used for the NMR sample.

EI-MS proved effective for the analysis of **4.9**, yielding a fragmentation pattern of expected average isotopic distribution with the complex molecular ion visible at *m/z* = 622. Elemental microanalysis of crystalline **4.9** produced atomic composition data in agreement with the X-Ray solid state structure and NMR spectroscopic data gathered.

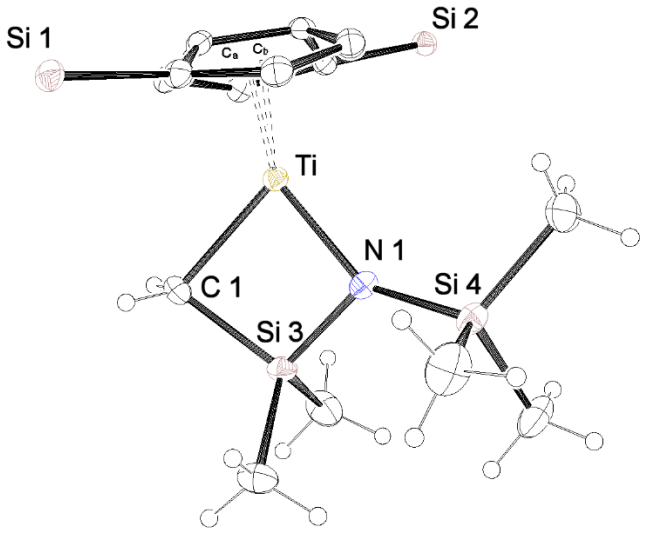

Figure 4.16 ORTEP diagram of complex **4.9**, pentalene ring hydrogen environments and TIPS groups omitted.

Parameter	Bond Length (Å)	Angle	(°)
Ti-C_a	1.972(2)	Hinge	0.13(2)
Ti-C_b	1.964(18)	Fold	34.44(12)
Ti-C 1	2.142(2)	Σ(X-N 1-Y)$_{Angles}$	358.20(16)
Ti-N 1	1.938(18)		
Bridgehead C-C	1.459(14)		

Table 4.8 Selected measurements and bond lengths for compound **4.9**.

The pentalene ligand angles of **4.9** are congruous with the η^{8-}pentalene binding mode; as with other complexes featuring this conformation, the ligand shows a fold angle of 34.44(12)°, rather than the negligible folding seen in the [μ:η^5,η^5] bridging motif (of which **4.8** is a prime example). The Ti-N 1 distance of 1.938(18) Å is in good agreement for a Ti-N single σ-bond interaction, with the comparatively elongated 2.146(3) Å for the L-donating isocyanide **4.3**. The xylylisocyanide adduct of **1.1**, complex **5.3** (see Chapter 5) also displays L-type donation, with a bond length of 2.197(4) Å.

The Ti-C 1 distance of 2.142(2) Å is similar to the Ti-Me σ-bonds in **4.1**, which measure at 2.144(13) Å and 2.121(17) Å. From the bond metrics (and the diamagnetic NMR spectra obtained), it is possible to deduce that **4.9** possesses a CBC classification of ML_4X_4, with a total electron count of $14e^-$ and a formal Ti(IV) centre.

Despite the similarities to other M-C σ-bond distances, the Ti-CH_2 bond in **4.9** is slightly shorter than crystallographically characterised tuck-in compounds reported in the literature. By comparison, the decamethyltitanocene CH_2 tuck-in derivative isolated[173] by Fischer *et al.* in 1996 (**Figure 4.17**) displays a Ti-CH_2 distance of 2.281(14) Å. The dimeric uranium Cp* tuck-in, "tuck-over" complex reported by the Evans group shows greater elongation,[174] with a U-CH_2 tuck-in σ-bond distance of 2.564(1) Å. The "tuck-over" U-CH_2 interaction, in which the CH_2 bound to one Cp* group is metallated onto a uranium core not ligated to that Cp* group through the ring system, is further lengthened at 2.640(1) Å. In addition to bond distance increases caused by the geometry of this species, U-Me σ-bonds are inherently lengthened in comparison to transition metal M-Me single bonds[174] by around 0.3 Å (at *ca*. 2.4 Å to 2.1 Å respectively).[73,174,175]

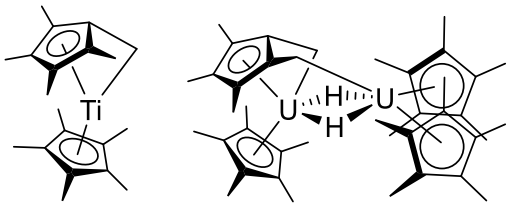

Figure 4.17 A titanium tuck-in compound and a combination tuck-in and "tuck-over" uranium complex.

The most likely reason for the shortened Ti-C bond of **4.9** lies with the ligand sterics of the system. The decamethyltitanocene tuck-in carbon is a dehydrogenated methyl substituent of the Cp* ligand. This imposes a degree of restriction on the minimum Ti-C distance due to the rigidity of the Cp*-CH_2 bond and the Ti-Cp* centroid distance. Similarly, the bridging dimeric uranium tuck-in species possesses a total of four sterically demanding Cp* rings, the twisted comformation of which precludes any closer bonding. By contrast, complex **4.9** is not a homoleptic sandwich complex and instead possesses a single pentalene ligand capping one face of the titanium atom coordination sphere, with the opposite face entirely occupied by only the

trimethylsilylamide fragment. This moiety is symmetrical prior to bonding and acts directly as the tuck-in donor ligand rather than a methyl group bound to the pentalene ligand itself (or TIPS substituent). Unlike Cp* tuck-ins, this means there is no restriction placed upon the Ti-C distance by the ligand geometry and the binding of the $N(SiMe_3)_2$ moiety to the open face results in no obstruction of the tuck-in bond by other sterically demanding ligands in proximity. This results in a shorter Ti-C bond more akin to a generic metal alkyl complex than a traditional "tuck-in" species. As previously discussed, shorter M-C bonds cannot be simply assumed to inherently produce more stable products, though **4.9** is noticeably less prone to thermal decomposition in comparison to many of the other Ti-alkyl complexes produced in this chapter. The shorter M-C length may be one possible reason for this, though DFT study of the complex is necessary to yield a definitive answer.

Conclusions

A total of eight novel Ti(Pn†) compounds possessing metal-carbon σ-bonds were successfully synthesised and characterised where possible by ^{1}H, ^{13}C and ^{29}Si NMR spectroscopy. These species include the dimethyl complex $[Ti(Me)_2(\eta^8\text{-}Pn^{\dagger})]$ **4.1**, which when reacted with CO_2 produced the di-carboxylate complex $[Ti(OAc)_2(\eta^8\text{-}Pn^{\dagger})]$ **4.2** in analogous fashion to the Pn* variant of the compound.[67]

An example of isocyanide insertion into a titanium methyl bond was observed during the reaction of **4.1** and xylylisocyanide, forming $[Ti(\eta^8\text{-}Pn^{\dagger})(\eta^3\text{-}C_8H_9NCMe)_2]$, **4.3**. Unlike all other species isolated in this chapter, this compound proved stable at ambient temperature and was characterised by elemental microanalysis.

Further isolated species included the *bis*-benzyl compound $[Ti(Bn)_2(\eta^8\text{-}Pn^{\dagger})]$ **4.4** and an η^8-Pn† "half-sandwich" compound with bridging chloride groups in addition to terminal methyl moieties, $[TiMe(\eta^8\text{-}Pn^{\dagger})]_2(\mu\text{-}Cl)_2$ **4.5**.

Unfortunately, attempts at confirming reactivity of **4.1** with CO were inconclusive, despite ^{13}C and ^{1}H NMR evidence that binding of the gas has occurred. Gas reactions performed with **4.4** and **4.5** also showed no evidence of success.

Reactions with $LiCH_2TMS$ and neopentyl lithium produced *anti*-bimetallics **4.6** and **4.7** respectively. Compound **4.7** shows formation of a TIPS-group tuck-in interaction though the reasons behind its formation remain unclear. Although the two compounds

are isoelectronic and the steric demands of the CH_2TMS and neopentyl groups are similar, **4.6** displays a marked lack of tuck-in behaviour. Both lithiated pentalene complexes may prove useful precursors in the synthesis of further bimetallic species.

A crystal of an *anti*-bimetallic titanium tri-methyl compound **4.8** was isolated through serendipity. Initial attempts to reproduce formation of this complex through rational methods failed, though further investigation is of future interest. Finally, an unidentified compound **3.1.U** was synthesised by the reaction of **3.1** *in situ* with two equivalents of $MgMe_2$. Preliminary investigation suggests that the asymmetric species characterised by ^{1}H NMR spectroscopy may correspond to $[TiMe(\mu{:}\eta^5,\eta^5\text{-}Pn^{\dagger})]_2$, corroborated by observation of the characteristic molecular ion by EI-MS. However, further investigation is required to definitively reveal the identity of this compound.

Finally, reaction of **3.4** with four equivalents of KHMDS yielded **4.9**, an M-C bonded species featuring a TMS group tuck-in bond to the metal centre.

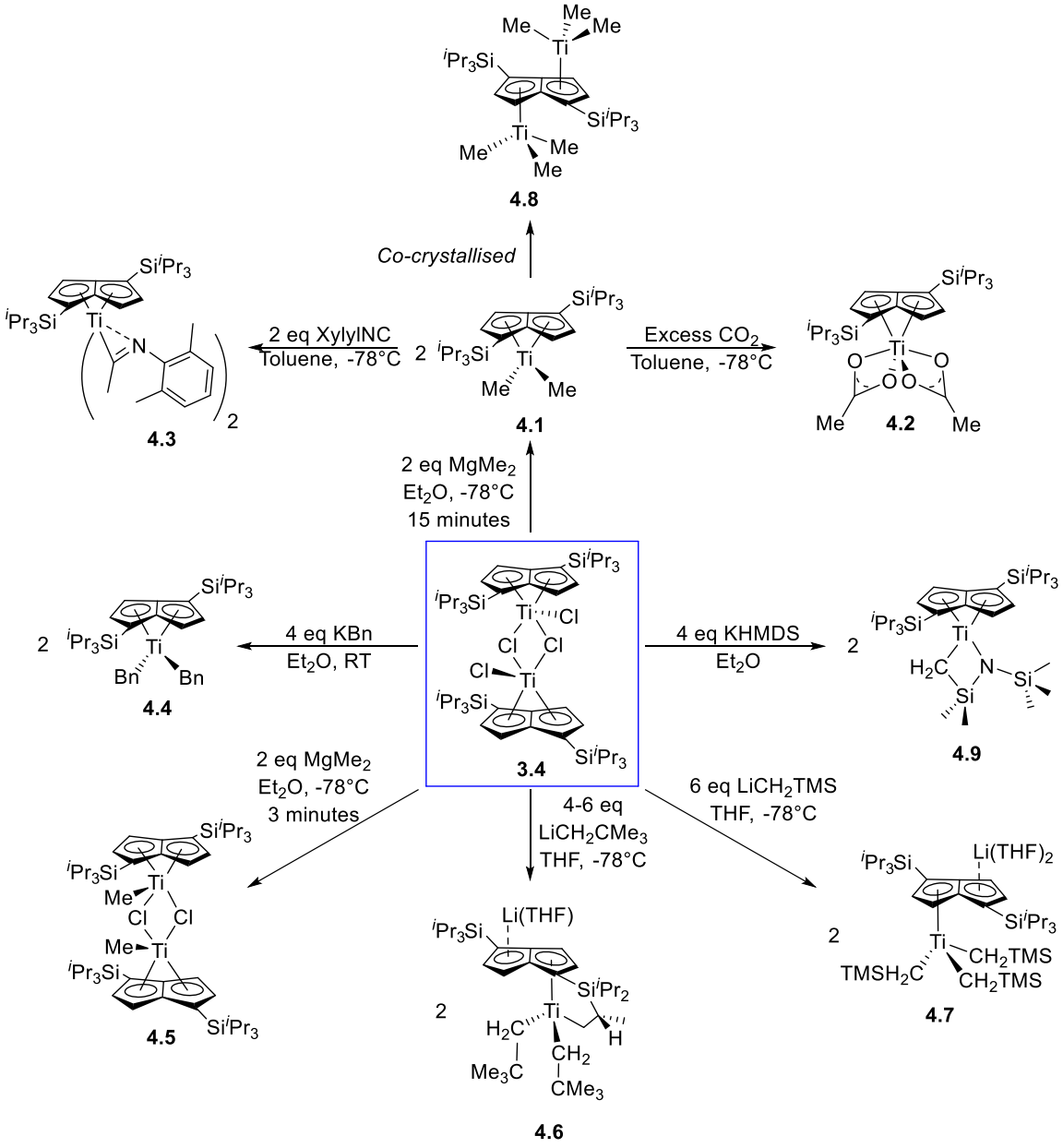

Scheme 4.21 Summary of isolated products (Chapter 4).

Chapter 4 Experimental Data

R4.1) Synthesis of [Ti(Me)$_2$(η^8-Pn†)] (4.1)

100 mg of [TiCl(η^8-Pn†)]$_2$(μ-Cl)$_2$ (0.09 mmol) was added to a small Young's tap ampoule equipped with a magnetic stirrer bar and 20 mg of $MgMe_2$ (0.36 mmol) was transferred to the vessel *via* a glass funnel. The ampoule was placed within a slush bath at -78°C and 5 mL of diethyl ether was added. An immediate colour change to brown was witnessed. Stirring was continued for 15 minutes at this temperature. The ether was then removed *in vacuo* at -78°C. Attempts to bind the $MgCl_2$ in solution with 1,4-dioxane resulted in decomposition of the final product. Instead, the complex was extracted with around 5 mL of pentane, with vigorous shaking to ensure maximum possible dissolution. The resulting orange solution was then filtered twice through a Celite® packed pipette. A Celite® frit was used for larger preparations.

Following filtration, solvent was evaporated to the point of product saturation and red block crystals were obtained from a pentane solution at -35°C. The resulting complex is unstable at ambient temperature, and so must be stored at -35°C.

Yield: 25 mg (0.0522 mmol), 58%.

^{1}H NMR: δ_H 6.49 (2H, d, $^3J_{HH}$ = 3.30 Hz, Pn H), 5.75 (2H, d, $^3J_{HH}$ = 3.30 Hz, Pn H), 1.25 (12H, m, methine CH), 1.16 (18H, d, $^3J_{HH}$ = 7.35 Hz, ^{i}Pr$_3$Si CH$_3$), 1.14 (18H, d, $^3J_{HH}$ = 5.18 Hz, ^{i}Pr$_3$Si CH$_3$), 0.66 (6H, s, metal-ligated CH$_3$).

^{13}C NMR: δ_C 147.7 (Pn C), 129.0 (Pn C), 116.1 (Bridgehead Pn C), 110.7 (Pn C), 47.3 (Titanium bound CH$_3$ C), 37.6 (^{i}Pr$_3$Si CH$_3$ C), 19.0 (^{i}Pr$_3$Si CH$_3$ C), 12.1 (^{i}Pr$_3$Si CH$_3$ C).

^{29}Si{^{1}H} NMR: δ_{Si} 0.04 (^{i}Pr$_3$Si).

Crystallographic data for [Ti(Me)$_2$(η^8-Pn†)]:

Formula weight: 492.76

Triclinic. Space group P-1, clear intense red cube. a = 8.1972(5) Å, b = 13.2152(11) Å, c = 13.9066(6) Å, α = 95.580(5)°, β = 99.384(5 °, γ = 93.766(6)°.

Volume = 1474.16(17) Å^3, T = 173 K, Z = 2, R_{int} = 0.0786, Cu(Kα) λ = 1.54184 Å.

Maximum θ = 71.01°, R_1 [I>2σ(I)] = 0.0931, wR_2 (all data) = 0.255, GooF = 1.033.

R4.2.1) Reaction of [Ti(Me)$_2$(η^8-Pn†)] with $^{13}CO_2$ (4.2)

80 mg (0.16 mmol) of [Ti(Me)$_2$(η^8-Pn†)] was prepared *in situ* inside a Young's tap sealed ampoule with a cone sidearm piece and a magnetic stirrer bar. The sample was degassed on a high vacuum line and 2 equivalents (0.16 mmol, 11cm^3 Hg) of $^{13}CO_2$ was administered to the vessel at -78°C *via* Toeppler pump. After stirring the solution for 10 minutes at -78°C a colour change from bright red to orange was observed. The sample was then allowed to warm to room temperature. Orange crystals were obtained from a saturated pentane solution at -35°C.

Yield: 73 mg (0.13 mmol), 81%.

^{1}H NMR (C_7D_8): δ_H 6.60 (2H, d, $^3J_{HH}$ = 3.47 Hz, Pn H), 5.80 (2H, d, $^3J_{HH}$ = 3.26 Hz, Pn H), 1.66 (6H, d, $^2J_{CH}$ = 6.58 Hz, O_2CCH_3), 1.44 (6H, m, methine CH), 1.28 (18H, d, $^3J_{HH}$ = 7.35 Hz, ^{i}Pr$_3$Si CH$_3$ C), 1.24 (18H, d, $^3J_{HH}$ = 7.35 Hz, ^{i}Pr$_3$Si CH$_3$ C).

^{13}C{^{1}H} NMR (C_7D_8): δ_C 190.7 (bound O_2CCH_3 CO_2 C), 189.7 (bound O_2CCH_3 CO_2 C), 153.6 (Pn C), 152.2 (Pn C), 135.0 (Pn C), 134.2 (Pn C), 102.6 (Pn bridgehead C), 99.4 (Pn bridgehead C), 97.0 (Pn bridgehead C), 94.3 (Pn bridgehead C), 19.9 (^{i}Pr$_3$Si CH$_3$ C), 19.7 (^{i}Pr$_3$Si CH$_3$ C), 12.7 (^{i}Pr$_3$Si CH C).

^{13}C NMR (C_7D_8): δ_C 190.7 (q, $^2J_{CH}$ = 6.70 Hz, bound O_2CCH_3 CO_2 C), 189.7 (bound O_2CCH_3 CO_2 C), 153.6 (Pn C), 152.2 (Pn C), 135.0 (Pn C), 134.2 (Pn C), 102.6 (Pn bridgehead C), 99.4 (Pn bridgehead C), 97.0 (Pn bridgehead C), 94.3 (Pn bridgehead C), 19.9 (^{i}Pr$_3$Si CH$_3$ C), 19.7 (^{i}Pr$_3$Si CH$_3$ C), 12.7 (^{i}Pr$_3$Si CH C).

^{29}Si{^{1}H} NMR (C_7D_8): δ_{Si} 0.58 (^{i}Pr$_3$Si Si), 0.26 (^{i}Pr$_3$Si Si).

Crystallographic data for [Ti(OAc)$_2$(η^8-Pn†)]:

Formula weight: 580.79

Triclinic. Space group P-1, dull orange block. a = 9.7781(4) Å, b = 11.8616(5) Å, c = 15.5766(5) Å, α = 100.402(3)° β = 97.588(3)°, γ = 112.234(4)°.

Volume = 1604.49(12) Å^3, T = 173 K, Z = 2, R_{int} = 0.0208, Cu(Kα) λ = 1.54184 Å.

Maximum θ = 71.59°, R_1 [I>2σ(I)] = 0.0346, wR_2 (all data) = 0.0986 , GooF = 1.088.

R4.3) Synthesis of [Ti(η^8-Pn†)(η^2-$C_8H_9NCMe)_2$] (4.3)

100 mg (0.20 mmol) of [Ti$(Me)_2$(η^8-Pn†)] was synthesised *in situ* within a Rotaflow sealed ampoule. Xylylisocyanide was added to the vessel *via* microsyringe from a 1.43 M stock solution in toluene (0.40 mmol, 280 μL) at -78°C. Addition of the isocyanide produced an immediate colour change to dark brown. The solution was stirred for 2 hours at -78°C before slowly warming to room temperature. Brown plate crystals were obtained from a saturated pentane solution stored at -35°C.

Yield: 95 mg (0.13 mmol), 64%

^{1}H NMR: δ_H 7.01 (1H, s, br, Pn H), 6.71 (2H, s, br, Pn H), 6.22 (1H, s, br, Pn H), 5.98 (2H, s, br, Pn H), 5.92 (1H, s, br, Pn H), 5.49 (2H, s, br, Pn H), 3.29 (3H, s, NC-CH_3), 1.50 (5H, br, s, methine CH), 1.17 (36H, s, ^{i}Pr$_3$Si CH_3), 1.06 (6H, s, br, ^{i}Pr$_3$Si CH_3), 0.97 (12H, br, s, ^{i}Pr$_3$Si CH_3).

^{13}C{^{1}H} NMR (C_7D_8): δ_C 147.8 (Pn C), 143.7 (Pn C), 128.6 (Pn C), 125.0 (Pn C), 119.6 (Pn C), 115.0 (Pn C), 109.4 (Pn C), 107.7 (Pn C), 47.9 (**4.1** Ti-Me), 19.3 (^{i}Pr$_3$Si CH_3 C), 19.2 (^{i}Pr$_3$Si CH_3 C), 19.1 (^{i}Pr$_3$Si CH_3 C), 19.0 (^{i}Pr$_3$Si CH_3 C), 12.8 (^{i}Pr$_3$Si CH C), 12.0 (^{i}Pr$_3$Si CH C), 5.1 (^{i}Pr$_3$Si CH C), 4.7 (^{i}Pr$_3$Si CH C), 2.6 (^{i}Pr$_3$Si CH C).

Crystallographic data for [Ti($(Me)_2C_6H_3NCMe)_2$(η^8-Pn†)]:

Formula weight: 921.24

Monoclinic. Space group $P2_1/c$, irregular clear pale yellow. a = 11.647(2) Å, b = 36.011(6) Å, c = 10.3402(17) Å, α = 90°, β = 96.699(15)°, γ = 90°.

Volume = 4307.4(13) Å^3, T = 173 K, Z = 4, R_{int} = 0.0853, Cu(Kα) λ = 1.54184 Å.

Maximum θ = 70.64°, R_1 [I>2σ(I)] = 0.0693, wR_2 (all data) = 0.249, GooF = 0.954.

R4.4) Synthesis of [Ti$(Bn)_2$(η^8-Pn†)] (4.4)

100 mg (0.09 mmol) of [TiCl(η^8-Pn†)$]_2(\mu$-$Cl)_2$ was added to a Young's tap ampoule equipped with a glass stirrer bar. 50 mg of potassium benzyl (0.38 mmol) was added *via* a glass funnel. 5 mL of diethyl ether was added at room temperature and the reaction proceeded with stirring for 15 minutes. An immediate colour change to orange was observed. The solvent was removed under vacuum conditions and the resulting product was extracted in pentane. Crystals were obtained from trimethylsilane at -35°C. The

sample exhibited temperature sensitivity in solution, decaying in around 12 hours. Storage of the crystalline solid at -35°C preserved the sample indefinitely.

Yield: 24 mg (0.04 mmol), 40%

^{1}H NMR (C_6D_{12}): δ_H 7.10 (4H, t, aromatic *meta* CH), 7.01 (4H, d, $^{3}J_{HH}$ = 7.52 Hz, aromatic *ortho* CH), 6.81 (2H, t, aromatic *para* CH), 6.02 (2H, d, $^{3}J_{HH}$ = 2.96 Hz, Pn H), 5.61 (2H, $^{3}J_{HH}$ = 3.01 Hz), 2.29 (2H, d, $^{2}J_{HH}$ = 10.26 Hz, benzyl CH_2) 2.18 (2H, d, $^{2}J_{HH}$ = 10.33 Hz, benzyl CH_2), 1.18 (12H, m, methine CH), 1.11 (36H, d, $^{3}J_{HH}$ = 6.95 Hz, $^{i}Pr_3Si$ CH_3), 1.04 (36H, d, $^{3}J_{HH}$ = 7.05 Hz, $^{i}Pr_3Si$ CH_3).

^{13}C NMR: δ_C 146.8 (*ipso* Ph C), 144.8 (Pn C), 130.7 (Pn C), 126.4 (*ortho* Ph C), 122.6 (*meta* Ph C), 122.1 (*para* Ph C), 117.9 (Pn C), 111.1 (Pn C), 66.4 (Bn CH_2), 19.7 ($^{i}Pr_3Si$ CH_3 C), 13.5 ($^{i}Pr_3Si$ CH C).

^{29}Si{^{1}H} NMR: δ_{Si} 0.21 ($^{i}Pr_3Si$ Si).
EI-MS: *m/z* = 663 $[Ti(\eta^8\text{-}Pn^{\dagger})(Bn)_2]^+$ (fluorine ion adduct).
Crystallographic data for $[Ti(\eta^8\text{-}Pn^{\dagger})(Bn)_2]$:

Formula weight: 644.96.

Triclinic. Space group P-1, lustrous intense red plate. a = 9.2686(12) Å, b = 9.3367(11) Å, c = 22.587(3) Å, α = 82.797(10)°, β = 79.552(11)°, γ = 75.554(11)°.

Volume = 1854.8(4) Å^3, T = 173 K, Z =2, R_{int} = 0.1354, Cu(Kα) λ = 1.54184 Å.

Maximum θ = 71.01°, R_1 [I>2σ(I)] = 0.1158, wR_2 (all data) = 0.3626, GooF = 1.118.

R4.5) Synthesis of $[TiMe(\eta^8\text{-}Pn^{\dagger})]_2(\mu\text{-}Cl)_2$ (4.5)

80 mg of $[TiCl(\eta^8\text{-}Pn^{\dagger})]_2(\mu\text{-}Cl)_2$ (0.08 mmol) was added to a small Rotaflow ampoule with magnetic stirrer bar and 17 mg of $MgMe_2$ (0.31 mmol) was added. The vessel was cooled to -78°C and 5 mL of diethyl ether was added. An immediate colour change to brown was witnessed. The mixture was allowed to stir at -78°C for 3 minutes. Solvent was then stripped from the sample *in vacuo* at -78°C. Work-up was repeated as with $[Ti(Me)_2(\eta^8\text{-}Pn^{\dagger})]$, with extraction in pentane followed by double filtration through Celite® packed pipettes.

Following filtration, solvent was evaporated to the point of product saturation and brown crystals were obtained from a pentane solution at -35°C. The sample may be stored at -35°C indefinitely, but decays rapidly at room temperature.

Yield: 55 mg (0.05 mmol), 68%.

^{1}H NMR: δ_H 6.35 (2H, d, $^{3}J_{HH}$ = 3.30 Hz, Pn H), 5.85 (2H, s, Pn H), 1.23 (12H, br, m, ^{i}Pr$_3$Si methine CH), 1.15 (36H, d, $^{3}J_{HH}$ = 5.83 Hz, ^{i}Pr$_3$Si CH$_3$), 1.08 (obscured, titanium-ligated methyl), 1.09 (36H, d, $^{3}J_{HH}$ = 6.23 Hz, ^{i}Pr$_3$Si CH$_3$).

^{13}C NMR: δ_C 129.3 (Pn C), 118.3 (Bridgehead Pn C), 110.7 (Pn C), 48.7 (Titanium bound CH$_3$ C), 19.5 (^{i}Pr CH$_3$ C), 19.4 (^{i}PrSi CH$_3$ C), 12.4 (^{i}Pr$_3$Si CH C).

^{29}Si{^{1}H} NMR: δ_{Si} 0.45 (TIPS Si).
EI-MS: *m/z* = 1026 [[Ti(η^8-Pn†)MeCl]$_2$]$^+$

Crystallographic data for [Ti(η^8-Pn†)(MeCl)]$_2$:

Formula weight: 513.19

Monoclinic. Space group C2/c, translucent light brown block. a = 26.8823(18) Å, b = 8.5532(2) Å, c = 28.2922(13) Å, α = 90°, β = 114.115(7)°, γ = 90°.

Volume = 5939.1(6) Å^3, T = 173 K, Z = 8, R_{int} = 0.0269, Cu(Kα) λ = 1.54184 Å.

Maximum θ = 71.50°, R_1 [I>2σ(I)] = 0.0428, wR_2 (all data) = 0.112, GooF = 1.026.

R4.6) Synthesis of [Ti(CH$_2$^{t}Bu)$_2$(η^5:η^1-Pn†(Si(iPr)$_2$CH$_3$CHCH$_2$)][Li(THF)] (4.6)
100 mg (0.09 mmol) of [TiCl(η^8-Pn†)]$_2$(μ-Cl)$_2$ was placed within a Rotaflow sealed ampoule containing a magnetic stir bar. 120 μL (0.36 mmol) of 3.0 M neopentyl lithium solution in hexane (0.36 mmol) was added *via* microsyringe. 5 mL of THF was added at -78°C to the mixed solids and a colour change to brown was observed. The solvent was removed under vacuum conditions at -78°C after 10 minutes. Extraction was performed in pentane, followed by filtration through Celite®. Crystals were obtained from a saturated pentane solution at -35°C. The resulting tuck-in complex was stored at -35°C, but proved susceptible to decay at this temperature.

Yield: Negligible, characterised *in situ*. Small number of crystals (*ca.* 5 mg) isolated for XRD study.

ESI-MS: *m/z* = 603 [Ti(η^5-Pn†)(η^1-CHCH$_3$CH$_2$Si*i*Pr$_2$Pn†)]$^-$

Crystallographic data for [Ti(η^5-Pn†)(η^1-CHCH$_3$CH$_2$CH$_0$Si*i*Pr$_2$Pn†)]:

Formula weight: 1366.03

Triclinic. Space group P-1, clear light red plate. a = 12.3478(10) Å, b = 12.8010(7) Å, c = 14.8716(9) Å, α = 80.609(5)°, β = 88.545(6)°, γ = 66.610(6)°.

Volume = 2126.6(3) Å^3, T = 173 K, Z = 1, R_{int} = 0.0253, Cu(Kα) λ = 1.54184 Å.

Maximum θ = 71.02°, R_1 [I>2σ(I)] = 0.0447, wR_2 (all data) = 0.123, GooF = 1.057.

R4.7) Synthesis of [Ti(CH$_2$TMS)$_3$(η^5-Pn†)][Li(THF)$_2$] (4.7)

100 mg (0.09 mmol) of [TiCl(η^8-Pn†)]$_2$(μ-Cl)$_2$ was added to a Young's tap ampoule equipped with a magnetic stirrer bar. 61 mg of LiCH$_2$TMS (0.56 mmol) was placed within the vessel. 5 mL of THF was added at -30°C to the mixed solids and a colour change to brown was observed. The solvent was removed *in vacuo* at -30°C after 20 minutes. The product compound was extracted in pentane and filtered through Celite®. Crystals were obtained from a saturated ether solution at -35°C. The sample decays within 2 hours when in solution at room temperature, but may be stored indefinitely at -35°C.

Yield: 40 mg (0.05 mmol), 28%.

^{1}H NMR: δ_H 7.09 (1H, d, $^3J_{HH}$ = 3.66 Hz, Pn H), 6.65 (1H, d, $^3J_{HH}$ = 3.41 Hz, Pn H), 6.54 (1H, d, $^3J_{HH}$ = 3.86 Hz, Pn H), 6.12 (1H, d, $^3J_{HH}$ = 3.66 Hz, Pn H), 2.20-1.64 (9H, m, ^{i}Pr$_3$Si CH, ^{i}Pr$_3$Si CH$_3$), 1.37 (18H, m, ^{i}Pr$_3$Si CH$_3$)

0.42 (9H, s, TMS CH$_3$), 0.35 (9H, s, TMS CH$_3$), 0.00 (9H, s, TMS CH$_3$).

^{13}C NMR: δ_C 126.9 (Pn C), 102.2 (Pn C), 101.2 (Pn C), 98.0 (Pn C), 93.9 (Pn C), 81.9 (Pn bridgehead C), 79.7 (Pn bridgehead C), 35.4 (LiCH$_2$TMS CH$_2$ C), 31.4 (LiCH$_2$TMS CH$_2$ C), 24.8 (LiCH$_2$TMS CH$_2$ C), 22.1 (^{i}Pr$_3$Si CH$_3$ C), 20.2 (^{i}Pr$_3$Si CH$_3$ C), 20.0 (^{i}Pr$_3$Si CH$_3$ C), 19.9 (^{i}Pr$_3$Si CH$_3$ C), 19.8 (^{i}Pr$_3$Si CH$_3$ C), 19.7 (^{i}Pr$_3$Si CH$_3$ C), 19.7 (^{i}Pr$_3$Si CH$_3$ C), 19.6 (^{i}Pr$_3$Si CH$_3$ C), 13.9 (^{i}Pr$_3$Si CH C), 12.9 (^{i}Pr$_3$Si CH C), 12.8 (^{i}Pr$_3$Si CH C), 12.5 (^{i}Pr$_3$Si CH C), 12.0 (^{i}Pr$_3$Si CH C), 11.9 (^{i}Pr$_3$Si CH C), 2.8 (TMS CH$_3$ C), 2.7 (TMS CH$_3$ C), -0.0 (TMS CH$_3$ C).

^{29}Si{^{1}H} NMR: δ_{Si} 5.88 (^{i}Pr$_3$Si Si), -0.58 (^{i}Pr$_3$Si Si), -2.04 (^{i}Pr$_3$Si Si), -2.08 (^{i}Pr$_3$Si Si), -2.21 (^{i}Pr$_3$Si Si).

ESI-MS: *m/z* = 653 $[Ti(\eta^5\text{-}Pn^\dagger)(CH_2TMS)_3]^-$ (minus fragmented TMS).
Crystallographic data for $[Ti(\eta^5\text{-}Pn^\dagger)(CH_2TMS)_3]$:

Formula weight: 348.59

Monoclinic. Space group $P2_1/n$, pale red block. a = 14.7292(3) Å, b = 16.4402(3) Å, c = 23.1619(5) Å, α = 90°, β = 94.849(2)°, γ = 90°.

Volume = 5588.6(2) $Å^3$, T = 173 K, Z = 10, R_{int} = 0.0394, Cu(Kα) λ = 1.54184 Å.

Maximum θ = 72°, R_1 [I>2σ(I)] = 0.0568, wR_2 (all data) = 0.161, GooF = 1.032.

R4.8) Synthesis of $[(Ti(Me)_3)_2(\mu{:}\eta^5,\eta^5\text{-}Pn^\dagger)]$ (4.8)

Complex isolated serendipitously from a synthetic mixture predominantly yielding **4.1**. Sample size of **4.8** restricted to a single red crystal used for X-Ray crystallography.

Formula weight: 286.38

Triclinic. Space group P-1, clear light red plate. a = 8.6904 (12) Å, b = 9.122(3) Å, c = 11.884(4) Å, α = 90.09(2)°, β = 100.96(2)°, γ = 108.70(2)°.

Volume = 871.4(1) $Å^3$, T = 173 K, Z = 2, R_{int} = 0.0254, Cu(Kα) λ = 1.54184 Å.

Maximum θ = 49.86°, R_1 [I>2σ(I)] = 0.0642, wR_2 (all data) = 0.157, GooF = 1.045.

R4.9) Synthesis of Unknown Complex [4.1.U]

50 mg of $[Ti(\mu{:}\eta^5,\eta^5\text{-}Pn^\dagger)]_2$ (0.05 mmol) was added to a Young's tap sealed ampoule and 2 molar equivalents of ^{t}BuCl were added (10 mg, 0.11 mmol). An immediate colour change to brown was observed, and the solvent was removed *in vacuo* at -78°C. A pre-prepared solution of $MgMe_2$ (8 mg, 0.15 mmol) was added, producing a colour change to purple. The mixture was dried under vacuum conditions after one minute, an aliquot of the sample was extracted for analysis by EI-MS and the remaining solution was stored at -35°C.

^{1}H NMR: δ_H 7.94 (1H, d, $^3J_{HH}$ = 3.48 Hz, Pn H), 7.85 (1H, d, $^3J_{HH}$ = 3.28 Hz, Pn H), 6.80 (1H, d, $^3J_{HH}$ = 3.36 Hz, Pn H), 6.54 (1H, d, $^3J_{HH}$ = 3.30 Hz, Pn H), 6.41 (1H, d, $^3J_{HH}$ = 3.06 Hz, Pn H), 6.38 (1H, d, $^3J_{HH}$ = 3.06 Hz, Pn H), 5.71 (1H, d, $^3J_{HH}$ = 3.05 Hz, Pn H), 5.43 (1H, d, $^3J_{HH}$ = 2.87 Hz, Pn H), 2.28 (2H, s, Me CH_3), 2.12 (1H, s, Me CH_3).

EI-MS: *m/z* = 996 $[[TiCl(\mu{:}\eta^5,\eta^5\text{-}Pn^\dagger)]_2]^+$

R4.10) Synthesis of $[Ti(\eta^8\text{-}Pn^\dagger)(\eta^2\text{-}CH_2SiMe_2NSiMe_3)]$ (4.9)

100 mg (0.09 mmol) of $[TiCl(\eta^8\text{-}Pn^\dagger)]_2(\mu\text{-}Cl)_2$ was added to a Rotaflow sealed ampoule equipped with a magnetic stirrer bar. 75 mg (0.38 mmol) of KHMDS was added and the mixed solids were dissolved in 2 mL of ether. A colour change to brown was observed immediately. After 30 minutes the solvent was removed *in vacuo* and brown crystals of $[Ti(\eta^8\text{-}Pn^\dagger)(\eta^2\text{-}CH_2SiMe_2NSiMe_3)]$ were obtained from a Celite® pipette filtered pentane solution kept at -35°C.

Yield: 75 mg (0.13 mmol), 70%.

^{1}H NMR: δ_H 6.36 (1H, d, $^3J_{HH}$ = 3.52 Hz, Pn H), 6.30 (1H, d, $^3J_{HH}$ = 3.36 Hz, Pn H), 5.97 (1H, d, $^3J_{HH}$ = 3.48 Hz, Pn H), 5.91 (1H, d, $^3J_{HH}$ = 3.37 Hz, Pn H), 1.64 (1H, d, $^2J_{HH}$ = 13.81 Hz, CH of titanium bound CH_2), 1.49 (1H, d, $^2J_{HH}$ = 13.64 Hz, CH of titanium bound CH_2), 1.25 (12H, d, $^3J_{HH}$ = 7.31 Hz, ^{i}Pr CH_3), 1.22 (3H, d, $^3J_{HH}$ = 6.36 Hz, ^{i}Pr CH_3), 1.18 (9H, d, $^3J_{HH}$ = 6.36 Hz, ^{i}Pr CH_3), 1.13 (12H, d, $^3J_{HH}$ = 6.66 Hz, ^{i}Pr CH_3), 0.51 (3H, s, TMS CH_3), 0.29 (3H, s, TMS CH_3), 0.14 (9H, s, TMS CH_3).

^{13}C{^{1}H} NMR: δ_C 148.2 (Pn C), 144.1 (Pn C), 129.1 (Pn C), 125.5 (Pn C), 120.0 (Bridgehead Pn C), 115.4 (Bridgehead Pn C), 109.8 (Pn C), 108.1 (Pn C), 48.3 (Titanium bound CH_2 C), 19.7 (^{i}Pr CH_3), 19.6 (^{i}Pr CH_3), 19.5 (^{i}Pr CH_3), 19.5 (^{i}Pr CH_3), 13.3 (^{i}Pr CH_3), 12.4 (^{i}Pr CH_3), 5.6 (TMS C), 5.1 (TMS C), 3.1 (TMS C).

^{29}Si{^{1}H} NMR: δ_{Si} -0.04 (^{i}Pr$_3$Si Si), -0.09 (^{i}Pr$_3$Si Si), -3.37 (Me$_3$Si Si), -34.88 (solvent impurity).
EI-MS: *m/z* = 622 $[Ti(\eta^8\text{-}Pn^\dagger)_2(\eta^2\text{-}CH_2SiMe_2NSiMe_3)]^+$.
Elemental analysis (calculated for $C_{32}H_{63}NSi_4Ti$): C, 58.34 (61.79); H, 10.81 (10.21); N, 1.95 (2.25)%.

Crystallographic data for $[Ti(\eta^8\text{-}Pn^\dagger)(\eta^2\text{-}CH_2SiMe_2NSiMe_3)]$:

Formula weight: 622.09.

Orthorhombic. Space group $P2_12_12_1$, dark red plate. a = 8.7606(10) Å, b = 17.1765(2) Å, c = 24.7654(4) Å, α = 90° β = 90°, γ = 90°.

Volume = 3726.61(9) Å^3, T = 173 K, Z = 4, R_{int} = 0.0260, Cu(Kα) λ = 1.54184 Å.

Maximum θ = 70.68°, R_1 [I>2σ(I)] = 0.0356, wR_2 (all data) = 0.0899, GooF = 1.023.

R4.10.2) Reaction of 3.4 with 1 Equivalent of KHMDS

50 mg (0.05 mmol) of $[TiCl(\eta^8\text{-}Pn^{\dagger})]_2(\mu\text{-}Cl)_2$ was placed within a small ampoule sealed with a Rotaflow tap and equipped with a magnetic stir bar. 10 mg (0.05 mmol) of KHMDS was added and the ampoule was charged with 2 mL of diethyl ether. The mixture displayed a colour change from red to brown and the solvent was removed under vacuum conditions after 30 minutes. The product was not isolated.

^{1}H NMR: δ_H 6.57 (1H, d, $^3J_{HH}$ = 2.95 Hz, Pn H), 6.45 (1H, d, $^3J_{HH}$ = 3.56 Hz, Pn H), 6.31 (1H, d, $^3J_{HH}$ = 3.46 Hz, Pn H), 6.26 (1H, d, $^3J_{HH}$ = 2.80 Hz, Pn H), 6.07 (1H, d, $^3J_{HH}$ = 3.29 Hz, Pn H), 6.05 (1H, d, $^3J_{HH}$ = 3.40 Hz, Pn H), 5.92 (1H, d, $^3J_{HH}$ = 3.18 Hz, Pn H), 5.87 (1H, d, $^3J_{HH}$ = 3.43 Hz, Pn H), 1.58 (2H, d $^2J_{HH}$ = 13.27 Hz, CH of titanium bound CH_2), 1.42 (6H, m, ^{i}Pr$_3$Si CH), 1.23 (18H, d, $^3J_{HH}$ = 7.52 Hz, ^{i}Pr$_3$Si CH_3), 1.16 (18H, d, $^3J_{HH}$ = 8.34 Hz, ^{i}Pr$_3$Si CH_3), 1.12 (36H, d, $^3J_{HH}$ = 6.02 Hz, ^{i}Pr$_3$Si CH_3), 0.45 (2H, s, TMS CH_3), 0.32 (6H, s, TMS CH_3), 0.29 (6H, s, TMS CH_3), 0.26 (2H, s, TMS CH_3), 0.24 (2H, s, TMS CH_3), 0.10 (6H, s, TMS CH_3), 0.08 (9H, s, TMS CH_3).

Chapter 5 – Reactivity of $[Ti(\mu:\eta^5,\eta^5\text{-}Pn^\dagger)]_2$ with Neutral L Type Ligands

Introduction

Many chemically transformative catalytic processes rely on initial L-type coordination from a π-donor ligand. The classical example of this is the interaction of metal alkyl olefin polymerisation catalysts with alkenes. A neutral alkenyl L-type adduct forms with the metal centre, followed by insertion into an M-C bond (as discussed in Chapter 4).[176] Group IV cyclopentadienyl complexes showcase rich chemistry in this field, as electron deficient early transition metals show a particularly strong affinity for the coordination of L-type ligands.[100]

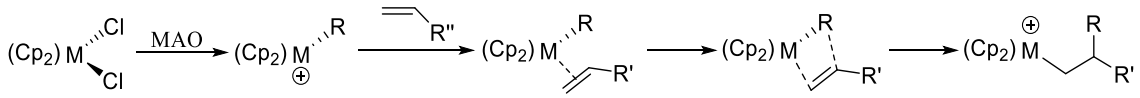

Scheme 5.1 Alkene insertion into an M-C bond.[177,178]

The manipulation of side-on bound alkenes is not always dependent on the presence of an "M-X" bond, however. Work by Mach *et al.* demonstrates[179] this with the insertion of 2-butyne into a Cp* titanocene species bound to η^2 coordinated ethylene. The ability of titanocenes to to mediate the formation of carbocycles is well documented.[145,179–181]

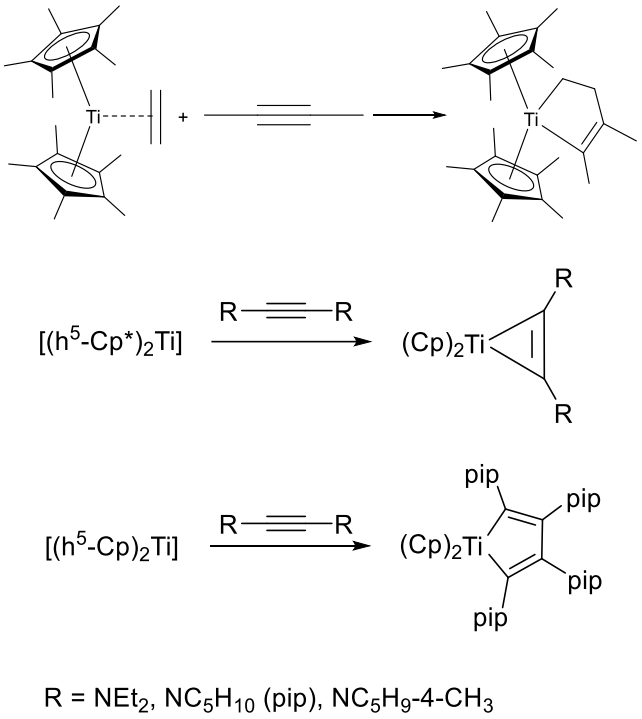

Scheme 5.2 Ti(II) carbocycles and insertion chemistry.[179,180]

The bimetallic nature of **1.1** and the existence of the Ti-Ti double bond grants the complex an additional dimension of potential reactivity over monometallic titanocenes.

The presence of two metal centres produces the possibility of either increasing the reaction rate or producing unique interactions between the ligands across the metal centres (*i.e.* formation of a bimetallic macrocycle, or asymmetric cooperative catalysis).[182]

Reactions were conducted between **1.1** and neutral L-type ligands with the goal of further probing the reactivity of the Ti-Ti double bond and the effect of the bimetallic configuration on any observed catalysis or insertion chemistry.

Reaction of 1.1 with Ethylene

Ethylene was reacted with **1.1** at -78°C, with the progress of the reaction monitored with *in situ* IR spectroscopy. A signal was recorded at 1123 cm^{-1} upon pressurisation of the vessel and as the temperature was lowered a second peak at 947 cm^{-1} grew from the baseline, representative of the formation of a metal alkene adduct. As this peak appeared, a colour change to green was evident. This colour and the requisite signal at 947 cm^{-1} is only witnessed with a constant overpressure of gas and the alkene de-ligates

rapidly upon warming. This requirement of a constant ethylene atmosphere precluded isolation of crystalline material for X-Ray diffraction. Unfortunately, useful ^{1}H NMR spectroscopic analysis was also hindered by the thermal instability of the compound.

Compound **1.1** was also reacted with CO *in situ* at -78°C after the addition of ethylene. No interaction between CO and the coordinated alkene is observed; the ethylene ligand is instead displaced and the same mix of *bis*-oxo and *bis*-carbonyl products is formed as when directly reacting **1.1** with CO. The $^{13}C\{^{1}H\}$ NMR shows bound CO at δ_C 231 ppm, in agreement for the values seen for the di-carbonyl adduct of **1.1**. Bound CO is also apparent at δ_C 297.1 ppm; indicating the presence of the mono-carbonyl complex in solution.[38]

Reaction of 1.1 with Butadiene

Complex **1.1** was next reacted with an excess of 1,3-*trans*-butadiene, with the goal of mimicking the adduct formation observed with C_2H_4 with a bulkier alkene capable of providing sufficient stability to allow isolation of the product. As before, introduction of the gas resulted in a colour change to dark green. An overpressure of gas and maintenance of temperature at -78°C was no longer required to sustain the resulting complex, with one stoichiometric equivalent of butadiene resulting in successful and long-lasting binding of the alkene.

X-Ray diffraction of crystalline material isolated from pentane at -35°C confirmed side-on η^2, η^2 coordination of one butadiene molecule to both metal centres to form the complex $[Ti_2(\mu{:}\eta^4\text{-}C_4H_6)(\mu{:}\eta^5,\eta^5\text{-}Pn^{\dagger})_2]$, **5.1**.

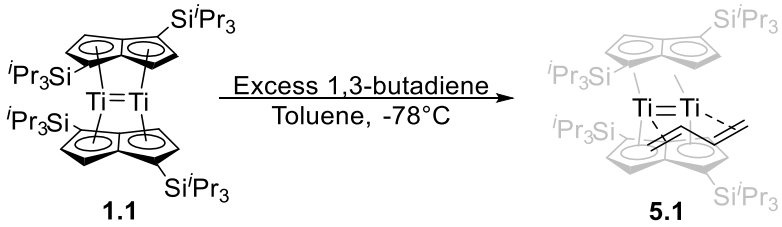

1.1 **5.1**

Scheme 5.3 Synthesis of the butadiene adduct of **1.1**, complex **5.1**

Characterisation of [$Ti_2(\mu:\eta^4\text{-}C_4H_6)(\mu:\eta^5,\eta^5\text{-}Pn^{\dagger})_2$] (5.1)

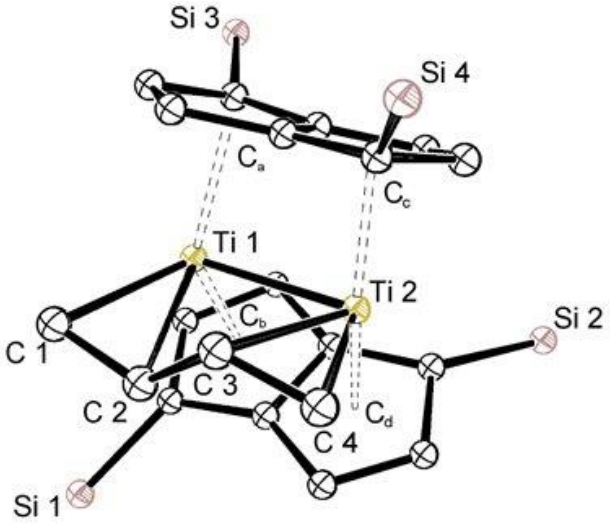

Figure 5.1 ORTEP diagram of **5.1**, ellipsoids at 50%, H atoms omitted.

Parameter	Bond Length (Å)	Angle	(°)
Ti 1-Ti 2	2.463(6)	Hinge	1.70(16)
Ti 1-C_a	2.098(2)	Fold	5.45(16)
Ti 1-C_b	2.097(6)	Twist	3.20(2)
Ti 1-C 1	2.333(4)	C_a-Ti 1-C_b	136.13(3)
Ti 1-C 2	2.437(4)	C_c-Ti 2-C_d	136.49(3)
Ti 2-C_c	2.109(7)		
Ti 1-C_d	2.112(7)		
Ti 2-C 3	2.434(3)		
Ti 2-C 4	2.325(4)		
C 1-C 2	1.400(5)		
C 2-C 3	1.415(5)		
C 3-C 4	1.410(5)		
Bridgehead C-C	1.447(5)		

Table 5.1 Selected measurements for compound **5.1**.

Bond lengths measured for Ti-C σ bond interactions in titanium alkyl compounds range from 2.082(5) Å to 2.163(3) Å. By contrast, the Ti-C distances in **5.1** vary between 2.333(4) Å and 2.437(4) Å, characteristic of "L" type π-donation over any degree of direct σ-type bonding. The conformation of the ligand in the X-Ray structure further supports this, showing a side-on binding mode with one C-C double bond interaction

per metal centre. The compound is diamagnetic by ^{1}H NMR, ruling out uneven σ-bonding from the butadiene moiety to yield a mixed valence species.

The Ti-Ti bond length in **1.1** is 2.399(8) Å, while the Ti-Ti length of **5.1** is lengthened to 2.463(14) Å. As with previous metric observations, this slight degree of lengthening alone is not enough to infallibly predict the retainment or loss of the Ti-Ti double bond. However, given the L_2 ligation mode of the alkene, it is likely that the Ti-Ti double bond is unaffected by coordination of the butadiene molecule.

Assuming no loss of the Ti-Ti double bonding character, each metal centre can thus be assigned a Ti(II) formal oxidation state and an MLX configuration of ML_5X_4, with a total electron count of 18 e^-.

Coordination of the butadiene unit near halves the fold angle of **5.1** from 8.72(4)° in **1.1** to 5.45(16)°. This geometrical alteration is likely reactionary to the increased steric protection afforded by the butadiene ligand, which prompts a shift away from "umbrella" steric shielding of the titanium core by the pentalene ligand in favour of greater electronic contribution to the metal centre. This is accomplished by the heightened degree of aromaticity gained by the diminished bridgehead C-C fold angle.

Entropic concerns pertaining to the chelate effect are also a factor with regard to the increased longevity of the butadiene adduct over the ethylene complex. Coordination of two ethylene molecules is entropically less favourable than adduct formation with one bidentate ligand.[183]

NMR spectroscopic data is supportive of all assertions made based on the results of X-Ray diffraction analysis. The ^{1}H NMR spectrum of the compound displays four Pn-H peaks in solution at δ_H 7.85 ppm, 6.51 ppm, 5.64 ppm and 5.57 ppm. Three resonances pertaining to the butadiene ligand are observed. The butadiene CH group labelled H_C is exhibited as a multiplet at δ_H 5.87 ppm and δ_H 3.80 ppm signifies the proximal CH_2 proton H_b, which manifests as a doublet. Finally, a second doublet at δ_H 3.06 ppm signifies butadiene CH group H_a. These groups have been labelled for convenience in **Figure 5.2**.

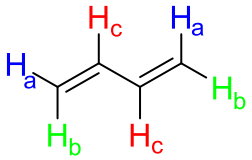

Figure 5.2 Bound butadiene proton environments identified by ^{1}H NMR spectroscopy.

$^{13}C\{^{1}H\}$ NMR and $^{29}Si\{^{1}H\}$ NMR spectra are in agreement with all other characteristic data. The former displays eight pentalene carbon environments, with the butadiene CH_2 visible as an antiphase peak at δ_C 52.8 ppm when scrutinised by a DEPT-135 experiment. The $^{29}Si\{^{1}H\}$ NMR data displays a total of two silicon triisopropylsilyl environments, indicative of C_s symmetry in solution.

Infrared analysis of the product in comparison to the base IR spectrum of **1.1** depicted three new peaks. A broad 3365 cm^{-1} signal and a sharp peak at 2865 cm^{-1} are indicative of CH_2 stretching,[184] while a second broad resonance at 1592 cm^{-1} is characteristic of butadiene CH scissoring.

EI-MS of crystalline **5.1** produced a characteristic molecular ion at 979 *m/z* in addition to the fragmentation pattern of the sample conforming to the expected average isotopic distribution. Elemental composition was confirmed by combustion analysis.

Reactivity of $[Ti_2(\mu{:}\eta^4\text{-}C_4H_6)(\mu{:}\eta^5,\eta^5\text{-}Pn^{\dagger})_2]$ (5.1)

Gas reactions conducted with **5.1** and ^{13}CO at -78°C produced identical results to the *in situ* gas reactions performed with the ethylene adduct, resulting in the loss of the coordinated butadiene molecule to yield the mono-carbonyl products, identifiable by the coordinated $^{13}C\{^{1}H\}$ CO signal at 297.1 ppm.

Attempts were made to repeat the reported[179] reactivity of Ti(II) ethylene compounds with alkynes with **5.1**, utilising the one coordinated molecule of butadiene between two metal centres as a replacement for the singular equivalent of ethylene reported for the monometallic permethylcyclopentadiene sandwich. Unfortunately, it was found that reaction with two equivalents of 2-butyne at room temperature results once again in a loss of the butadiene moiety in favour of binding one butyne unit between the two metal centres. This is observed as a colour change from green to dark brown, resulting in the asymmetric diamagnetic complex $[Ti_2(\mu{:}\eta^2\text{-}CH_3CCCH_3)(\mu{:}\eta^5,\eta^5\text{-}Pn^{\dagger})_2]$ **5.2**, obtained in

high purity at 80% yield. **5.2** was isolated as a brown crystalline solid and characterised by X-Ray diffraction, ^{1}H, ^{13}C and ^{29}Si spectroscopy.

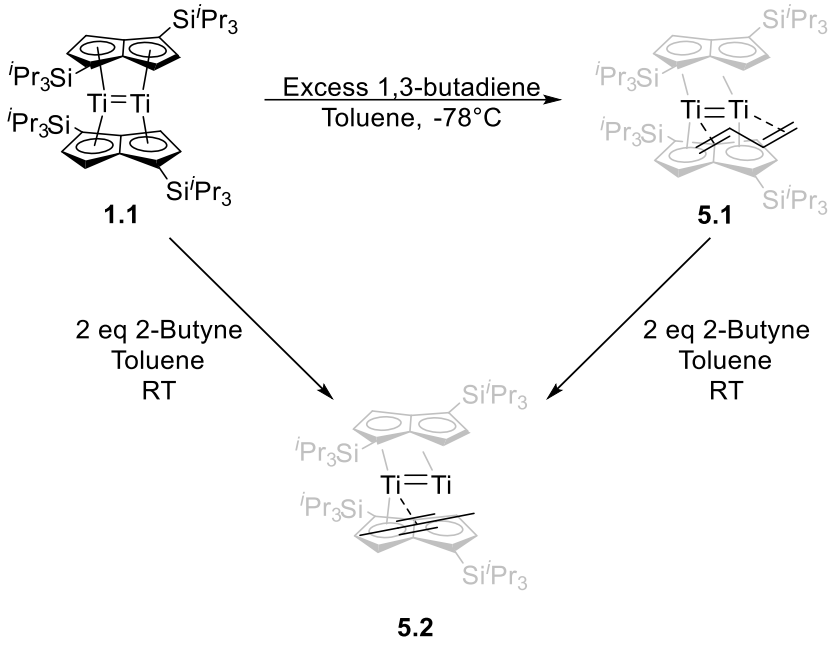

Scheme 5.4 Synthesis of **5.2** from **1.1** and **5.1**.

Characterisation of $[Ti_2(\mu{:}\eta^2\text{-}CH_3CCCH_3)(\mu{:}\eta^5,\eta^5\text{-}Pn^{\dagger})_2]$ (5.2)

^{1}H NMR spectroscopic analysis of the solution shortly after mixing shows four pentalene aromatic CH resonances at δ_H 7.85, 6.51, 5.64 and 5.57 attributable to **5.1**. Also present are eight pentalene environments from δ_H 7.29 ppm to 5.82 ppm characteristic of the formation of **5.2**. The butyne methyl groups present as 3H integration signals at δ_H 2.69 ppm and -0.39 ppm. With the α proximity of each methyl group to the alkyne C-C triple bond, the clear chemical shift difference between these two values is likely indicative of uneven distribution of electrons across the C-C triple bond. The 2.69 ppm methyl group, C 4 on the X-Ray structure ORTEP diagram (**Figure 5.3**), is comparatively deshielded due to its close (1.397(5) Å) proximity to the metal C=C π interaction. C 1 by contrast is located at a more conventional CH_3 shift region.

Free butadiene is seen at δ_H 4.96 and 5.08 ppm in the crude reaction mixture. Within one hour the ^{1}H NMR spectrum confirms full loss of butadiene coordination by the disappearance of **5.1**, leaving only free butadiene and **5.2**.

The $^{13}C\{^{1}H\}$ data shows a total of 16 pentalene aromatic peaks in addition to four separate signals for the butyne alkyne and alkyl environments. $^{29}Si\{^{1}H\}$ NMR data is

also indicative of the asymmetry of **5.2**, with the TIPS group silicons displayed as four separate signals from δ_{Si} 3.64 ppm to δ_H 1.13 ppm.

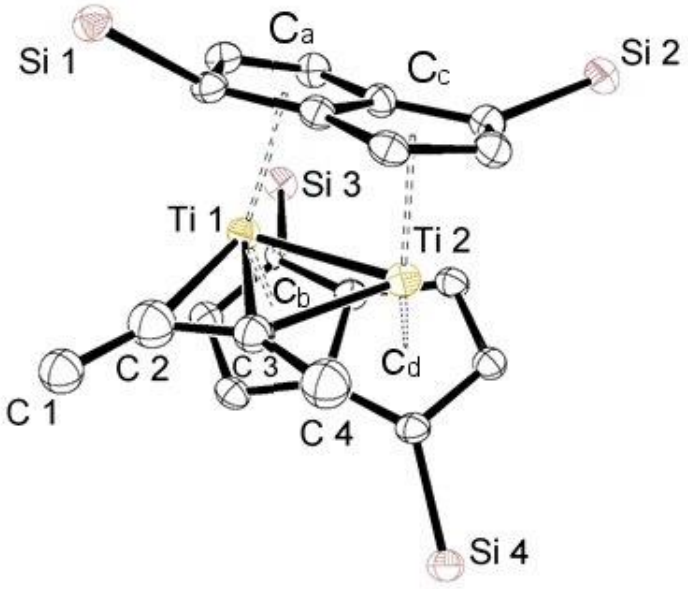

Figure 5.3 ORTEP diagram of **5.2**, ellipsoids at 50% probability. Hydrogen atoms and erroneous fifth 2-butyne carbon atom omitted.

Parameter	Bond Length (Å)	Angle	(°)
Ti 1-Ti 2	2.419(11)	Hinge	1.65(15)
Ti 1-C_a / Ti 2-C_b	2.139(5)	Fold	2.67(15)
Ti 1-C_b / Ti 2-C_a	2.078(6)	Twist	42.03
Ti 1-C 2 / Ti 2-C 4	2.332(5)	C_a-Ti 1-C_b	136.99(3)
Ti 1-C 3 / Ti 2-C 3	2.182(4)	C_c-Ti 2-C_d	136.99(3)
Ti 1-C 1	3.591(7)		
Ti 1-C 4	3.424(5)		
C 1-C 2	1.297(8)		
C 2-C 3	1.397(5)		
Bridgehead C-C	1.443(4)		

Table 5.2 Selected bond length and angle measurements for **5.2**.

The diffraction pattern of **5.2** appears to show five carbon atoms coordinated rather than the four indicated by NMR analysis and that should logically be expected from ligation of a C_4 unit. These five carbon atoms are shown in a horseshoe shape, bound between the metal centres in a perfectly symmetrical conformation. This is in fact an issue with the butyne group lying directly across a plane of symmetry rather than an indication of

erroneous characterisation. The structure shown in **Figure 5.3** has been simplified to more accurately represent the true structure of the complex, with purposeful omission of hydrogen atoms and "C 5", the anomalous carbon atom observed in a mirror position to C 1. Given the diamagnetic nature of the complex, it is likely the oxidation state of each titanium core remains at (II), with L type bonding to one metal centre from the alkyne triple bond. At 2.419(11) Å, the Ti-Ti bond length of **5.2** is one of the shortest recorded in this work, differing by only 0.02 Å from the value of 2.399(2) of **1.1**. This is strongly suggestive of M-M double bond retainment. **5.2** also displays an acute centroid-metal-centroid angle typical of ligation of a bulky group to one face of the structure. Additionally, twist angles between the pentalene ligands are significant at 42.03°, symptomatic of the asymmetric mode of binding butyne displays.

The C-C alkyne bond in **5.2** is elongated to 1.397(5) Å in comparison to literature measurements for titanocene side-on alkyne complexes, which state values between 1.301(19) Å and 1.294(4) Å.[179] The shortened Ti-C 3 distance of 2.182(4) is 0.1 Å greater than Ti-C σ bond interaction lengths recorded in this work. However, Mach *et al*. in fact describe shorter Ti-alkyne-C lengths of 2.073(12) Å and 2.076(13) Å.[179] Thus, the Ti-C distances are within established ranges for a side-on π interaction, with no evidence for σ-type bonding. There is also a notable shortening of the C 1-C 2 bond to 1.297(8) Å, in contrast with C-C single bond distances of 1.410(5) observed for butadiene in **5.1**. A published study of 2-butyne concludes that this C-C distance is 1.45 Å,[185] suggesting that coordination of the butyne fragment in **5.2** has resulted not only in weakening of the C-C triple bond interaction, but strengthening of the C-C single bonds. The exact reason for this remains unclear, though DFT studies may prove useful for further analysis of bonding in the system.

Repetition of the reaction between **5.1** and 2-butyne at an elevated temperature (60°C) again results in replacement of the butadiene group by 2-butyne, with no evidence by ^{1}H NMR of insertion chemistry. Compound **5.2** may also be synthesised by direct reaction of **1.1** with 2-butyne.

Synthesis of [Ti(μ:η^5,η^5-Pn†)]$_2$(μ:η^2-C$_8$H$_9$NC)] (5.3)

It was discovered in previous work by the Cloke group[66] that compound **1.1** reacts with methyl isocyanide to produce an adduct in which NC binds side-on, bridging the two metal centres (*vide infra*).

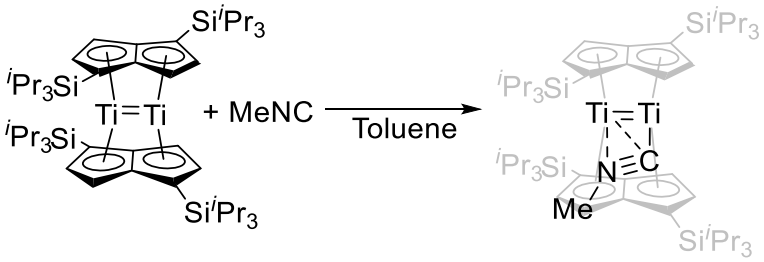

Scheme 5.5 Reaction of methylisocyanide with **1.1**.[66]

A reaction was performed with **1.1** and the bulkier xylylisocyanide to obtain a second example of an isocyanide adduct with differing steric properties. Observations noted over the course of the experiment were consistent with the methylisocyanide reaction, with formation of a purple complex after addition of the isocyanide to a toluene solution of **1.1** at ambient temperature. Crystals of [Ti(μ:η^5,η^5-Pn†)]$_2$(μ:η^2-C$_8$H$_9$NC)] **5.3** were furnished from a pentane solution at -35°C and analysed by X-Ray diffraction. The structure obtained was confirmed by further characterisation with ^{1}H, ^{13}C{^{1}H} and ^{29}Si{^{1}H} NMR spectroscopy and EI-MS techniques.

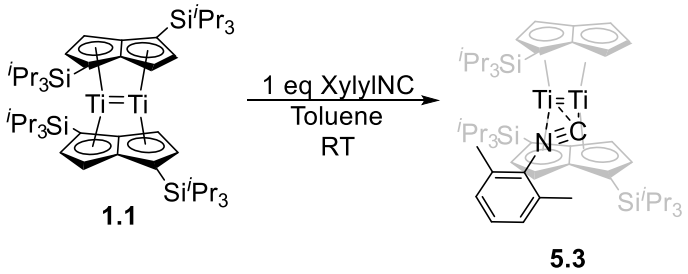

Scheme 5.6 Reaction of xylylisocyanide with **1.1**

Characterisation of [Ti(μ:η^5,η^5-Pn†)]$_2$(μ:η^2-C$_8$H$_9$NC)] (5.3)

As with methyl isocyanide, xylyl isocyanide adopts a side-on binding motif, bridging the bimetallic core. The ^{1}H NMR spectrum shows eight pentalene aromatic doublets consistent with this non-symmetric binding of the isocyanide ligand. The aromatic region also contains the xylyl group protons, which are clearly distinguished by

multiplicity. A triplet at δ_H 6.93 ppm marks the *para* aromatic CH, while doublets at 7.06 ppm and 6.72 ppm are characteristic of the CH groups proximal to the quaternary carbons bound to the xylyl methyl groups.

$^{13}C\{^1H\}$ NMR data further supports the structure depicted in the ^1H NMR and X-Ray diffraction data, with the depiction of 16 pentalene carbon environments. The bound isocyanide carbon is seen at an extreme downfield shift of δ_C 298.2 ppm in contrast to the literature reported value of δ_C 169.5 ppm for the free isocyanide.[153] This is also in agreement with the resonance at δ_C 289 ppm described for the ligated isocyanide carbon in the methyl isocyanide complex.[66]

$^{29}Si\{^1H\}$ spectrum of the complex displays four silicon environments, consistent with full asymmetry of the triisopropylsilyl groups. EI-MS analysis of the complex yielded the molecular ion value of 1055 *m/z* in addition to the unbound isocyanide at 130 *m/z*.

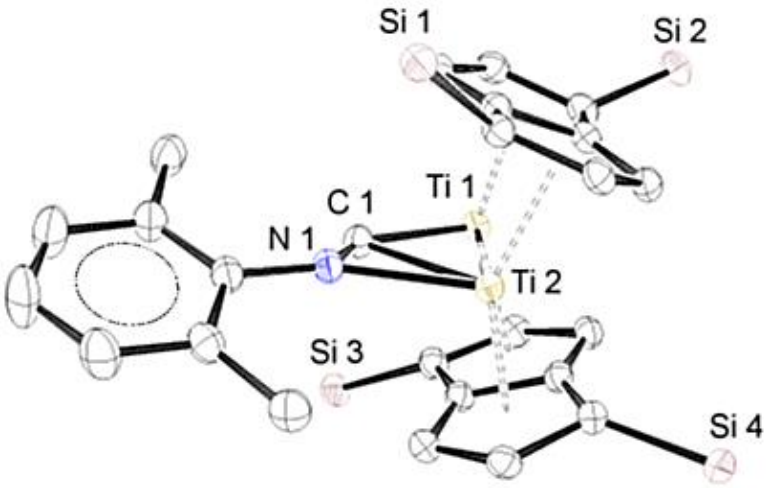

Figure 5.4 ORTEP diagram of xylylisocyanide adduct **5.3**. Ellipsoids are set at 50% probability. ^{i}Pr and hydrogen atoms have been omitted.

Parameter	Bond Length (Å)	Angle	(°)
Ti 1-Ti 2	2.414(7)	Hinge	2.47(5)
Ti 1-C_a	2.075(4)	Fold	4.49(11)
Ti 1-C_b	2.051(3)	Twist	36.15(7)
Ti 2-C_c	2.089(3)	C_a-Ti 1-C_b	147.28(5)
Ti 1-C_d	2.147(4)	C_c-Ti 2-C_d	139.68(9)
Ti 1-C 1	2.017(4)		
Ti 2-N 2	2.197(4)		
N 1-C 1	1.266(3)		
Bridgehead C-C	1.449(3)		

Table 5.3 Selected structural metrics for **5.3**.

The bond lengths measured for **5.3** are consistent with DFT calculations for the methyl isocyanide complex (for which only mediocre X-Ray diffraction data was obtained).[66] The Ti-Ti distance of 2.414(7) Å shows only 0.002 Å of deviation from the calculated value of 2.4120(15) Å given for the MeNC compound.

The centroid-Ti-centroid angle given for the MeNC adduct is 142.94(11)°,[66] in comparison to mean value in **5.3** of 143.48°. The twist angle is notably doubled in **5.3** with respect to the MeNC adduct, likely due to the increased bulk of the xylyl group. The IR spectrum of **5.3** shows the *ν*(CN) stretch at 1572.2 cm^{-1}, similar to the reported $[Ti(\mu{:}\eta^5,\eta^5\text{-}Pn^\dagger)]_2(\mu{:}\eta^2\text{-MeNC})$ *ν*(CN) stretch of 1642 cm^{-1}. This is an unusually low[66] value for a bridging isocyanide compound, though similar M-M dimers with tungsten centres have displayed comparable stretch wavenumbers of ~1530 cm^{-1}.[186]

These lower values have been determined to arise from back-donation from the metal d-orbitals to the π* anti-bonding orbitals of the isocyanide. This weakens the π-bonding interaction between the metal and NC group. In the particular case of $[Ti_2(\mu{:}\eta^5,\eta^5\text{-}Pn^\dagger)_2(\mu{:}\eta^2\text{-MeNC})]$, significant back-donation from the $Ti_2(Pn)_2$ fragment HOMO was determined by DFT studies to be responsible for this effect.[38,65,66] This is also observed in reactions with CO, resulting in a predilection towards side-on ligation so this back-donation can occur.[65,66] It is notable that due to this effect, both methyl isocyanide and xylylisocyanide show a total preference for bridging ligation of a single isocyanide unit even in the presence of excess isocyanide in solution.

In addition to 2,6-dimethylphenylisocyanide, reactions were also attempted with ^{t}BuNC; unfortunately, the resulting mixture proved intractable.

Reactivity of 1.1 with Azides and Nitrile Groups

Compound **1.1** was also reacted with a number of azides and organic nitriles. These experiments resulted in visible colour changes and show asymmetric ^{1}H NMR spectra suggestive of adduct formation. Adducts resulting from reaction of **1.1** with trityl azide and adamantyl azide have been observed by EI-MS. However, these reactions produced complicated mixtures and showed a tendency to form oils and amorphous, impure solids when recrystallisation was attempted. Characterisation of these adducts was therefore not pursued further beyond EI-MS of the crude reaction mixtures, though preliminary spectroscopic and experimental details are described in the Experimental section for further reference.

Conclusions

The formation of two alkene adducts, created by the reaction of **1.1** with ethylene and 1,3-*trans*-butadiene respectively, was observed by *in situ* IR spectroscopy. The butadiene complex $[Ti_2(\mu{:}\eta^4\text{-}C_4H_6)(\mu{:}\eta^5,\eta^5\text{-}Pn^{\dagger})_2]$ **5.1** proved isolable and was studied in further detail.

Gas reactions with these alkene adducts proved unfruitful. Reactions of **5.1** with 2-butyne did not result in novel insertion chemistry or formation of a carbocycle bound to titanium, as was intended based on a literature precedent for this chemistry. Instead the compound $[Ti_2(\eta^2\text{-}CH_3CCCH_3)(\mu{:}\eta^5,\eta^5\text{-}Pn^{\dagger})_2]$ **5.2** was isolated and characterised.

A xylylisocyanide complex, $[Ti_2(\mu{:}\eta^5,\eta^5\text{-}Pn^{\dagger})_2(\mu{:}\eta^2\text{-}C_8H_9NC)]$ **5.3**, was also synthesised and compared with the resulting compound from a previously reported reaction between **1.1** and MeNC.

Additional reactions were attempted between **1.1** and trityl azide, adamantyl azide, tetracyanoethylene and fumaronitrile, but the results of these experiments were inconclusive.

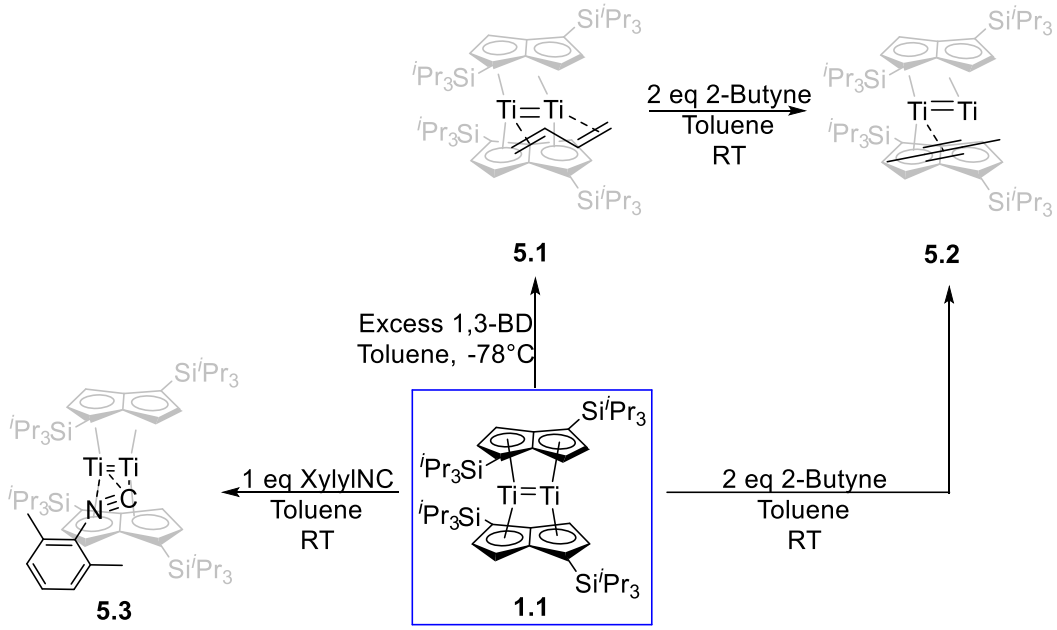

Scheme 5.7 Summary of products isolated (Chapter 5).

Chapter 5 Experimental Data

R5.1) Reaction with Ethylene (Excess)

20 mg (0.02 mmol) of **1.1** was dissolved in d^8-toluene and cooled to -78°C in an IMS/cardice bath. Two equivalents of ethylene gas were introduced *via* Toeppler line (1.8 cm^3 Hg). The sample was kept cold to prevent decomposition and NMR experiments were conducted at 0°C.

^{1}H NMR ($C_6D_5CD_3$), 399.5 MHz, -273.15 K): δ_H 8.20 (2H, d, $^3J_{HH}$ = 3.08 Hz, Pn H), 7.21 (2H, d, $^3J_{HH}$ = 2.85 Hz, Pn H), 6.67 (2H, d, $^3J_{HH}$ = 2.62 Hz, Pn H), 6.57 (2H, d, $^3J_{HH}$ = 2.62 Hz, Pn H), 6.31 (2H, d, $^3J_{HH}$ = 3.08 Hz, Pn H), 6.20 (2H, d, $^3J_{HH}$ = 3.54 Hz, Pn H), 5.86 (2H, d, $^3J_{HH}$ = 3.60 Hz, Pn H), 5.65 (2H, d, $^3J_{HH}$ = 2.70 Hz, Pn H), 4.96 (2H, m, ethylene CH_2), 4.40 (2H, m, ethylene CH_2), 1.74 (3H, m, ^{i}Pr$_3$Si CH), 1.44 (3H, m, ^{i}Pr$_3$Si CH), 1.37 (6H, d, $^3J_{HH}$ = 8.99 Hz, ^{i}Pr$_3$Si CH_3), 1.29 (3H, m, ^{i}Pr$_3$Si CH), 1.19 (18H, m, ^{i}Pr$_3$Si CH_3), 1.15 (9H, d, $^3J_{HH}$ = 7.28 Hz, ^{i}Pr$_3$Si CH_3), 1.10 (3H, d, $^3J_{HH}$ = 7.28 Hz, ^{i}Pr$_3$Si CH_3), 1.00 (12H, d, $^3J_{HH}$ = 7.64 Hz, ^{i}Pr$_3$Si CH_3), 0.86 (12H, m, ^{i}Pr$_3$Si CH_3), 0.75 (6H, d, $^3J_{HH}$ = 7.04 Hz, ^{i}Pr$_3$Si CH_3), 0.50 (6H, d, $^3J_{HH}$ = 7.64 Hz, ^{i}Pr$_3$Si CH_3).

^{13}C{^{1}H} NMR ($C_6D_5CD_3$), 100.5 MHz, -273.15 K): δ_{Si} 135.7 (Pn C), 133.6 (Pn C), 132.7 (Pn C), 132.2 (Pn C), 131.7 (Pn C), 126.5 (Pn C), 122.9 (Pn C), 121.9 (Pn C), 111.1 (Pn C), 110.7 (Pn C), 108.8 (Pn C), 107.1 (Pn C), 100.5 (Pn C), 99.1 (Pn C), 87.9 (Pn C), 86.8 (Pn C), 14.5 (^{i}Pr$_3$Si CH C), 14.3 (^{i}Pr$_3$Si CH C), 13.9 (^{i}Pr$_3$Si CH C), 13.6 (^{i}Pr$_3$Si CH C), 13.0 (^{i}Pr$_3$Si CH C), 12.2 (^{i}Pr$_3$Si CH C).

R5.2) Reaction of $Ti_2(Pn^\dagger)_2(C_2H_4)$ with ^{13}CO

20 mg (0.02 mmol) of [$Ti_2(Pn^\dagger)_2(C_2H_4)$] was dissolved in d^8-toluene and cooled to -78°C in an IMS/cardice slush bath. One equivalent of ^{13}CO was introduced *via* Toeppler line (2.9 cm^3 Hg). NMR experiments were conducted at 0°C to prevent degradation of the complex.

^{1}H NMR ($C_6D_5CD_3$), 399.5 MHz, -273.15 K): δ_H 1.54 (6H, m, ^{i}Pr$_3$Si CH), 1.23 (18H, d, $^3J_{HH}$ = 7.87 Hz, ^{i}Pr$_3$Si CH_3), 0.94 (9H, d, $^3J_{HH}$ = 7.07 Hz, ^{i}Pr$_3$Si CH_3), 0.90 (18H, d, $^3J_{HH}$ = 6.69 Hz, ^{i}Pr$_3$Si CH_3)

Note: The aromatic region of this spectrum contains a large number of singlets and multiplets unassignable to any one pentalene species.

$^{13}C\{^{1}H\}$ NMR ($C_6D_5CD_3$), 100.5 MHz, -273.15 K): δ_{Si} 297.2 (ligated CO, monocarbonyl adduct), 231.3 (ligated CO, *bis*-carbonyl adduct).

R5.3) Synthesis [$Ti_2(\mu:\eta^4\text{-}C_4H_6)(\mu:\eta^5,\eta^5\text{-}Pn^{\dagger})_2$] (5.1)

59 mg (0.06 mmol) of complex **1.1** was dissolved in toluene (5 mL). The sample was degassed by the freeze-pump-thaw method at -78°C three times. 1,3-butadiene (1.1 atm) administered at this temperature. The solution immediately changed colour from red to dark green upon addition of the gas. The sample was gradually warmed to room temperature. After removal of solvent *in vacuo* the sample was recrystallised from pentane to yield green crystals of [$Ti_2(\mu:\eta^4\text{-}C_4H_6)(\mu:\eta^5,\eta^5\text{-}Pn^{\dagger})_2$], complex **5.1**. These crystals were isolated *via* decantation and dried under vacuum conditions.
Yield: 33 mg (0.03 mmol), 56%.

^{1}H NMR: δ_H 7.85 (2H, d, $^{3}J_{HH}$ = 3.56 Hz, Pn H), 6.51 (2H, d, $^{3}J_{HH}$ = 3.32 Hz, Pn H), 5.87 (2H, m, butadiene H_c CH), 5.64 (2H, d, $^{3}J_{HH}$ = 3.23 Hz, Pn H), 5.57 (2H, d, $^{3}J_{HH}$ = 3.30 Hz, Pn H), 3.80 (2H, d, $^{3}J_{HH}$ = 13.75, butadiene H_b CH_2), 3.06 (2H, d, $^{3}J_{HH}$ = 6.86 Hz, butadiene H_a CH_2), 1.67 (6H, m, $^{i}Pr_3Si$ CH), 1.47 (6H, m, $^{i}Pr_3Si$ CH_3), 1.28 (18H, d, $^{3}J_{HH}$ = 7.30 Hz, $^{i}Pr_3Si$ CH_3), 1.28 (36H, d, $^{3}J_{HH}$ = 7.42 Hz, $^{i}Pr_3Si$ CH_3), 0.97 (18H, d, $^{3}J_{HH}$ = 7.48 Hz, $^{i}Pr_3Si$ CH_3)
$^{13}C\{^{1}H\}$ NMR: δ_{Si} 131.5 (Pn C), 129.0 (Pn C), 127.0 (Butadiene CH C), 123.4 (Pn C), 118.9 (Pn C) 117.0 (Pn C), 105.9 (Pn C) 94.3 (Pn Bridgehead C), 91.0 (Pn Bridgehead C), 52.4 (Butadiene CH_2 C), 20.2 ($^{i}Pr_3Si$ CH_3 C), 20.1 ($^{i}Pr_3Si$ CH_3 C), 19.9 ($^{i}Pr_3Si$ CH_3 C), 19.6 ($^{i}Pr_3Si$ CH_3 C), 14.5 ($^{i}Pr_3Si$ CH C), 14.3 ($^{i}Pr_3Si$ CH C), 13.0 ($^{i}Pr_3Si$ CH C), 12.9 ($^{i}Pr_3Si$ CH C).
$^{29}Si\{^{1}H\}\{^{1}H\}$ NMR: δ_{Si} 2.59 ($^{i}Pr_3Si$ Si), 2.44 ($^{i}Pr_3Si$ Si).
EI-MS: *m/z* = 979 $[Ti_2(Pn^{\dagger})_2](\mu:C_4H_6)]^+$; 924 $[Ti_2(Pn^{\dagger})_2]^+$
IR cm^{-1} 3365 (br), 2865 (sharp), 1592 (br).
Elemental analysis (calculated for $C_{54}H_{96}Si_4Ti_2$): C, 68.49 (68.67); H, 9.96 (10.02)%.

R5.4) Reaction of 5.1 with ^{13}CO

9 mg (0.01 mmol) of **5.1** was dissolved in d^8-toluene and cooled to -78°C in a dry ice bath. Two equivalents of ^{13}CO gas were added *via* Toeppler line (2.80 cm^3 Hg). The sample was left to warm slowly to room temperature overnight. A gradual colour change from green to orange was observed.

^{1}H NMR ($C_6D_5CD_3$), 399.5 MHz, -273.15 K): δ_H 6.52 (2H, d, $^3J_{HH}$ = 3.19 Hz, Pn H), 6.21 (2H, m, butadiene H_c CH), 5.69 (2H, d, $^3J_{HH}$ = 3.06 Hz, Pn H), 5.06 (2H, d, $^3J_{HH}$ = 15.80 Hz, butadiene H_b CH), 4.95 (2H, d, $^3J_{HH}$ = 9.11 Hz, butadiene H_a CH), 1.23 (6H, m, ^{i}Pr$_3$Si CH), 1.16 (36H, d, $^3J_{HH}$ = 6.88 Hz, ^{i}Pr$_3$Si CH$_3$), 1.10 (36H, d, $^3J_{HH}$ = 7.02 Hz, ^{i}Pr$_3$Si CH$_3$).

^{13}C{^{1}H} NMR ($C_6D_5CD_3$), 100.5 MHz, -273.15 K): δ_{Si} 231.3 (ligated CO), 35.0 (^{i}Pr$_3$Si CH$_3$ C), 23.3 (^{i}Pr$_3$Si CH$_3$ C), 14.8 (^{i}Pr$_3$Si CH C), 14.5 (^{i}Pr$_3$Si CH C), 13.0 (^{i}Pr$_3$Si CH C), 12.5 (^{i}Pr$_3$Si CH C).

R5.5) Reaction of 5.1 with 2-Butyne (2 Equivalents)

30 mg (0.03 mmol) of [Ti$_2$(μ:η^4-C$_4$H$_6$)(μ:η^5,η^5-Pn†)$_2$] **5.1** was dissolved in deuterated toluene within a Young's NMR tube. 5 μL of 2-butyne was added *via* microsyringe. A colour change to brown was seen within two minutes.

Yield: 18 mg (0.02 mmol), 66%.

^{1}H NMR: δ_H 7.85 (2H, d, $^3J_{HH}$ = 3.39 Hz, **5.1** Pn H), 7.29 (1H, d, $^3J_{HH}$ = 3.41 Hz, **5.2** Pn H), 6.91 (1H, d, $^3J_{HH}$ = 3.49 Hz, **5.2** Pn H), 6.51 (2H, d, $^3J_{HH}$ = 3.18 Hz, **5.2** Pn H), 6.30 (1H, d, $^3J_{HH}$ = 1.44 Hz, **5.2** Pn H), 6.29 (1H, d, $^3J_{HH}$ = 3.76 Hz, **5.2** Pn H), 6.21 (1H, d, $^3J_{HH}$ = 3.18 Hz, **5.2** Pn H), 6.02 (1H, d, $^3J_{HH}$ = 3.94 Hz, **5.1** Pn H), 5.87 (1H, d, $^3J_{HH}$ = 3.22 Hz, **5.2** Pn H), 5.82 (1H, d, $^3J_{HH}$ = 3.41 Hz, **5.2** Pn H), 5.64 (2H, d, $^3J_{HH}$ = 3.99 Hz, **5.1** Pn H), 5.57 (2H, d, $^3J_{HH}$ = 2.83 Hz, **5.1** Pn H), 5.08 (2H, d, $^3J_{HH}$ 15.87, free butadiene), 4.96 (2H, d, $^3J_{HH}$ 8.70, free butadiene), 3.84 (2H, d, $^3J_{HH}$ = 13.93, **5.1** butadiene H_b CH$_2$), 3.06 (2H, d, $^3J_{HH}$ = 6.86 Hz, **5.1** butadiene H_a CH$_2$), 2.69 (3H, s, **5.2** butyne CH$_3$), -0.39 (3H, s, butyne CH$_3$), 1.27 (m, ^{i}Pr$_3$Si CH), 1.23 (24H, d, $^3J_{HH}$ = 7.82 Hz, **5.2** ^{i}Pr$_3$Si CH$_3$), 1.16-1.03 (66H, m, ^{i}Pr$_3$Si CH$_3$).

R5.6) Synthesis of [Ti_2(μ:η^2-CH_3CCCH_3)(μ:η^5,η^5-$Pn^\dagger$)$_2$] (5.2)

49 mg (0.05 mmol) of complex **1.1** was measured into a small ampoule equipped with a magnetic stir bar and Young's valve. **1.1** was dissolved in 1 mL of toluene and 4 μL (0.11 mmol) of 2-butyne was added *via* microsyringe. A colour change to brown was observed over the course of stirring for five minutes.

Brown crystals of **5.2** were obtained from pentane at -35°C.

Yield: 37.16 mg (0.04 mmol), 76%.

^{1}H NMR: δ_H 7.30 (1H, d, $^3J_{HH}$ = 3.21 Hz, Pn H), 6.90 (1H, d, $^3J_{HH}$ = 3.21 Hz, Pn H), 6.30 (1H, d, $^3J_{HH}$ = 3.39 Hz, Pn H), 6.29 (1H, d, $^3J_{HH}$ = 3.76 Hz, Pn H), 6.21 (1H, d, $^3J_{HH}$ = 3.39 Hz, Pn H), 6.03 (1H, d, $^3J_{HH}$ = 3.40 Hz, Pn H), 5.87 (1H, d, $^3J_{HH}$ = 3.22 Hz, Pn H), 5.82 (1H, d, $^3J_{HH}$ = 3.39 Hz, Pn H), 2.69 (3H, s, butyne CH_3), 1.51 (6H, m, ^{i}Pr$_3$Si CH), 1.40 (6H, m, ^{i}Pr$_3$Si CH), 1.23 (12H, d, $^3J_{HH}$ = 7.45 Hz, ^{i}Pr$_3$Si CH_3), 1.16 (6H, d, $^3J_{HH}$ = 7.45 Hz, ^{i}Pr$_3$Si CH_3), 1.12 (6H, d, $^3J_{HH}$ = 4.86 Hz, ^{i}Pr$_3$Si CH_3), 1.07 (9H, d, $^3J_{HH}$ = 8.14 Hz, ^{i}Pr$_3$Si CH_3), -0.39 (3H, s, butyne CH_3).
^{13}C{^{1}H} NMR: δ_{Si} 193.4 (Butyne alkyne C), 162.5 (Butyne alkyne C), 133.0 (Pn C), 132.7 (Pn C), 132.4 (Pn C), 131.0 (Pn C), 129.6 (Pn C), 127.2 (Pn C), 125.7 (Pn C), 121.1 (Pn C), 115.3 (Pn C), 110.2 (Pn C), 110.1 (Pn C), 105.4 (Pn C), 102.8 (Pn bridgehead C), 94.6 (Pn bridgehead C), 90.1 (Pn bridgehead C), 89.8 (Pn bridgehead C), 34.0 (^{i}Pr$_3$Si CH_3 C), 25.0 (^{i}Pr$_3$Si CH_3 C), 22.3 (^{i}Pr$_3$Si CH_3 C), 14.0 (^{i}Pr$_3$Si CH C), 13.7 (^{i}Pr$_3$Si CH C), 12.3 (^{i}Pr$_3$Si CH C), 12.1 (^{i}Pr$_3$Si CH C), 1.0 (Butyne CH_3 C), -1.7 (Butyne CH_3 C).

^{29}Si{^{1}H} NMR: δ_{Si} 3.64 (^{i}Pr$_3$Si Si), 2.59 (^{i}Pr$_3$Si Si), 2.42 (^{i}Pr$_3$Si Si), 1.13 (^{i}Pr$_3$Si Si).

EI-MS: *m/z* = 924 [Ti(μ:η^5,η^5-$Pn^\dagger$)$_2$]$^+$; 979 [Ti($Pn^\dagger$)$_2$(μ:C_4H_6)]$^+$, 1033 [Ti($Pn^\dagger$)$_2$(C_4H_6)$_2$]$^+$

Crystallographic data for [Ti_2(μ:η^5,η^5-$Pn^\dagger$)(μ-C_4H_6)]:

Formula weight: 981.51.

Monoclinic. Space group C2/c, brown block. a = 19.5148(9) Å, b = 20.5302(8) Å, c = 15.1138(7) Å, α = 90° β = 109.650(5)°, γ = 90°.

Volume =5702.6(5) Å^3, T = 173 K, Z = 5, R_{int} = 0.0430, Cu(Kα) λ = 1.54184 Å.

Maximum θ = 70.98°, R_1 [I>2σ(I)] = 0.0617, wR_2 (all data) = 0.1943, GooF = 1.068.

R5.8) Synthesis of [Ti(μ:η^5,η^5-Pn†)]$_2$(μ:η^2-C$_8$H$_9$NC)] (5.3)

80 mg (0.08 mmol) of compound **1.1** was dissolved in toluene (2 mL). A toluene solution (2 mL) containing 11 mg (0.09 mmol) of 2,6-dimethylphenylisocyanide was transferred *via* cannula, stirring vigorously. A colour change from crimson to purple was observed over the course of an hour. After removal of volatiles *in vacuo* the purple solid was redissolved in the minimum volume of pentane and crystals were obtained after storage of the sample at -35°C.

Yield: 65 mg (0.06 mmol), 69%.

^{1}H NMR: δ_H 7.64 (1H, d, $^3J_{HH}$ = 3.26 Hz, Pn H), 7.06 (1H, d, $^3J_{HH}$ = 7.46 Hz, aromatic CH), 6.72 (1H, d, $^3J_{HH}$ = 7.59 Hz, aromatic CH), 6.93 (1H, m, aromatic CH), 6.29 (^{1}H, d, $^3J_{HH}$ = 2.89 Hz, Pn H), 6.40 (1H, d, $^3J_{HH}$ = 2.93 Hz, Pn H), 6.24 (1H, d, $^3J_{HH}$ = 3.32 Hz, Pn H), 6.11 (1H, d, $^3J_{HH}$ = 3.61 Hz, Pn H), 6.08 (1H, d, $^3J_{HH}$ = 3.32 Hz, Pn H), 5.81 (1H, d, $^3J_{HH}$ = 3.03 Hz, Pn H), 5.76 (H, d, $^3J_{HH}$ = 3.31 Hz, Pn H), 3.14 (3H, s, CH_3), 2.06 (3H, s, xylyl CH_3), 1.46 (6H, m, ^{i}Pr$_3$Si CH), 1.38 (6H, m, ^{i}Pr$_3$Si CH), 1.38 (6H, m, ^{i}Pr$_3$Si CH), 1.25 (12H, d, $^3J_{HH}$ = 7.32 Hz, ^{i}Pr$_3$Si CH_3), 1.19 (18H, d, $^3J_{HH}$ = 8.19 Hz, ^{i}Pr$_3$Si CH_3), 1.19 (18H, d, $^3J_{HH}$ = 8.19 Hz, ^{i}Pr$_3$Si CH_3), 1.13-1.04 (24H, m, ^{i}Pr$_3$Si CH_3), 1.01 (9H, d, $^3J_{HH}$ = 2.53 Hz, ^{i}Pr$_3$Si CH_3), 0.99 (9H, d, $^3J_{HH}$ = 2.52 Hz, ^{i}Pr$_3$Si CH_3).

^{13}C{^{1}H} NMR: δ_C 298.2 (NC C), 141.0 (Pn C), 134.9 (aromatic C), 133.4 (Pn C), 132.2 (aromatic C), 131.9 (Pn C), 131.6 (Pn C), 130.1 (Pn C), 129.9 (aromatic C), 129.8 (Pn C), 126.3 (aromatic C), 125.0 (Pn C), 122.1 (aromatic C), 113.6 (aromatic C), 113.1 (Pn C), 112.6 (Pn C), 107.8 (Pn C), 106.9 (Pn C), 94.7 (Pn bridgehead C), 93.4 (Pn bridgehead C), 93.1 (Pn bridgehead C), 92.6 (Pn bridgehead C), 23.3 (xylyl group CH_3 C), 20.1 (^{i}Pr$_3$Si CH_3 C), 20.0 (^{i}Pr$_3$Si CH_3 C), 19.9 (^{i}Pr$_3$Si CH_3 C), 19.7 (^{i}Pr$_3$Si CH_3 C), 19.6 (^{i}Pr$_3$Si CH_3 C), 19.4 (^{i}Pr$_3$Si CH_3 C), 19.3 (^{i}Pr$_3$Si CH_3 C), 19.2 (^{i}Pr$_3$Si CH_3 C), 18.7(^{i}Pr$_3$Si CH_3 C), 19.6 (^{i}Pr$_3$Si CH_3 C), 19.2 (^{i}Pr$_3$Si CH_3 C), 14.3 (^{i}Pr$_3$Si CH C), 14.1 (^{i}Pr$_3$Si CH C), 13.8 (^{i}Pr$_3$Si CH C), 13.6 (^{i}Pr$_3$Si CH C), 12.12 (^{i}Pr$_3$Si CH C).

^{29}Si{^{1}H} NMR: δ_{Si} 2.16 (^{i}Pr$_3$Si Si), 1.99 (^{i}Pr$_3$Si Si), 1.40 (^{i}Pr$_3$Si Si), 0.34 (^{i}Pr$_3$Si Si).

EI-MS: *m/z* = 130 [Xylyl-NC]$^+$; 877 [Ti(η^8-Pn†)$_2$]$^+$; 956 [[Ti(η^8-Pn†)](μ-O)]$_2$]$^+$; 1055 [Ti$_2$(μ:η^5,η^5-Pn†)$_2$(μ:η^2-C$_8$H$_9$NC)]$^+$

Crystallographic data for [Ti$_2$(μ:η^5,η^5-Pn†)(μ-(CH$_3$)$_2$C$_6$H$_3$NC)]:

Formula weight: 1057.59.

Monoclinic. Space group $P2_1/n$, brown plate. a = 12.828(3) Å, b = 33.485(7) Å, c = 14.703(3) Å, α = 90° β = 96.56(3)°, γ = 90°.

Volume = 6274(2) $Å^3$, T = 173 K, Z = 5, R_{int} = 0.0372, Mo(Kα) λ = 0.71073 Å.

Maximum θ = 71.42°, R_1 [I>2σ(I)] = 0.0574, wR_2 (all data) = 0.1830, GooF = 1.054.

R5.9) Reaction with Trityl Azide

10 mg (0.01 mmol) of **1.1** was added into a Young's NMR tube. 6 mg (0.02 mmol) of trityl azide was added in solid form. Upon dissolving the solids in C_6D_6, the solution displayed a colour change from red to dark brown.

^{1}H NMR: δ_H 7.98 (1H, s, Pn H), 7.88 (1H, s, Pn H), 6.85 (1H, s, Pn H), 6.58 (1H, s, Pn H), 6.42 (1H, s, Pn H), 6.33 (1H, s, Pn H), 5.74 (1H, s, Pn H), 5.48 (1H, s, Pn H), 1.76 (6H, d, 7.93 Hz, ^{i}Pr$_3$Si CH$_3$), 1.58 (6H, d, 7.73 Hz, ^{i}Pr$_3$Si CH$_3$), 1.30 (18H, d, 7.73 Hz, ^{i}Pr$_3$Si CH$_3$), 0.91 (18H, d, 5.49 Hz, ^{i}Pr$_3$Si CH$_3$), 0.77 (6H, d, 6.37 Hz, ^{i}Pr$_3$Si CH$_3$), 0.68 (9H, d, 7.12 Hz, ^{i}Pr$_3$Si CH$_3$), 0.52 (3H, d, 7.26 Hz, ^{i}Pr$_3$Si CH$_3$).
EI-MS: *m/z* = 1209 $[Ti_2(Pn^†)_2(Ph_3CN_3)]^+$; 1196 $[Ti_2(Pn^†)_2(Ph_3CN_2)]^+$; 877 $[Ti(\eta^8\text{-}Pn^†)_2]^+$

R5.10) Reaction with Adamantyl Azide

10 mg (0.01 mmol) of **1.1** was added *via* spatula into a Young's tap NMR tube and dissolved in C_6D_6. 4 mg (0.02 mmol) of solid adamantyl azide was added. Upon mixing, the solution displayed a colour change from red to brown.
^{1}H NMR: δ_H 6.82 (4H, $^3J_{HH}$ = 3.53 Hz, Pn H), 6.34 (4H, $^3J_{HH}$ = 2.96 Hz, Pn H), 1.76-1.46 (12H, m, br), 0.92 (32H, d, $^3J_{HH}$ = 7.38 Hz, ^{i}Pr CH$_3$), 0.77 (28H, d, $^3J_{HH}$ = 7.24 Hz, ^{i}Pr CH$_3$).
EI-MS: *m/z* = 1209 $[Ti_2(Pn^†)_2(C_{10}H_{15}CN_3)]^+$; 1101 $[Ti_2(Pn^†)_2(C_{10}H_{15}N_2)]^+$; 879 $[Ti(\eta^8\text{-}Pn^†)_2]^+$

R5.11) Reaction with Trimethylsilyl Azide

10 mg (0.01 mmol) of **1.1** and 4 mg (0.02 mmol) of TMS azide were added to a Young's NMR tube. Upon addition of C_6D_6, the solution displayed a colour change from red to brown.

^{1}H NMR: δ_H 7.06 (1H, d, $^3J_{HH}$ = 3.24 Hz, Pn H), 6.87 (1H, d, $^3J_{HH}$ = 2.32 Hz, Pn H), 6.68 (1H, d, $^3J_{HH}$ = 2.70 Hz, Pn H), 6.59 (1H, d, $^3J_{HH}$ = 3.01 Hz, Pn H), 6.53 (1H, d, $^3J_{HH}$ = 3.47 Hz, Pn H), 6.46 (1H, d, $^3J_{HH}$ = 3.47 Hz, Pn H), 6.38 (1H, d, $^3J_{HH}$ = 3.24 Hz, Pn H), 6.33 (1H, d, $^3J_{HH}$ = 3.24 Hz, Pn H), 6.38 (1H, d, $^3J_{HH}$ = 2.70 Hz, Pn H), 6.33 (1H, d, $^3J_{HH}$ = 3.24 Hz, Pn H), 6.32 (1H, d, $^3J_{HH}$ = 3.01 Hz, Pn H), 6.13 (1H, d, $^3J_{HH}$ = 3.78 Hz, Pn H), 5.91 (1H, d, $^3J_{HH}$ = 3.24 Hz, Pn H), 5.82 (1H, d, $^3J_{HH}$ = 3.24 Hz, Pn H), 5.80 (1H, d, $^3J_{HH}$ = 3.01 Hz, Pn H), 5.18 (1H, d, $^3J_{HH}$ = 2.17 Hz, Pn H), 0.38 (3H, s, TMS CH_3), 0.26 (6H, s, TMS CH_3), 0.23 (6H, s, TMS CH_3), 0.10 (6H, s, TMS CH_3), 0.07 (2H, s, TMS CH_3).

Note: 2 asymmetric pentalene species present by ^{1}H NMR of crude solution. Aliphatic region consists of broad multiplets and sharp indistinct singlets.

R5.12) Reaction with Fumaronitrile (1 Equivalent)

39 mg (0.04 mmol) of compound **1.1** was dissolved in toluene (10 mL) within an ampoule. A solution of 4 mg $C_4H_2N_2$ (0.05 mmol) in toluene was added slowly *via* cannula transfer. An immediate colour change to purple was observed. The volatiles were removed *in vacuo* leaving a purple solid. This solid was filtered and washed with pentane. After removal of solvent under vacuum conditions, recrystallisation was attempted from THF at -35°C.

^{1}H NMR: δ_H 7.21 (^{1}H, d, $^3J_{HH}$ = 4.01 Hz, Pn H), 7.17 (^{1}H, d, $^3J_{HH}$ = 4.00 Hz, Pn H), 7.05 (^{1}H, d, $^3J_{HH}$ = 3.49 Hz, Pn H), 6.93 (^{1}H, d, $^3J_{HH}$ = 3.75 Hz, Pn H), 6.87 (^{1}H, d, $^3J_{HH}$ = 3.75 Hz, Pn H), 6.33 (^{1}H, d, $^3J_{HH}$ = 3.04 Hz, Pn H), 5.88 (^{1}H, d, $^3J_{HH}$ = 3.42 Hz, Pn H), 5.81 (^{1}H, d, $^3J_{HH}$ = 2.93 Hz, Pn H), 1.55 (6H, m, ^{i}Pr$_3$Si CH), 1.43 (6H, m, ^{i}Pr$_3$Si CH), 1.35 (12H, d, $^3J_{HH}$ = 6.91 Hz, ^{i}Pr$_3$Si CH_3), 1.26 (36H, d, $^3J_{HH}$ = 7.34 Hz, ^{i}Pr$_3$Si CH_3), 1.17 (12H, d, $^3J_{HH}$ = 3.13 Hz, ^{i}Pr$_3$Si CH_3), 1.15 (12H, d, $^3J_{HH}$ = 3.56 Hz, ^{i}Pr$_3$Si CH_3), 1.07 (36H, d, $^3J_{HH}$ = 7.22 Hz, ^{i}Pr$_3$Si CH_3).

R5.13) Reaction with Tetracyanoethylene (1 Equivalent)

50 mg (0.05 mmol) of **1.1** was mixed with 14 mg (0.11 mmol) of tetracyanoethylene within a small ampoule with Young's valve seal. The solids were dissolved in 1 mL of toluene and an immediate colour change to purple was observed. The solution was left stirring for 3 days, at which point the reaction had proceeded to completion by ^{1}H NMR.

^{1}H NMR: δ_H 7.99 (1H, d, $^{3}J_{HH}$ = 3.71 Hz, Pn H), 7.88 (1H, d, $^{3}J_{HH}$ = 3.33 Hz, Pn H), 6.87 (4H, d, $^{3}J_{HH}$ = 3.05 Hz, **1.1** Pn H), 6.82 (4H, d, $^{3}J_{HH}$ = 3.70 Hz, Pn H), 6.60 (1H, d, $^{3}J_{HH}$ = 3.15 Hz, Pn H), 6.57 (1H, d, $^{3}J_{HH}$ = 3.33 Hz, Pn H), 6.34 (4H, d, $^{3}J_{HH}$ = 3.42 Hz, **1.1** Pn H), 5.76 (1H, d, $^{3}J_{HH}$ = 3.15 Hz, Pn H), 5.74 (1H, d, $^{3}J_{HH}$ = 3.70 Hz, Pn H), 5.48 (1H, d, $^{3}J_{HH}$ = 2.87 Hz, Pn H), 1.76 (6H, d, $^{3}J_{HH}$ = 7.76 Hz, ^{i}Pr$_3$Si CH$_3$), 1.58 (9H, d, $^{3}J_{HH}$ = 7.31 Hz, ^{i}Pr CH$_3$), 1.11 (12H, d, $^{3}J_{HH}$ = 4.79 Hz, ^{i}Pr$_3$Si CH$_3$), 0.92 (27H, d, $^{3}J_{HH}$ = 7.41 Hz, ^{i}Pr$_3$Si CH$_3$), 0.77 (27H, d, $^{3}J_{HH}$ = 7.39 Hz, ^{i}Pr$_3$Si CH$_3$), 0.69 (6H, d, $^{3}J_{HH}$ = 7.78 Hz, ^{i}Pr$_3$Si CH$_3$), 0.53 (3H, d, $^{3}J_{HH}$ = 7.48 Hz, ^{i}Pr$_3$Si CH$_3$).

Appendix – Supplementary Data

A disc attached to this document contains a complete record of the raw NMR, IR and X-Ray diffraction data described in this thesis.

Bibliography

1 H. Li, H. Feng, W. Sun, Y. Xie, R. B. King and H. F. Schaefer III, *New J. Chem.*, 2011, **35**, 1718--1729.

2 D. Astruc, *Eur. J. Inorg. Chem.*, 2017, **2017**, 6–29.

3 G. Wilkinson, *J. Am. Chem. Soc.*, 1954, **76**, 209–211.

4 P. L. Pauson, *J. Am. Chem. Soc.*, 1954, **76**, 2187–2191.

5 J. J. Eisch, *Organometallics*, 2012, **31**, 4917–4932.

6 H. Blaser, W. Brieden, B. Pugin, F. Spindler, M. Studer and A. Togni, *Top. Catal.*, 2002, **19**, 3–16.

7 D. Santamaría, J. Cano, P. Royo, M. E. G. Mosquera, T. Cuenca, L. M. Frutos and O. Castaño, *Angew. Chemie - Int. Ed.*, 2005, **44**, 5828–5830.

8 J. W. Armit and R. Robinson, *J. Chem. Soc. Dalt. Trans.*, 1922, **121**, 827–839.

9 E. Le Goff, *J. Am. Chem. Soc.*, 1962, **84**, 3975–3976.

10 Cloke. F. G. N. and O. T. Summerscales, *Coord. Chem. Rev.*, 2007, **124**, 2239–2242.

11 A. E. Ashley, A. R. Cowley and D. O'Hare, *Chem. Commun.*, 2007, 1512–1514.

12 H. Butenschon, *Angew. Chem. Int. Ed.*, 1997, **36**, 1695–1697.

13 F. G. N. Cloke, J. C. Green, A. F. R. Kilpatrick and D. O. Hare, *Coord. Chem. Rev.*, 2017, **344**, 238–262.

14 S. Knox and F. Stone, *Acc. Chem. Res.*, 1974, **7**, 321–328.

15 K. Hafner and M. Goltz, *Angew. Chem. Int. Ed. Engl.*, 1982, **21**, 695–696.

16 O. Tsuge, S. Okita, M. Noguchi and S. Kanemasa, *Chem. Lett.*, 1982, **11**, 993–996.

17 F. Xu, L. Peng, K. Shinohara, T. Nishida, K. Wakamatsu, M. Uejima, T. Sato, K. Tanaka, N. Machida, H. Akashi, A. Orita and J. Otera, *Org. Lett.*, 2015, **6**, 3014–3017.

18 Z. U. Levi and T. D. Tilley, *J. Am. Chem. Soc.*, 2009, **131**, 2796–2797.

19 S. A. R. Knox, R. J. Mckinney and G. A. Stone, *J. Chem. Soc. Dalt. Trans.*,

1980, 235–239.

20 M. Jones Jr. and L. O. Schwab, *J. Am. Chem. Soc.*, 1968, **90**, 6549–6550.

21 F. G. N. Cloke, M. C. Kuchta, R. M. Harker, P. B. Hitchcock and J. S. Parry, *Organometallics*, 2000, **19**, 5795–5798.

22 O. T. Summerscales, A. S. P. Frey, F. G. N. Cloke and P. B. Hitchcock, *Chem. Commun. (Camb).*, 2009, 198–200.

23 A. E. Ashley, A. R. Cowley and D. O'Hare, *Eur. J. Org. Chem.*, 2007, **2007**, 2239–2242.

24 A. E. Ashley, R. T. Cooper, G. G. Wildgoose, J. C. Green and D. O'Hare, *J. Am. Chem. Soc.*, 2008, **130**, 15662–15677.

25 M. Baird and C. Reese, *Tetrahedron Lett.*, 1976, **17**, 2895–2898.

26 U. H. Brinker and I. Fleischhauer, *Chem. Ber. Recl.*, 1987, **120**, 501–506.

27 A. F. R. Kilpatrick, *PhD Thesis*, University of Sussex, 2014.

28 R. Arkin and A. Kerim, *Chem. Phys. Lett.*, 2012, **546**, 144–149.

29 C. Zhu, X. Zhou, H. Xing, K. An, J. Zhu and H. Xia, *Angew. Chem. Int. Ed.*, 2015, **54**, 3102–3106.

30 T. Bally, S. Chai, M. Neuenschwander and Z. Zhu, *J. Am. Chem. Soc.*, 1997, **119**, 1869–1875.

31 S. Zilberg and Y. Haas, *Int. J. Quantum Chem.*, 1998, **71**, 133–145.

32 T. Katz and M. Rosenberger, *J. Am. Chem. Soc*, 1968, **84**, 865–866.

33 M. L. H. Green and G. Parkin, *J. Chem. Educ.*, 2014, **91**, 807–816.

34 P. Atkins, T. Overton, J. Rourke, M. Weller and F. A. Armstrong, *Inorganic Chemistry - 5th Edition*, 2010.

35 P. Aguirre-Etcheverry and D. O'Hare, *Chem. Rev.*, 2010, **110**, 4839–4864.

36 K. Jonas, P. Kolb, G. Kollbach, B. Gabor, R. Mynott, K. Angermund, O. Heinemann and C. Krüger, *Angew. Chemie Int. Ed. English*, 1997, **36**, 1714–1718.

37 F. G. N. Cloke, P. B. Hitchcock, M. C. Kuchta and N. A. Morley-Smith,

Polyhedron, 2004, **23**, 2625–2630.

38 A. F. R. Kilpatrick, J. C. Green and F. G. N. Cloke, *Organometallics*, 2015, **34**, 4830–4843.

39 Q. A. Abbasali, F. G. N. Cloke, P. B. Hitchcock and S. C. P. Joseph, 1997, **4**, 1541–1542.

40 S. Bendjaballah, S. Kahlal, K. Costuas, E. Bévillon and J. Y. Saillard, *Chem. - A Eur. J.*, 2006, **12**, 2048–2065.

41 T. J. Katz and J. J. Mrowca, *J. Am. Chem. Soc.*, 1967, **89**, 1105–1111.

42 F. G. N. Cloke, *Pure Appl. Chem.*, 2001, **73**, 233–238.

43 F. G. N. Cloke and P. B. Hitchcock, *J. Am. Chem. Soc.*, 2002, **124**, 9352–9353.

44 N. Tsoureas, A. F. R. Kilpatrick, O. T. Summerscales, J. F. Nixon, F. G. N. Cloke and P. B. Hitchcock, *Eur. J. Inorg. Chem.*, 2013, **2013**, 4085–4089.

45 J. C. T. R. B. Laurent, M. A. King, H. W. Kroto, J. F. Nixon and R. J. Suffolk, *J. Chem. Soc. Dalt. Trans.*, 1983, **4**, 755–759.

46 M. Aulbach, F. Kuber, F. M. Riedel and Helmer-Metzmann F., *Pat. Appl. CA2179355 A1*, 1996.

47 G. J. P. Britovsek, V. C. Gibson and D. F. Wass, *Angew. Chemie - Int. Ed.*, 1999, **38**, 428–447.

48 F. M. Chadwick, R. T. Cooper, A. E. Ashley, J. C. Buffet and D. M. O'Hare, *Organometallics*, 2014, **33**, 3775–3785.

49 B. Oelckers, I. Chavez, J. M. Manriquez and E. Roman, *Organometallics*, 1993, **12**, 3396–3397.

50 T. J. Katz, N. Acton and J. McGinnis, *J. Am. Chem. Soc.*, 1972, **94**, 6205–6206.

51 A. F. R. Kilpatrick, J. C. Green, F. G. N. Cloke and N. Tsoureas, *Chem. Commun.*, 2013, **49**, 9434–6.

52 M. C. Kuchta, F. G. N. Cloke and P. B. Hitchcock, *Organometallics*, 1998, **17**, 1934–1936.

53 F. M. Chadwick, A. E. Ashley, R. T. Cooper, L. A. Bennett, J. C. Green and D. M. O. Hare, *Dalt. Trans.*, 2015, **44**, 20147–20153.

54 C. Morales-Verdejo, I. Martínez-Díaz, C. Adams, J. Felipe, L. Oehninger, D. M. Carey, A. Muñoz-Castro, R. Arratia-Pérez, I. Chávez and J. Manuel, *Polyhedron*, 2014, **69**, 15–24.

55 A. E. Ashley, A. R. Cowley, J. C. Green, D. O. Hare, G. Balázs, A. R. Cowley, J. C. Green and D. O'Hare, *Organometallics*, 2007, **26**, 5517–5521.

56 G. R. Whittell and I. Manners, *Adv. Mater.*, 2007, **19**, 3439–3468.

57 W. E. Geiger, *Organometallics*, 2007, **26**, 5738–5765.

58 L. Bogani, A. Vindigni, R. Sessoli and D. Gatteschi, *J. Mater. Chem.*, 2008, **18**, 4750.

59 S. C. Jones and D. O'Hare, *Chem. Commun.*, 2003, 2208–2209.

60 Y. Portilla, I. Chávez, V. Arancibia, B. Loeb, J. M. Manríquez, A. Roig and E. Molins, *Inorg. Chem.*, 2002, **41**, 1831–1836.

61 F. Burgos, I. Chávez, J. M. Manriquez, M. Valderrama, E. Lago, E. Molins, F. Delpech, A. Castel, P. Rivière, I. Cha, J. M. Manriquez, F. Delpech, A. Castel and P. Rivie, *Organometallics*, 2001, **20**, 1287–1291.

62 F. Burgos, I. Chávez, J. M. Manriquez, M. Valderrama, E. Lago, E. Molins, F. Delpech, A. Castel and P. Riviére, *Organometallics*, 2001, **20**, 1287–1291.

63 P. Day, N. S. Hush and R. J. H. Clark, *Philos. Trans. A. Math. Phys. Eng. Sci.*, 2008, **366**, 5–14.

64 A. D. Smith, *MChem Dissertation*, 2012, University of Sussex.

65 A. F. R. Kilpatrick and F. G. N. Cloke, *Chem. Commun.*, 2014, **50**, 2769–71.

66 A. F. R. Kilpatrick, J. C. Green and F. G. N. Cloke, *Organometallics*, 2017, **36**, 352–362.

67 A. F. R. Kilpatrick, J. C. Green and F. G. N. Cloke, *Organometallics*, 2015, **34**, 4816–4829.

68 J. M. de Wolf, A. Meetsma and J. H. Teuben, *Organometallics*, 1995, **14**, 5466–5468.

69 T. Shima, S. Hu, G. Luo, X. Kang, Y. Luo and Z. Hou, *Science*, 2013, **27**, 1549–1553.

70 S. P. Semproni, C. Milsmann and P. J. Chirik, *Organometallics*, 2012, **31**, 3672–3682.

71 N. Tsoureas, J. C. Green and F. G. N. Cloke, *Chem. Commun.*, 2017, **53**, 13117–13120.

72 R. T. Cooper, F. M. Chadwick, A. E. Ashley and D. O'Hare, *Organometallics*, 2013, **32**, 2228–2233.

73 R. T. Cooper, F. M. Chadwick, A. E. Ashley and D. O'Hare, *Chem. Commun.*, 2015, **51**, 11856–9.

74 F. H. Stephens, V. Pons and R. Tom Baker, *Dalton Trans.*, 2007, **2**, 2613–2626.

75 M. C. Denney, V. Pons, T. J. Hebden, D. M. Heinekey and K. I. Goldberg, *J. Am. Chem. Soc.*, 2006, **128**, 12048–12049.

76 D. Pun, E. Lobkovsky and P. J. Chirik, *Chem. Commun.*, 2007, 3297–3299.

77 A. Kumar, H. C. Johnson, T. N. Hooper, A. S. Weller, A. G. Algarra and S. A. Macgregor, *Chem. Sci.*, 2014, **5**, 2546.

78 C. T. Aitken, E. Samuel and J. F. Harrod, 1995, **2**, 4059–4066.

79 A. Gluer, M. Forster, V. R. Celinski, J. Schmedt Auf Der Gunne, M. C. Holthausen and S. Schneider, *ACS Catal.*, 2015, **5**, 7214–7217.

80 M. E. Sloan, A. Staubitz, T. J. Clark, C. A. Russell, G. C. Lloyd-Jones and I. Manners, *J. Am. Chem. Soc.*, 2010, **132**, 3831–3841.

81 T. J. Clark, C. A. Russell and I. Manners, *J. Am. Chem. Soc.*, 2006, **128**, 9582–9583.

82 R. J. Keaton, J. M. Blacquiere and R. T. Baker, *J. Am. Chem. Soc.*, 2007, **129**, 1844–1845.

83 H. Dorn, R. A. Singh, J. A. Massey, J. M. Nelson, C. A. Jaska, A. J. Lough and I. Manners, *J. Am. Chem. Soc.*, 2000, **122**, 6669–6678.

84 T. Jurca, T. Dellermann, N. E. Stubbs, D. A. Resendiz-Lara, G. R. Whittell and I. Manners, *Chem. Sci.*, 2018, **9**, 3360–3366.

85 E. M. Staudt, G. M. Whitesides, M. Hackett, R. L. Brainard, J. P. P. M. Lavalleye, A. F. Sowinski, A. N. Izumi, S. S. Moore and D. W. Brown,

Organometallics, 1985, **4**, 1819–1830.

86 J. K. Dunleavy, *Platin. Met. Rev.*, 2006, **50**, 156.

87 H. A. Kalviri, F. Gartner, G. Ye, I. Korobkov and R. T. Baker, *Chem. Sci.*, 2015, **6**, 618–624.

88 A. F. R. Kilpatrick, J. C. Green and F. G. N. Cloke, *Organometallics*, 2015, **34**, 4816–4829.

89 C. a. Jaska, K. Temple, A. J. Lough and I. Manners, *J. Am. Chem. Soc.*, 2003, **125**, 9424–9434.

90 X. Chen, J. Zhao and S. G. Shore, *J. Am. Chem. Soc.*, 2010, **132**, 10658–10659.

91 G. R. Fulmer, A. J. M. Miller, N. H. Sherden, H. E. Gottlieb, A. Nudelman, B. M. Stoltz, J. E. Bercaw and K. I. Goldberg, *Organometallics*, 2010, **29**, 2176–2179.

92 L. J. Farrugia, *J. Appl. Crystallogr.*, 2012, **45**, 849–854.

93 O. V. Dolomanov, L. J. Bourhis, R. J. Gildea, J. A. K. Howard and H. Puschmann, *J. Appl. Crystallogr.*, 2009, **42**, 339–341.

94 W. L. F. Armarego and C. L. L. Chai, *Purification of Laboratory Chemicals*, Elsevier, Amsterdam, 6th Edition, 2009.

95 A. C. Cope, *J. Am. Chem. Soc.*, 1935, **57**, 2238–2240.

96 B. P. Whim and P. G. Johnson, *Directory of Solvents*, Springer Publications, New York, 1st Edition, 2012, p. 139.

97 T. Sasaki, S. Eguchi, T. Katada and O. Hiroaki, *J. Org. Chem.*, 1977, **42**, 3741–3743.

98 F. A. Carey and R. J. Sundberg, in *Advanced Organic Chemistry: Reaction and Synthesis Part B*, Springer Publications, New York, 5th Edition, 2007, pp. 365–400.

99 L. E. Manxzer, J. Deaton, P. Sharp and R. R. Schrock, *Inorg. Synth.*, 1982, **21**, 135–140.

100 R. A. Collins, A. F. Russell and P. Mountford, *Appl. Petrochemical Res.*, 2015, **5**, 153–171.

101 F. A. Hicks, N. M. Kablaoui and S. L. Buchwald, *J. Am. Chem. Soc.*, 1999, **121**, 5881–5898.

102 G. A. Luinstra and J. H. Teuben, *J. Chem. Soc. Chem. Commun.*, 1990, 1470–1471.

103 M. Hargittai, *Chem. Rev.*, 2000, **100**, 2233–2301.

104 G. Cavallo, P. Metrangolo, R. Milani, T. Pilati, A. Priimagi, G. Resnati and G. Terraneo, *Chem. Rev.*, 2016, **116**, 2478–2601.

105 M. Horacek, V. Kupfer, U. Thewalt, P. Stepnica, M. Polasek and K. Mach, *Organometallics*, 1999, **18**, 3572–3578.

106 D. F. Herman and W. K. Nelson, *J. Am. Chem. Soc.*, 1953, **75**, 3877–3882.

107 L. Summers, R. H. Uloth and A. Holmes, *J. Am. Chem. Soc.*, 1955, **77**, 3604–3606.

108 L. Summers and R. H. Uloth, *J. Am. Chem. Soc.*, 1954, **76**, 2278–2279.

109 T. S. Piper and G. Wilkinson, *J. Inorg. Nucl. Chem.*, 1956, **3**, 104–124.

110 G. G. Hlatky, *Coord. Chem. Rev.*, 1999, **181**, 243–296.

111 J. A. Higgins, F. G. N. Cloke and S. M. Roe, *Organometallics*, 2013, **32**, 5244–5252.

112 A. R. Siedle, W. M. Lamanna, R. A. Newmark and J. N. Schroepfer, *J. Mol. Catal. A Chem.*, 1998, **128**, 257–271.

113 K. C. Jayaratne and L. R. Sita, *J. Am. Chem. Soc.*, 2000, **122**, 958–959.

114 V. C. Gibson and S. K. Spitzmesser, *Chem. Rev.*, 2003, **103**, 283–315.

115 J. Saßmannshausen, A. K. Powell, C. E. Anson, S. Wocadlo and M. Bochmann, *J. Organomet. Chem.*, 1999, **592**, 84–94.

116 P. J. W. Deckers, B. Hessen and J. H. Teuben, *Organometallics*, 2002, **21**, 5122–5135.

117 Q. Wang, R. Quyoum, D. J. Gillis, M.-J. Tudoret, D. Jeremic, B. K. Hunter and M. C. Baird, *Organometallics*, 1996, **15**, 693–703.

118 M. Aresta and A. Dibenedetto, *Dalton Trans.*, 2007, 2975–2992.

119 R. R. Schrock and G. W. Parshall, *Chem. Rev.*, 1976, **76**, 243–268.

120 E. M. Matson, W. P. Forrest, P. E. Fanwick and S. C. Bart, *J. Am. Chem. Soc.*, 2011, **133**, 4948–54.

121 T. J. Schmeier, N. Hazari, C. D. Incarvito and J. A. Raskatov, *Chem. Commun.*, 2011, **47**, 1824–1826.

122 J. Campos, J. Lopez-Serrano, R. Peloso and E. Carmona, *Chem. - A Eur. J.*, 2016, **22**, 6432–6457.

123 H. Masai, K. Sonogashira and N. Hagihara, *Bull. Chem. Soc. Jpn.*, 1968, **41**, 1954–1955.

124 I. S. Kolomnikov, M. E. Volpin and T. S. Lobeeva, *Zhurnal Obs. Khimii*, 1972, **42**, 2232.

125 R. Waterman, *Organometallics*, 2013, **32**, 7249–7263.

126 A. F. Dunlop-Brière, P. H. M. Budzelaar and M. C. Baird, *Organometallics*, 2012, **31**, 1591–1594.

127 F. A. Cotton, *Chem. Rev.*, 1955, **55**, 551–594.

128 G. Wilkinson, *Pure Appl. Chem.*, 1972, **30**, 627–636.

129 E. L. Muetterties, G. F. Schmidt, M. A. Beno and J. M. Williams, *Proc. Natl. Acad. Sci.*, 1981, **78**, 1318–1320.

130 U. Giannini and U. Zucchini, *Chem. Commun.*, 1968, 940a.

131 W. Bruser, K. H. Thiele, P. Zdunneck and F. Brune, *J. Organomet. Chem.*, 1971, **32**, 335–341.

132 J. A. M. Simões and J. L. Beauchamp, *Chem. Rev.*, 1990, **90**, 629–688.

133 J. A. Labinger and J. E. Bercaw, *Organometallics*, 1988, **7**, 926–928.

134 P. E. M. Siegbahn, *J. Phys. Chem.*, 1995, **99**, 12723–12729.

135 H. A. Skinner and J. A. Connor, *Pure Appl. Chem.*, 1985, **57**, 79–88.

136 J. J. Eisch, A. A. Adeosun, S. Dutta and P. O. Fregene, *European J. Org. Chem.*, 2005, 2657–2670.

137 C. P. Gordon, K. Yamamoto, K. Searles, S. Shirase, R. A. Andersen, O.

Eisenstein and C. Copéret, *Chem. Sci.*, 2018, **9**, 1912–1918.

138 D. J. Cardin, B. Cetinkaya and M. F. Lappert, *Chem. Rev.*, 1972, **72**, 545–574.

139 M. M. Franc, W. J. Pietro, R. F. Hout and W. J. Hehre, *Organometallics*, 1983, **2**, 281–286.

140 R. S. Grainger and K. R. Munro, *Tetrahedron*, 2015, **71**, 7795–7835.

141 E. O. Fischer and A. Maasböl, *Angew. Chem. Int. Ed.*, 1964, **3**, 580–581.

142 D. Bourissou, O. Guerret, F. P. Gabbai and G. Bertrand, *Chem. Rev.*, 2000, **100**, 39–91.

143 P. de Frémont, N. Marion and S. P. Nolan, *Coord. Chem. Rev.*, 2009, **253**, 862–892.

144 T. M. Trnka and R. H. Grubbs, *Acc. Chem. Res.*, 2001, **34**, 18–29.

145 R. Beckhaus, in *Metallocenes: Synthesis Reactivity Applications*, ed. A. Togni, R. L. Halterman, Wiley Online Library, Hoboken, 1st Edition, 2008, Chapter 4, p. 167.

146 T. Takeda, *Chem. Rec.*, 2007, **7**, 24–36.

147 P. D. Bolton and P. Mountford, *Adv. Synth. Catal.*, 2005, **347**, 355–366.

148 R. F. Johnston and J. C. Cooper, *Organometallics*, 1987, **6**, 2448–2449.

149 P. K. Hurlburt, J. J. Rack, J. S. Luck, S. F. Dec, J. D. Webb, O. P. Anderson and S. H. Strauss, *J. Am. Chem. Soc.*, 1994, **116**, 10003–10014.

150 J. Zakzeski, S. Burton, A. Behn, M. Head-Gordon and A. T. Bell, *Phys. Chem. Chem. Phys.*, 2009, **11**, 9903–9911.

151 K. I. Gell, B. Posin, J. Schwartz and G. M. Williams, *J. Am. Chem. Soc.*, 1982, **104**, 1846–1855.

152 F. E. Hahn, *Angew. Chem. Int. Ed. Eng.*, 1993, **33**, 650–665.

153 R. W. Stephany, M. J. A. de Bie and W. Drenth, *Org. Magn. Reson.*, 1974, **6**, 45–47.

154 J. G. P. Delis, P. G. Aubel, K. Vrieze, P. W. N. M. Van Leeuwen, N. Veldman, A. L. Spek and F. J. R. Van Neer, *Organometallics*, 1997, **16**, 2948–2957.

155 G. Bellachioma, G. Cardaci, A. Macchioni and G. Reichenbach, *Inorg. Chem.*, 1992, **31**, 63–66.

156 M. Luo, L. Long, H. Zhang, Y. Yang, Y. Hua, G. Liu, Z. Lin and H. Xia, *J. Am. Chem. Soc.*, 2017, **139**, 1822–1825.

157 J.-M. Basset, D. E. Berry, G. K. Barker, M. L. H. Green, J. A. K. Howard and F. G. A. Stone, *J. Chem. Soc. Dalt. Trans.*, 1979, 1003–1011.

158 J. Chen, N. Yassin, T. Gunasekara, J. R. Norton and M. Rauch, *J. Am. Chem. Soc.*, 2018, **140**, 8980–8989.

159 R. C. Cookson, T. A. Crabb, J. J. Frankel and J. Hudec, *Tetrahedron*, 1966, **22**, 355–390.

160 V. N. Fishman, B. Linclau, D. P. Curran and K. V Somayajula, *Am. Soc. Mass Spectrom.*, 2001, **0305**, 1050–1054.

161 U. Zucchini, E. Albizzati and U. Giannini, *J. Organomet. Chem.*, 1971, **26**, 357–372.

162 I. W. Bassi, G. Allegra, R. Scordamaglia and G. Chioccola, *J. Am. Chem. Soc.*, 1971, **93**, 3787–3788.

163 F. Mark Chadwick, R. T. Cooper and D. O'Hare, *Organometallics*, 2016, **35**, 2092–2100.

164 R. P. Stewart and P. M. Treichel, *J. Am. Chem. Soc.*, 1970, **92**, 2710–2718.

165 R. R. Schrock, *Acc. Chem. Res.*, 1979, **12**, 98–104.

166 Z. J. Tonzetich, *PhD. Thesis*, University of Rochester, 2002.

167 D. Tapu, D. A. Dixon and C. Roe, *Chem. Rev.*, 2009, 3385–3407.

168 A. F. R. Kilpatrick and F. G. N. Cloke, *Dalt. Trans.*, 2017, **46**, 5587–5597.

169 F. G. N. Cloke, P. B. Hitchcock, M. C. Kuchta and N. A. Morley-Smith, *Polyhedron*, 2004, **23**, 2625–2630.

170 M. Schlegel and K. H. Thiele, *Zeitschrift fuer Anorg. und Allg. Chemie*, 1985, **526**, 43–47.

171 E. Aldeco-Perez, A. J. Rosenthal, B. Donnadieu, P. Parameswaran, G. Frenking and G. Bertrand, *Science*, 2009, **326**, 556–559.

172 A. Vicancos, C. Segarra and M. Albrecht, *Chem. Rev.*, 2018, **118**, 9483–9586.

173 J. M. Fischer, W. E. Piers and V. G. Young, *Organometallics*, 1996, **15**, 2410–2412.

174 W. J. Evans, K. A. Miller, A. G. DiPasquale, A. L. Rheingold, T. Stewart and R. Bau, *Angew. Chemie - Int. Ed.*, 2008, **47**, 5075–5078.

175 N. R. Andreychuk, S. Ilango, B. Vidjayacoumar, D. J. H. Emslie and H. A. Jenkins, *Organometallics*, 2013, **32**, 1466–1474.

176 A. F. Dunlop-Brière, M. C. Baird and P. H. M. Budzelaar, *Organometallics*, 2015, **34**, 5245–5253.

177 L. Guo, W. Liu and C. Chen, *Mater. Chem. Front.*, 2017, 2487–2494.

178 W. L. Carrick, *Fortschritte der Hochpolymeren-Forschung*, conference proceedings, Springer Publications, New York, 1973, pp. 65–86.

179 J. Pinkas, I. Cisarova, R. Gyepes, J. Kubista, M. Horacek and K. Mach, *Organometallics*, 2012, **31**, 5478–5493.

180 O. Arias, A. R. Petrov, T. Bannenberg, K. Altenburger, P. Arndt, P. G. Jones, U. Rosenthal and M. Tamm, *Organometallics*, 2014, **33**, 1774–1786.

181 L. Clawson, J. Soto, S. L. Buchwald, M. L. Steigerwald and R. H. Grubbs, *J. Am. Chem. Soc.*, 1985, **107**, 3377–3378.

182 R. Breinbauer and E. N. Jacobsen, *Angew. Chem. Int. Ed.*, 2000, **39**, 3604–3607.

183 E. G. Moschetta, K. M. Gans and R. M. Rioux, *J. Catal.*, 2014, **309**, 11–20.

184 J. E. Bertie and D. A. Othen, *Can. J. Chem.*, 1973, **51**, 1155–1158.

185 E. Pignataro and B. Post, *Acta Crystallogr.*, 1955, **8**, 672–674.

186 M. H. Chisholm, D. L. Clark, J. C. Huffman and C. A. Smith, *Organometallics*, 1987, **6**, 1280–1291.